An investigation of *in vitro*-assembled chromatin as a novel vehicle for gene delivery

Melanie Johnson-Saliba

Division of Molecular Bioscience
John Curtin School of Medical Research
Australian National University

THE JOHN CURTIN SCHOOL OF MEDICAL RESEARCH
Health through Discovery

THE AUSTRALIAN NATIONAL UNIVERSITY

Thesis submitted for the degree
of
Doctor of Philosophy in Medical Sciences

January 2004

STATEMENT

Unless otherwise acknowledged in the text, this thesis represents my own work. It has not been presented for the purpose of gaining any other degree.

Melanie Johnson-Saliba

ACKNOWLEDGEMENTS

To my supervisors, Prof David Jans and Dr David Tremethick, for providing me with the opportunity to pursue a PhD that introduced me to the worlds of gene therapy, nuclear transport and chromatin. I am grateful to David Jans for his expertise, pertinent comments, encouragement and interest in my work and to David Tremethick for adopting me into his laboratory when David Jans relocated to Melbourne, for giving me the freedom to develop as a scientist and for his advice and support.

To my advisors, Dr Pat Ridgway and Dr Jun Fan, for whose support I am most grateful. Moreover, I am greatly indebted to Jun who helped me with several of the chromatin techniques that I used in my work

To Geoff Osbourne and Sabine Grüninger of the Flow Cytometry Unit for sharing their expertise in FACS and their unfailing willingness to lend a skilful hand with 'setting quadrants'.

To Dr Tim Senden of the Research School of Physical Sciences and Engineering for capturing the atomic force images and for introducing me to AFM with such infectious enthusiasm.

To Kerry McAndrew and Dr Peter Milburn of the Biomolecular Resource Facility for kindly synthesising the NLS peptides used in this study. I am also especially grateful to Milburn under whose expert eye the chromatography for this study was performed.

To my fellow 'official' members of the Nuclear Signalling Lab, Chee Kai Chan, Chong-Yun Xiao, Wei Hu, Torsten Jülich, Jade Forwood, Sophina Calanni, Anna John, Chenoa Barton, Patricia Jans, Mark Lam, Assad Jadeer and Jiansheng Zhou and 'unofficial' members, Tanya Soboleva and Yvonne Foong, for creating such an enjoyable work environment, both socially and intellectually. I feel very fortunate to have worked with all of them and to have witnessed the awarding of degrees, exchanging of marriage vows and bearing of children! I feel very fortunate also to have met Lakshmi Wijeyewickrema through the Nuclear Signalling Lab, who was such a treasure to have around and has become a very dear friend.

To the members of the Chromatin and Transcriptional Regulation Group, who accepted me by fire and ice (literally!) into their lab. I benefited greatly from our discussions on chromatin architecture. I am especially thankful to Luke Hyman and Ailsa Frew for their friendship and support and to Dr Danny Rangasamy for keeping up the friendly rivalry during the South Africa vs India cricket tours.

To Dr Frances Shannon and the Cytokine Gene Expression Group, particularly Karen Bunting, Ian Parish, Xin Xin Chen, Donna Woltring and Anna Moore for being such wonderful neighbours. I am especially grateful to Karen for kindly helping me with the luciferase assay.

To Dr Sudha Rao of the Molecular Mechanisms in Disease Group for her invaluable advice and support during the process of writing this thesis.

To my family, my mom Pam and my parents-in-law, John and Grace, for understanding that I could not let the opportunity to do this research pass, even though it was so far away from home. I am thankful for their enduring support, love and encouragement.

To my friend, my mentor and my surrogate supervisor, Milburn, for nurturing me as a scientist and always being in my corner. I am exceptionally grateful.

To my husband Kevin for riding the rollercoaster of this PhD with me, for being my inspiration as a scientist and my biggest fan.

To my dad for being my strength.

PUBLICATIONS

Johnson-Saliba M., Siddon N.A., Clarkson M.J., Tremethick D.J. and Jans D.A. (2000). Distinct importin recognition properties of histones and chromatin assembly factors. *FEBS Letters* **467**: 169-174.

Johnson-Saliba M. and Jans D.A. (2001). Gene Therapy: Optimising DNA delivery to the nucleus. *Current Drug Targets* **2**: 371-399.

PUBLISHED ABSTRACT

Johnson-Saliba M., Fan J-Y., Senden T.J., Tremethick D.J. and Jans D.A. (2003). 'Chromatinisation' of plasmid DNA does not enhance reporter gene expression. *Journal of Gene Medicine* **5**: S19, P9.

ABSTRACT

A fundamental problem in non-viral gene delivery is the poor efficiency of DNA transfer into the nucleus. In the work described in this thesis, *in vitro*-assembled chromatin was investigated for the first time as a potential vehicle for non-viral gene delivery. Chromatin is formed by a hierarchical process of sequential folding and compaction of DNA, beginning with the formation of the basic repeating unit, the nucleosome, comprised of two turns of DNA around an octameric association of the core histones. It was reasoned that chromatin-induced compaction might facilitate the nuclear entry of large plasmids (greater than 5 kb) and provide resistance to cytoplasmic degradation. In addition, histones have intrinsic nuclear localisation sequences (NLSs) that mediate their passage to the nucleus and may provide a means for the nuclear import of the *in vitro*-assembled chromatin constructs as well. Since chromatin is the physiological form in which DNA occurs in the nucleus, endogenous mechanisms for the decompaction of chromatin exist, which might also facilitate decompaction and expression of the chromatinised plasmid.

Histone octamers were reconstituted from recombinant *Xenopus laevis* core histones H2A, H2B, H3 and H4 and assembled *in vitro* with the reporter plasmid, pGeneGrip-RFP, into chromatin. A range of constructs was generated with stoichiometries between 0 and 40 octamers per plasmid. Chromatin formation was verified using sedimentation velocity ultracentrifugation, DNA supercoiling, micrococcal nuclease digestion and atomic force microscopy. Chromatinised constructs were transfected into Cos-7 and HTC cells using electroporation and lipofection and reporter gene expression was quantitated by flow cytometry. Unexpectedly, reporter gene expression decreased upon plasmid chromatinisation at high nucleosome densities. pGeneGrip-RFP was labelled using a fluorescein-conjugated peptide nucleic acid (PNA) hybridisation probe in order to analyse gene expression and tracking in the same experiment. Flow cytometric analysis of isolated nuclei revealed that chromatinisation at high nucleosome densities corresponded to diminished nuclear accumulation of the plasmid. Greater proportions of nuclei accumulated plasmid chromatinised at high histone octamer stoichiometries than proportions of cells that expressed the reporter gene. This suggested that, in addition to reduced nuclear accumulation, gene expression may have been further compromised with chromatinisation at high nucleosome densities.

A high affinity interaction between histones and nuclear import proteins, mediated predominantly by importin β, was demonstrated using a modified ELISA method. Importin binding affinity was abolished when histones were assembled with DNA into chromatin, implying that nuclear import of the chromatin constructs was unlikely to be mediated via this pathway.

Incorporation of an optimised Simian Virus 40 large tumour-antigen NLS peptide into the chromatin transfection constructs was investigated as a means to enhance their nuclear uptake. A carboxy-terminal fusion protein comprised of histone H2A and the NLS sequence was generated but this did not assemble into a histone octamer under standard reconstitution conditions. The same NLS peptide was synthesised and coupled to the reporter plasmid via a PNA-maleimide linker. Transfection efficiency in the presence of the coupled NLSs was decreased relative to in their absence but appeared to be rendered insensitive to the degree of chromatinisation of the plasmid. As a means to potentiate the transcriptional permissiveness of the chromatinised plasmid, chromatin was assembled using histone octamers containing H2AZ instead of H2A, since H2AZ had been implicated in the formation of transcriptionally primed regions of chromatin. However, the impairment of transfection efficiency was more pronounced with chromatinisation at higher stoichiometries of H2AZ-containing histone octamers. An alternative reporter gene expression system involving the plasmid pGMLuc, which contains the endogenous granulocyte-monocyte colony stimulating factor promoter known to recruit transcription complexes in Jurkat cells, was investigated. Reporter gene expression in Jurkat cells using pGMLuc was not repressed upon chromatinisation at increasing nucleosome densities. In contrast, reporter gene expression in Jurkat cells using the chromatinised pGeneGrip-RFP plasmid was inhibited, consistent with the trend observed in HTC and Cos-7 cells.

Overall, the results indicate that both the nuclear uptake and the transcriptional permissiveness of transfection constructs are limiting factors for efficient transgene expression using non-viral methods of gene delivery. Furthermore, with incorporation of appropriate promoter elements into the plasmid, which are able to recruit chromatin decompaction and transcription complexes, *in vitro*-assembled chromatin may have potential for use as a gene delivery vehicle in the context of tissue-specific transgene expression.

TABLE OF CONTENTS

CHAPTER 2: Materials and Methods

ABBREVIATIONS

7-AAD	7-amino-actinomycin D
AAV	adeno-associated virus
ATP	adenosine 5'-triphosphate
B_{max}	level of maximum binding
bp(s)	base pair(s)
C-terminal	carboxyl-terminal
CB	chromatin buffer (135 mM NaCl/10 mM Tris)
CLSM	confocal laser scanning microscopy
CMV	cytomegalovirus
Da	Dalton
ddH_2O	double-distilled deionised water
DMEM	Dulbecco's modified Eagle's medium
DNA	deoxyribonucleic acid
CB	chromatin buffer
ε	extinction coefficient
EDTA	ethylene diamine tetraacetic acid
ELISA	enzyme-linked immunosorbent assay
FACS	fluorescence activated cell sorting
FITC	fluorescein isothiocyanate
GMCSF	granulocyte-monocyte colony stimulating factor
GST	glutathione-S-transferase
GTP	guanine triphosphate
HIV	human immunodeficiency virus
HSV	herpes simplex virus
HVJ	haemagglutinating virus of Japan (Sendai virus)
Imp	importin
IPTG	isopropyl-β-thiogalatopyranoside
Kap	karyopherin
kb	kilobases
K_D	apparent dissociation constant
kDa	kiloDalton
LB	Luria-Bertani medium
l	litre
MCS	multiple cloning site
MNase	micrococcal nuclease
MW	molecular weight
MWCO	molecular weight cut-off
M	molar
mg	milligram
ml	millilitre
mM	millimolar
mol	moles
min	minute(s)
µg	microgram
µl	microlitre
µM	micromolar

N-terminal	amino-terminal
NAP-1, Nap1p (yeast)	nuclear assembly protein 1
NE	nuclear envelope
NLS	nuclear localisation sequence
NPC	nuclear pore complex
ng	nanogram
nM	nanomolar
OD	optical density (absorbance)
PBS	phosphate buffered saline
PCR	polymerase chain reaction
PEI	polyethylenimine
PI	propidium iodide
pLy	poly-L-lysine
PNA	peptide nucleic acid
pmol	picomoles
RFP	red fluorescent protein
RNA	ribonucleic acid
rpm	revolutions per minute
s-coefficient	sedimentation coefficient (Svedberg units, *S*)
SDS-PAGE	sodium dodceyl sulphate-polyacrylamide gel electrophoresis
SEM	standard error of the mean
SV40 T-ag	Simian Virus 40 large tumour antigen
Tris	tris(hydroxymethyl) aminoethane
UV	ultraviolet
WGA	wheat germ agglutinin

CHAPTER 1

Introduction

1.1. OVERVIEW

The successful alleviation of human disease using gene therapy has been anticipated keenly since the first approved clinical trial, which was conducted over 10 years ago (Rosenberg *et al.*, 1990). In this trial, a neomycin resistance reporter gene was introduced *ex vivo* into tumour-infiltrating lymphocytes of cancer patients as a proof-of-principle. The reporter gene was detected for up to two months in the circulating transduced cells, demonstrating the potential of this therapeutic strategy. Several thousand patients since have been involved in clinical trials for the treatment of diseases such as severe combined immunodeficiency-adensosine deaminase disorder (SCID-ADA), cystic fibrosis, haemophilia and cancer. Only recently though have clinically significant outcomes been achieved in a trial for the treatment of X-chromosome-linked SCID (Hacein-Bey-Abina *et al.*, 2002; Cavazzana-Calvo *et al.*, 2000). Despite initially encouraging results, these clinical trials were marred by one of the disadvantages of the therapeutic approach used – random genomic insertion of the therapeutic gene. The insertion occurred adjacent to a human T-cell oncogene locus, *LMO2*, and resulted in the development of T-cell leukaemia condition in two of the ten patients treated (ESOGT, 2003; Hacein-Bey-Abina *et al.*, 2003a; Hacein-Bey-Abina *et al.*, 2003b). This highlights not only the complexities associated with gene therapy but, also, is a reminder of the risks involved with this emerging therapeutic strategy.

Methods of introducing genes into cells are conventionally grouped into viral- and non-viral-based gene delivery systems. Viral delivery systems use the genome of viruses as the vector into which the genes of interest are inserted and the viral capsid to transport this therapeutic vector. In non-viral methods of gene delivery, the DNA may be introduced into cells encapsulated within a lipid formulation (liposomes), by electroporation, complexed to heavy metal particles such as gold that are introduced into cells ballistically, or by receptor-mediated endocytosis where the DNA is linked to a receptor-specific ligand and taken up into only those cells expressing the receptor.

Whether viral or non-viral gene delivery systems are used, the vector must overcome each of several obstacles which exist in the cell before ultimately reaching the nucleus (Figure 1.1). The first limitation to entry into the cell is the plasma membrane, which must be traversed. Depending on the mode of uptake into the cell, the vector may be internalised within an endosome from which it must escape. Surviving passage through the cytoplasm is the next crucial step before the final barrier, the nuclear envelope (NE), is reached. The ultimate transfection efficiency of the gene delivery vehicle is the product of overcoming all of these barriers. As viruses have evolved mechanisms in order to overcome each of these, viral-based gene delivery vectors have proven to be highly efficient in gene transfer but are difficult to control. In contrast, while non-viral vectors have exhibited disappointing transfection efficiency, they have advantages over viral-based gene delivery systems such as being non-immunogenic and non-pathogenic.

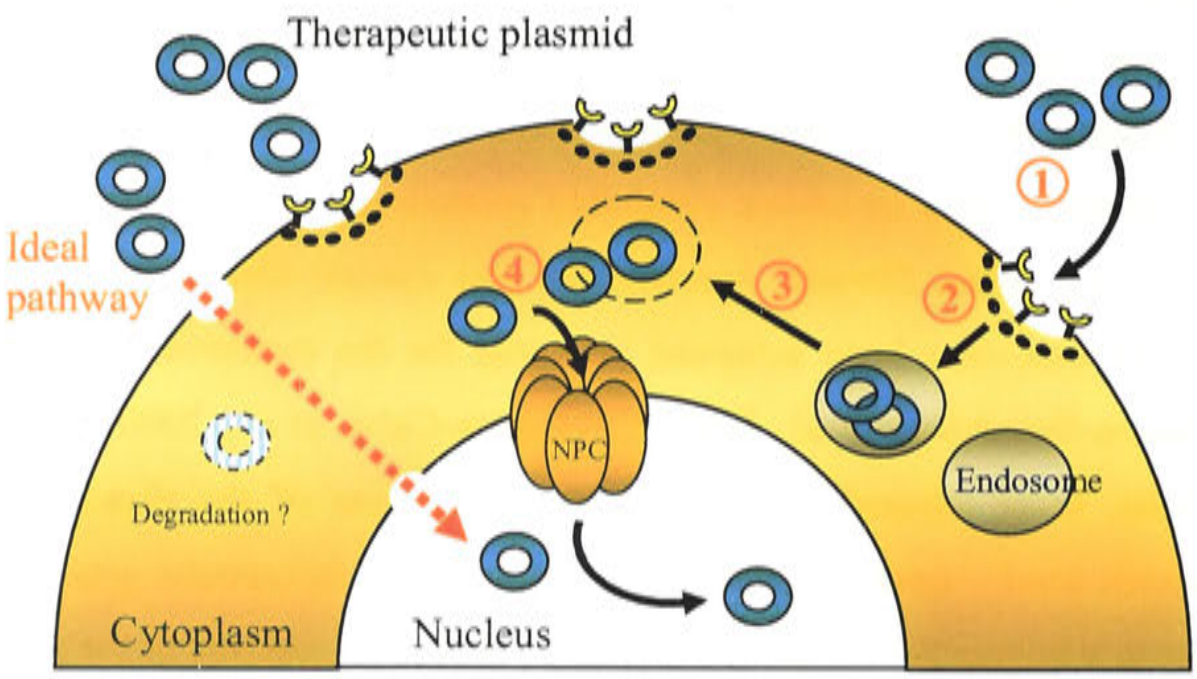

Figure 1.1. Cellular barriers to non-viral gene delivery. A schematic representation of the path of therapeutic plasmid DNA to the nucleus of a target cell is shown. Barriers to the passage of plasmid DNA are numbered in red. Entry into the cell across the plasma membrane is either mediated by endocytosis for receptor-mediated and liposomal delivery ① or is directly into the cytoplasm when using electroporation and ballistic delivery. Internalisation ② in receptor-mediated uptake or liposomal delivery results in sequestration within endosomes or vesicles and subsequent endosomal exit ③ is crucial for the DNA to be able to reach the nucleus. This may be facilitated by chloroquine, endosomal exit sequences or pH-sensitive lipids within the transfection constructs. Once in the cytoplasm, the DNA may be subjected to degradation by cytosolic nucleases. Finally, uptake into the nucleus, which occurs through nuclear pore complexes (NPCs) ④, is a key limiting step in non-viral gene delivery. The ideal pathway for gene delivery is delineated in red.

Specialised peptide sequences, that act as ligands for cell surface receptors to facilitate cell-specific uptake or nuclear localisation sequences (NLSs) that mediate nuclear uptake, may be incorporated into the non-viral vector in order to enhance transfection efficiency. This may also be achieved by usurping endogenous cellular mechanisms, such as the trafficking pathways of

certain proteins into the nucleus. A number of proteins, such as transcription factors and histones, have efficient nuclear transport pathways, presented in Sections 1.3.3.3 and 1.5.2, respectively, which, when combined with their intrinsic capacity for binding DNA, warrants their investigation as potential enhancers of transfection efficiency. Indeed, transfection studies using individual histones suggested that histone/DNA complexes constituted a promising non-viral DNA delivery vehicle (Section 1.5.3). The desire for the delivery of large plasmids, however, necessitates the use of DNA-compacting agents. Physiologically, in the form of histone octamers, histones fulfil this role also, whereby large lengths of DNA are compacted into chromatin in the nucleus.

In this chapter, the gene delivery systems are reviewed briefly and the means by which cellular barriers are circumvented are discussed. The current view on the nuclear import of plasmid DNA is presented and, finally, the premise for investigating transgene delivery into cells in the form of 'chromatinised' plasmids is expanded upon.

1.2. GENE DELIVERY SYSTEMS

The viral and non-viral gene delivery systems differ fundamentally in several ways; the capacity of DNA construct that can be accommodated, the manner of integration into the host genome and whether expression of the transgene is transient or stable. A transfection vehicle may therefore be engineered to a particular outcome, depending upon the application.

Viruses are exceptionally efficient at introducing their genetic material into host cells, which makes them attractive as vehicles for gene delivery (for reviews see Johnson-Saliba and Jans, 2001; Robbins and Ghivizzani, 1998). Their use, however, may be associated with some degree of risk to the patient, such as oncogenicity, pathogenicity and the stimulation of an immune or inflammatory reaction. In order to address some of these disadvantages, non-viral gene delivery systems were developed.

Advantages of non-viral systems include the lack of pathogenicity and immunogenicity and the capacity to accommodate large inserts of exogenous genetic material (for reviews see Johnson-Saliba and Jans, 2001; Pouton and Seymour, 2001; Luo and Saltzman, 2000). The lack of intrinsic mechanisms to overcome the cellular membrane barriers shown in Figure 1.1 is, however, a major limitation of non-viral gene delivery. As a result, the major challenge in non-viral gene delivery continues to be potentiating the level of transfection efficiency at each of the membrane barriers.

The more extensively used and, consequently, investigated systems of both viral- and non-viral-mediated gene delivery are presented in this section and the defining properties of each system are detailed in Tables 1.1 and 1.2, respectively.

1.2.1. Viral-mediated gene delivery

1.2.1.1. Retroviral vectors

Retroviruses are RNA viruses that can infect animal and human hosts (Weiss and Tailor, 1995). The genome is comprised of a single strand of RNA of 7 - 10 kilobases (kb) containing the *gag, pro, pol* and *env* genes (encoding proteins involved in viral replication and virion packaging) and the long terminal repeat regions (facilitating transcriptional control and integration into the host genome; Cullen, 1992). The *pol*-encoded reverse-transcriptase converts the viral RNA into double-stranded DNA, which then accesses the nucleus.

The majority of retroviral vectors are based on the murine Moloney leukaemia virus (MMLV). The gene delivery vector is generated by delecting the genes that encode proteins involved in viral proliferation. This reduces the probablity of the viral particles re-infecting cells and serves to create the capacity to carry 6 - 7 kb of exogenous therapeutic DNA (Miller *et al.*, 1993). The process of cell division, which involves breakdown of the NE, is essential for the retrovirus to gain access to the nucleus. Here, aided by the viral integrase and the long terminal repeat regions, the viral vector integrates randomly into the host genome (Roe *et al.*, 1993). Since the site of integration is not specific, the possibility of insertional mutagenesis or oncogenesis has been of major concern in gene therapy trials (Dave *et al.*, 2004). On the other hand, an advantage of genomic insertion is stable integration, should long-term expression of the gene product be desired (Bordignon *et al.*, 1995).

A limitation of the use of retroviral vectors, such as MMLV, is the requirement for a mitotic cycle in order for nuclear entry to occur, restricting their use to dividing cells only. Lentiviruses, a subgroup of retroviruses, of which the human immunodeficiency virus (HIV) is a member, are able to infect non-dividing cells and thus provide a broader target cell range when used as therapeutic vectors (Miyake *et al.*, 1998; Naldini *et al.*, 1996a; Naldini *et al.*, 1996b). As HIV exhibits a natural tropism for haematopoietic cells, HIV-based vectors have potential in the treatment of diseases such as AIDS and T-cell pathologies (Costello *et al.*, 2000). Current clinical trials that involve retroviral vectors are directed at treating SCID, haematological neoplasias, tumours of the central nervous system (CNS), a variety of peripheral solid tumours (in conjunction with chemotherapy) and chronic granulomatous disease (see websites http://clinicaltrials.gov/ct/gui and http://www.wiley.co.uk/genetherapy/clinical/).

1.2.1.2. Adenoviral vectors

Adenovirus is a linear double-stranded DNA virus that infects a wide range of tissues (Bergelson *et al.*, 1997; Wickham *et al.*, 1993) and may cause infections of the gastroenteric and upper respiratory tracts (Albert, 1986). Adenovirus infects non-dividing cells and does not need to integrate into the host genome for propagation. Deletion of the adenoviral genes that orchestrate viral gene expression, replication and propagation generates a replication-defective viral vector which may accommodate up to 35 kb of inserted DNA (Fisher *et al.*, 1996; Kochanek *et al.*, 1996; Bett *et al.*, 1994).

A disadvantage of using adenoviral vectors, particularly for *in vivo* applications, is that a vigorous host immune response directed against the adenoviral structural proteins is elicited. This immune response is both humoral and cell-mediated and infected cells are rapidly cleared, thus eliminating the therapeutic vector within 1 - 2 weeks post-infection (Yang and Wilson, 1995). While the cell-mediated response results in a localised inflammatory reaction, the humoral response was found to decrease the chance for successful re-introduction of the vector (Jooss *et al.*, 1998; Mack *et al.*, 1997).

Most of the clinical protocols involving adenoviral vectors are for the treatment of cystic fibrosis (http://clinicaltrials.gov/ct/gui; http://www.wiley.co.uk/genetherapy/clinical/), however encouraging results have also been observed in the treatment of cancer (Alemany *et al.*, 2000; Hu and Garen, 2000; Roth *et al.*, 1998) and neurodegenerative diseases such as Parkinson's disease and motor neuron disorders (Barkats *et al.*, 1998).

1.2.1.3. Adeno-associated viral vectors

The adeno-associated virus (AAV) is a single-stranded DNA virus that infects eukaryotic cells but without related pathology, which enhances its utility for gene therapy purposes (for review see Athanasopoulos *et al.*, 2000). In addition, unlike the other viruses used for gene delivery, AAV exhibits the unique property of site-specific integration into the host genome (human chromosome 19Q13.3qter; Young *et al.*, 2000; Surosky *et al.*, 1997; Samulski, 1993). Here, the virus remains dormant in the form of a provirus until a helper virus such as adenovirus (Ding *et al.*, 1997; Weger *et al.*, 1997) or herpes simplex virus (HSV) (Buller *et al.*, 1981) induces infectivity. Since AAV is also able to infect non-dividing cells (Russell *et al.*, 1994), collectively, these characteristics make it an attractive vector for gene therapy.

The genome of AAV is around 4.7 kb comprising the *rep* and *cap* genes, flanked by inverted terminal repeat regions (Chiorini *et al.*, 1999; Srivastava *et al.*, 1983). The *rep*-encoded proteins

are responsible for DNA binding (Im and Muzyczka, 1992; Im and Muzyczka, 1989) and site- and strand-specific integration (Young *et al.*, 2000; Im and Muzyczka, 1992; Im and Muzyczka, 1990). AAV vectors have been generated by deleting the *rep* and *cap* genes but leaving the inverted terminal repeat regions intact to function in viral integration (Xiao *et al.*, 1997b; Rolling and Samulski, 1995). This allows around 4.5 kb of exogenous DNA to be cloned within the inverted terminal repeat regions of the vector. In the absence of the *rep* gene, however, integration into the host genome reverts to being random (Kearns *et al.*, 1996) and the likelihood of insertional mutagenesis or, in certain cell types, episomal maintenance of the viral DNA is increased (Ferrari *et al.*, 1996). In an elegant series of experiments, *rep* cloned outside of the inverted terminal repeat regions was shown to restore site-specific integration of the reporter gene (Pieroni *et al.*, 1998). Although some rearrangement or partial deletion of the inserted gene and flanking regions occurred at the site of integration, this functionality of *rep* in *trans* demonstrated potential for the site-specific integration of therapeutic DNA (Pieroni *et al.*, 1998).

AAV vectors have been used to transfect muscle (Fisher *et al.*, 1997; Xiao *et al.*, 1996b), brain (Kaplitt *et al.*, 1994), liver (Koeberl *et al.*, 1997), lung (Flotte *et al.*, 1993) as well as haematopoietic cells (FisherAdams *et al.*, 1996). Clinical trials have focused mainly on the treatment of cystic fibrosis (see websites http://clinicaltrials.gov/ct/gui and http://www.wiley.co.uk/genetherapy/clinical/).

1.2.1.4. Herpes Simplex viral vectors

HSV type 1 is a double-stranded DNA virus that, through its ability to attach to cell surface heparan sulphate moieties common to many different cells (Yeung *et al.*, 1999; Gruenheid *et al.*, 1993), is able to infect a broad range of cell types (for review see Garner, 2003). HSV has become a promising candidate vector for the gene therapy of certain neurological disorders (Latchman, 2003; Lachmann and Efstathiou, 1999) due to its natural tropism for neural tissue in which it is able to establish lifelong latency (Lachmann *et al.*, 1999; Wagner and Bloom, 1997).

The 152 kb HSV genome encodes 84 known genes which are expressed sequentially at different stages of infection. Replication-defective HSV vectors have been generated by deletion of the 'immediate-early' genes which are involved in viral protein expression, DNA replication and virion production. In addition to rendering the virus incapable of replication and thus suitable as a gene delivery vector, this deletion provides accommodation for the insertion of 10 - 100 kb of exogenous DNA (Krisky *et al.*, 1998a; Krisky *et al.*, 1998b; Marconi *et al.*, 1996). This is the largest DNA carrying capacity amongst the viral-based gene delivery systems developed thus far (Wang *et al.*, 2000; Table 1.1). Replication-defective HSV vectors have

been used to transfect melanoma cells (Krisky *et al.*, 1998a), muscle (Akkaraju *et al.*, 1999) and synovial fibroblast cells (Oligino *et al.*, 1999). Amplicon HSV vectors differ from replication-defective HSV vectors in that they still contain the viral origin of replication but have a defective packaging sequence (Federoff *et al.*, 1997). These have been investigated for therapeutic gene delivery to the CNS (Herrlinger *et al.*, 2000; Dumas *et al.*, 1999).

HSV infection may be either lytic or latent. Lytic infection is suitable for the treatment of cancer (for review see Lou, 2003), whereby cellular toxicity due to HSV proteins and altered host cell protein synthesis (Greco *et al.*, 2000) is exploited to mediate anti-tumour effects (Miyatake *et al.*, 1999; Toda *et al.*, 1999; Todryk *et al.*, 1999). With the exception of cancer treatment, cytotoxicity is a major obstacle that limits the application of HSV vectors as gene delivery vehicles and, furthermore, has been shown to result in suppression of transgene expression within two weeks of transfection (Huard *et al.*, 1997). In contrast, latent infection, which is mediated by the neurotropic latency promoter, was shown to maintain gene expression for up to 18 months in the CNS (Lachmann and Efstathiou, 1999). Efforts to minimise toxicity, maximise the term of gene expression and maintain cell-specificity could enhance the utility of HSV-derived gene delivery vectors and broaden their range of applications.

1.2.2. Non-viral-mediated gene delivery

1.2.2.1. Liposomes

Liposomes are the most extensively used means of non-viral gene delivery. They have been derived using the basic principles of lipid chemistry and are comprised of a polar component attached to a non-polar component so that water-soluble material such as plasmid DNA may be encapsulated in a hydrophillic recess surrounded by a lipid bilayer (Figure 1.2).

Liposomes may be cationic, anionic or neutral, depending on the charge on the polar head group of the lipid used (for review see Katsel and Greenstein, 2000). Cationic liposomes set the precedent for the rational use of liposomes as pharmacological agents. The liposome formulation comprised an equal ratio mixture of N-[1-(2,3-dioleyloxy)propyl]-N,N,N-trimethylammonium chloride (DOTMA) and dioleoyl phosphotidylethanolamine (DOPE), in which DNA formed a complex with DOTMA through electrostatic interactions and the 'helper lipid' DOPE increased the capacity of the liposome to fuse with the cell membrane.

Table 1.1. Characteristics of viral-mediated gene delivery systems.

Viral vector	Infectivity	Genome	Capacity	Site of integration	Expression	Advantages	Disadvantages	Applications[A]
Retrovirus	MMLV infects wide variety of tissues with cell entry via Ram-1 receptor (Porter *et al.*, 1996; Weiss and Tailor, 1995; Miller *et al.*, 1994; Vanzeijl *et al.*, 1994) HIV infects $CD4^+$ T-cells (Costello *et al.*, 2000; Suzuki and Shimada, 2000)	RNA, transcribed into double-stranded DNA ~ 7 - 10 kb	6 - 7 kb	Genomic (Miyake *et al.*, 1998; Naldini *et al.*, 1996a; Roe *et al.*, 1993)	Stable (Bordignon *et al.*, 1995)	Stable expression Efficient transfer	Infects dividing cells (Roe *et al.*, 1993) but HIV-based vectors can infect non-dividing cells Random integration Insertional mutagenesis Risk of replication	Haematological neoplasias, CNS tumours and various solid tumours in conjunction with chemotherapy Chronic granulomatous disease
Adenovirus	Wide variety of tissues Cell entry via CAR, integrins and heparan sulphate (Bergelson *et al.*, 1997; Wickham *et al.*, 1994; Wickham *et al.*, 1993)	Linear double-stranded DNA ~ 36 kb	~ 35 kb (Fisher *et al.*, 1996; Kochanek *et al.*, 1996; Bett *et al.*, 1994)	Episomal (Zeng *et al.*, 1997)	Transient	Can infect non-dividing cells Efficient transfer	Immunogenicity (Jooss *et al.*, 1998; Mack *et al.*, 1997; Yang and Wilson, 1995) Risk of replication-competency at high viral titres	Cystic fibrosis Urea cycle disorders such as ornithine transcarbamylase deficiency Various solid tumours
Adeno-associated virus	Brain (Kaplitt *et al.*, 1994), liver (Koeberl *et al.*, 1997), lung (Flotte *et al.*, 1993), muscle (Fisher *et al.*, 1997; Xiao *et al.*, 1996b), vascular endothelial and haematopoietic cells (FisherAdams *et al.*, 1996), via HSP, FGF1 and integrin receptors (Summerford *et al.*, 1999; Summerford and Samulski, 1998)	Single-stranded DNA ~ 4.7 kb	~ 4.5 kb (Rolling and Samulski, 1995)	Episomal or site-specific into chromosome 19Q13.3 (Young *et al.*, 2000; Pieroni *et al.*, 1998; Surosky *et al.*, 1997; Samulski, 1993)	Transient or stable	Site-specific genomic integration (Pieroni *et al.*, 1998) Can infect non-dividing cells (Russell *et al.*, 1994) Efficient transfer Low immunogenicity	Small insert DNA capacity Risk of replication Rearrangement of DNA insert during integration (Pieroni *et al.*, 1998) Loss of site-specific integration in absence of *rep* (Kearns *et al.*, 1996)	Cystic fibrosis
Herpes Simplex virus	Latent infectivity of neural cells (Lachmann *et al.*, 1999; Wagner and Bloom, 1997) Broad infectivity - cell surface heparan sulphates (Yeung *et al.*, 1999; Gruenheid *et al.*, 1993)	Linear double-stranded DNA ~ 152 kb	10 - 100 kb (Krisky *et al.*, 1998b; Marconi *et al.*, 1996)	Stable episomal	Transient, but up to 18 months in CNS (Lachmann and Efstathiou, 1999)	Tropism for neural tissue Large DNA insert capacity Efficient transfer Unlikely reactivation of latency promoter (Wang *et al.*, 1997)	Pathogenicity Cytotoxicity (Greco *et al.*, 2000; Miyatake *et al.*, 1999; Toda *et al.*, 1999; Todryk *et al.*, 1999) Latency in neural tissues	Brain tumours

[A] See websites http://clinicaltrials.gov/ct/gui and http://www.wiley.co.uk/genetherapy/clinical/ for current clinical trials.

Unlike earlier some formulations (Wang and Huang, 1984; Schaeferridder *et al.*, 1982), the DOTMA/DOPE formulation entrapped DNA completely and enhanced gene transfer by 5 - 100-fold in a range of cultured cells (Felgner *et al.*, 1987).

Liposome structure may be unilamellar (Gershon *et al.*, 1993) or multilamellar. Multilamellar liposomes consist of alternate layers of lipid membrane and DNA (Battersby *et al.*, 1998; Radler *et al.*, 1997), an example of which is shown in Figure 1.2. Formation of the final structure is believed to occur in two steps; initially a rapid exothermic electrostatic interaction between DNA and the liposome surface, followed by a slower endothermic reaction resulting in coalescence of the DNA and lipid components (Pector *et al.*, 2000). Variations of polar head groups, counterions and the nature of the acyl chains determine the properties of each liposome formulation and influence their potential as gene transfer agents (for review see Katsel and Greenstein, 2000). The lipid to DNA ratio, the size and shape of the liposome/DNA complex and the type of cells transfected play an important role in transfection efficiency (Wangerek *et al.*, 2001; Liu *et al.*, 1997).

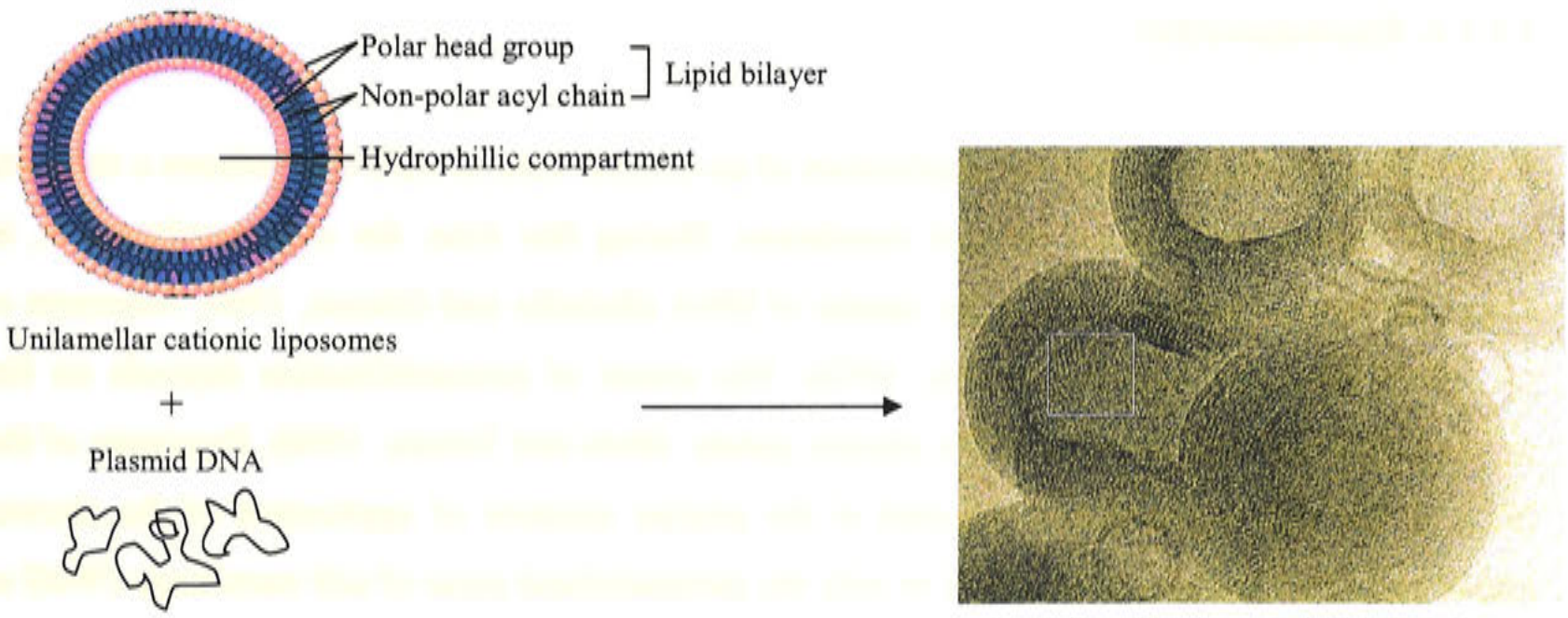

Figure 1.2. Formation of cationic lipid/DNA complexes. Model proposed by Battersby *et al.* (1998), whereby unilamellar cationic liposomes and DNA spontaneously form cationic lipid/DNA complexes comprising of spherical multilamellar liposomes. The image shown is from Battersby *et al.* (1998), obtained by cryo-electron microscopy of cationic lipid/DNA complexes embedded in vitreous ice. The DNA is believed to be aligned between the lipid bilayers in parallel helices with orthorhombic or tetragonal packing, seen as a fingerprint-like pattern within the complexes (boxed).

Cellular uptake of liposomes occurs primarily through endocytosis (Matsui *et al.*, 1997; Zabner *et al.*, 1995). After internalisation, liposomes have been shown to exhibit perinuclear localisation within large endosomal aggregates (Zabner *et al.*, 1995). Endosomal sequestration is one of the major disadvantages of using liposomes for gene delivery. It is crucial that the

DNA escapes sequestration in order to be able to enter the nucleus so that the transgene can be expressed. Other disadvantages associated with the use of liposomes *in vivo* include rapid clearance of liposomes from the bloodstream and uptake by the reticulo-endothelial system (within minutes of intravenous injection, liposomes are detected in the liver, spleen or lungs) (for review see Pouton and Seymour, 2001). This problem has been largely overcome by the addition of polyethylene glycol to the liposome surface, which inhibits binding of serum proteins. In so doing, this decreases clearance of the liposomes by macrophages, increasing their plasma circulation time (Allen *et al.*, 1991; Klibanov *et al.*, 1990; Allen *et al.*, 1989).

Liposomes may be produced on a large-scale, are available commercially, lack the immunogenicity and pathgogenicity of viruses and impose only a modest restriction on the size of DNA accommodated (Compton *et al.*, 2000). In addition, liposomes are easily modified to incorporate moieties that enhance transfection efficiency, facilitating cell-specific targeting or endosomal escape (Sections 1.3.1 and 1.3.2). Despite these advantages, around only 15 % of all gene therapy protocols in clinical trials involve the use of liposomes (http://clinicaltrials.gov/ct/gui and http://www.wiley.co.uk/genetherapy/clinical/).

1.2.2.2. Electroporation

Electro-gene therapy involves the application of an electric field to cells that induces a transient structural re-organisation of the cell membrane. During this time, the cell membrane is, in effect, permeabilised to facilitate the uptake of DNA (Robello and Gliozzi, 1989; Neumann *et al.*, 1982; Neumann and Rosenheck, 1972). The extent of permeabilisation depends on the number, intensity and duration of the electric pulses (Rols and Teissie, 1990). Proximity of the DNA at the cell membrane is required at the precise moment of application of the electric pulses and DNA transfer is localised to only the permeabilised areas of cell membrane (Wolf *et al.*, 1994).

In vitro electro-gene transfer has been applied to various cell types, in suspension or monolayer culture, and large volumes of cells may be electroporated at a time (Rols *et al.*, 1992). Transfection efficiencies when using electroporation have been reported to be comparable and, in some cases, even superior to transfection using liposomes (Wells *et al.*, 2000; Yanez and Porter, 1999; Spiller *et al.*, 1998).

Electroporation techniques have been described for applications *in vivo*, in which electrodes have been applied *in situ* to target tissue into which plasmid DNA had been injected (for review see Muramatsu *et al.*, 1998). Although the injection of the therapeutic plasmid and application of electrodes favours selective uptake in only the target tissue, a potential problem is that the

electric field may extend to non-target cells within the tissue. These cells could be rendered permeable to the plasmid simply by proximity ('bystander effect'), leading to possible undesirable side-effects if the therapeutic gene product is toxic. This concern may be addressed by optimising parameters influencing the efficiency of plasmid uptake, such as the electric field itself and the concentration of DNA (high concentrations may lead to cell lysis; Wolf *et al.*, 1994).

Using *in situ* electroporation, transgenes have been expressed at various sites in rats, including the liver (Heller *et al.*, 2000; Suzuki *et al.*, 1998) and brain (Nishi *et al.*, 1996), and in mice, including in breast (Wells *et al.*, 2000) and colon adenocarcinoma cells maintained subcutaneously (Goto *et al.*, 2000). *In situ* electro-gene therapy has also proven successful in skeletal muscle, which is reputedly difficult to transfect using cationic liposomes (Mathiesen, 1999); expression of fibroblast growth factor could be maintained for up to nine months in mouse, rat, rabbit and monkey (Mir *et al.*, 1999) and expression of erythropoietin in mice for at least six months (Rizzuto *et al.*, 1999). This demonstrates the potential of skeletal muscle to be utilised for the production of proteins with therapeutic value, in addition to the potential of electro-gene therapy in the treatment of muscle disorders.

1.2.2.3. Receptor-mediated gene delivery

Receptor-mediated gene delivery facilitates the uptake of transgenes in a cell-specific manner. By conjugating the DNA to ligands for cellular receptors, receptor-specific binding may be achieved which, in turn, initiates the process of cellular internalisation by endocytosis (for review see Varga *et al.*, 2000). The ligand may be covalently attached by conventional cross-linking procedures to a DNA-binding moiety, such as poly-L-lysine (pLy) (Chan and Jans, 2001; Chan *et al.*, 2000; Chan and Jans, 1999; Synnes *et al.*, 1999) or a DNA-binding protein (Uherek *et al.*, 1998; Paul *et al.*, 1997; Fominaya and Wels, 1996). Bi-functional fusion proteins capable of binding to both a specific receptor and DNA have also been described (Chan and Jans, 2001; Chan and Jans, 1999).

The stability of the DNA/ligand complex, the distribution and number of receptors on the cell surface, receptor-DNA/ligand complex binding affinity and the efficiency of endocytosis all influence the efficacy of receptor-mediated gene delivery. In order to promote cellular uptake, naked DNA may be condensed into a more compact form, for which purpose pLy not only functions as the DNA-binding moiety but is also the most commonly used DNA-condensing agent (for review see Garnett, 1999).

The liver has been a frequently targeted organ in receptor-mediated gene delivery applications (Smith and Wu, 1999), primarily via the asialoglycoprotein (Edwards *et al.*, 1996; Perales *et al.*, 1994) and galactose (Han and Il Yeom, 2000) receptors expressed on hepatocytes. The first reported study using receptor-mediated gene delivery involved the galactose receptor and its ligand, asialioorosomucoid, which was linked via pLy to a reporter plasmid (Wu and Wu, 1988; Wu and Wu, 1987). Reporter gene expression was detected in cultured hepatocytes expressing the receptor, but not in cells lacking it. Since then, this approach has been applied to a number of other receptors, including mannose receptors on alveolar macrophages (Liang *et al.*, 1996), lactose receptors on respiratory epithelial cells (Kollen *et al.*, 1999), the epidermal growth factor (EGF) receptor on squamous carcinoma cells (Chen *et al.*, 1998; Chen *et al.*, 1994b) and tyrosine kinase receptors on neuroblastoma cells (Yano *et al.*, 2000).

A limitation of receptor-mediated gene delivery is that cellular uptake is by endocytosis and, thus, invariably leads to endosomal sequestration. A consequence of this may be degradation of the transfection construct within lysosomes. Endosomolytic agents are therefore often used in conjunction with this mode of delivery and are discussed in Section 1.3.2.

1.2.2.4. Ballistic particle-mediated gene delivery

Ballistic particle-mediated gene transfer was originally developed to deliver genes into plant cells (Klein *et al.*, 1992). DNA is precipitated onto gold or tungsten particles and accelerated into cells by a helium propellant using a 'gene gun' (Williams *et al.*, 1991). The gold particles (1 - 5 μm diameter) are small enough to traverse the cell membrane without measurable damage and have a carrying capacity of 0.5 - 5 μg of DNA per milligram of gold.

Using the gene gun, neither the target cell type nor the size of the transfecting DNA is restricted, there is no risk of immunogenicity or toxicity and plasmids may be re-introduced into cells as often as required. Another distinct advantage of this method is the ability to deliver multiple genes encoded by several different plasmids simultaneously. A disadvantage, however, is that the particles penetrate only through the epidermis, and a few layers intradermally (Tanigawa *et al.*, 2000), which possibly limits use to the treatment of cutaneous disorders (for review see Lin *et al.*, 2000). Recently though, *in situ* introduction of DNA into the heart (Nishizaki *et al.*, 2000) liver (Kuriyama *et al.*, 2000) and cornea (Blair-Parks *et al.*, 2002; Tanelian *et al.*, 1997) has been reported.

The gene gun has been used extensively in the development of DNA vaccines (for review see Robinson, 1999), particularly against cancer (Irvine *et al.*, 1996; Yang and Sun, 1995). In this application, expression of an antigen-encoding gene introduced into the skin was reportedly

maintained for up to one month, during which time predominantly $CD8^+$ T-cells were shown to be recruited in the immune response (Irvine *et al.*, 1996; Yang and Sun, 1995). Other cancer vaccine applications have described the introduction of recombinant cytokines, such as granulocyte-monocyte colony stimulating factor (GMCSF) (Tanigawa *et al.*, 2000; Turner *et al.*, 1998; Mahvi *et al.*, 1996), interleukin-12 (Sakai *et al.*, 2000; Rakhmilevich *et al.*, 1999) or interferon-α (Tuting *et al.*, 1997), near to the tumour in order to enhance the immune response locally.

Although non-viral-mediated gene delivery methods have not been subject to the problems associated with viral-mediated gene delivery, such as random genomic insertion of the transgene, immune reactivity and cytotoxicity, the efficiency of transgene delivery using viral vectors is superior in comparison. Viral vectors are, however, restricted in terms of the size of the DNA that may be accommodated. In combination in a hybrid system, the advantageous properties of viral-and non-viral mediated gene delivery may overcome the limitations of both of these gene delivery systems (Kaneda, 2000).

1.3. BARRIERS TO GENE DELIVERY

Whether viral or non-viral gene delivery systems are used, the therapeutic plasmid faces a challenging route to the nucleus that necessitates traversing a series of membrane barriers and running the gauntlet of cytosolic nucleases (Pollard *et al.*, 2001; Lechardeur *et al.*, 1999) before the NE is reached, which plays a crucial role also in limiting transfection efficiency (Zabner *et al.*, 1995) (Figure 1.1). This is attested to by the low transfection efficiency of non-viral gene delivery systems, using which, an estimated 0.01 - 10 % of the original transfected DNA has been shown to reach the nucleus (Chu *et al.*, 1990; Capecchi, 1980).

Viruses have evolved intrinsic mechanisms that enable them to bind selected host cells, cross the cell membrane, escape endosomal sequestration and enter the nucleus (Figure 1.3). Efforts to enhance viral gene delivery have therefore focused on targeting cells other than those corresponding to the innate tropism of the virus (Anderson *et al.*, 2000; Chandler *et al.*, 2000; Curiel, 1999; Doukas *et al.*, 1999; Douglas *et al.*, 1996). In contrast, the rational design of non-viral vectors requires a comprehensive understanding of each of the membrane barriers and the nuclear transport processes. In this section the membrane barriers and the approaches adopted to optimise non-viral gene delivery are examined in more detail.

Table 1.2. Characteristics of non-viral-mediated gene delivery systems.

	Liposomes	Receptor-mediated	Electroporation	Ballistic
Capacity	No limitation	No limitation	No limitation	No limitation
Primary site of vector	Episomal	Episomal	Episomal	Episomal
Expression	Transient	Transient	Transient Up to 9 months in muscle (Mir *et al.*, 1999; Rizzuto *et al.*, 1999)	Transient Up to 2 months expression in muscle (Zelenin *et al.*, 1997)
Advantages	Controlled encapsulation capacity (Liu *et al.*, 1997) Easily modified with targeting ligands (Cao and Suresh, 2000; Maruyama, 2000; Ward, 2000; Singh, 1999; Hart *et al.*, 1998) Variable lipid composition (Saravolac *et al.*, 2000; Zou *et al.*, 2000)	Targets specific cells	Target specific tissue by *in situ* application of electrodes (Goto *et al.*, 2000; Heller *et al.*, 2000; Wells *et al.*, 2000; Yoshizato *et al.*, 2000; Muramatsu *et al.*, 1998; Suzuki *et al.*, 1998; Nishi *et al.*, 1996) Introduction of multiple genes	Target specific tissue by *in situ* application of the gene gun (Kuriyama *et al.*, 2000; Nishizaki *et al.*, 2000; Tanelian *et al.*, 1997) Possible introduction of multiple genes encoded by several different plasmids
Disadvantages	Rapid plasma clearance (Allen *et al.*, 1989; Poste *et al.*, 1982) Systemic toxicity at high concentrations Perinuclear aggregation (Zabner *et al.*, 1995)	Requires endosomal escape agent	Transfection of adjacent cells; 'bystander effect'	Primarily suitable for cutaneous delivery (Lin *et al.*, 2000) Expensive
Applications[A]			*In vitro* and animal trials only *In situ* application of electodes for subcutaneous, liver and muscle gene delivery	DNA vaccines (Tanigawa *et al.*, 2000; Rakhmilevich *et al.*, 1999; Robinson, 1999; Turner *et al.*, 1998; Rakhmilevich *et al.*, 1997; Tuting *et al.*, 1997; Irvine *et al.*, 1996; Mahvi *et al.*, 1996; Yang and Sun, 1995) Cutaneous disorders

[A] See websites http://clinicaltrials.gov/ct/gui and http://www.wiley.co.uk/genetherapy/clinical/ for current clinical trials.

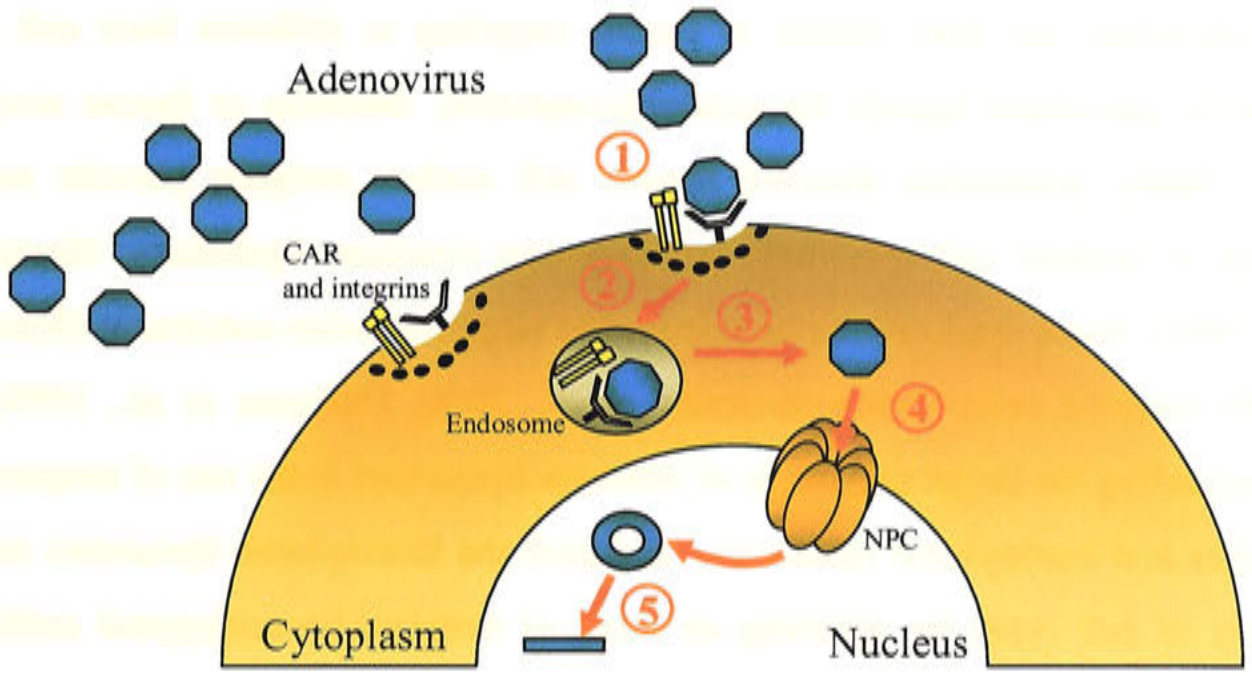

Figure 1.3. Cellular uptake and nuclear translocation of an adenoviral vector. A schematic diagram of the pathway of internalisation and nuclear translocation of an adenoviral vector is shown, illustrating the intrinsic properties of viruses utilised in viral-based gene delivery systems. Adenoviral capsid proteins attach to the Coxsackie and Adenovirus receptor (CAR), integrins and heparan sulphate proteoglycans on the cell surface (Bergelson *et al.*, 1997; Wickham *et al.*, 1994; Wickham *et al.*, 1993) ①. Internalisation occurs by receptor-mediated endocytosis into an endosome ②. The acidic environment of the endosome induces a conformational change in the capsid proteins, which disrupts the endosome and the adenoviral capsid is released into the cytoplasm (Seth *et al.*, 1984) ③. Docking of the adenovirus capsid occurs at the NPC, where histone H1 binds the adenoviral capsid and initiates disassembly. Nuclear transport proteins bind to H1 and translocate the partially disassembled capsid and viral DNA into the nucleus (Trotman *et al.*, 2001) ④. Within the nucleus, the viral capsid is lost and the viral vector is free to be transcribed ⑤.

1.3.1. Crossing the cell membrane

The outer cell membrane consists of a lipid bilayer punctuated by pores, channels, transporters and receptors, each of which displays unique properties in controlling what enters and leaves the cell. Cellular uptake occurs through a number of mechanisms, including pinocytosis, phagocytosis, fusion with the cell membrane or receptor-mediated endocytosis, dictated largely by the nature of the molecules presenting at the cell surface.

Particular membrane receptors expressed exclusively on certain cell types provide the basis for viral tropism but, also, facilitate a conduit for cell-specific non-viral gene delivery. An understanding of the differential expression profiles of cell-surface proteins is important in order to ensure that the gene delivery vector targets only the desired cells. This becomes extremely important when toxic gene products are produced, such as in an anti-cancer therapy.

By incorporating receptor-specific ligands into the liposomal membrane, cells expressing EGF (Chen *et al.*, 1998; Uherek *et al.*, 1998; Foster and Kern, 1997), integrin (Compton *et al.*, 2000; Hart *et al.*, 1998), folate (Reddy and Low, 2000; Reddy *et al.*, 1999; Lee and Huang, 1996) and

transferrin (Simoes *et al.*, 1999; Simoes *et al.*, 1998) have been targeted successfully. Glycosylation of liposomes has been shown to enable targeting to different liver cell types through the respective glycolipid-ligands for asialoglycoprotein, mannose or fucose receptors (Kawakami *et al.*, 2000). Antibodies directed against cell surface antigens provide another avenue along which to mediate cell-specificity of liposomes (immuno-liposomes; Martin and Papahadjopoulos, 1982). Some applications have included targeting colon carcinoma (Kamps *et al.*, 2000) and HIV-infected cells (Bestman-Smith *et al.*, 2000; Dufresne *et al.*, 1999). An effective way of expanding the target cell range of immuno-liposomes is the use of streptavidin-conjugated antibodies and biotinylated liposomes, in which the biotinylated liposomes may be targeted to a variety of cell types by selecting an array of streptavidin-conjugated antibodies (Cao and Suresh, 2000).

The repertoire of cell-surface receptors and antigens is vast, making the scope for designing cell-specific gene delivery systems considerable. The major caveat of gene delivery approaches that occur via cell-surface receptors, however, remains that following internalisation the vectors become entrapped within endosomes.

1.3.2. Sequestration within endosomes

Ligands that bind to external cellular receptors initiate receptor-mediated endocytosis, whereby the ligand-receptor complexes are internalised within endosomes (Figure 1.4). Apart from receptor-mediated gene delivery, transfection using liposomes also proceeds via endocytosis (Zabner *et al.*, 1995; Zhou and Huang, 1994; Legendre and Szoka, 1992). Sequestration imposes a significant limitation on gene delivery methods that target the endosomal pathway (Zabner *et al.*, 1995). Since endosomes mature through various stages of acidification and eventually fuse with lysosomes which contain degradative enzymes, prior escape of the transfecting DNA is critical. Moreover, notwithstanding degradation, entrapment of the therapeutic constructs also decreases the quantity available for nuclear uptake.

Viruses which enter their host cells by receptor-mediated uptake have specialised 'endosomal escape mechanisms' (see Figure 1.3). For example, adenovirus takes advantage of the decreased pH within the endosomes that causes the hydrophobic domains of the adenoviral capsid proteins become exposed. This facilitates interaction with the endosomal membrane in such a way as to bring about endosomal disruption (Seth *et al.*, 1984). In order to extend this function to non-viral gene delivery systems, adenoviral particles have been incorporated into non-viral vectors by co-infection (Curiel *et al.*, 1991), covalent linking (Ogier *et al.*, 1994), non-covalent interactions (Fasbender *et al.*, 1997), bi-functional antibodies and streptavidin-biotin bridges between adenoviral particles and the DNA complexes (Gao *et al.*, 1993).

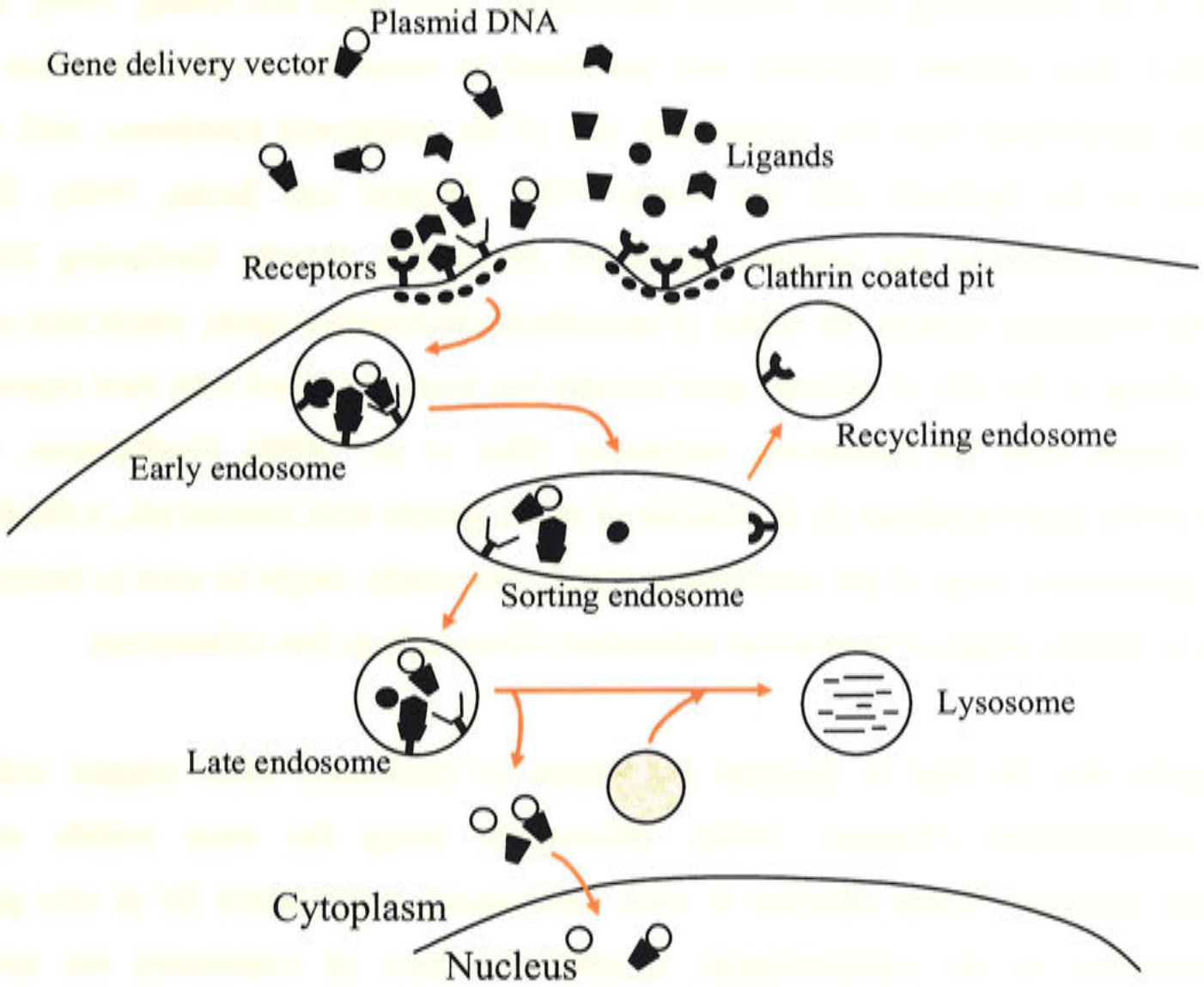

Figure 1.4. General endocytosis pathway for gene delivery mediated by receptors on the cell surface. Endocytosis is initiated by ligands binding to their associated receptors on the cell surface. Internalisation occurs through clathrin-coated pits, in the process forming early endosomes. Within these, receptors are sorted and are either returned to the cell surface via recycling endosomes or late endosomes are formed. Late endosomes may fuse with vesicles containing lysosomal degradative enzymes, forming lysosomes. Throughout this process, endosomes undergo progressive acidification from pH ~ 7 at the cell surface to pH ~ 4 within lysosomes. It is imperative that the gene delivery vectors escape endosomal sequestration to avoid degradation within lysosomes. Adapted from Varga *et al.* (2000).

The amino terminal peptide of influenza virus (haemagglutinin HA-2) has been coupled to pLy-condensed DNA and was shown to enhance transgene expression by greater than 5000-fold upon lipofection into cultured liver cells (Plank *et al.*, 1994). The authors proposed that the acidic interior of the endosome (pH ~ 5) induced a conformational change to an α-helix within the HA-2 peptide, that enabled it to insert into the endosomal membrane, thereby facilitating fusion between the liposomal and endosomal membranes and, hence, enabling extrusion of the liposome contents into the cytoplasm. Synthetic peptides have been derived from this archetype, some of which form pores in the endosomal membrane (Chung and Thompson, 1996), while others, such as GALA (Plank *et al.*, 1994; Parente *et al.*, 1990; Subbarao *et al.*, 1987) and KALA (Wyman *et al.*, 1997) have fusogenic activity.

Fusion of the liposomal and endosomal membranes appears to be essential in order to bring about release of the transfecting DNA (Wrobel and Collins, 1995; Zhou and Huang, 1994). The release of DNA from cationic liposomes was postulated to occur due to the interaction of anionic lipids, destabilised from the cytoplasmic side of the endosomal membrane, with the cationic lipids of the liposome (Xu and Szoka, 1996; Zelphati and Szoka, 1996). This interaction would neutralise the cationic lipid/DNA interaction, thereby facilitating DNA release into the cytoplasm. Indeed, the ability of specialised pH-sensitive lipids, which take on a net positive charge at low pH, to mediate gene transfer has been correlated with their capacity to facilitate fusion with the endosomal membrane (Mui *et al.*, 2000). Furthermore, the modification of the lipid membrane by attachment of amine groups with selected pK_a's (Budker *et al.*, 1996) generated a range of pH sensitivities which, potentially, might be used to facilitate DNA release at various stages of endosomal maturation (from early to late endosomes).

Chemical agents may be used to facilitate the release of transfected DNA trapped within endosomal compartments (Wagner, 1998); chloroquine being the most widely used lysosomotropic chemical. While effective *in vitro*, chloroquine is unsuitable for *in vivo* gene therapy applications as the concentrations required for lysis of endosomes are toxic. Polyethylenimine (PEI) has a similar endosomalytic mechanism of action to chloroquine and has become a widely used non-viral DNA delivery agent (Abdallah *et al.*, 1996; Behr, 1994 and for review see Remy *et al.*, 1998). The mechanism of action of these lysosomotropics has been demonstrated recently (Sonawane *et al.*, 2003). As these agents are polybasic, they accumulate in acidic compartments (such as endosomes) inside the cell, where they become protonated. This removes free H^+ from the endosomal interior, prompting these agents to be termed 'proton sponges'. An influx of counterions (Cl^-) occurs due to the depletion of H^+ (to restore a net neutral charge) and concomitant osmotic swelling causes the endosome to burst (Sonawane *et al.*, 2003). In addition, the shift towards basic pH would inhibit lysosomal enzymes and thus reduce the degradation of DNA complexes (Seglen, 1983).

1.3.3. Transport into the nucleus

Transfected DNA must reach the nucleus in order for transcription to occur so that the desired gene product is ultimately expressed. As viruses have intrinsic mechanisms that enable them to access the nucleus (for review see Whittaker *et al.*, 2000), these may be extended to the viral-based gene delivery systems. In contrast, non-viral gene delivery systems require additional extrinsic modifications to enhance the nuclear delivery step.

1.3.3.1. The nuclear membrane

The nucleus is bound by a double membrane called the NE. It partitions the cell into two specialised compartments by separating nuclear material and activity from that in the cytoplasm. In so doing, this necessitates a mechanism which allows regulated communication between the two compartments. This portal is provided by nuclear pore complexes (NPCs), distributed within the NE (Figure 1.5). All nuclear transport takes place through the NPC (Rout *et al.*, 2003). The number of NPCs in a single cell varies according to cell type and metabolic activity. A yeast cell contains around 200 NPCs (Rout and Blobel, 1993), a proliferating human cell several thousand and a mature *Xenopus laevis* oocyte around 5×10^7 (Cordes *et al.*, 1995).

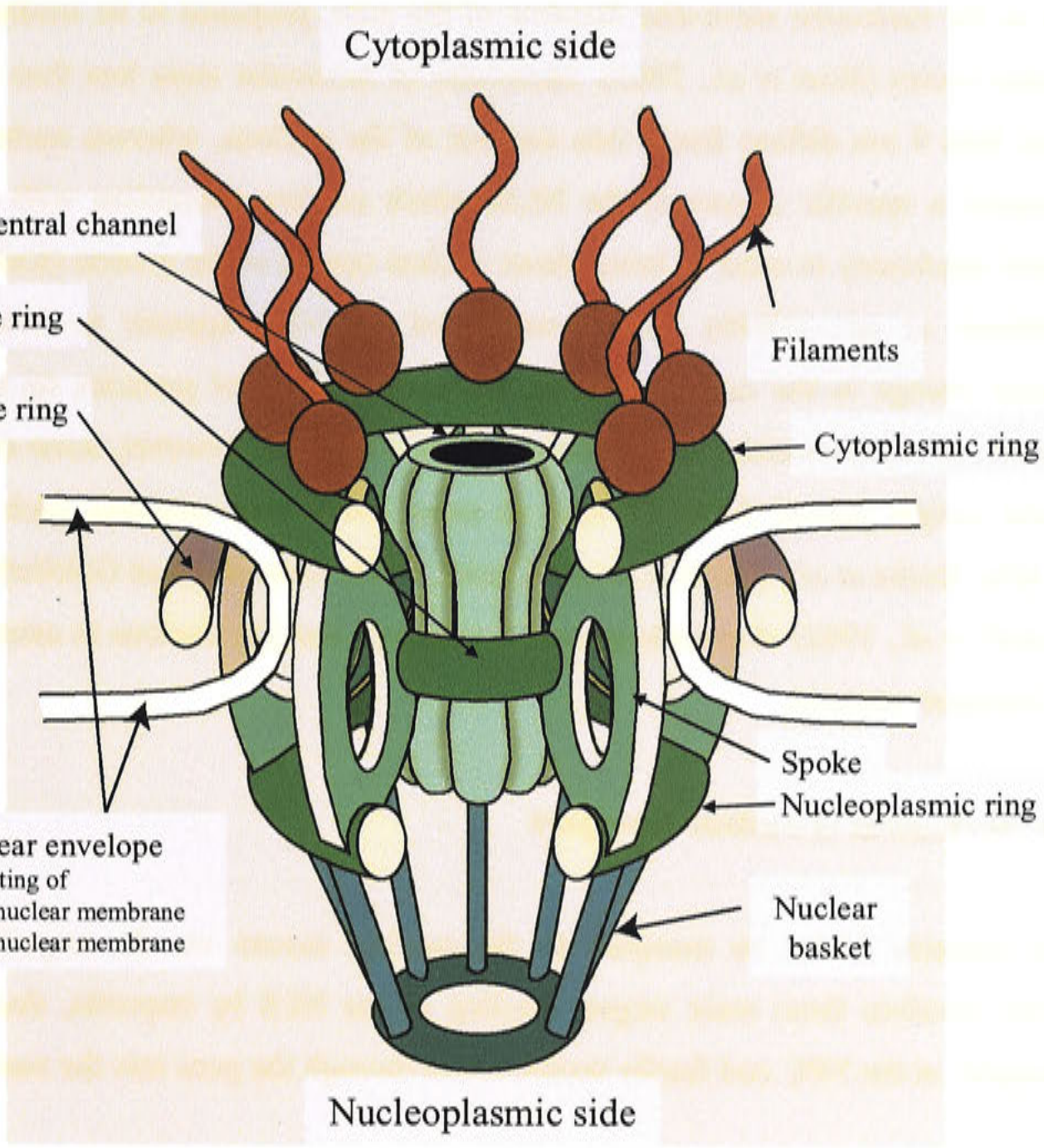

Figure 1.5. Model of the nuclear pore complex. The NPC consists of a central channel, comprising around 30 different proteins (nucleoporins) which associate to form a basic repeated subunit, and attached filaments, which extend outwards on the cytoplasmic side and join to form a basket-like structure on the nucleoplasmic side (from Blobel and Wozniak, 2000).

The NPC is an intricate, cylindrical, multi-subunit arrangement, with attached fibrils or filaments on the cytoplasmic side and a basket-like structure on the nucleoplasmic side (Blobel

and Wozniak, 2000) (Figure 1.5). This overall structure is highly species-conserved, implying a fundamental role in nuclear transport processes. A group of around 30 different proteins, termed nucleoporins, make up 5 - 10 % of the NPC mass and provide around 150 docking sites at hydrophobic repeat sequences (Phe-Gly) for nuclear transport complexes during their transit into the nucleus (Rout and Aitchison, 2001; Blobel and Wozniak, 2000). The NPC may be blocked by interaction between a lectin, wheat germ agglutinin (WGA), and N-acetylglucosamine groups on its cytoplasmic side (Finlay *et al.*, 1987). WGA has been used extensively in nuclear transport experiments to determine whether transport may be inhibited, thereby demonstrating involvement of the NPC.

The diameter of the central channel of the NPC is around 9 nm. It is the central channel which plays a role in the molecular sieve-like function of the pore, proposed to be mediated through entropy related events (Rout *et al.*, 2003). Molecules of molecular mass less than 45 kDa and diameter less than 9 nm diffuse freely into and out of the nucleus, whereas molecules larger than this require a specific sequence, the NLS, which confers interaction with the cellular nuclear import machinery in order to bring about nuclear uptake of the protein (Kalderon *et al.*, 1984a; Kalderon *et al.*, 1984b). The presence of an NLS appears to bring about a conformational change in the central channel, allowing passage of particles up to 26 nm in diameter (Akey, 1990; Dworetzky and Feldherr, 1988). There are, however, some exceptions to this molecular weight cut-off (MWCO) rule, as some lower mass proteins, such as histones (around 14 kDa; Baake *et al.*, 2001b; Lin and Clarke, 1996; Breeuwer and Goldfarb, 1990) and tRNAs (Zasloff *et al.*, 1982) also undergo active transport into the nucleus in association with the nuclear transport proteins.

1.3.3.2. The mechanism of nuclear transport

If a protein contains NLSs, its transport to the nucleus occurs via the importin-mediated pathway. This involves three main stages: binding of the NLS by importin, docking of the transport complex at the NPC and finally translocation through the pore into the nucleus.

In the 'conventional pathway' of importin-mediated nuclear transport (Figure 1.6), a heterodimeric complex consisting of importin α (karyopherin; Kap60p in yeast) and importin β1 (Kap95p in yeast) forms the 'NLS receptor'. Importin α presents two functional domains, namely an importin β-binding domain (Gorlich *et al.*, 1996) and an NLS-binding site (Conti *et al.*, 1998). Binding of importin β to the importin β-binding domain within importin α displaces an auto-inhibitory sequence from the NLS-binding site (Kobe, 1999), allowing importin α to bind the NLS-containing protein specifically (Gorlich *et al.*, 1995; Imamoto *et al.*, 1995b;

Imamoto *et al.*, 1995a; Moroianu *et al.*, 1995a; Moroianu *et al.*, 1995b; Radu *et al.*, 1995). Importin β mediates docking of the importin α/β heterodimer/NLS-protein transport complex to the distal end of the cytoplasmic fibrils of the NPC (see Figure 1.5) through high affinity interactions with hydrophobic amino acids (Moroianu *et al.*, 1995a). The complex is subsequently transferred to the central channel and, through a series of docking events involving different nucleoporins within the NPC, travels 100 - 120 nm to the nucleoplasmic side (Bayliss *et al.*, 2000).

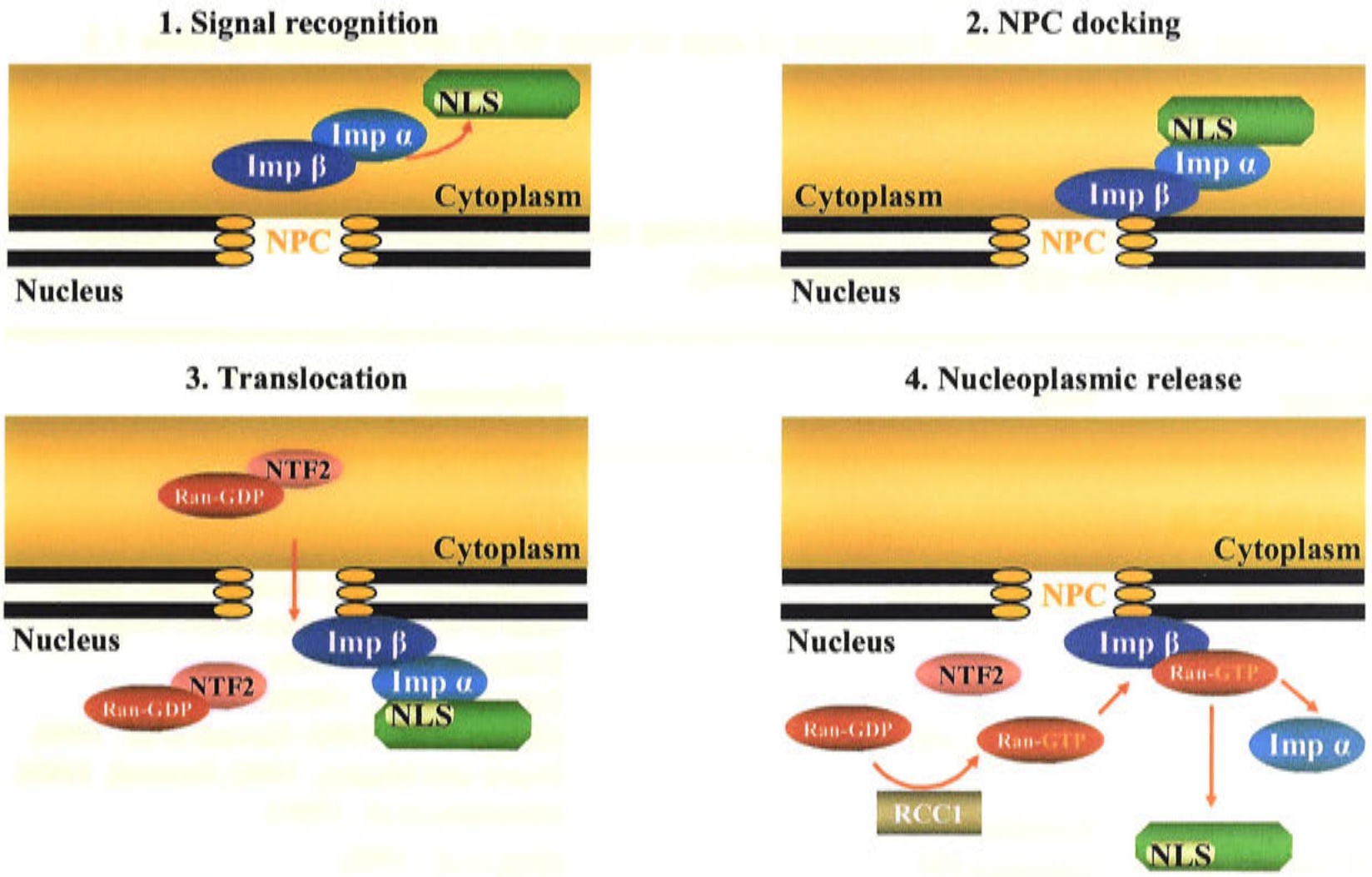

Figure 1.6. NLS-dependent nuclear import of proteins. A schematic representation of the nuclear uptake of an NLS-containing protein is shown. Nuclear translocation of proteins that contain an NLS is mediated through the 'NLS receptor', a heterodimeric complex of importin α, which specifically binds the NLS (**1**) and importin β, which mediates docking at the NPC (**2**). Translocation through the NPC occurs via a series of interactions with nucleoporins within the pore (**3**). The complex is dissociated in the nucleus when Ran-GTP, generated by the nucleotide exchanger RCC1, binds importin β (**4**). The nuclear transport factor NTF2 transports Ran in its GDP-bound form from the cytoplasm into the nucleus in order to replenish the stores of nuclear Ran.

The monomeric guanine nucleotide binding-protein Ran, in its GTP bound form (mediated by the nucleotide exchanger RCC1; Klebe *et al.*, 1995), dissociates the transport complex from the nucleoplasmic side of the NPC by binding to importin β (Gorlich *et al.*, 1995; Moroianu *et al.*, 1995b). The NLS-containing protein and importin α are thus released into the nucleus, while importin β remains at the NPC.

1.3.3.3. Classes of nuclear localisation sequences

NLSs may be characterised into 3 major classes: those resembling the NLS of the Simian Virus 40 large tumour antigen (SV40 T-ag) that are comprised of a short stretch of basic amino acids (PKKKRKV[133], referred to as 'classical' NLSs; Kalderon *et al.*, 1984a; Kalderon *et al.*, 1984b; Lanford and Butel, 1984), those which consist of two stretches of basic amino acids separated by 10 - 12 amino acids (referred to as bipartite NLSs; Robbins *et al.*, 1991) and a third, less well-defined class made up of NLSs resembling those of the yeast homeodomain containing protein Matα2 in which charged or polar residues are interspersed with non-polar residues (Hall *et al.*, 1990; Hall *et al.*, 1984). Examples of each of these NLSs are presented in Table 1.3.

Table 1.3. Selected examples of NLSs conferring nuclear import by the 'conventional pathway' (importin α/β and Ran-dependent).

Protein	NLS[A]	References
T-ag-like NLSs		
SV40 T-ag	PKKKRKV[132]	(Xiao *et al.*, 1998; Hubner *et al.*, 1997; Xiao *et al.*, 1997a; Jans *et al.*, 1991; Kalderon *et al.*, 1984a; Kalderon *et al.*, 1984b)
Dorsal	RRKRQR[340]	(Briggs *et al.*, 1998; Govind *et al.*, 1996; Norris and Manley, 1992; Steward, 1989)
c-rel	KAKRQR[294]	(Mosialos *et al.*, 1991)
NF-κB p65 (RelA)	EEKRKR[286]	(Beg *et al.*, 1992; Shirakawa and Mizel, 1989)
Bipartite NLSs		
SWI5	KK -10 aa spacer- RKRGRPRK[655]	(Jans *et al.*, 1995; Moll *et al.*, 1991)
Rb	KR -11 aa spacer- KKLR[869]	(Efthymiadis *et al.*, 1997)
Nucleoplasmin	KR - 9 a.a. spacer- KKKKL[171]	(Vancurova *et al.*, 1995)
N1/N2	RKKRK - 12 a.a. spacer- KKSK [551]	(Hu and Jans, 1999)
Matα2-like NLSs		
Matα2	MNKIPIKDLLNPQ[13] VRILESWFAKNI[159]	(Hall *et al.*, 1990; Hall *et al.*, 1984)

[A] The single letter amino acid code is used.

All three classes of NLSs are recognised specifically by the importin α/β heterodimer during the first step of nuclear transport (Hu and Jans, 1999; Hubner *et al.*, 1999; Efthymiadis *et al.*, 1997; Smith *et al.*, 1997). Competition for this nuclear import pathway is significant in the context of the whole cell, considering the large number of nuclear import substrates (Jans *et al.*, 2000a). In response, higher eukaryotes express multiple forms of importin α (8 in human; 6 in mouse), all of which are believed to function as a heterodimer with importin β1 yet retain discrete NLS-substrate binding properties and transport efficiencies (Kohler *et al.*, 1999; Prieve *et al.*, 1998; Hubner *et al.*, 1997; Miyamoto *et al.*, 1997; Nadler *et al.*, 1997; Rexach and Blobel, 1995).

The NLS/importin α/β-mediated nuclear import pathway is not the only signal-dependent pathway capable of targeting proteins to the nucleus. Certain 'classical' NLSs may be bound by importin β in the absence of importin α, which is also not required for subsequent transport into the nucleus. HIV-1 Rev protein (Truant and Cullen, 1999; Henderson and Percipalle, 1997), transcription factors such as GAL4, (Chan *et al.*, 1998), AP-1 (Forwood *et al.*, 2001a), CREB (Forwood *et al.*, 2001a), SRY (Forwood *et al.*, 2001b) and TRF1 (Forwood and Jans, 2002), parathyroid hormone related protein (Lam *et al.*, 1999) and histones (Baake *et al.*, 2001a; Muhlhausser *et al.*, 2001; Johnson-Saliba *et al.*, 2000; Jakel *et al.*, 1999) are amongst the importin β-recognised nuclear import 'substrates'.

There are around 24 homologues of importin β in eukaryotes, having specific import (as well as export) roles for particular classes of proteins (Jans *et al.*, 2000a). Importin β2 (Kap104p/transportin) mediates both the nuclear import and export of mRNA-binding proteins by specifically binding to sequences homologous to a 38-amino acid sequence (termed M9) within the human mRNA-binding protein hnRNP A1 (Michael *et al.*, 1997). Importin β3 mediates the nuclear import of the transcription factor Pho4 (Komeili and O'Shea, 1999; Kaffman *et al.*, 1998). Other proteins are trafficked by more than one importin β homologue; the presence of a β-importin-like binding or 'BIB' domain within ribosomal proteins, for example, has been shown to confer binding affinity for any one of importin β1, β2, β3 or Imp7 (Jakel and Gorlich, 1998).

There are additional signal-dependent but importin- and Ran-independent pathways. The HIV-1 Tat protein, for example, is bound neither by importin α nor importin β, but the Tat NLS (GRKKRRQRRRAP[59]) has been shown to target β-galactosidase to the nucleus and appears to have both nuclear entry and retention functions (Truant and Cullen, 1999; Efthymiadis *et al.*, 1998; Siomi *et al.*, 1990). In contrast, the HIV-1 Vpr protein does not have a distinct NLS but displays cytosolic factor-dependent intranuclear binding, independent of importin α/β or Ran

(Jans *et al.*, 2000b). Another example of importin-independent nuclear localisation is β-catenin, which is able to bind directly to nucleoporins within the NPC in order to initiate translocation (Fagotto *et al.*, 1998).

It is apparent that a range of nuclear import pathways exists, enabling translocation of proteins into the nucleus that is mediated through different types of targeting signals. Many NLS-containing proteins are, however, not constitutively nuclear due to mechanisms that modulate NLS function and accessibility (for review see Jans *et al.*, 2000a). A comprehensive understanding of both the pathways that provide access to the nucleus and their associated regulatory mechanisms is paramount if these endogenous processes are to be exploited for purposes such as enhancing gene delivery to the nucleus.

1.4. Optimising DNA translocation into the nucleus

Translocation into the nucleus, as discussed earlier, is governed by the NPCs which present an apparent size exclusion barrier. Linear DNA greater than 2 kb in length was found to enter the nucleus with reduced efficiency compared to a 1 kb fragment (Ludtke *et al.*, 1999). Given that most therapeutic DNA constructs are well in excess of 2 kb, it is clear how transport into the nucleus could be a severely limiting step in non-viral gene delivery systems. In a seminal study, microinjection of DNA into the nucleus of cultured mammalian cells produced levels of transfection greater than 50 %, whereas microinjection into the cytoplasm led to gene expression in less than 0.01 % of the cells (Capecchi, 1980).

1.4.1. The nuclear import of DNA

Initial studies to delineate the nuclear transport mechanism involved microinjection of gold-labelled plasmid DNA into cultured cells (Dowty *et al.*, 1995). Detection using electron microscopy revealed the DNA to be located at the NPC or within the nucleus. As gene expression could be inhibited by the nucleoporin-binding lectin WGA (see Section 1.3.3.1), the NPC was implicated as the route of entry into the intact nucleus (Dowty *et al.*, 1995). Similarly, using a digitonin-permeabilised cell system, in which nuclear import was reconstituted, fluorescently-labelled linear DNA fragments were found to enter the nucleus through the NPC and in a strictly size-dependent manner (Ludtke *et al.*, 1999; Hagstrom *et al.*, 1997).

In the afore-mentioned reconstituted nuclear import system, nuclear import by passive diffusion was found to occur but only for linear DNA fragments of less than 310 bp (Ludtke *et al.*, 1999). For larger DNA fragments of 510 - 1500 bp, nuclear uptake was shown to be energy-dependent, implying an active process. However, the even larger 2 and 3 kb plasmids did not accumulate in

the nucleus within the one hour time frame of the experiment (Ludtke *et al.*, 1999; Hagstrom *et al.*, 1997). Microinjection into the cytoplasm of intact cells yielded similar results; after 4 hours DNA fragments less than 1 kb accumulated in the nuclei, while the larger DNA fragments of 1.5, 2 and 3 kb did not enter the nucleus (Ludtke *et al.*, 1999). In contrast to these studies, Salman *et al.* (2001) found that the nuclear uptake of linear double stranded DNA (bacteriophage λ DNA) occured passively, independently of ATP consumption in a *Xenopus laevis* oocyte model of reconstituted nuclear transport. Collectively, these studies agreed that nuclear import of DNA did not require the addition of cytosolic factors. This, the authors suggested, implied a nuclear import pathway distinct from that mediated by importins (Salman *et al.*, 2001; Ludtke *et al.*, 1999; Hagstrom *et al.*, 1997). Competition experiments in which an excess of NLS-fusion proteins did not inhibit DNA transport also suggested divergence from the importin-mediated uptake pathway (Hagstrom *et al.*, 1997).

While shown to be energy-dependent and occur through the NPC, the nuclear import of plasmid DNA appears to be different from that of linear DNA. The nuclear import of plasmid DNA was found to be sequence dependent (Dean *et al.*, 1999; Dean, 1997) with an absolute requirement for cytoplasmic extract (Wilson *et al.*, 1999). The SV40 promoter/enhancer sequence was shown to elicit uptake of plasmid DNA into the nucleus (Dean, 1997). When the plasmid contained other sequences derived from SV40, the Roux sarcoma virus promoter region or the human cytomegalovirus (CMV) promoter region, nuclear localisation was not observed (Dean *et al.*, 1999). The authors proposed that the SV40 sequence contains binding sites for transcription factors which contain NLSs, by virtue of which the SV40-plasmid may be transported into the nucleus along the importin-mediated nuclear import pathway (Dean *et al.*, 1999; Dean, 1997). In addition to this, only when in combination could importins α and β, Ran and nuclear extract support plasmid uptake, further implicating the 'conventional' nuclear import pathway. As has been observed for the linear fragments of DNA (Ludtke *et al.*, 1999) upon completion of the four hour time course, the larger plasmid DNA (14.4 kb) displayed perinuclear retention, whereas the comparatively smaller plasmid (4.2 kb) had accumulated in the nucleus (Wilson *et al.*, 1999).

Taken together, these results suggest that the nuclear import pathway of linear DNA fragments may be distinct from that of plasmid DNA, with plasmids possibly requiring additional import factors and a more stringent import mechanism to access the nucleus. For both linear and circular plasmid DNA, size-dependency was shown to be critical with larger molecules appearing to be precluded from nuclear uptake.

1.4.2. DNA condensation

While there is no formal consensus on a relationship between DNA condensation and gene transfer efficiency, evidence from a number of experimental systems alludes to a positive correlation (Chan *et al.*, 2000; Chan and Jans, 1999; Ziady *et al.*, 1999; Perales *et al.*, 1997; Vitiello *et al.*, 1996). Condensation of DNA has been reported to facilitate an easier passage across cell membranes, including the NE, with a 1.7-fold enhancement in nuclear uptake attributed to condensation of the plasmid DNA (Chan and Jans, 1999). Additionally, condensed DNA has been shown to be protected from degradation by cytosolic nucleases (Pollard *et al.*, 2001; Baeza *et al.*, 1987).

pLy is the most commonly used DNA-condensing agent (Garnett, 1999). Other molecules with DNA condensing properties that have been studied extensively for gene delivery applications include protamine (Sorgi *et al.*, 1997; Chen *et al.*, 1995), histones (Fritz *et al.*, 1996; Chen *et al.*, 1994a; Wagner *et al.*, 1991), synthetic cationic peptides (YKAKKKKKKKKWK; Gottschalk *et al.*, 1996) and, more recently, cationic detergents (Dauty *et al.*, 2001; Blessing *et al.*, 1998).

As all of these agents are cationic, interaction with DNA occurs on the basis of electrostatic charge. Condensation into a variety of forms has been shown, including rod shapes, toroids, spheroids and 'flowers' (for review see Vijayanathan *et al.*, 2002). Using atomic force and electron microscopy, the step-wise condensation of plasmid DNA upon the addition of increasing amounts of pLy was shown to proceed from an open, irregular structure through intermediate toroid structures (60 nm in diameter) and, finally, into spheroid structures (16 nm in diameter; Chan *et al.*, 2000; Wagner *et al.*, 1991). Similarly condensed structures have been reported using individual histones, H1 and H4 (Lucius *et al.*, 2001; Fritz *et al.*, 1996; Wagner *et al.*, 1991).

In addition to the compaction of the DNA itself, the size and shape of the transfection complexes as a whole have also been found to influence gene transfer efficiency. Complexes containing lipid, protamine (or pLy) and DNA were shown to rearrange into virus-like particles upon mixing, having diameters not greater than 100 nm. Compared to particles containing only lipid and DNA, upon inclusion of the polycation, luciferase reporter gene expression was enhanced by 10 - 30-fold (Gao and Huang, 1996). Similar nanometric particles have been assembled using PEI as the DNA-complexing agent that, additionally, has endosomalytic activity (see Section 1.3.2); this dual functionality makes it highly efficient in gene transfer (for review see Remy *et al.*, 1998).

1.4.3. The use of nuclear localisation sequences

NLSs have been incorporated into transfection constructs in order to enhance import of plasmid DNA into the nucleus. This has been achieved in a variety of ways including direct coupling of the NLS to the DNA and indirect coupling by conjugating the NLS to a DNA-carrier molecule (for reviews see Escriou *et al.*, 2003; Cartier and Reszka, 2002; Bremner *et al.*, 2001).

Linking NLSs directly to DNA has involved a number of resourceful chemical and molecular approaches. Zanta *et al.* describe the covalent attachment of the SV40 T-ag NLS to a linear DNA fragment at a terminal stem-loop secondary structure via a modified oligonucleotide (Zanta *et al.*, 1999). Compared to the control constructs (closed circular plasmid, linearised plasmid and linear plasmid presenting a mutated form of the NLS), gene expression was enhanced 10 - 1000-fold across the range of cell lines tested.

Another approach is the use of sequence-specific hybridisation to couple functional peptides (such as NLSs) to the DNA (Roulon *et al.*, 2002; Branden *et al.*, 1999; Neves *et al.*, 1999a; Neves *et al.*, 1999b; Sebestyen *et al.*, 1998). The basis of this technology is the initial hybridisation through Watson-Crick base pairing between a site within the reporter plasmid and a complementary oligonucleotide to which the NLS has been conjugated. The resulting hybrid rearranges into a hairpin-loop triplex structure which has been shown to be extremely stable (Zelphati *et al.*, 2000; Zelphati *et al.*, 1999). Collectively, these studies reported that transgene expression had occurred upon transfection into cultured cells, however, relative enhancement of gene expression due to the NLS was observed in only one of the studies, with an 8-fold increase in transfection efficiency (Branden *et al.*, 1999).

In order to incorporate NLSs into the transfection constructs through the DNA-binding moiety, Chan *et al.* crosslinked an optimised SV40 T-ag NLS to pLy and demonstrated condensation of DNA, nuclear targeting and a 1.3-fold enhanced reporter gene expression (Chan and Jans, 2001; Chan *et al.*, 2000; Chan and Jans, 1999). Fusion proteins consisting of a DNA-binding domain and NLS peptide have also been generated between, for example, histone H1 and the SV40 T-ag NLS (Fritz *et al.*, 1996; Hagstrom *et al.*, 1996). While the transfection efficiency of the reporter plasmid was enhanced when associated with H1, no further enhancement was achieved in the presence of the NLS (Fritz *et al.*, 1996).

All of the NLSs listed in Table 1.3 are potential candidates for use in DNA transfection constructs to enhance importin-mediated nuclear import. By deleting an inhibitory regulatory element (the cyclin-dependent kinase phosphorylation site; Thr to Ala substitution) within the SV40 T-ag NLS without affecting the enhancing sequences, an optimised NLS was generated,

which was found to enhance nuclear transport efficiency up to 100-fold (Hubner *et al.*, 1997; Xiao *et al.*, 1997a). Furthermore, when coupled to transfection constructs, the optimised SV40 T-ag NLS enhanced plasmid uptake into the nucleus (Chan and Jans, 2001; Chan *et al.*, 2000; Chan and Jans, 1999; Akhlynina *et al.*, 1995; Akhlynina *et al.*, 1993). Modification of NLS peptides so that they are either constitutively active or differentially regulated in response to cellular signals is another possibility for NLS optimisation (Xiao and Jans, 1998; Xiao *et al.*, 1998; Xiao *et al.*, 1996a; Jans and Jans, 1994).

1.4.4. The use of modular DNA-carrier proteins

Several peptides have been demonstrated to have the capacity to mediate the passage of transfected DNA through the cell, endosomal and nuclear membranes. Combinatorial approaches, in which all of these sequences are included in one transfection construct, may have the potential to enhance non-viral DNA delivery greatly (Figure 1.7).

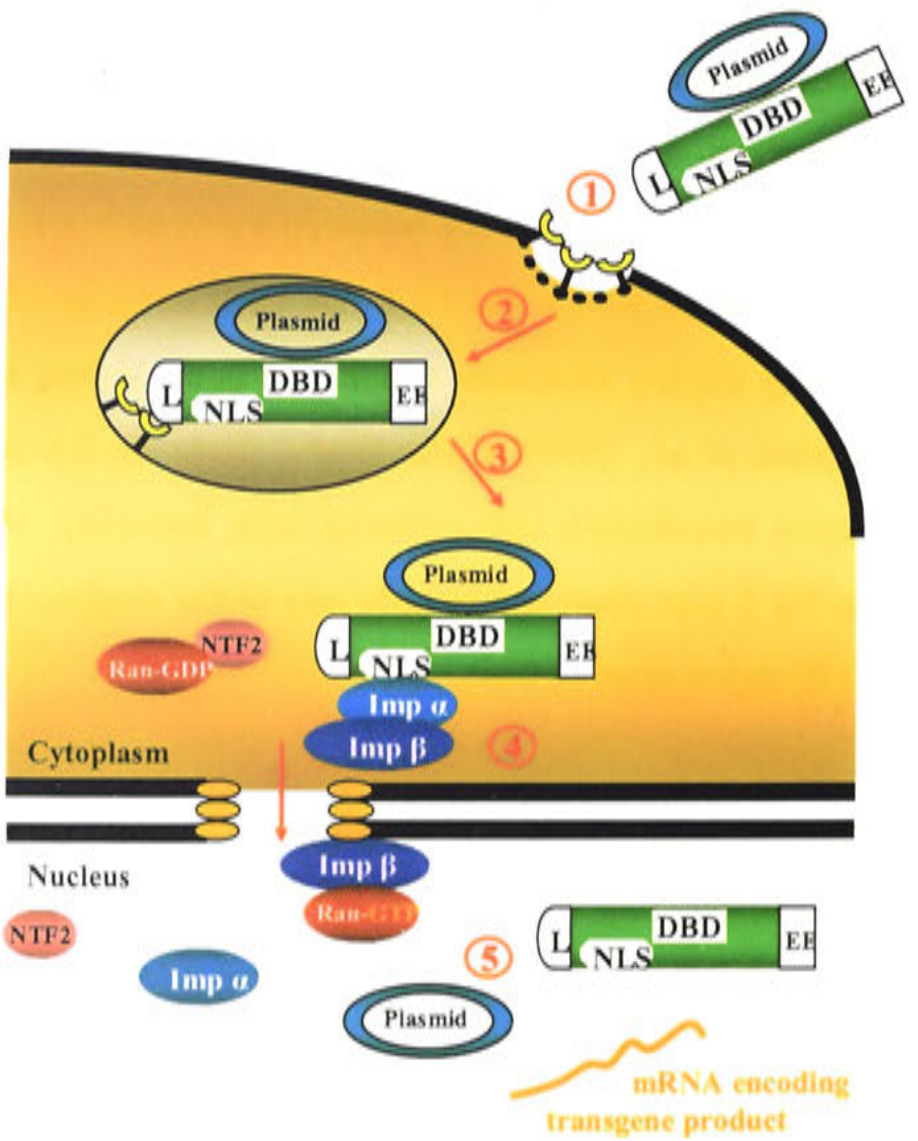

Figure 1.7. Enhancement of nuclear gene delivery using modular targeting sequences. An idealised fusion protein is shown, comprising a receptor-specific ligand (L), NLS, endosome exit sequence (EE) and DNA binding domain (DBD), complexed with plasmid DNA. Cell surface receptor binding is facilitated through the L moiety ①. The complex is internalised into an endosome ② where the EE brings about endosomal disruption and escape into the cytoplasm ③. Here, the NLS confers interaction with importins, which facilitate nuclear translocation ④. Ran-GTP mediates release of the plasmid from the nuclear transport complex ⑤ and the transgene may be transcribed. The overall enhanced transfection efficiency and transgene expression may be reflected in the increased nuclear accumulation of the plasmid. Examples using some elements of the modular approach include GAL4 as the DBD (Chan and Jans, 2001; Chan *et al.*, 1998) the optimised NLS of the SV40 T-ag as the NLS (Chan and Jans, 2001; Chan and Jans, 1999) the diphtheria toxin T-domain as the EE (Uherek *et al.*, 1998; Fisher and Wilson, 1997; Fominaya and Wels, 1996) and MSH as L (Chan and Jans, 2001).

These constructs might be generated by cross-linking individual peptides to a DNA-carrier protein or by expressing fusion proteins comprising of a series of different peptide sequences to produce a single chimeric protein with modular functionality. A non-viral transfection construct incorporating all of the modular targeting elements illustrated in Figure 1.7 has been described recently (Deas *et al.*, 2002). The construct was based around neutravidin, to which various functional moieties were attached using biotinylation, including a biotinylated monoclonal antibody to target kidney tumour cells, a biotinylated fusogenic peptide to initiate endosomolysis and biotinylated histone H1, which in addition contains intrinsic NLSs, to bind and compact the plasmid DNA (Deas *et al.*, 2002). This approach was effective both *in vitro*, where a 30-fold increase in reporter gene expression was detected, and *in vivo*, where only cells expressing the antigen were found to express the reporter gene.

1.5. THE USE OF CHROMATIN AS A NOVEL VEHICLE FOR GENE DELIVERY

Histones have multiple innate functions that could be beneficial in a modular transfection construct: histones are able to bind DNA and therefore may act as DNA-carrier proteins; histones are able to condense DNA, a property which has been suggested to enhance nuclear transport; histones contain intrinsic NLSs which may facilitate import into the nucleus. In this section, these properties of individual histones are discussed and their potential utility in the context of a transfection construct comprising of *in vitro* assembled chromatin is presented.

1.5.1. The structure of chromatin

Approximately 2 m of DNA is condensed into the nucleus, which is typically 5 - 10 μm in diameter. This is achieved through a highly ordered process of folding and compaction into a protein/DNA assembly called chromatin. The protein component consists primarily of histones, of which there are five main sub-types, namely H2A, H2B, H3, H4, termed the 'core histones, and H1, termed the 'linker histone'. Two copies of each of H2A, H2B, H3 and H4 associate into an octamer and form the 'core particle' (Figure 1.8a). The core particle is stabilised as approximately 146 base pairs of superhelical DNA are wrapped around twice to form a nucleosome (Figure 1.8b). The nucleosome forms the basic structural unit of chromatin and is repeated in a regular fashion, separated by approximately 80 - 120 base pairs of 'linker DNA' (Figure 1.8b).

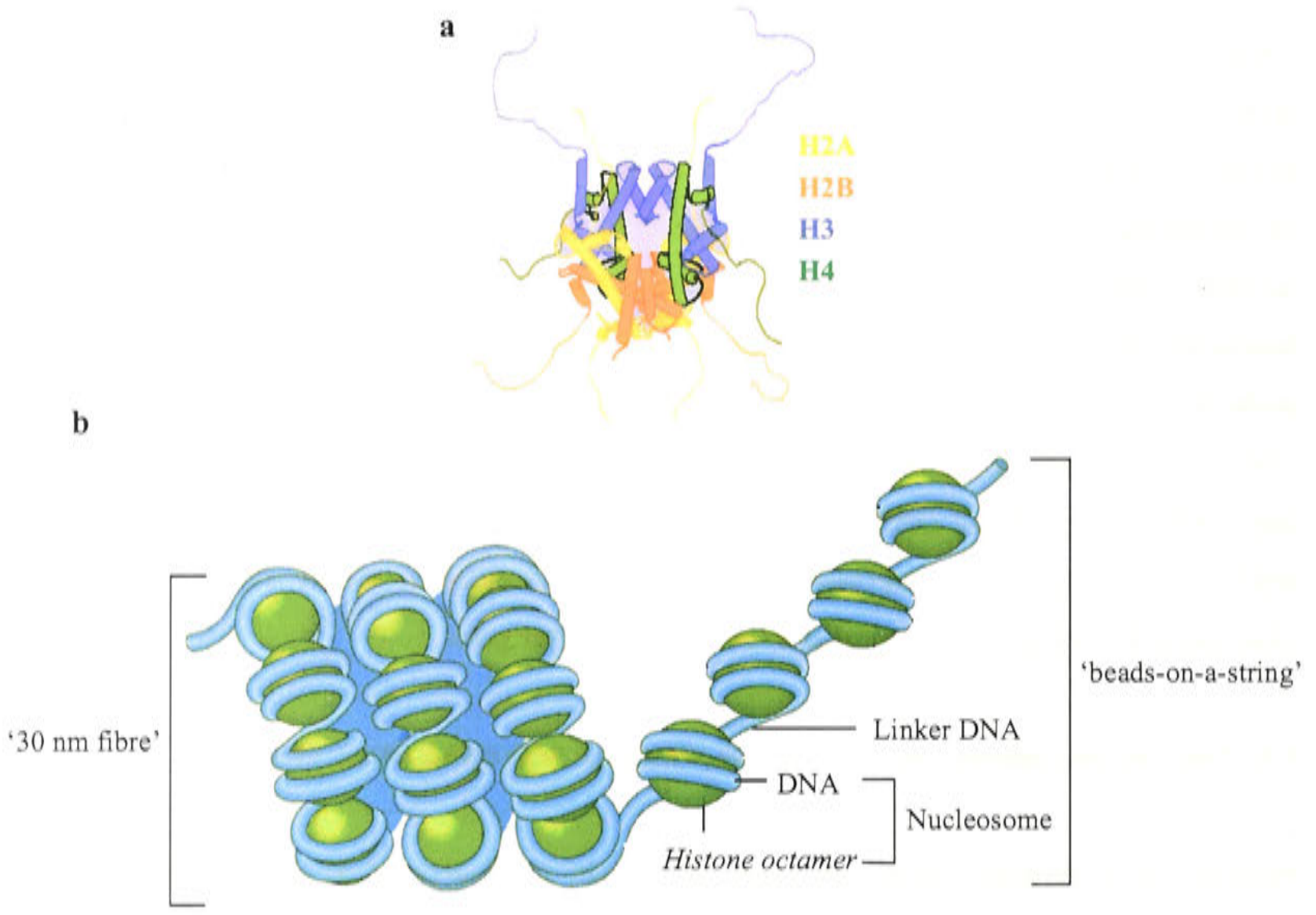

Figure 1.8. The basic structure of chromatin. Chromatin is formed by a hierarchical process of folding and compaction of DNA complexed with histones within the nucleus. Two of each histone, H2A, H2B, H3 and H4, highlighted in different colours, associate to form an octamer (**a**). 146 base pairs of superhelical DNA are wrapped twice around the octamer to form the basic repeated unit of chromatin, the nucleosome (**b**). Consecutive nucleosomes constitute the first level of chromatin packaging into the 'beads-on-a-string' array. Further packaging into the '30 nm fibre' is mediated through inter-nucleosomal interactions facilitated by the histone tail regions. Histone H1 interacts with linker DNA between consecutive nucleosomes, enabling stabilisation of the '30 nm fibre'.

The core histones H2A, H2B, H3 and H4 are structurally similar small proteins, ranging from 11 - 15 kDa, and exhibit high sequence conservation (Wells and McBride, 1989). There are three domains: the amino and carboxy terminal domains, that are highly basic, pliant and irregular, and the central globular domain, constituting the well-defined histone-fold region which is involved in inter-histone contacts within the nucleosome core (Luger *et al.*, 1997). Variant histones with different amino acid sequences and expression profiles exist. Although the role of these variant histones is not yet clear, they are believed to be important in modulating chromatin structure, which in turn may regulate transcriptional activity. An example of this is the variant histone H2AZ, which has been shown to affect nucleosome stability and localised chromatin structure (Fan *et al.*, 2002; Suto *et al.*, 2000).

Members of the H1 family, comprising H1°, H5 and H1, are termed the 'linker histones' as they interact with the 'linker DNA' between consecutive nucleosomes. They have a molecular mass of around 22 kDa. Like the core histones, there are three structural domains, but these differ

between the histone H1 subtypes in the distribution of the basic amino acid residues (Doenecke and Tonjes, 1986). The H1 subtypes are all involved in higher order condensation of chromatin; the central globular domain maintains the two turns of DNA around the nucleosome core (Allan *et al.*, 1980), while the C-terminal domain is involved in further compaction into higher order chromatin structures (Thoma *et al.*, 1983). Differences in the amino acid composition serve to confer functional differences and each variant has a particular role in the stabilisation of the higher order chromatin structures formed.

Several chromatin assembly factors and histone chaperone proteins, such as N1/N2 and NAP-1, are involved in the formation of chromatin (Akey and Luger, 2003). H3 and H4 associate in the cytoplasm to form tetramers (Chang *et al.*, 1997) and are believed to be chaperoned by N1/N2 into the nucleus (Dilworth *et al.*, 1987). H2A and H2B form dimers in the cytoplasm and are chaperoned into the nucleus by NAP-1 (Mosammaparast *et al.*, 2002a; Mosammaparast *et al.*, 2001; Ito *et al.*, 1996). Here, according to the current model, the chaperone proteins deposit one H3/4 tetramer, followed by two H2A/2B dimers onto the DNA (Nakagawa *et al.*, 2001), to form a single core histone octamer (Figure 1.8a).

Chromatin may be assembled *in vitro*; nucleosomes are distributed successively along the DNA template, in localised arrays, in a process that requires ATP and is driven by the ATP-dependent chromatin assembly factor (Fyodorov and Kadonaga, 2002). The globular domain of H1, the tail domains of H1 or the N-terminal domain of H3 may act to neutralise the charge on the linker DNA between consecutive nucleosomes and facilitate the organisation of the nucleosomal array ('beads-on-a-string' model) into the more compact canonical '30 nm fibre' structure (Leuba *et al.*, 1998; Bustamante *et al.*, 1997; see Figures 1.8 and 7.2). *In vivo*, the chromatin fibre undergoes further compaction into higher order structures to finally form the characteristically shaped chromosomes (for review see Horn and Peterson, 2002).

1.5.2. Transport of histones to the nucleus

Histones are synthesised in the cytoplasm and, because they are absolutely required as the scaffolding proteins in chromatin architecture, must be translocated into the nucleus efficiently. Experiments in yeast were the first to suggest that H2A and H2B are transported to the nucleus in the form of a heterodimer (Moreland *et al.*, 1987). As the chromatin assembly chaperone proteins NAP-1 (Ito *et al.*, 1996; Dilworth *et al.*, 1987) and N1/N2 (Chang *et al.*, 1997; Dilworth *et al.*, 1987) are associated with H2A/2B and H3/4, respectively, in the cytoplasm and transfer the histones onto DNA during chromatin assembly, they were assigned a putative 'shuttle' function to facilitate the nuclear transport of these histones. Considering that the molecular weight of histones (11 - 15 kDa) is well within the nuclear pore exclusion limit (~ 45

kDa), it would not have been unreasonable to suppose that, alternatively, simple diffusion is the mechanism of nuclear uptake. However, as discussed below, several groups have shown that histone transport into the nucleus is mediated by the importin nuclear transport proteins and requires Ran and ATP.

In the absence of ATP or at 4°C, histone H1 was no longer transported to the nucleus (Lin and Clarke, 1996; Breeuwer and Goldfarb, 1990). Nuclear uptake of the core histones H2A, H2B, H3 and H4 was also later demonstrated to be energy-dependent (Baake *et al.*, 2001a; Langer, 2000). These studies established that diffusion does not contribute significantly to the nuclear uptake of histones and implicated active transport for the nuclear uptake of the linker and core histones.

Protein transfer into the nucleus is generally mediated by the various members of the importin family of nuclear transport proteins which bind to NLSs within the protein to be transported (presented in Section 1.3.3). The first of the core histone NLSs to be identified as being sufficient to mediate nuclear transport was that of yeast H2B (Moreland *et al.*, 1987). This function was localised to the amino-terminal (N-terminal) amino acids 21 – 33 and, due to sequence homology with the SV40 T-ag NLS, it was suggested that nuclear import of H2B is facilitated by importin α.

In order to investigate this interaction further, and since histones are transported to the nucleus with their binding partners, the *in vitro* binding affinities of importins were quantitated for the core histones in the form of the H2A/2B dimer and H3/4 tetramer using a modified ELISA (Johnson-Saliba *et al.*, 2000 and see Section 3.2). Although all the histones tested were indeed bound with high affinity by importin α/β, binding by importin β was predominant. Moreover, the binding affinity of importin α was lower than importin β for each of H1, H2A/2B and H3/4. The results implied that the nuclear import of histones would be mediated predominantly by importin β and not importin α.

Subsequently, several members of the importin β family were shown to play a role in the nuclear transport of both H2A and H2B in yeast (Mosammaparast *et al.*, 2001). These included Kap114p, 121p, 123p and 95p, which correspond to the mammalian importins 9, β3, β4 and β1, respectively (Mosammaparast *et al.*, 2001). In this study, as had been suggested by Moreland *et al.* (1987), nuclear localisation of H2B was attributed to the N-terminal amino acids 21 - 33. Amino acids 1 – 52, in the form of a green fluorescent protein-fusion peptide, were shown by fluorescence microscopy to result in greater nuclear accumulation, assigning nuclear import function also to sequences flanking the amino acids 21 – 33. The NLS of yeast H2A was

similarly mapped to amino acids 24 - 46 and with the inclusion of important flanking sequences was extended to encompass amino acids 1 – 46 (Mosammaparast *et al.*, 2001).

In a similar series of experiments to those delineating H2A and H2B nuclear import, Mosammaparast *et al.* (2002b) identified the nuclear import proteins involved in H3 and H4 translocation in yeast. Kap123p and 121p were shown to specifically bind NLSs located in the N-terminal domains amino acids 1 – 28 in H3 and amino acids 1 - 42 in H4.

Mosammaparast *et al.* (Mosammaparast *et al.*, 2002a) provided insight into the role of the chromatin assembly protein Nap1p (eukaryotic NAP-1) in the nuclear transport of H2A and H2B in yeast (Figure 1.9). Nap1p was found to bind to Kap114p; the interaction shown to increase the affinity of Kap114p for the histone NLSs but decrease affinity for the other Kaps. The authors postulated that, in this way, Kap114p is primed as the predominant importin involved in the rapid nuclear translocation of H2A/2B. Once inside the nucleus, RanGTP dissociates Kap114 from the complex. This leaves Nap-1 to deposit its histone cargo onto 'chromatinising' DNA. Using a yeast strain lacking Nap1p, H2A and H2B were, however, still found to localise to the nucleus, suggesting that Nap1p is not absolutely required for H2A/2B nuclear uptake and that Kap114p alone may fulfil the nuclear import function (Mosammaparast *et al.*, 2001).

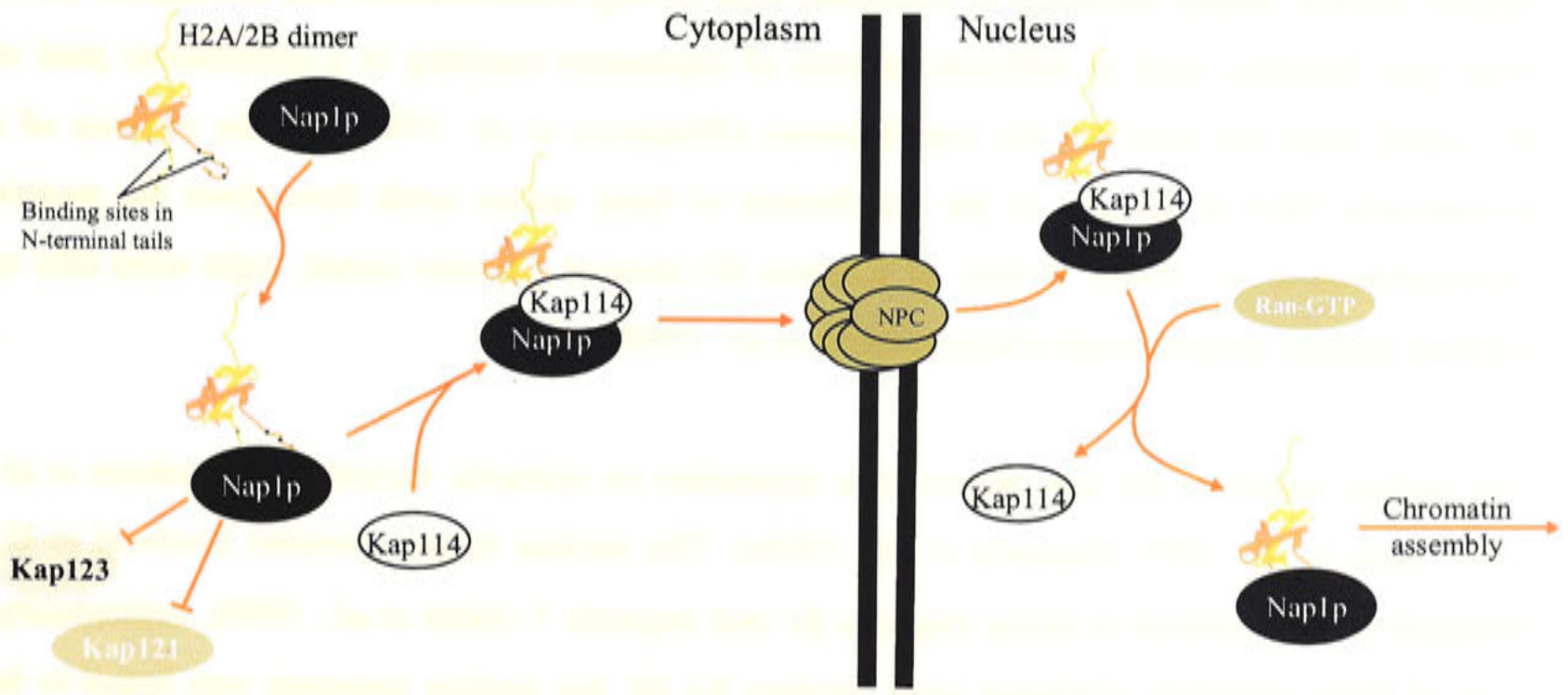

Figure 1.9. The dual role of Nap1p in nuclear transport and chromatin assembly in yeast. Model of H2A/2B Nap1p-mediated nuclear transport according to Mosammaparast *et al.* (2002a). Nap1p binds Kap114p, increasing the binding affinity of Kap114p for NLSs in the N-terminal tails of H2A and H2B. This inhibits the binding of Kap121p and Kap123p for the histones. Kap114p translocates H2A/2B and Nap1p into the nucleus. Here, RanGTP dissociates Kap114 from the complex and Nap1p fulfils its role as a chromatin assembly factor, depositing H2A/2B onto chromatinising DNA. Adapted from Mosammaparast *et al.* (2002a).

The nuclear import pathways of core histones have been investigated in vertebrate systems. In order to define the NLSs, Baake *et al.* (Baake *et al.*, 2001a) generated fusion proteins comprising β-galactosidase and the core histones, or peptides thereof, and determined their subcellular location using an antibody directed against β-galactosidase. Using this approach, groups of basic amino acids in the N-terminal domains were found to function as NLSs. The overall globular structure of the histones was shown to be important also, analogous to the role of the 'flanking sequences' purported to play a role in conferring nuclear localisation of histones in the yeast (Mosammaparast *et al.*, 2002b; Mosammaparast *et al.*, 2001). Several members of the importin β family, including importin β, transportin, importin 5, importin 7 and a novel importin, importin 9, were identified using affinity chromatography as binding to immobilised histones and using fluorescence microscopy were shown to mediate nuclear transport of fluorescein-labelled histones in a model digitonin permeabilised cell system (Baake *et al.*, 2001b; Muhlhausser *et al.*, 2001).

The nuclear import pathway of the H1 linker histones was shown to be distinct from that of core histones (Baake *et al.*, 2001b). Competition experiments showed that an excess of the linker histone H1 diminished, but did not entirely abolish, nuclear accumulation of core histones, suggesting that while some receptors are common, alternative import receptors exist for the core histones. In contrast, each core histone inhibited the nuclear uptake of the other histones, implying a communal nuclear import mechanism (Baake *et al.*, 2001b). Having distinct nuclear import pathways is consistent with having characteristics that distinguish linker from core histones, such as different patterns of expression resulting in a cytoplasmic pool of H1 which does not exist for the core histones (Zlatanova *et al.*, 1990) and the absence of a conspicuous NLS in H1 due to the distribution of basic amino acids throughout the protein (Schwamborn *et al.*, 1998). In fact, of fourteen H1-derived peptides tested, eight were able to mediate nuclear accumulation (Schwamborn *et al.*, 1998).

The nuclear import of H1 was shown to be dependent on cytosolic factors (Schwamborn *et al.*, 1998; Kurz *et al.*, 1997; Imamoto *et al.*, 1995a). The nuclear import proteins involved in H1 transport were identified as being importin β1 and importin 7 (Jakel *et al.*, 1999). Individually, each of these importins exhibited weak binding for H1 but nuclear transport was found to be mediated through the formation of a heterodimer, impβ1/imp7. Within the heterodimer, importin β1 was found to have the more dominant import function and also played a role in interaction with RanGTP to disassemble the transport complex. Impβ1/imp7 was shown to be the only import receptor involved in H1 nuclear translocation (Bauerle *et al.*, 2002). Bauerle *et al.* (2002) also investigated putative NLSs within H1 for importin binding activity. The N-terminal domain amino acids 1 - 20 did not function as an NLS. The central globular domain

(amino acids 21 - 95) was found to associate with importin β1 and the carboxy-terminal (C-terminal) domain (amino acids 95 - 193) with impβ1/imp7. Smaller peptides (>50 amino acids > 20) within the C-terminal domain were transported to the nucleus by importin β, transportin, importin 5 and importin 7, as are the core histones. The authors suggested that the length of the NLS, therefore, may be a key determinant in differentiating between nuclear import pathways.

Collectively, these studies show that distinct import pathways are involved in the uptake of histones into the nucleus and that several pathways may exist to ensure that these crucial architectural proteins reach the nucleus. These pathways may provide a direct route into the nucleus for histones serving as carrier-proteins of plasmid DNA in gene delivery applications.

1.5.3. The use of histones as DNA-carrier proteins for gene delivery

The ability to bind and compact DNA, as well as harbouring intrinsic NLSs which facilitate their passage to the nucleus (a crucial step to ensure efficient DNA delivery), suggests the use of histones as DNA carrier proteins for gene delivery purposes. The first report outlining the use of nuclear proteins for DNA delivery described the co-introduction of DNA with chromatin associated high mobility group (HMG)-1 and DNA-binding protein extracts from *Xenopus laevis* oocytes into cells in culture (Kaneda *et al.*, 1989). Nuclear accumulation and reporter gene activity were enhanced compared to co-introduction of DNA with non-nuclear proteins. These results were substantiated *in vivo* whereupon 4 days post-injection into the portal veins of rats, radio-immunostaining revealed that approximately 10 % of the liver cells had expressed the transgene.

Histones have since been assessed for their ability to function as carriers of DNA for gene delivery applications. While in the presence of histones transfection efficiency was enhanced, consensus on which histone has superior transfection efficiency has not been reached. These studies are presented below.

1.5.3.1. The use of H1 for gene delivery

Fractions containing H1, HMG17 and, to a lesser extent, HMG1, obtained from acid extraction of the nucleus, were identified to be the most active in enhancing transfection (Bottger *et al.*, 1998; Zaitsev *et al.*, 1997). This group further demonstrated that H1 could facilitate transfection of DNA in cardiomyocytes, demonstrating, as a 'proof of principle', DNA delivery into primary cells which are usually problematic to transfect (Kott *et al.*, 1998). Compared to the other histone subtypes, H2A, H2B, H3 and H4, Chen *et al.* (Chen *et al.*, 1994a) reported 11 times

greater chloramphenicol acetyl transferase reporter gene activity when H1 was used as the DNA-carrier protein. In this series of experiments, the histones were galactosylated to facilitate receptor-mediated endocytosis into hepatocytes (HepG2 cells). Transfection activity using H1 was shown to be a function of the histone and not the degree of galactosylation (Haberland *et al.*, 1999; Chen *et al.*, 1994a).

Similar results were obtained using short peptides derived from H1. H1 alone and the C-terminus of H1 (amino acids 99 - 193) expressed as a recombinant fusion protein with the T-ag NLS were complexed with a luciferase reporter plasmid and found to yield luciferase expression 20 - 45 times that of plasmid DNA alone (Fritz *et al.*, 1996). This was also markedly greater than when H2A/2B- and H3/4-DNA complexes were transfected. Interestingly, H1 mediated transfection in both the absence and presence of the cationic lipid delivery agent used. Evidence for how this was possible was provided by a subsequent study which showed that despite H1-NLS-bound DNA being located on the outside of the anionic liposomes, the complexes were able to mediate transfection (Hagstrom *et al.*, 1996).

1.5.3.2. The use of H3 and H4 for gene delivery

H4 was shown to enhance gene transfer to an extent greater than that of H3 and H1 in K-562 cells (Wagner *et al.*, 1991). The histones were incubated with DNA that had been pre-condensed using a transferrin-pLy conjugate. Electron microscopy revealed that the level of DNA condensation achieved with the transferrin-pLy conjugate alone was greater than that in the presence of H4, yet the respective transfection activities were similar and, moreover, were enhanced up to 7-fold when a higher ratio of H4 to transferrin-polylysine was used. The authors suggested that the transfection capacity of H4 was independent of its condensation effect.

H3 and H4 were shown to mediate transfection of the HIV-1 Tat gene in a model T-cell line (Jurkat), whereas H1 and H2A were not (Demirhan *et al.*, 1998). Anti-histone IgG was found to specifically diminish the transfection activity of H3 and H4 within a histone-based transfection system (Hasselmayer *et al.*, 2001). Furthermore, as pLy was unable to facilitate gene expression in the transfection system described by Demirhan *et al.* (1998), together, these studies implied that histone-mediated transfection was not due simply to the cationic nature and DNA-condensing ability of the histones.

1.5.3.3. The use of H2A for gene delivery

H2A has also been shown to mediate transfection; firstly, as part of a retroviral gene delivery system (Singh and Rigby, 1996) and, secondly, in an elegantly conducted series of experiments

in which Balicki *et al.* described the use of H2A for gene transfer *in vitro* and *in vivo* (Balicki *et al.*, 2002; Balicki *et al.*, 2000; Balicki and Beutler, 1997).

H2A was found to enhance the levels of β-galactosidase reporter expression *in vitro* (Cos-7 cells) compared to when H2B, H3, H4, H1 and pLy were used as the DNA-carriers (Balicki and Beutler, 1997). This system was applied *in vivo* to a mouse model of neuroblastoma (Balicki *et al.*, 2000). A plasmid encoding the Il-2 cytokine gene, complexed with H2A, was transferred into neuroblastoma cells in culture, which were then injected subcutaneously into mice. Mice receiving cells transformed with single chain IL-2 did not develop liver or bone marrow metastases and demonstrated an elevated cytotoxic T-lymphocyte and interferon-γ response, consistent with protective immunity.

Various peptides spanning the full length of H2A were generated and assessed for their ability to mediate gene transfer (Balicki *et al.*, 2002). Activity was localised to a 37-amino acid sequence located within the N-terminus of H2A. The authors postulated that the secondary structure (α–helix) and positively charged residues in this region played a vital role in DNA-binding and nuclear localisation, respectively. In the context of the nucleosome core particle, H2A is the only histone to harbour a cluster of DNA binding sites located near to its NLS (Luger *et al.*, 1997). This, the authors suggested, would impart on H2A dual DNA binding and nuclear targeting functionality within a structurally distinct region, making H2A a superior mediator of transfection compared to the other core histones tested.

Collectively, all of these studies demonstrated the capacity for gene delivery purposes; however, transfection efficiency of the individual histones appeared to be highly dependent on both the type of histone and cultured cells transfected.

1.6. Hypothesis, aims and scope of this project

Although there have been many recent advances in the improvement of non-viral transfer, the gene transfer efficiency of viral-based delivery systems remains far superior. This is due mainly to the intrinsic ability of viruses to target specific cells, circumvent endosomal sequestration and enter the nucleus efficiently. Approaches using engineered fusion proteins displaying modular characteristics beneficial for gene delivery represent a leap forward in mimicking viral systems and might be an indispensable asset to non-viral gene delivery. The aim of this thesis was to explore the potential of *in vitro* assembled chromatin as a novel vehicle for non-viral gene delivery. The reasoning for this was based on the observation that chromatin has modular properties which may enhance DNA delivery into the nucleus.

Firstly, in the form of chromatin, at the first level of compaction, DNA is condensed in length up to 5-fold by association with the core histones into a nucleosomal array (Van Holde *et al.*, 1980). Condensation has been shown to shield the DNA from degradation in the cytoplasm and, potentially, allows the accommodation of larger, or even multiple, genes. Condensed DNA also has been reported to be transported more efficiently across the nuclear membrane (Chan and Jans, 1999). Secondly, in addition to their DNA-carrier protein function, histones contain intrinsic NLSs which promote their rapid uptake into the nucleus (Section 1.5.2). This could provide a pathway along which a gene delivery vehicle based on chromatin may be targeted to the nucleus. Thirdly, as histones may be expressed in recombinant form, they may be modified and generated as fusion proteins, incorporating functional sequences for cellular targeting, endosomal escape or nuclear import. Finally, chromatin is the physiological form in which condensed DNA is found in the nucleus. As mechanisms exist in the nucleus to de-condense chromatin and transcribe the DNA (Horn and Peterson, 2002; Kadonaga, 1998), a transfection construct based on chromatin may therefore circumvent problems relating to the inhibition of gene expression that has been observed previously in the presence of artificial DNA condensing agents (Bielinska *et al.*, 1997; Zabner *et al.*, 1995).

Published data demonstrated the capacity of individual histones to mediate transfection (presented in Section 1.5.3). In order to characterise the histone nuclear import pathways, which may serve as routes for gene delivery, the binding properties of importins to the core histones were determined. This work, presented in Chapter 3, additionally formed the first reported study delineating the pathway of histone nuclear import (Johnson-Saliba *et al.*, 2000). As most prior studies involving *in vitro* assembled chromatin were conducted using a linear DNA template of specified sequence or small plasmids (Forte *et al.*, 1989; Hansen *et al.*, 1989; Simpson *et al.*, 1985), appropriate assembly of large plasmid DNA into chromatin had to be verified before transfection into cultured cells could be performed. In Chapter 4, the characterisation of chromatinised plasmid DNA assembled at various stoichiometries of recombinant histone octamers, using assays including sedimentation velocity ultracentrifugation, DNA supercoiling, micrococcal nuclease digestion and atomic force microscopy, is described. Upon transfection of the chromatin constructs into cells in culture, reporter gene expression was found to decrease concomitantly with chromatinisation at increasing nucleosome densities. In Chapter 5, possible reasons for this unexpected pattern of transfection efficiency were examined. Based on these results, a number of strategies, described in Chapter 6, were investigated as a means to improve transfection efficiency, namely improving nuclear import of the chromatinised plasmids by incorporating exogenous SV40 T-ag NLS peptides and potentiating their transcriptional permissiveness by altering the histone composition of the chromatin.

In addition to providing a rational approach to the design of non-viral gene delivery vectors, this study highlighted the problems associated with large plasmid delivery into the nucleus. Transport into the nucleus and the transcriptional permissiveness of the transfection constructs were found to be key determinants for gene delivery efficiency. This thesis details these findings.

CHAPTER 2

Materials and Methods

2.1. MATERIALS

2.1.1. Chemicals and reagents

All chemicals and enzymes used in this study were of analytical grade or higher.

2.1.2. Culture media, buffers and solutions

All cell culture media, solutions and buffers were prepared with double-distilled deionised water (ddH_2O) and sterilised by autoclaving at 112°C for 20 minutes. Luria-Bertani (LB) and all cell culture media were prepared by the Media Unit, JCSMR. Solutions for plasmid DNA manipulation, protein purification, chromatin assembly and *in vitro* assay techniques are tabulated below.

Table 2.1. Media for bacterial and cell culture

Use	Name of solution	Composition	Comments
Bacterial culture	Luria-Bertani (LB)	per litre: 10 g bacto-tryptone 5 g bacto-yeast extract 10 g NaCl	Autoclaved at 121°C for 20 minutes. Added antibiotics before use.
	SOB medium	per 100 ml: 2 g bacto-tryptone 0.55 g bacto-yeast extract 1 ml 1 M NaCl 1 ml 1 M KCl	Autoclaved at 121°C for 20 minutes.
	SOC medium	per 10 ml SOB medium: 100 µl 2 M $MgCl_2/MgSO_4$ (1:1, v/v) 100 µl 2 M glucose	All solutions filtered through 0.22 µm Millex® syringe driven filter unit (Millipore).

CHAPTER 2

Materials and Methods

2.1. MATERIALS

2.1.1. Chemicals and reagents

All chemicals and enzymes used in this study were of analytical grade or higher.

2.1.2. Culture media, buffers and solutions

All cell culture media, solutions and buffers were prepared with double-distilled deionised water (ddH_2O) and sterilised by autoclaving at 112°C for 20 minutes. Luria-Bertani (LB) and all cell culture media were prepared by the Media Unit, JCSMR. Solutions for plasmid DNA manipulation, protein purification, chromatin assembly and *in vitro* assay techniques are tabulated below.

Table 2.1. Media for bacterial and cell culture

Use	Name of solution	Composition	Comments
Bacterial culture	Luria-Bertani (LB)	per litre: 10 g bacto-tryptone 5 g bacto-yeast extract 10 g NaCl	Autoclaved at 121°C for 20 minutes. Added antibiotics before use.
	SOB medium	per 100 ml: 2 g bacto-tryptone 0.55 g bacto-yeast extract 1 ml 1 M NaCl 1 ml 1 M KCl	Autoclaved at 121°C for 20 minutes.
	SOC medium	per 10 ml SOB medium: 100 µl 2 M $MgCl_2/MgSO_4$ (1:1, v/v) 100 µl 2 M glucose	All solutions filtered through 0.22 µm Millex® syringe driven filter unit (Millipore).

Cell Culture	PBS	137 mM NaCl 6.75 mM Na_2HPO_3 2.5 mM NaH_2PO_3	Autoclaved at 121°C for 20 minutes.
	DMEM	per litre: 9.99 g H16 powder (Gibco cat. no. 31600-091) 3.7 g $NaHCO_3$ 0.2g Streptomycin (Thermo Trace cat. no. 60-005-PF) 0.12g Penicillin (Thermo Trace cat. no. 60-004-P2)	pH 6.8 - 7.5 with CO_2. Sterilised using Millipore filter 0.22 µm.
	RPMI-1640	per litre: 10.44 g RPMI powder (Gibco, cat. no. 31800-105) 2 g $NaHCO_3$	pH 6.9 - 7.0with CO_2. Sterilised using Millipore filter 0.22 µm.

Table 2.2. Solutions used for DNA methods.

Use	Name of solution	Composition	Comments
Gel loading dye	6 × DNA loading buffer	60 mM Tris-HCl 75.4 mM EDTA 2.8 % sarkosyl 0.25 % bromophenol blue 0.25 % xylene cyanol 40 % sucrose	
Gel electrophoresis buffer	50 × TAE	2 M Tris 5.71 % glacial acetic acid 0.05 M EDTA (pH 8.0)	
DNA storage buffer	TE	10 mM Tris-HCl (pH 8) 1 mM EDTA (pH 8)	

Table 2.3. Solutions used for protein detection and analysis.

Use	Name of solution	Composition	Comments
Bacterial cell lysis	Lysis solution	1 % SDS 0.03 % β-mercaptoethanol	
Protein loading dye	2 × SDS-loading dye	0.1 M Tris-HCl (pH 6.8) 0.2 M DTT 4 % SDS 0.005 % bromophenol blue 20 % glycerol	
Gel electrophoresis buffer	5 × SDS-PAGE buffer	0.25 M Tris 2 M Glycine 0.5 % SDS	
Gel staining solution	Coomassie blue	0.25 % Coomassie brilliant blue R250 45 % methanol: ddH_2O (1:1, v/v) 10 % glacial acetic acid	
Gel destaining solution	Coomassie blue destain	5 % acetic acid 5 % isopropanol	
Western blot	Transfer buffer	20 % methanol 25 mM Tris 192 mM glycine 0.1 % SDS	
	Ponceau S stain	0.5 % Ponceau S 1% acetic acid	
	Ponceau S destain	7 % acetic acid	
	TBST	10 mM Tris (pH 8) 150.5 mM NaCl 0.05 % Tween-20	Made to 800 ml with ddH_2O, pH to 8.0, then added Tween-20 and ddH_2O to 1 L.
	Blocking solution	100 ml TBST 5 g skim milk powder (Carnation milk)	Filtered using 0.22 µm Millex® syringe driven filter unit (Millipore).

Table 2.4. Buffers and solutions used for purification of histones.[A]

Use	Name of solution	Composition	Comments
Preparation of inclusion bodies	Wash buffer	50 mM Tris-HCl (pH 7.5) 100 mM NaCl 1 mM EDTA 0.5 mM PMSF	
	TW buffer	1% Triton X-100 in Wash buffer	
	Unfolding buffer	7 M urea 20 mM Tris-HCl (pH 7.5) 10 mM DTT	DTT added just before use.
FPLC	SAU-1000	7 M urea 20 mM NaOAc (pH 5.2) 1 M NaCl 5 mM β-mercaptoethanol 1 mM EDTA	
	SAU-600	as above, but 600 mM NaCl	
	SAU-200	as above, but 200 mM NaCl	
Octamer reconstitution	Refolding buffer	2.2 M NaCl 10 mM Tris-HCl (pH 7.5) 1 mM EDTA 5 mM β-mercaptoethanol	

[A] Buffer composition is as described in Luger *et al.* (1999).

Table 2.5. Solutions used for chromatin assembly.

Use	Name of solution	Composition	Comments
Octamer transfer by salt dialysis method	1 M NaCl buffer	1 M NaCl 0.01 M Tris-HCl	pH 7.5
	0.75 M NaCl buffer	0.75 M NaCl 0.01 M Tris-HCl	pH 7.5
	Chromatin buffer (CB) 0.135 M NaCl buffer	0.135 M NaCl 0.01 M Tris-HCl	pH 7.5

NAP-1 method		See section 2.5.1 for details

[A] Buffers were adapted from Luger *et al.* (1999).

Table 2.6. Solutions used for the Luciferase assay.[A]

Use	Name of solution	Composition	Comments
Cell lysis	Lysis buffer	100 mM K_2HPO_4 buffer 2 % Triton X-100 20 % glycerol 4 mM DTT	
Assay buffer	Luciferase assay buffer	100 mM K_2HPO_4 2 mM DTT 8 mM MgSO4, 175 µM coenzyme A 750 µM ATP	Solutions stored at 4°C. Assembled buffer allowed to equilibrate at room temperature before use.
Initiate light reaction	D-luciferin	1 mM D-luciferin 5 mM K_2HPO_4 buffer	

[A] Buffer composition is as described in Himes and Shannon (2000).

Table 2.7. Solutions used for ELISA.

Use	Name of solution	Composition	Additional information
Coating microtitre plates	Coating buffer	100 mM NaHCO3 (pH 9.6)	2 × stock solution
	Intracellular buffer (IB)	440 mM KCl 20 mM NaHCO3 20 mM MgCl2 4 mM EGTA 0.4 mM CaCl2 80 mM Hepes	4 × stock solution. pH to 7.4 using NaOH. Stored at 4°C.
Rinsing plates before addition of importins	Hybridisation buffer (HB)	150 ml 4 × IB 1 mM DTT	
Blocking and buffer for importin dilutions	HB/BSA	HB/1 % BSA	Stored at 4°C
Washing microtitre plates	Wash buffer	0.3 % Tween-20 in PBS	

Solution for primary and secondary antibodies	Antibody buffer	PBS/0.3 % Tween-20 1 % BSA	
Visualisation of antibody reaction	10 % diethanolamine buffer	10 % diethanolamine in 0.5 mM $MgCl_2$ (pH 9.8)	Stored at 4°C. Covered with aluminium foil.

2.1.3. Bacterial strains

Table 2.8. Bacterial strains used in this study.

Strain	Genotype
DH5α	F- *deo*R *rec*A1 *end*A1 *hsd*R17(r_k^-, m_k^+) *sup*E44 λ^- *thi*-1 *gyr*A96 *rel*A1
BL21(DE3)pLysS	F- *ompT* *hsdS*$_B$ ($r_B^-m_B^-$) *gal* *dcm* (DE3) pLysS (Cam^R)
DB3.1™	F- *gyr*A462 *end*A1 Δ(*sr*1- *rec*A) mcrB *mrr* *hsd*S20(r_B^-,m_B^-) *sup*E44 *ara*14 *gal*K2 *lac*Y1 *pro*A2 *rps*L20(Sm^r) *xyl*5 Δ*leu* *mtl*1

2.1.4. Plasmids and expression vectors

Table 2.9. Plasmids used in this study.

Name	Description
pET3a-H2A	Contains the coding region of histone H2A (*Xenopus*) subcloned into the pET3a vector by M. Clarkson (Chromatin and Transcriptional Regulation Group, JCSMR). Amp^R.
pET3a-H2AZ	Contains the coding region of histone H2AZ (mouse) subcloned into the pET3a vector by M. Clarkson (Chromatin and Transcriptional Regulation Group, JCSMR). Amp^R.
pET3a-H2B	Contains the coding region of histone H2B (*Xenopus*) subcloned into the pET3a vector by M. Clarkson (Chromatin and Transcriptional Regulation Group, JCSMR). Amp^R.
pPR28	pPR2 vector containing optimised SV40 T-ag NLS. Amp^R. See Hubner *et al.* (1997) and Rihs *et al.* (1998).

pET5a	Cloning vector purchased from Promega. Amp^R.
pET5a-H2Anls	pET5a vector containing the coding region of H2A subcloned from pET3a-H2A and the SV40 T-ag NLS subcloned from pPR28 (P10) as a C-terminal fusion H2A-NLS. Amp^R. Generated by Dr M. Lam (Nuclear Signalling Group, JCSMR) and sequenced by M. Johnson-Saliba.
pGeneGrip™	Cloning vector purchased from Gene Therapy Systems. Contains GeneGrip™ site for PNA labelling. Contains MCS downstream of CMV promoter. Kan^R.
pDsRed-C1	Expression vector (Clontech). Contains coding region of red fluorescent protein from *Discosoma sp*. C-terminal to the MCS. Expression driven by CMV promoter. Kan^R/Neo^R. Kindly donated by Dr M. Whitelaw, Adelaide.
pDONR201™	Gateway™ 'Donor' vector containing *att*P sites for recombination 'BP reaction' with *att*B-containing vectors. Kan^R/$Chlor^R$. Kindly donated by Dr M. Robertson, Plant Industries, CSIRO, Canberra.
pEntry-RFP	Gateway™ generated 'Entry' vector containing the coding region of RFP (bases 601 - 1365), flanked by *att*L sites. Kan^R. Derived in this study.
pGeneGrip-DestA	Gateway™ compatible 'Destination' vector. Generated by ligation of Gateway™ reading frame A cassette into the EcoRV site of pGeneGrip MCS. Kan^R/$Chlor^R$. Can only be propagated in *E. coli* DB3.1 cells. Derived in this study.
pGeneGrip-RFP	Gateway™ generated 'Expression' vector. Generated through recombination of pEntry-RFP and pGeneGrip-DestA using 'LR reaction'. Contains the coding region of RFP, flanked by *att*B sites. RFP expression driven by the CMV promoter. Kan^R. Derived in this study.
pGMCSF-1(2)TK-luc+ (pGMLuc)	Luciferase reporter plasmid. Luciferase gene expression driven by a fragment of the human GMCSF promoter region (– 620 to + 37). Kindly provided by K. Bunting (Cytokine Gene Expression Group, JCSMR). See Himes *et al*. (1993).

2.1.5. Primers

Table 2.10. Oligonucleotides used in this study.

Name	Sequence
H2A-NLS primers	
H2A5'	5'-gcCAtATGAgCGCTTCAGGAAGAGGCAAACAAGGC-3'
H2A3'	5'-GCGactagtCTTGCTCTTGGCAGATTTGGC-3'
H2A3'NLS	5'-GCGaagcttCTTGCTCTTGGCAGATTTGGC-3'
P105'	5'-cggaagcttTCCTCTAGTGATGATGAGGC-3'
P103'	5'-cgcGGATCCctatGCactagtCCGGGGGGTCTTCTACC-3'

Gateway™ primers[A]	
*att*B1RFP	5'-**GGGG ACA AGT TTG TAC AAA AAA GCA GGC** TCC CCG GTC GCC ACC ATG GTG CGC TCC-3'
*att*B2RFP	5'-**GGGG AC CAC TTT GTA CAA GAA AGC TGG GT**G TTA TCT AGA TCC GGT GGA TCC CGG GCC-3'
pGeneGrip sequencing primers	
5' forward primer	5'-CAGACTAACAGACTGTTC-3'
3' reverse primer	5'-GGCAAACAACAGATGGC-3'

[A] The *attB* sites are highlighted in bold type-face.

2.1.6. Enzymes

Table 2.11. Enzymes used in this study.

Enzyme	Source
Restriction endonucleases	
BamHI	New England Biolabs
Cla I	Bresatec
EcoRV	New England Biolabs
HpaI	Promega
HindIII	Promega
SacII	Promega
SalI	Promega
XhoI	New England Biolabs
Ligation and recombination	
T4 DNA ligase	Boehringer
Calf intestinal phosphatase (CIP)	Boehringer
BP clonase	Life Technologies
LR clonase	Life Technologies
PCR	
Taq polymerase	Fermentas
Pfu turbo	Stratagene
Platinum Taq	Life Technologies
Chromatin characterisation	
Topoisomerase I	Promega
S4 micrococcal nuclease (MNase)	Roche

2.1.7. Antibodies and conjugates

Table 2.12. Primary and secondary antibodies used in this study.

Antibody	Description	Source
H2Anls immunoblotting		
1° H2A antibody	Raised in sheep. Directed against C-terminal epitope Used at 1:500.	Chiron mimotopes
2° alkaline phosphatase-conjugated anti-sheep antibody	Anti-sheep. Used at 1:1000.	Sigma
ELISA		
1° anti-GST antibody	Raised in goat. Used at 1:1000.	Amersham Pharmacia
2° alkaline phosphatase-conjugated anti-goat antibody	Anti-goat. Used at 1:25000.	Sigma

2.1.8. Kits

Table 2.13. Molecular biology kits used in this study.

Name	Company
Plasmid MiniPrep and MaxiPrep kits	Qiagen
BRESA-clean gel extraction kit	BRESAGEN
SuperSignal West Pico Western Blot Kit	Pierce
Gateway™ vector conversion system	Life Technologies
Gateway™ BP clonase	Life Technologies
Gateway™ LR clonase	Life Technologies
NE-PER™ cytoplasmic and nuclear extraction reagents	Pierce
pGeneGrip™ fluorescein PNA label	Gene Therapy Systems
pGeneGrip™ maleimide PNA label	Gene Therapy Systems

2.1.9. Molecular mass markers

Table 2.14. Molecular mass markers used in this study.

Name	Application	Company
GeneRuler 1kb DNA ladder	DNA agarose gels (500 kb to 10 000 kb)	Fermentas
1kb Plus DNA ladder	DNA agarose gels (100 bp to 12 000 bp)	Fermentas
Benchmark protein ladder	SDS-PAGE (Coomassie blue stain)	GibcoBRL
Benchmark Pre-stained protein Ladder	SDS-PAGE (Western blot)	Invitrogen

2.1.10. Miscellaneous materials

All other materials used in this study are described in the text.

2.2. General DNA methods

2.2.1. *E. coli* cells

2.2.1.1. Preparation of competent cells

E.coli cells competent for transformation by heat shock were prepared using $CaCl_2$. *E. coli* cells were spread onto an agar plate and cultured overnight at 37°C. A single colony was used to inoculate 3 ml of LB, which was incubated overnight at 37°C with agitation at 220 rpm in a Controlled Environment Incubator Shaker (New Brunswick Scientific Co. Inc., USA). This culture was used to inoculate a second overnight culture of 100 ml, which in turn was used to inoculate 400 ml LB the following morning. This was cultured to an OD_{600} of 0.8 - 1.0 at 37°C with vigorous shaking. The cultures were chilled on ice for 15 min, the cell suspension transferred into 500 ml centrifuge tubes and centrifuged in a GS-3 rotor (Sorvall RC5C, Sorvall Instruments, DuPont) for 15 minutes at 4800 rpm and 4°C. The supernatant was discarded and the pellet resuspended in 50 ml of cold, sterile $CaCl_2$ (0.1 M). After overnight incubation at 4 °C, the cell suspension was centrifuged for 5 minutes at 5000 g. The supernatant was removed and the pellet resuspended in 5 ml of cold 0.1 M $CaCl_2$/glycerol (85:15, v/v). The cell suspension was transferred in aliquots of 100 µl into pre-chilled Eppendorf tubes and stored at

-70 °C. Bacterial stocks were stored for no longer than 6 months.

2.2.1.2. Transformation of competent cells by heat shock

Transformation of competent bacteria was achieved using heat shock, based on the procedure described by Sambrook *et al.* (1989). Competent cells were removed from storage at -70°C and thawed on ice for 10 minutes. Plasmid DNA (1 - 10 ng) was pipetted into the vial containing competent cells (100 µl) and incubated on ice for a further 30 min. The cells were plunged into a 42°C water bath for 45 seconds and then returned to ice for 2 minutes. Following this, 1 ml of LB or SOC medium (Table 2.1) was added and the cell suspension incubated for 1 hour at 37°C with agitation at 220 rpm. For routine plasmid transformations, 50 - 200 µl of the transformation culture was plated onto agar plates containing suitable antibiotic(s) for selection. In the case of ligations, 50 µl of the bacterial culture was spread and the remaining culture centrifuged, resuspended in 50 µl of LB and then spread onto agar. Agar plates were incubated at 37°C overnight. Individual colonies were selected the following day and used to inoculate 5 ml overnight cultures for DNA or protein purification.

2.2.1.3. Long-term storage

For storage purposes, *E. coli* strains transformed with various plasmids were cultured to late log phase (OD_{600nm} ~ 1.0). Together, 850 µl of bacterial culture and 150 µl sterile 80 % glycerol/LB were pipetted into sterile cryotubes (Nunc). The cell suspension was gently mixed and stored at -70°C.

2.2.2. Plasmid purification

Purification of up to 500 µg of plasmid DNA was carried out using kits (Table 2.13); the Qiagen MiniPrep kit was used for plasmid purification from 2 ml of bacterial culture, whereas the MaxiPrep kit was used to purify plasmid from 200 ml of bacterial culture. Bacteria were cultured at 37°C overnight with agitation at 220 rpm in the presence of appropriate antibiotic. Bacterial cells were collected by centrifugation and plasmid DNA purified according to the protocol recommended by the manufacturer. All buffers used were supplied in the kits and were stored according to the manufacturer's instructions. Purified plasmid DNA was quantitated using spectrophotometry (Section 2.2.3) and quality was verified by agarose gel electrophoresis (Section 2.2.4).

2.2.3. Quantitation of DNA

DNA samples were quantitated spectrophotometrically. Samples were measured in quartz cuvettes, having a path length of 1 cm. The absorbance readings were measured at 260 nm and 280 nm and were normalised to reference solutions. The concentration of DNA in plasmid preparations was calculated using the equation:

$$\text{Concentration } (\mu g/ml) = \text{Absorbance}_{260\,nm} \times 50 \times \text{dilution factor}$$

2.2.4. Agarose gel electrophoresis

Separation of DNA fragments greater than 100 bp was performed by electrophoresis through horizontal slab agarose gels (BioRad gel apparatus) in TAE buffer (Table 2.2). Depending on the separation required, 1 or 1.5 % agarose gels were used. Samples were typically made up to a final volume of 12 µl using TE and 6 × DNA loading dye (Table 2.2). Electrophoresis was performed at a voltage between 60 - 120 V for 2 - 4 h, or until the marker dye front reached the end of the gel. Agarose gels were stained in 0.5 µg/ml ethidium bromide for 20 minutes with gentle agitation, followed by destaining in ddH_2O for an equal period of time. DNA fragments were visualised under UV light (Gel Documentation System, Novaline).

2.2.5. DNA extraction from agarose gels

DNA fragments were separated using agarose gel electrophoresis (see above). The band of interest was located using a UV transilluminator (Gel Documentation System, Novaline) and excised with a scalpel. The piece of gel was placed into an eppendorf tube and the DNA extracted using a gel extraction kit according to the manufacturer's instructions (BRESAGEN; Table 2.13).

2.2.6. Phenol/chloroform/isoamyl alcohol purification

An equal volume of phenol/chloroform/isoamyl alcohol (24:1:1 v/v/v, Sigma) was added to the DNA sample to be purified. Thorough mixing was achieved by vortexing for ~ 20 seconds. Samples were centrifuged at 14000 rpm for 10 minutes (Eppendorf centrifuge, 5415C). The aqueous phase was transferred into a clean eppendorf tube. Ethanol precipitation of the DNA was carried out as described in the next section.

2.2.7. Ethanol precipitation

For precipitation, to the sample containing DNA, 1/10 of the sample volume of 3M NaOAc (pH 5.2) and 2.5 × the sample volume of ice-cold 100% EtOH were added. Samples were incubated overnight at -70°C. Precipitated DNA was collected by centrifugation at 14000 rpm for 30 minutes (Eppendorf centrifuge, 5415C) and at 4°C. The supernatant was discarded and the pellet briefly rinsed in 500 µl of cold 70% EtOH and re-centrifuged at 14000 rpm for 10 minutes at 4°C (Eppendorf centrifuge, 5415C). The resulting supernatant was carefully aspirated and the DNA pellet was air-dried in order to remove any trace of EtOH. The pellet was resuspended in TE buffer (Table 2.2) and stored at either 4°C or -20°C until use.

2.2.8. Ammonium acetate precipitation

Ammonium acetate (NH_4OAc) was used preferentially for precipitation of DNA in the supercoiling assay (Section 2.5.4). To each of the DNA samples, 53 µl of 7.5 M NH_4OAc and 265 µl of ice-cold 100 % ethanol were added. Samples were retained at -70°C for 1 hour, after which DNA was collected by centrifugation, as described above.

2.2.9. Restriction endonuclease digestion

Plasmid DNA or oligonucleotides were digested using 1 unit of a restriction endonuclease (see Table 2.11) per µg of DNA in the presence of the appropriate buffer (supplied by the manufacturer) and BSA (1 µg/ml final concentration). Reactions were typically carried out in a total volume of 10 µl. Digestion was allowed to proceed for 1 - 3 h at the optimal temperature for enzymatic activity (usually 37°C). The progress of the reaction was monitored using agarose gel electrophoresis (Section 2.2.4). The reaction was terminated by heating at 65 - 85°C for 15 - 20 minutes. For the digestion of more than 1 µg of DNA, reactions were scaled up accordingly. For use in ligation reactions, the digested DNA was purified using agarose gel electrophoresis and gel extraction (Section 2.2.4 and 2.2.5).

2.2.10. Dephosphorylation

Linearised plasmid DNA was dephosphorylated before blunt-ended ligations were performed. Calf intestinal phosphatase (CIP, Boehringer) was added to a final concentration of 0.5 U/µg of plasmid DNA in One-Phor-All buffer (Gibco BRL, Pharmacia). Reactions were incubated at 37°C for 15 min. This was followed by heat inactivation of the enzyme at 45°C for 5 minutes and 85°C for 15 minutes. Phenol/chloroform/isoamyl alcohol purification (Section 2.2.6) followed by ethanol precipitation (Section 2.2.7) were performed in order to remove the CIP and purify the DNA.

2.2.11. Ligation

Ligation of DNA fragments was achieved by combining the insert DNA with the linearised vector at a molar ratio of 10:1. The ligation mixture also contained 1× T4 DNA ligase buffer (Boeringer) and 400 U T4 DNA ligase (Boehringer). If blunt ended ligations were performed (see Section 2.2.10), 1× polyethylene glycol (Boehringer) was also included in the reaction mix. The final reaction volume was 20 µl. Reactions were incubated at 22°C for 4 hours or at 15°C overnight. Half of the ligation mix was used to transform competent *E. coli* cells using the heat shock method (Section 2.2.1.2). In order to confirm that ligation had occurred, 500 ng of DNA from each component of the ligation reaction (insert, vector, ligation mix before addition of ligase and ligation mix after the reaction) was analysed using agarose gel electrophoresis (Section 2.2.4). The presence of high molecular weight bands and the disappearance of the insert band in the post-ligation sample indicated a successful ligation. A negative control in which the DNA insert was replaced with an equal volume of ddH_2O was included in all ligation experiments in order to establish the probability of re-ligation of the vector.

2.2.12. Polymerase chain reaction (PCR)

PCR was carried out to amplify DNA fragments for cloning or to screen for the insertion of a fragment of interest in recombinant plasmids. High fidelity Pfu Turbo DNA polymerase was used for cloning experiments, whereas Taq DNA polymerase was used for analysis or screening purposes. Polymerase enzymes were purchased with the requisite nucleotides and buffers (Table 2.11). The primers used are shown in Table 2.10.

PCR reactions were assembled on ice. Into each sterile PCR tube was added 4 µl of dNTP cocktail, comprising of 2.5 mM each of dATP, dCTP, dGTP and dTTP, 5µl of 10 × PCR buffer (100 mM Tris-HCl, 15 mM $MgCl_2$ and 500 mM KCl pH 8.3), a final concentration of 250 nM of each primer, 0.5 units of Taq polymerase (or 2.5 units of Pfu turbo) and sterile ddH_2O to a final volume of 48 µl. The remaining 2 µl was made up by DNA of concentration 50 ng/µl (or sterile ddH_2O to constitute the 'blank' control sample).

Conditions for PCR were optimised for each DNA fragment with respect to DNA concentration and thermal cycling, using a temperature gradient (BioRad i-cycler). Typically, the reactions were carried out under the following conditions: pre-amplification denaturation ('hot start') at 94°C for 30 seconds, followed by 30 cycles, each consisting of denaturation 94°C for 30 seconds, primer annealing at temperatures 4 - 10°C below the T_m of the primers for 30 seconds, and extension at 72°C for 1 minute per kilobase of the product (Taq polymerase) or 2 minutes per kilobase of the product (Pfu turbo). A 10 µl aliquot of each PCR product was analysed using

agarose gel electrophoresis (Section 2.2.4). Samples were retained at 4°C until use.

2.2.13. Polymerase chain reaction from bacterial colonies

PCR performed directly on transformed *E. coli* cells was used to screen for the presence of the DNA insert of interest. Single colonies were picked with a sterile pipette tip and spotted onto a fresh agar plate before resuspending in 50 µl of sterile water. Lysis was completed by heating for 10 min at 65°C. The lysate was retained on ice while the PCR reaction was prepared essentially as described above, with the exception that the final volume of the reaction mix was 45 µl, with the remaining volume being 5 µl of lysate. The thermal cycle program was used, as described above. PCR products were analysed using 1 % agarose gel electrophoresis (Section 2.2.4).

2.2.14. DNA sequencing

Cloning was verified by restriction digest analysis and direct sequencing of DNA. Each sequencing reaction contained 500 ng of plasmid, 3.2 pmol of sequencing primer, 8 µl of BigDye Terminator Mix (ABI Prism) and sterile water, to a total volume of 20 µl. The sequencing reaction was performed through 25 thermal cycles consisting of 96°C for 10 seconds, 50°C for 5 seconds, and 60°C for 4 minutes (BioRad i-cycler). Unincorporated dye-labelled terminator nucleotides were removed from the mixture by ethanol precipitation (by adding 2 µl 3M NaOAC and 50 µl 100% EtOH). The mixture was incubated on ice for 7 minutes and centrifuged at 14000 rpm for 30 minutes in a benchtop centrifuge (Eppendorf centrifuge, 5415C). The supernatant was discarded and the pellet was washed briefly with 500 µl 70% EtOH. The pellet was re-centrifuged at 14000 rpm for 10 minutes and air-dried. The sequence was determined using the Perkin Elmer ABI Prism 377 DNA sequencer (Biomolecular Resource Facility, JCSMR).

2.2.15. Generation of the reporter plasmid used in this study using the Gateway™ cloning system

Gateway™ cloning technology (Life Technologies) was used to generate the reporter plasmid, pGeneGrip-RFP, used in this study. The Gateway™ cloning system is based on site-specific recombination reactions of bateriophage λ in *E. coli*, mediated by proteins from both organisms. Recombination sites (*att*) flank the genes of interest and interact during two sequential events:

attB x *attP* ⇒ *attL*-flanked gene within the Entry clone

attL x *attR* ⇒ *attB*-flanked gene within the Expression clone.

The cloning technology involves generation of an Entry vector containing the gene of interest, flanked by *attL* sites. The gene of interest is recombined into a cassette flanked by *attR* sites

within a Destination vector containing the plasmid backbone of interest. This recombination produces an Expression clone comprising the plasmid backbone of interest into which the gene of interest has been transferred.

2.2.15.1. Construction of the Entry clone using the 'BP recombination reaction'

The coding region of the red fluorescent protein (RFP) was PCR amplified (Pfu Turbo, Section 2.2.12) from pDSRed (Table 2.9) (Clontech) using custom-made primers designed to insert *attB* sites flanking the gene (Table 2.10; thermal cycling at 95°C for 5 minutes, 25 cycles of 95°C for 30 seconds, 74°C for 30 seconds, 72°C for 2 minutes and an extension of 72°C for 5 minutes). The PCR product (*attB*-flanked *RFP* gene) was gel purified (Section 2.2.5). pDONR201™ (Table 2.9) was amplified by bacterial culture and purified using a plasmid miniprep kit (Qiagen; Section 2.2.2). The plasmid was further purified by phenol/chloroform/isoamyl alcohol extraction (Section 2.2.6). The *attB*-flanked *RFP* gene and pDONR201™ were recombined in the presence of BP clonase™ enzyme mix in a 'BP reaction' according to the manufacturer's protocol (Life Technologies; Table 2.11). From the reaction mix, 1 µl was used to transform competent DH5α *E. coli* cells (Table 2.8) using the heat shock method (Section 2.2.1.2). Transformed cells were selected overnight at 37°C on agar plates containing 50 µg/ml kanamycin. Colonies were picked the following morning and positive recombination clones were identified by restriction digest analysis using HpaI and SacII (Section 2.2.9). A positive clone was selected, amplified by bacterial culture and purified using the plasmid maxiprep kit (Qiagen) for use in the 'LR recombination reaction' (Section 2.2.15.3). This clone was named pEntry-RFP.

2.2.15.2. Construction of the Destination vector

pGeneGrip™ (Table 2.9) was converted into a Gateway™-compatible Destination vector by inserting a suitable reading frame Destination cassette (*ccdB* gene, Chloramphenicol^R; Gateway™ vector conversion system, Life Technologies). Destination cassette A was inserted by blunt-end ligation into the EcoRV site within the multiple cloning site (MCS) of pGeneGrip (see Sections 2.2.9, 2.2.10 and 2.2.11). The ligation product was transformed into DB3.1™ competent cells (Table 2.8, donated by M. Roberston, Plant Industries, CSIRO, Canberra) using the heat shock method (Section 2.2.1.2) and plated onto agar containing chloramphenicol (30 µg/ml). Positive clones were identified by restriction digest analysis using EcoRV and SalI (Section 2.2.9) and colony PCR (Taq polymerase, Section 2.2.13) using the pGeneGrip sequencing primers designed to sequence across the pGeneGrip MCS (Gene Therapy Systems; Table 2.10; thermal cycling at 95°C for 5 minutes, 25 cycles of 95°C for 30 seconds, 55°C for

30 seconds, 72°C for 30 seconds minutes and an extension of 72°C for 5 minutes). A positive clone, pGeneGrip-DestA (Kanamycin^R/Chloramphenicol^R; Table 2.9) was amplified in DB3.1™ *E. coli* cells (Table 2.8) which contain a gyrase mutation conferring resistance to the otherwise lethal *ccdB* gene within the Destination cassette. pGeneGrip-DestA was purified using the plasmid maxiprep kit (Section 2.2.2; Qiagen).

2.2.15.3. Construction of the Expression clone using the 'LR recombination reaction'

The pGeneGrip-DestA destination vector and the pEntry-RFP entry clone were recombined according to the protocol provided by Life Technologies using an 'LR reaction', mediated by LR Clonase™ (Life Technologies). The recombination reaction was transformed into competent DH5α *E. coli* cells (Table 2.8) using the heat shock method (Section 2.2.1.2) and plated onto agar. Kanamycin (50 µg/ml) resistance and the loss of the *ccdB* gene, which permitted propagation of DH5α *E. coli* cells, provided the basis for selection of positive recombination clones containing the pGeneGrip vector with the RFP gene. Colonies were screened by PCR (Taq polymerase, Section 2.2.13) using primers for the pGeneGrip MCS (Gene Therapy Systems; Table 2.10; thermal cycling at 95°C for 5 minutes, 25 cycles of 95°C for 30 seconds, 55°C for 30 seconds, 72°C for 30 seconds minutes and an extension of 72°C for 5 minutes). Restriction digestion using EcoRV and XhoI was performed also to verify the presence and orientation of the inserted *RFP* gene (Section 2.2.9). The resulting expression vector was named pGeneGrip-RFP. pGeneGrip-RFP served as the reporter plasmid used in this study.

2.2.16. Labelling of pGeneGrip-RFP using peptide nucleic acid hybridisation

pGeneGrip™ vector (Gene Therapy Systems) contains a region comprising 8 concatameric binding sites to which short, linear peptide nucleic acid (PNA) molecules can hybridise in a sequence specific manner and with high affinity (Zelphati *et al.*, 2000; Zelphati *et al.*, 1999). PNA 'clamps' have been conjugated to a variety of molecules, such as fluorescein and maleimide. In this study, PNA chemistry was used to label the pGeneGrip-RFP reporter plasmid with fluorescein, which allowed tracking of the DNA within transfected cells. PNA-maleimide labelling facilitates coupling of peptides containing a cysteine residue by thiol alkylation chemistry and was used to conjugate optimised NLS peptide to the pGeneGrip-RFP reporter plasmid. Fluoresceination of the NLS peptide enabled DNA tracking of the NLS-coupled plasmid. As the plasmid DNA retains a supercoiled conformation and is transcriptionally active (Gene Therapy Systems), expression of a reporter gene is unhindered by the labelling process, permitting DNA tracking and gene expression to be analysed in tandem.

2.2.16.1. pGeneGrip-RFP labelling with PNA-fluorescein

The PNA-fluorescein labelling kit (Table 2.13) was purchased from Gene Therapy Systems and the protocol followed was according to the manufacturer's instructions. Briefly, pGeneGrip-RFP was purified by phenol/chloroform/isoamyl alcohol (Sections 2.2.6 and 2.2.7) and resuspended in 50 µl ddH_2O according to the calculation:

$$X = [(\text{plasmid size in kb})/5] \times 100, \text{ where X is } \mu g \text{ of plasmid DNA}$$

To the DNA solution, 100µl of 2 × labelling buffer and 50µl PNA-fluorescein label were added. The labelling reaction was incubated at 37°C for 2 hours. To remove unincorporated label, isopropanol precipitation was used. The salt concentration was brought to 1 M using 3 M NaOAc (pH 5.6) (100 µl) and 0.7 × the volume of isopropanol (210 µl) was added. The solution was mixed well by pipetting and centrifuged at 14000 rpm for 20 minutes (Eppendorf centrifuge, 5415C). The supernatant was discarded, the DNA pellet rinsed with 500µl of 70% ethanol and re-centrifuged to recover the DNA. The pellet was air-dried for 10 minutes and the plasmid resuspended in 100 µl of 1 × labelling buffer. The labeled DNA was quantitated spectrophotometrically (Section 2.2.3) and used immediately for assembly into chromatin (Section 2.5.2), during the dialysis procedure of which, any remaining unbound label was further removed.

PNA-fluorescein labelling was verified using agarose gel electrophoresis (Section 2.2.4). A 50 ml horizontal slab agarose gel was prepared. An ethidium-free gel apparatus was used. pGeneGrip-RFP and fluorescein-labelled pGeneGrip-RFP were electrophoresed side-by-side (1.2 and 2.4 µg/well). The presence of fluorescein was visualised using a Fluorimager (FLA-3000, Fuji, excitation 473 nm; emission 538 nm). DNA was visualised by EtBr staining under UV illumination (FLA-3000, Fuji, excitation 473 nm; emission 580 nm). Co-incidence of fluorescein-positive and EtBr stained bands confirmed labelling.

2.2.16.2. Conjugation of NLS peptide, with and without FITC, to pGeneGrip-RFP using PNA-maleimide

The pGeneGrip-RFP plasmid was labelled with PNA-maleimide using the PNA-maleimide labelling kit (Table 2.13) as recommended by the manufacturer (Gene Therapy Systems), essentially as described above for PNA-fluorescein.

An optimised NLS peptide (Xiao and Jans, 1998; Xiao *et al.*, 1998; Hubner *et al.*, 1997), comprising the SV40 T-ag amino acids CG^{110}PGSDDEAAADAQHAAP**PKKKRKV**^{132}GY was synthesised with and without an FITC group on the N-terminal cysteine residue (K.N.

McAndrew, Biomolecular Resource Facility, JCSMR). The N-terminal cysteine residue was included in the NLS peptide in order to provide the means for coupling to the maleimide moiety using thiol alkylation chemistry (see Figure 6.6). The final product is formed via a chemically stable thioether bond involving the nucleophilic addition of cysteine-thiolate to the maleimide derivative.

Immediately after performing the PNA-maleimide labelling reaction, 6 nmoles of NLS peptide ± FITC (corresponding to a 20-fold molar excess) was added, as recommended by Gene Therapy Systems. The reaction mix was incubated at room temperature for 4 hours and then retained at 4°C overnight. The following day, labelled DNA was precipitated using isopropanol (as described above in Section 2.2.16.1) and the pellet resuspended in 1 × labelling buffer. This step was repeated to ensure removal of excess PNA-maleimide and NLS peptide. The labeled DNA was quantitated spectrophotometrically (Section 2.2.3) and used immediately for chromatin assembly (Section 2.5.2). Any remaining unbound label was further removed during the chromatin dialysis procedure.

2.3. GENERAL PROTEIN METHODS

2.3.1. Quantitation

2.3.1.1. BioRad protein assay

The concentration of proteins was determined using the BioRad protein assay according to manufacturer's instructions (BioRad). Briefly, solutions containing 2 - 14 µg of bovine serum albumin (BSA) made up to 800 µl in ddH_2O were used to produce a standard curve. Similarly, dilutions of the test protein were prepared. The BioRad protein binding reagent was added (200 µl) to the solutions to a final volume of 1 ml and mixed thoroughly by pipetting. Reactions were incubated for 10 minutes at room temperature. Absorbance was measured at 595 nm and values were corrected using a reference solution containing 800 µl of ddH_2O and 200 µl of BioRad reagent. The concentration of protein was calculated using the BSA standard curve.

2.3.1.2. Spectrophotometry

The concentrations of individual histones and the reconstituted octamers were determined spectrophotometrically at 276 nm. Histone solutions were normalised to background at 600 nm. Absorbance was then measured at 276 nm and 320 nm. The absorbance at 320 nm was subtracted from the absorbance at 276 nm and the average of three readings was calculated. The equation $A = \varepsilon c l$ where l is 1 cm and ε is the extinction coefficient, provided in Luger *et al.*

(1999) was used to determine c, the concentration in mg/ml.

2.3.2. SDS-polyacrylamide gel electrophoresis

Proteins were separated using SDS-polyacrylamide gel electrophoresis (SDS-PAGE), providing information on their purity and molecular weight. Typically, 18 % SDS-PAGE was used for analysis of histones.

A protein mini-gel apparatus (BioRad) was assembled. The 18 % running gel solution was prepared in a final volume of 10 ml (18 % acrylamide-bis, 0.39 M Tris-HCl pH 8.8, 0.1 % SDS, 0.5 % ammonium persulphate, 0.05 % TEMED) and pipetted between the glass plates to 1 cm below the lower edge of the comb. The gel was overlaid with butanol (which facilitates setting to yield a smooth gel surface) and allowed to polymerise for at least 1 hour at room temperature. The butanol was removed and a 4% stacking gel prepared in a final volume of 4 ml (4 % acrylamide-bis, 0.125 M Tris-HCl pH 6.8, 1 % SDS, 1 % ammonium persulphate, 0.1 % TEMED) was carefully layered above the running gel. The comb was inserted and the gel was also allowed to set for 1 hour.

Protein samples were prepared for loading into the gel by adding an equal volume of 2 × SDS loading buffer (Table 2.3). Each lane accommodated 20 µl of sample. Electrophoresis was carried out in 1 × SDS-PAGE buffer (Table 2.3), initially at 80 V until the bromophenol blue dye marker reached the top of running gel and then at 120 V through the running gel. Gels were either stained with Coomassie brilliant blue or prepared for Western blot transfer (Sections 2.3.3 and 2.3.4).

2.3.3. Coomassie blue staining

Gels were stained in Coomassie brilliant blue solution (Table 2.3) overnight and destained for at least 2 - 5 hours with several changes of destaining buffer (Table 2.3). Destaining was performed with gentle rocking on a Platform rocker (setting 5, Bio-line, Edwards Instrument Company). The molecular weight of the protein was estimated by comparison with the bands of a standardised pre-stained molecular weight marker (Benchmark Pre-stained protein ladder, GibcoBRL).

2.3.4. Western blot

Western blotting (immunoblotting) to detect the protein of interest consisted of three stages: transfer of the protein onto a nitrocellulose (NC) membrane, probing the membrane with

antibodies and visualisation using chemiluminescence.

Protein samples were electrophoresed through duplicate 18 % SDS-polyacrylamide gels. A 'transfer sandwich' was constructed consisting of layers in order of, firstly, foam backing, followed by Whatman paper (Advantec MFS), the SDS- polyacrylamide gel, one NC transfer membrane (Optitran BA-S 85, Schleicher & Schuell) (cut to the size of the gel), Whatman paper and lastly, foam backing. Air-bubbles were removed from the 'sandwich' by gently rolling over with a pipette. All components were equilibrated briefly in transfer buffer (Table 2.3). The transfer apparatus (Mini Trans-Blot Transfer apparatus, BioRad) was assembled according to the manufacturer's instructions and filled with transfer buffer (Table 2.3). Transfer was performed at room temperature overnight at 10 V and with stirring of the buffer. The remaining duplicate gel was analysed using Coomassie blue staining (Section 2.3.3).

The efficiency of transfer was monitored by staining the NC membrane in Ponceau S (Table 2.3) for 15 minutes at room temperature with gentle agitation (setting 5, Bio-line, Edwards Instrument Company). The membrane was destained in two steps of 5 minutes each in Ponceau S destain (Table 2.3), before rinsing with ddH_2O. A digital image of the Ponceau S-stained NC membrane was captured using the LAS-1000 imaging system (Fuji, Japan). The NC membrane was placed in Blocking solution (Table 2.3) and incubated overnight at 4°C, with gentle agitation (setting 5, Bio-line, Edwards Instrument Company).

The NC membrane was incubated in primary antibody (Table 2.12; diluted in Blocking solution) for 90 minutes at room temperature, washed 3 times for 10 minutes each time with TBST solution (Table 2.3) and incubated for an additional hour at room temperature in secondary antibody (Table 2.12; diluted in Blocking solution). This was followed by another series of washes using TBST and a final brief rinse in ddH_2O. All incubations and washing steps were carried out with gentle agitation (setting 5, Bio-line, Edwards Instrument Company). For visualisation of the protein of interest, the SuperSignal detection kit (Table 2.13; Pierce) was used. The protocol supplied by the manufacturer was followed. Digital images were captured using the LAS-1000 (Fuji, Japan) on 'chemiluminescence' settings.

2.3.5. Silver staining

After SDS-PAGE (Section 2.3.2) was performed, gels were fixed in 50 % MeOH for 40 minutes, with gentle agitation on a platform rocker (setting 5, Bio-line, Edwards Instrument Company). A solution of 0.36 % NaOH (0.9 ml of 10 M NaOH in 100ml ddH_2O) was prepared and 21 ml was transferred into a clean beaker. To this, 1.4 ml of concentrated NH_4OH was added. In a Falcon tube, 0.8 g of silver nitrate was dissolved in 4 ml ddH_2O. This solution was

carefully added drop-wise to the NaOH solution, with vigorous stirring to ensure that the silver remained in solution. The volume was made up to 100 ml with ddH_2O. The MeOH solution was poured off and the gel briefly rinsed in ddH_2O. The silver stain was poured onto the gel and incubated with gentle rocking for 15 minutes at room temperature. The gel was thereafter rinsed 3 times with ddH_2O and developed in developing solution (0.05 % formaldehyde, 0.005 % citric acid) until a desired level of staining was reached. The reaction was stopped with replacement of the developing solution with a solution of 40 % MeOH, 10 % acetic acid. All water used in the silver staining protocol was Milli Q filtered.

2.4. PREPARATION OF RECOMBINANT PROTEINS

2.4.1. Importin-GST fusion proteins

Importin α2 (pTAC58) and importin β1 (pTAC97) subunits from mouse were expressed as glutathione-S-transferase (GST)-fusion proteins and purified by glutathione affinity chromatography by Dr C-Y Xiao, A.P. John, C.L. Barton and L. Wijeyewickrema (Nuclear Signalling Laboratory, JCSMR), as described previously (Jans and Jans, 1994; Rihs *et al.*, 1991). All samples were stored in 20 µl aliquots at -70 °C until use.

2.4.2. Core histone proteins

Recombinant *Xenopus laevis* histones H2A and H2B were purified according to the method of Luger *et al.* (Luger *et al.*, 1999), described below in Sections 2.4.2.1 and 2.4.2.2. Recombinant *Xenopus laevis* histones H3 and H4 were kindly donated by Dr J-Y. Fan (Chromatin and Transcriptional Regulation Group, JCSMR). Histone dimers H2A/2B and H2AZ/2B were prepared according to the method of Hayes and Lee (Hayes and Lee, 1997), as described in Section 2.4.2.4. Histone dimers H2AZ/2B were kindly donated by M. Clarkson (Chromatin and Transcriptional Regulation Group, JCSMR). Histone tetramers H3/4 and acetylated H3/4 (H3/4-ac) were purified from chicken and HeLa cells, respectively, by L. Hyman (Chromatin and Transcriptional Regulation Group, JCSMR), as previously described (Simon and Felsenfeld, 1979). All chromatography was performed in the Biomolecular Resource Facility, JCSMR under the guidance of Dr P. Milburn.

2.4.2.1. Expression of recombinant histones in *BL21DE3lysS E.coli* cells

BL21DE3p(lysS) cells (Table 2.8; Promega and One Shot®, Invitrogen) were transformed with pET3a-H2A, pET3a-H2B (containing the coding region for *Xenopus laevis* histones H2A and

H2B, respectively; Table 2.9) or pET5a-H2A-NLS (containing the coding region for a C-terminal fusion of the *Xenopus laevis* histone H2A and the optimised SV40 T-ag NLS; Table 2.9) according to the manufacturer's instructions. Transformed cells were plated onto agar containing 100 µg/ml ampicillin and 30 µg/ml chloramphenicol and cultured overnight at 37°C. The following morning, colonies were selected and used to inoculate 8 to 10 5 ml starter cultures. These cultures were divided into 'non-induced' and 'induced' samples, according to treatment with 0.5 mM IPTG for 2 hours. SDS-PAGE (18 %) was used to identify the highest expressor (Section 2.3.2). This sample was used to inoculate a larger culture of 800 ml LB media (Table 2.1), containing 30µg/ml chloramphenicol and 100µg/ml ampicillin. The culture was incubated at 37°C and 180 rpm for ~ 2 hours or until the absorbance at 600 nm was ~ 0.6 (optimal level for induction). At this stage, 500µl of culture was removed and retained as the 'non-induced' sample. IPTG was added to a final concentration of 0.5 mM and the culture was incubated for a further 3 - 4 hours at 37°C and 180 rpm and then overnight at room temperature with gentle shaking (100 rpm). Another 500 µl sample ('post-induction') was retained for SDS-PAGE analysis. The culture was centrifuged at 4500 rpm for 15 min at room temperature (GSA rotor, Sorvall). The cell pellet was resuspended in 20 ml Wash buffer (Table 2.4) and stored at -20°C until further purification.

2.4.2.2. Purification of recombinant histones

Histone purification involved three steps; preparation of inclusion bodies, gel filtration and ion exchange chromatography. The purification procedure was essentially carried out as described by Luger *et al.* (1999), but was scaled down accordingly for a 1 litre bacterial culture. The buffers used for these procedures were also from Luger *et al.* (Luger *et al.*, 1999) and are detailed in Table 2.4. A Superdex 200 HR 10/30 column (Amersham Pharmacia Biotech) was used for gel filtration. A Resource S ion exchange column (Amersham Pharmacia) was used to recover the core histone proteins using a 200 - 600 mM NaCl gradient (SAU-200 and SAU-600, Table 2.4). Purified histones were lyophilised and stored at -20°C until reconstitution into an octamer, as described below.

2.4.2.3. Reconstitution of histone octamers from purified recombinant histones

Purified recombinant *Xenopus laevis* histones H2A, H2B, H3 and H4 (Section 2.4.2.1 and 2.4.2.2) were reconstituted into octamers as described by Luger *et al.* (1999). The recombinant purified histones stored in lyophilised form were carefully solubilised by mixing, using a pasteur pipette, in 1.5 ml of Unfolding buffer (Table 2.4). Unfolding was allowed to proceed at room temperature for between 30 minutes and 3 hours, after which the concentration of histones was determined by measuring the absorbance at 276 nm, as described in Section 2.3.1.2. H2A

and H2B were mixed in equimolar proportions and H3 and H4 were added at 98 % that of H2A, so that the final molar ratios of H2A:H2B:H4:H4 were 1:1:0.98 0.98. The molar excess of H2A and H2B ensures maximal incorporation of H3 and H4 into the octamer as, under octamerisation conditions, excess H3 and H4 form tetramers which are difficult to purify from the octamer using gel filtration chromatography (Luger *et al.*, 1999). The concentration of the histone mix was determined and the final concentration adjusted to 1 mg/ml by adding Unfolding buffer (Table 2.4). The histone mix (typically having a volume between 2 – 4 ml) was transferred into dialysis tubing with a molecular weight cut off (MWCO) of 6000 – 8000 Da (Spectra/Por® membrane, flat width 10 mm, Spectrum Laboratories) and dialysed against 4 l of Refolding buffer (Table 2.4) at 4°C overnight, with at least 3 changes of buffer.

After overnight dialysis, the sample was concentrated to around 1 ml using a Centricon filter device (YM-10, Amicon) at 3000 rpm (Allegra 6 Centrifuge, Beckman) over a period of 3 hours. During this time, the gel filtration column (HiLoad 16/60 Superdex 200 prep grade, Pharmacia) was prepared by washing extensively with ddH_2O and then equilibrating in two column volumes (~ 120ml) of Refolding buffer (Table 2.4). Gel filtration was carried out at 4°C. The flow rate was set to 1 ml/min. A chromatogram was generated at 276 nm. The first 40 ml of flowthrough (waste material) was collected into a 50 ml Falcon tube, after which the fraction collector was set to recover 1 ml fractions every minute.

The fractions corresponding to peaks on the chromatogram were analysed using 18 % SDS-PAGE (Section 2.3.2). Fractions containing equimolar amounts of the constituent histones (indicating octamer formation) were pooled. The concentration of octamer was determined spectrophotometrically as described in Section 2.3.1.2 using the equation $A = \varepsilon cl$. The extinction co-efficient (ε) for the reconstituted histone octamer is 0.45 (Luger *et al.*, 1999).

Protease inhibitors were added (PMSF, 5.75 µl for every 10 ml from a 100 mM stock; Pepstatin A, 8 µl from 2.5 mg/ml stock; Leupeptin, 2 µl from a 10 mg/ml stock) and purified histone octamers were stored at 4 °C until use.

2.4.2.4. Dimerisation and refolding of recombinant H2A/2B

Equimolar amounts of recombinant *Xenopus laevis* H2A and H2B (Section 2.4.2.1 and 2.4.2.2) (typically of volume 2.5 ml) were pipetted into dialysis tubing with MWCO 6000 – 8000 Da (Spectra/Por® membrane, flat width 10 mm, Spectrum Laboratories). Dialysis was carried out overnight at 4°C against 0.5 M NaCl buffer I (500 mM NaCl, 50 mM HEPES pH 7.5, 1 mM DTT, 0.1 % NP-40, 0.05 mM PMSF), with one change the following morning. BioRex-70 resin was prepared by equilibrating 1 g in 0.5 M NaCl buffer II (500 mM NaCl, 50 mM HEPES pH

7.5, 0.05 mM PMSF) for 1 hour at 4°C. The resin was poured into a 14 ml round-bottomed Falcon tube to 1ml of settled volume and as much buffer as possible was aspirated. The dialysed histone sample was added to the resin. Following incubation at 4°C for 1 – 2 hours with gentle agitation (setting 5, Bio-line, Edwards Instrument Company), the resin slurry was transferred into a 10 ml poly-prep chromatography column (BioRad) and washed with 10 column volumes of 0.5 M NaCl buffer II. H2A/2B dimers were eluted by gravitational flow using 0.5 M NaCl buffer II. A total of 10 fractions of 300 µl each were collected. Typically, the dimers appeared in the second and third fractions.

Fractions containing the highest concentration of dimers were identified by SDS-PAGE (15 %, see Section 2.3.2) and silver staining (Section 2.3.5). These fractions were pooled and dialysed against H2A/2B buffer (200 mM NaCl, 10 mM HEPES pH 7.5, 0.1 mM EDTA). Aliquots of H2A/2B were stored at -70°C until use.

2.4.3. Recombinant chromatin assembly proteins NAP-1 and N1/N2

Recombinant NAP-1 and N1/N2 were kindly donated by N. Siddon (Chromatin and Transcriptional Regulation Group, JCSMR). Recombinant NAP-1 and N1/N2 were expressed from the plasmids pQE-N1/N2 and pQE-NAP-1 as described in Johnson-Saliba *et al.* (2000).

2.5. CHROMATIN METHODS

2.5.1. Chromatin assembly using NAP-1

Small scale assembly of 300 ng of plasmid DNA into chromatin was carried out using the NAP-1-based system for the purpose of performing a supercoiling assay (Section 2.5.4). The assembly reaction comprised of purified chicken H3/4 tetramer (Section 2.4.1), recombinant *Xenopus laevis* H2A/2B dimer (Section 2.4.2.4), recombinant NAP-1 (Section 2.4.3), 300 ng of plasmid DNA, 2 units Topoisomerase I (Promega) and 1.5 mM ATP. The reaction was performed in 1 × EB buffer (1 mM EGTA, 20 mM HEPES pH 7.0, 5 mM KCl, 10 % glycerol (v/v), 0.5 mM DTT and 10 mM β-glycerol phosphate) in a total volume of 12 µl. As each preparation of recombinant components of the reaction differed in their ability to induce supercoiling (Section 2.5.4), the volumes of the H2A/2B dimer, H3/4 tetramer and NAP-1 were determined by titration. Typically, 1.5 – 3 µl of H2A/2B dimer, 0.5 – 1 µl of H3/4 tetramer and 1 – 4 µl of NAP-1 were used. The reaction was performed at 27°C for 4 hours.

2.5.2. Chromatin assembly using octamer transfer by salt dialysis

Large scale assembly of 30 – 100 µg of plasmid DNA into chromatin was performed using purified recombinant histone octamers (Section 2.4.2.3) by stepwise dialysis from a high to low salt buffer essentially according to the method originally described by Thomas and Butler (Luger *et al.*, 1999; Richmond *et al.*, 1988; Thomas and Butler, 1977). The originally described dialysis buffers contained EDTA which is known to chelate metal ions, thus inhibiting the function of several key enzymes required for cell survival. This was believed to be responsible for cell lysis that was observed by light microscopy in the initial transfection experiments that were conducted using chromatin constructs in EDTA-containing buffer. Consequently, EDTA was thereafter omitted from the salt dialysis procedure, without any impact on the formation of chromatin. The physiological nucleosome density is 1 for every ~ 230 bps of DNA. The pGeneGrip-RFP reporter plasmid used in this study comprises 5889 bp and was calculated to be saturated (physiological nucleosome density) with 25 histone octamers. Chromatin constructs were therefore assembled at a stoichiometry of 0, 1, 2, 4, 10, 25 or 40 histone octamers per plasmid.

The chromatin assembly reaction contained DNA, 5 M NaCl/TE, histone octamer and TE, as set out below. All solutions were stored at 4°C but were retained on ice while the assembly reaction was composed. The reaction components were pipetted into eppendorf tubes in the following order:

1. DNA
2. TE (to final volume of 400 µl)
3. 5 M NaCl/TE
4. histone octamer.

Typically, 50 µg of pGeneGrip-RFP was assembled into chromatin per assembly reaction.

The volume of histone octamer was calculated using the equation:

$$r = \frac{\text{moles of octamer}}{\text{moles of DNA}}$$, where r is the ratio of octamers to DNA

$$= \frac{\text{conc. of octamer} \times \text{volume}}{\text{molar mass of octamer}} + \frac{\text{mass of DNA}}{\text{molar mass of DNA}}$$

The molar mass of a histone octamer containing H2A, [2(H2A/H2B)/($H3_2$/$H4_2$)], is 108486 µg/µmol. The molar mass of a histone octamer containing H2AZ, [2(H2AZ/H2B)/($H3_2$/$H4_2$)], is 107 408 µg/µmol.

The initial salt concentration of the assembly reaction was set to 2 M using 5 M NaCl/TE in order to maintain octamer stability (as the salt concentration falls below 2 M, the octamer is prone to dissociation). The volume of 5 M NaCl/TE added was calculated with respect to the volume of octamer using the equation:

$$5\ M \times X\ \mu l = 2\ M \times (\text{total reaction volume} - \text{volume of octamer})$$

TE was added to bring the final reaction volume to 400 µl. The assembly reactions were carefully transferred into dialysis tubing with a MWCO of 6000 – 8000 Da (Spectra/Por® membrane, flat width 10 mm, Spectrum Laboratories) that had been pre-soaked in the first dialysis buffer, 1 M NaCl/Tris-HCl (Table 2.5). Dialysis was performed at 4°C, with gentle stirring.The first stage of dialysis was carried out against 1 M NaCl buffer (Table 2.5) for 3 – 4 hours. The assembly reactions were thereafter transferred into 0.75 M NaCl buffer (Table 2.5) for a further 3 - 4 hours. The final dialysis step was carried out against 135 mM NaCl buffer (Table 2.5), overnight.

The DNA content of the chromatin constructs was quantitated spectrophotometrically (Section 2.2.3). Chromatin samples were stored at 4°C until use, for no longer than 6 weeks.

2.5.3. Sedimentation velocity ultracentrifugation

Sedimentation coefficients (*s*-values; Svedberg units, *S*) of the various chromatin constructs (Section 2.5.2) were determined using analytical ultracentrifugation, as described by Schwarz and Hansen (1994) and Carruthers *et al.* (1998). For sedimentation velocity ultracentrifugation experiments, chromatin was dialysed against a final buffer containing 2.5 mM NaCl/TE. This was to prevent the induction of non-specific salt-induced compaction that has been observed at physiological salt concentration of 135 mM (Section 2.5.2) (Carruthers *et al.*, 1998; Schwarz and Hansen, 1994).

Chromatin samples containing 6 µg of DNA were analysed in 2.5mM NaCl/TE buffer at a final volume of 380 µl. The reference sample contained 2.5mM NaCl/TE buffer alone at a final volume of 400 µl. Samples were transferred into ultracentrifuge cells and equilibrated at 20000 rpm for 1 hour and at 21°C (Beckman XL-A). The initial absorbance at 260 nm was 0.6 – 0.8. Ultracentrifugation was carried out overnight at 23000 rpm and 21°C. Typically, 30 absorbance scans were collected. Data were analysed as described by van Holde and Weischet (1978) using Ultrascan software (Linux), in which an algorithm divides each scan into 20 - 70 horizontal divisions and apparent *s*-values are calculated from the radial point of each division. The

apparent *s*-values are plotted against the inverse square root of time, generating a van Holde and Weischet extrapolation plot. The Ultrascan software (Linux) generates linear extrapolations through each series of horizontal divisions, which intercept the Y-axis. These intercepts are the true *s*-values for each boundary fraction. The boundary fraction was plotted against the *s*-values to obtain a van Holde and Weischet integral distribution plot. The sedimentation coefficient was read at the 0.5 (50%) boundary fraction.

2.5.4. Supercoiling assay

Prior to chromatin assembly, DNA was incubated with Topoisomerase I (Promega, 10 units/µl and used at 1 unit per µg DNA) for 1 hour at 27°C. Topoisomerase I cleaves one strand of the DNA duplex to remove negative supercoils from covalently closed circular DNA so that a relaxed, open circular structure is produced.

The chromatin assembly reactions were carried out as described (Sections 2.5.1 and 2.5.2) and the DNA content quantitated by spectrophotometry (Section 2.2.3). Around 500 ng of DNA was transferred into a clean Eppendorf tube and the volume adjusted to 50 µl with ddH_2O. SDS (2%, w/v) and proteinase K (10 mg/ml) were added at a volume of 8 µl each and the reaction was incubated either at 37°C overnight. Following this, 53 µl of 7.5 M ammominum acetate and 265 µl of ice-cold 100 % ethanol were added and the samples were retained for 1 hour at -70°C.

DNA was precipitated as described (Section 2.2.8). The recovered DNA was air-dried for 10 minutes and resuspended in 10 µl of TE buffer. To each sample, 2 µl of 6 × DNA loading dye was added (see Table 2.2) and analysis was performed using agarose gel electrophoresis (1 %, 90 V; Section 2.2.4).

2.5.5. Micrococcal nuclease digestion assay

Chromatin constructs were assembled at various stoichiometries of histone octamers (Section 2.5.2) and the DNA content was quantitated spectrophotometrically (Section 2.2.3). Chromatinised constructs containing 4µg of DNA was aliquotted for the micrococcal nuclease (MNase) assay. MNase S7 (Roche, 50 units/µl) was diluted one thousand fold in nuclease free ddH_2O (Promega, P119C) and retained on ice. The digestion reaction contained 2 mM $CaCl_2$, 10 mM Tris-Cl and 4 µg of DNA. The final reaction volume was 400µl, which was made up with nuclease free ddH_2O (Promega, P119C). To this, 25 milliunits of MNase per µg of DNA were added and reactions were allowed to proceed at room temperature. Reactions were stopped at 2, 10, 20 and 60 min by transferring 1 µg of DNA (100µl of each reaction) into 5 × Stop solution (2.5 % sarkosyl/100mM EDTA; 25 µl).

Digested DNA was purified using phenol-chloroform-isoamyl alcohol (Section 2.2.6) and recovered by ethanol precipitation (Section 2.2.7). Recovered samples were resuspended in 10µl of TE (pH 7.8), to which 2µl of 6 × DNA loading dye was added (Table 2.2). Sample analysis was performed by agarose gel electrophoresis (1.5 %, 200 ml horizontal slab gel, 90 V for around 4 hours, or until the marker dye front had migrated three quarters down the length of the gel; Section 2.2.4).

2.5.6. Atomic force microscopy

Chromatin assembly of the fully nucleosome-saturated 25 octamers per plasmid construct was carried out as described in Section 2.5.2. Non-chromatinised, naked plasmid DNA and the 25 octamers per plasmid samples were diluted to a final concentration of 10 ng/µl in 135mM NaCl/Tris-HCl.

Atomic force microscopy (AFM) was carried out as essentially as described by Hansma *et al.* (1998). Squares of mica (1.5 cm^2) were cleaved freshly, onto which 10 µl of sample was spotted. Samples were allowed to adsorb to the mica surface for 5 minutes, after which the surface was rinsed 3 times using 100 µl of sterile ddH_2O. Samples were dried briefly with a stream of compressed air. The AFM (MultiMode AFM and Nanoscope III, Digital Instruments) was operated by Dr T. Senden (Department of Applied Mathematics, Research School of Physical Sciences and Engineering, ANU). Tapping mode was performed using a 125 µm silicon cantilever, at a scanning rate of 1 – 2 Hz and oscillation 400 kHz. Images were analysed using Nanoscope software (Digital Instruments).

2.6. CELL CULTURE METHODS

2.6.1. HTC and Cos-7 cells

Hepatic tumour cells (HTC) derived from the rat Morris hepatoma 7288C cell line (Flow Laboratories, Bonn, Germany) were maintained in Dulbecco's modified Eagle's medium (DMEM; Table 2.1) containing 10 % foetal calf serum (FCS; CSL, Lot no. 097059101) which had been heat inactivated (56°C for 45 minutes). Cells were cultured in 25 cm^2 tissue culture flasks (Nunc) in a humidified incubator with atmosphere of 5 % CO_2 and maintained at 37°C (Forma Scientific Inc). Cells were subcultured every 3 – 4 days in a laminar flow hood (Airpure, Email Westinghouse) as described in Section 2.6.3.

The Cos-7 cell line, derived from the African green monkey, was provided by S. Ford (Cytokine Molecular Biology and Signalling Laboratory, JCSMR) and maintained as described above. As

the media used for HTC and Cos-7 cell culture were the same, two separate sets of culture media were used so as to minimise the possibility of cross-contamination.

For the purposes of transfection, HTC and Cos-7 cells were typically grown to 90 - 95 % confluence in 175 cm^2 tissue culture flasks (Nunc).

2.6.2. Jurkat cells

The human leukaemic T-cell line, Jurkat, was kindly provided by K. Bunting (Cytokine Gene Expression Group, JCSMR). Cells were maintained in suspension in 175 cm^2 tissue culture flasks (Nunc) in RPMI-1640 media (Table 2.1), supplemented with 10 % FCS (heat-inactivated; 56°C for 45 minutes), in a humidified incubator with atmosphere of 5 % CO_2 and at 37°C (Forma Scientific Inc). The presence of a pH indicator in the cell media was typically used to determine qualitatively when subculturing was required. Subculturing was carried out in a laminar flow hood (Airpure, Email Westinghouse) by physically agitating the cells in order to reduce the presence of clumps. Cells were counted (Section 2.6.4) and then diluted to the desired cell density using RPMI/10 % FCS. Cells were typically cultured to a concentration of 5×10^5 cells/ml prior to transfection experiments.

2.6.3. Harvesting of adherent cells

Culture media were aspirated and cells were rinsed briefly using sterile PBS. Detachment from the substratum was achieved by incubating HTC cells in 10 ml 1/10 (v/v) 0.25% Trysin-EDTA/PBS (Sigma) and Cos-7 cells in 10 ml of undiluted 0.25% Trysin/EDTA (Sigma) for up to 5 minutes in the incubator (Forma Scientific Inc). Detachment was aided by gentle physical agitation, after which the reaction was inhibited with the addition of 25 ml DMEM/10% FCS. The trypsinised cell suspension was transferred into a 50 ml Falcon tube and centrifuged at 640g (~ 1640 rpm.) (Allegra 6 Centrifuge, Beckman). The supernatant was discarded and the cell pellet was washed by resuspending in 30 ml PBS and re-centrifuging. Cells were thereafter resuspended in 2 ml PBS for counting and reseeding (Section 2.6.4) or in 500 µl PBS for analysis using flow cytometry (Section 2.9.1).

2.6.4. Cell counting

Cells were counted using a haemocytometer. Cell suspensions were diluted 1/10 in PBS, of which 10µl was applied onto the haemocytometer. Two separate fields were counted and the average count expressed as: number of cells/ml = average cell count × 10^4 × dilution factor.

2.6.5. Freezing and thawing cells

HTC and Cos-7 cells were routinely stored in liquid nitrogen. Cells were initially transferred onto dry ice from liquid nitrogen and then plunged into a water bath at 37°C until thawing was complete. Warm DMEM/10 % FCS (1 ml) was added drop wise to the thawed cells to a final volume of 10 ml. The cell suspension was centrifuged at 640 g (~ 1640 r.p.m.) (Allegra 6 Centrifuge, Beckman) and the supernatant (containing DMSO) discarded. Cells were resuspended in 10 ml DMEM/10 % FCS, transferred into 25 cm^2 tissue culture flasks (Nunc) and maintained as described in Section 2.6.1. Media were replaced the following day.

Cells were periodically frozen at low passage number. Cells were grown to confluence, detached from the substratum using trypsin (Section 2.6.3), resuspended in 2 ml of DMEM/10 % FCS and counted using a haemocytometer (Section 2.6.4). For storage, cells were resuspended at a final concentration of 5×10^6 cells/ml in DMEM/10 % FCS with 10 % DMSO (Sigma). Aliquots of 1 ml were transferred into cryotubes (Nunc) and retained on ice for 10 minutes, - 20 °C for 2 hours and - 70 °C overnight. The cryotubes were transferred into liquid nitrogen the following day.

2.7. TRANSFECTION OF CELLS IN CULTURE

2.7.1. Electroporation

Electroporation was carried out on HTC cells. Cells were aliquotted at a density of 5×10^6 cells in 200 µl in PBS (see Sections 2.6.1, 2.6.3 and 2.6.4) into electroporation cuvettes (BioRad, 0.4 cm gap), which had been previously sterilised by UV irradiation for 30 minutes in the laminar flow hood (Airpure, Email Westinghouse). Cuvettes were maintained on ice.

Chromatin constructs, assembled as described in Section 2.5.2, containing 10 µg of chromatinised DNA (or naked control plasmid) were transferred into sterile Eppendorf tubes and were brought to a final volume of 200 µl using 135 mM NaCl/Tris-HCl (Table 2.5). Chromatin samples were introduced carefully into the cell suspension and incubated on ice for 10 minutes.

Electroporation was carried out using a BioRad GenePulser II, with the pulse controller set to 'high range' and capacitance set to 'high capacity'. The optimal electroporation parameters were determined using FITC-labelled dextrans (see Sections 2.11.1 and 4.5.1). Subsequent electroporation experiments were carried out at 300 V and capacitance 500 µF. The cuvettes were pulsed (pulse times were typically around 25 msec) and were retained on ice for a further

10 minutes to allow the cells to recover. The electroporated cell suspensions were transferred, including the layer of dead cells, into 25 cm^2 tissue culture flasks (Nunc) containing 10 ml DMEM/10 % FCS. Transfected cells were cultured at 37°C in a humidified 5% CO_2 atomsphere (Forma Scientific Inc incubator) for 48 hours prior to analysis of reporter gene expression (Section 2.9.1).

2.7.2. Lipofection

HTC, Cos-7 and Jurkat cells were transfected using lipofection. HTC and Cos-7 cells were seeded at a density of 2×10^5 cells per 2 ml of DMEM/10 % FCS in each well of 6-well tissue culture plates (Nunc) prior to the day of transfection and were incubated overnight. Jurkat cells were seeded at a cell density of 5×10^5 cells per 0.5 ml of RPMI/10 % FCS into each well of 24-well tissue culture plates (Nunc) on the day of transfection.

Aliquots of chromatin samples containing 1 µg of chromatinised DNA (or naked control plasmid) were prepared for lipofection into each well. The aliquots were standardised to the maximum volume of each set of chromatin samples using chromatin buffer (CB, 135 mM NaCl/Tris-HCl; Table 2.5). The volume was brought to a final volume of 50 µl with serum-free DMEM for HTC and Cos-7 cells, or RPMI for Jurkat cells. Lipofectamine™ 2000 reagent (Invitrogen) was diluted 1:25 (v/v) in serum-free media and 50 µl was mixed promptly with 50 µl of each chromatin sample preparation. Formation of liposome/DNA complexes was allowed to proceed for 20 minutes at room temperature. During this time, the cell culture media of HTC and Cos-7 cells (DMEM/10 % FCS) were aspirated and cells were rinsed twice with serum-free media, which was also aspirated. Lipofectamine/DNA complexes (100 µl per well) were carefully distributed drop wise over the cells. Jurkat cells were returned to the incubator (Forma Scientific Inc incubator), while HTC and Cos-7 cells were incubated for a further 20 minutes and then overlaid with 2 ml of DMEM/DMEM with 10 % FCS (50/50, v/v) before returning to the incubator.

Cells were cultured at 37°C and in a humidified 5% CO_2 atomsphere (Forma Scientific Inc incubator) for 48 hours prior to analysis of reporter gene expression (Section 2.9).

2.8. Isolation of nuclei

Subcellular fractionation was performed in order to obtain pure nuclei in order to ascertain the level of DNA uptake into the nucleus following transfection of fluorescein-labelled chromatinised plasmid (Section 2.2.16). Cos-7 and HTC cells were harvested (Section 2.6.3) and resuspended in 500 µl of PBS. Cells were divided into two aliquots; one aliquot of which

was analysed as intact cells using flow cytometry (Section 2.9.1), the other aliquot of which was used to isolate nuclei, which were thereafter analysed using flow cytometry (Section 2.9.1). Nuclei were obtained using the method described in Rao *et al.* (2001) or using the NE-PER™ nuclear and cytoplasmic extraction kit (Pierce; Table 2.13).

Using the first method (Rao *et al.,* 2001), cells were collected by centrifugation at 640g (~ 1640 rpm; Allegra 6 Centrifuge, Beckman) and resuspended in 200 µl of ice-cold Nonidet P-40 lysis buffer containing 10 mM Tris (pH 7.4), 10 mM NaCl, 3 mM MgCl2, 0.5 % Nonidet P-40, 0.15 mM spermine and 0.5 mM spermidine. The cell suspension was incubated on ice for 5 minutes. Nuclei were recovered by centrifugation at 1000 rpm for 10 minutes (Eppendorf centrifuge, model 5415C). The supernatant was discarded and the pellet, containing the nuclei, was resuspended in 200 µl of PBS.

The second method involved using the NE-PER™ nuclear and cytoplasmic extraction kit (Pierce). Results obtained were consistent with the method described above. Reagents were used according to the manufacturer's protocol, with some adaptations. Briefly, the volumes of each reagent used were based on a packed cell volume of ~ 20 µl, corresponding to 5×10^6 cells. Samples were retained on ice throughout the procedure. The resupended cells were centrifuged at 1200 rpm for 5 minutes (Eppendorf centrifuge, model 5415C) in order to recover the cell pellet. Cell pellets were resuspended in 200 µl CER I reagent by vortexing for 15 seconds. Following a 10 minute incubation period on ice, 11 µl of CER II reagent was added to each sample. The samples were vortexed for 5 seconds and incubated for a further minute on ice. The samples were re-vortexed for 5 seconds and centrifuged at maximum speed in a benchtop centrifuge (14000 rpm, Eppendorf centrifuge, model 5415C) for 5 minutes. The supernatant, containing the cytoplasmic fraction, was discarded. The pellets, comprising the nuclei, were resuspended in 200 µl PBS by vortexing for 15 seconds in the first instance and then for 15 seconds every 10 minutes over a total period of 40 minutes with the samples retained on ice in between.

For both methods used, DNase I (Roche, 10 U/µl) was added to the final suspension of nuclei to disperse clumping (2 µl per sample). The samples were mixed gently by pipetting. If clumping persisted, an additional 2 µl of DNase I was added and the sample was incubated for a further 15 minutes. The nuclei suspension was brought to a final volume of 500 µl (in PBS) for analysis using flow cytometry (Section 2.9.1).

2.9. ANALYSIS OF TRANSFECTION EFFICIENCY

2.9.1. Flow cytometry

Flow cytometric (FACS) analysis was performed for the quantitation of transfection efficiency using the pGeneGrip-RFP plasmid (FACScan, FACScalibur or LSR, Becton Dickinson Immunocytometry Systems Inc; Flow Cytometry Unit, JCSMR). Cultured cells were transfected as described in Section 2.7. For FACS analysis, whole cells were resuspended in 500 µl (see Section 2.6.3 for harvesting of adherent cells) or nuclei were prepared (Section 2.8). The flow rate was set to 'medium'. When transfection experiments were conducted in order to ascertain reporter gene expression in whole cells, 100000 events were acquired in each scan. When transfection experiments were conducted using fluorescein-labelled chromatinised plasmids (Section 2.2.16) in order to relate plasmid uptake into the nucleus to reporter gene expression in whole cells, 30000 events were acquired in each scan for the whole cells and 5000 events for nuclei. For the analysis of whole cells, the forward light scatter parameter was set on a linear scale; for the analysis of nuclei, forward light scatter was set on a logarithmic scale. Events were analysed using CellQuest software (Becton Dickinson, Macintosh). Quadrants or regions were set according to negative control samples (non-transfected cells, 'no DNA transfections' with empty liposomes or non-labelled plasmid) or positive control samples (which generated known fluorescence events). The percentage of fluorescent events (cells) and the arithmetic and geometric means of fluorescence intensity were quantitated by the CellQuest software (Macintosh). Further mathematical analyses were performed using Microsoft Excel and SigmaPlot software.

Channel settings for the detection of fluorescence are indicated below. Multi-channel analyses were also performed, where possible, to ascertain the presence of several fluorescent molecules per cell.

2.9.1.1. Determination of cell viability using propidium iodide or 7-amino-actinomycin D

Cell viability was analysed using propidium iodide (PI, 5 µg/ml final concentration) or 7-amino-actinomycin D (7-AAD, 20 µl/sample; Via-Probe™, Roche). These reagents were added to the cell suspensions and were incubated in the dark for 10 minutes prior to FACS analysis. PI fluorescence was detected through channel FL2 using a standard filter configuration on the FACScan or FACScalibur or band pass filters 575/45 on the LSR. 7-AAD fluorescence was detected through channel FL3 using a standard filter configuration on the FACScan or FACScalibur or a 650 nm, long pass filter on the LSR.

2.9.1.2. Quantitation of RFP reporter gene expression

RFP fluorescence was detected through channel FL2 using a standard filter configuration on the FACScan or FACScalibur or band pass filter 575/45 on the LSR.

2.9.1.3. Quantitation of fluorescein fluorescence

Fluorescein (FITC) fluorescence was detected through channel FL1 using a standard filter configuration on the FACScan or FACScalibur or band pass filter 530/30 on the LSR. Nuclear FITC fluorescence originating from the FITC-labelled chromatin constructs was quantitated relative to nuclei isolated from cells transfected with either no construct or unlabelled construct.

2.9.2. Luciferase assay

The luciferase reporter plasmid pGMCSF-1(2)TK-luc+ was kindly provided by K. Bunting, Cytokine Gene Expression Group, JCSMR (pGMLuc; Table 2.9). pGMLuc was 6.1 kb and was calculated on the basis of physiological nucleosome density (~ 230 bps per nucleosome) to be saturated with 26 histone octamers. Chromatin constructs were assembled at stoichiometries of 0, 1, 2, 4 and 26 octamers per plasmid (Section 2.5.2). Jurkat cells were transfected by lipofection, as described in Section 2.7.2. Cells were allowed to recover post-lipofection for 30 - 34 hours before the pharmacological stimuli phorbol-12-myristate-13-acetate (PMA, Sigma) and calcium ionophore (A23187, Boehringer) were added to final concentration 20 ng/ml and 1 µM, respectively. Cells were cultured for a further 8 hours.

Cells were harvested by centrifugation for 5 minutes at 640 g (~ 1640 rpm; Allegra 6 Centrifuge, Beckman). Cells were washed twice with PBS, the cell pellets collected by re-centrifugation after each wash and the supernatants carefully aspirated. All material was thereafter retained on ice for the duration of the assay. The luciferase assay was conducted as set out by Himes and Shannon (2000). Briefly, cells were resuspended in 200 µl lysis buffer (Table 2.6) and lysed in three rounds of freezing and thawing using an ethanol/dry ice bath. Lysed cells were centrifuged at 14000 rpm for 5 minutes at 4°C (Eppendorf centrifuge, 5415C). The supernatant was retained and the protein concentration was determined using the BioRad protein assay (Section 2.3.1.1). Typically 50 µg (80 µl) of cell extract was pipetted per well of a 96-well black microtitre plate (Nunc). Luciferase assay buffer was assembled (Table 2.6) and allowed to equilibrate to room temperature, after which 200 µl were added to each well. In order to initiate the light reaction, 40 µl of D-luciferin (Table 2.6) was added. Luminescence was quantitated using a Top Count scintillation/luminescence counter (Packard).

2.10. ELISA

The importin binding affinities of histones, DNA or chromatin samples were determined using a modified enzyme-linked immunosorbent assay (ELISA), described previously (Hu and Jans, 1999; Hubner *et al.*, 1997; Xiao *et al.*, 1997a). This assay was conducted over three days and comprised three stages: adsorption the protein of interest, interaction with importins and, finally, analysis of the interaction based on visualisation using alkaline phosphatase.

Samples were brought to a concentration in the range of 0.1 to 1 µg per 100 µl in coating buffer (Table 2.7) and coated onto the surface of each well of a 96-well microtitre plate (Immuno™ plate MaxiSorp™ Surface, Nunc) in a volume of 100 µl per well. Plates were incubated overnight at 4°C to maximise adsorption.

The following day, the sample coating buffer was discarded and wells were rinsed briefly with hybridisation buffer (HB) containing 1 % BSA (HB/BSA, 300 µl per well) (Table 2.7). Blocking was carried out in HB/BSA (Table 2.7) for 1 hour at room temperature with gentle agitation (setting 5, Platform Rocker, Bio-line, Edwards Instrument Company). Following this, the wells were briefly rinsed again. This procedure was repeated using HB free of BSA (Table 2.7). Serial dilutions of the GST-tagged importin α (0 to 405 nM) and importin β (0 to 270 nM; see Section 2.4.1) were prepared in HB/BSA (Table 2.7). Importin α and β were also associated into a heterodimer by incubation of equimolar amounts (270 nM) at room temperature for 15 minutes in 1 × IB containing 1mM DTT (Table 2.7). Following pre-complexation, the heterodimer was similarly diluted in HB/BSA (Table 2.7). Each dilution of importin was added to triplicate wells at 100 µl, and incubated overnight at 4°C, with agitation (setting 5, Platform Rocker, Bio-line, Edwards Instrument Company).

The microtitre plates were washed 3 times using HB/BSA (Table 2.7), including incubation for 15 minutes at room temperature with gentle agitation (setting 5, Platform Rocker, Bio-line, Edwards Instrument Company). The anti-GST primary antibody (Table 2.12) was diluted in Antibody buffer (Table 2.7) and aliquotted at 500 ng per well. The reaction was incubated for 3 hours at room temperature on the platform rocker (setting 5, Bio-line, Edwards Instrument Company). Following extensive washing (10 times) using Wash buffer (Table 2.7), alkaline-phosphatase conjugated anti-goat secondary antibody (Table 2.12) was diluted 1:25000 in Antibody buffer (Table 2.7) and 100 µl were added per well. The reaction was incubated for 1 hour at room temperature, with gentle rocking, as described before. Following this, the plates were washed extensively using Wash buffer (Table 2.7). The protein/importin interaction was analysed using 1 mg/ml para-nitophenyl phosphate (Sigma) in 10 % diethanolamine buffer (Table 2.7), added at 100 µl/ per well. The change in absorbance was monitored at 405 nm over

90 minutes using a microtitre plate reader (Molecular Devices) and SoftMax™ software (Macintosh). Raw data were analysed using Microsoft Excel software. Values were corrected against the background absorbance at 0 minutes and wells which were incubated without importin. Data in the linear range were selected and the change in absorbance was plotted against time (KaleidaGraph software, Macintosh). The value of each gradient (OD/minute) was plotted against importin concentration. The resulting curves were fitted using the function:

$$B(x) = B_{max} (1 - e^{-kx})$$

where x is the concentration of importin, B is the level of importin bound and k is the slope of the curve (KaleidaGraph software, Macintosh or SigmaPlot, Jandel Scientific). The apparent dissociation constant (K_D) of the importin/protein interaction was determined from this equation as 0.693/k and represents the concentration of importins at which the level of binding was half the maximum.

2.11. CONFOCAL LASER SCANNING MICROSCOPY

The localisation of fluorescently labelled dextrans and DNA was monitored within the cell using confocal laser scanning microscopy (CLSM; MRC-600 and Radiance 2000, BioRad). Images obtained using CLSM were analysed using the NIH Image J 1.30 public domain software.

2.11.1. Subcellular localisation of FITC-dextrans following electroporation into cells

In order to determine the parameters for electroporation which would permit transfection of plasmid DNA exclusively into the cytoplasm of cells, while maintaining the integrity of the NE, the subcellular localisation of fluorescently labelled dextrans (FITC-dextran) introduced into HTC cells by electroporation was determined using CLSM. FITC-dextrans of MW 20 kDa and 70 kDa were included at a final concentration of 0.5 mg/ml in the electroporation mix. HTC cells were electroporated at a range of voltages from 200 – 300 V (essentially as described in Section 2.7.1, with FITC-dextrans substituted for DNA). Following post-electroporation recovery on ice for 10 minutes, cells were collected by centrifugation at 1500 rpm for 5 minutes (Eppendorf centrifuge, 5415C). The supernatant was discarded and the cells were rinsed twice in 500 µl of PBS, each time collected by centrifugation at 1500 rpm for 5 minutes (Eppendorf centrifuge, 5415C). Cells were finally resuspended in 500 µl of PBS.

Slides were prepared for microscopy by creating a 'chamber' on each slide using 0.1-mm-thick double-sided pressure-sensitive tape (Scotch 3M) into which a hole of 0.8 mm in diameter was punched. A volume of 5 µl of the cell suspension was pipetted into this well. The well was sealed using a coverslip. Cells were brought into focus using 60 × magnification with oil

immersion (Bio-Rad MRC-600). CLSM images were captured using 5 scans in Kalman filter mode at speed 1 scan/second and gain 900.

2.11.2. *In vitro* nuclear transport assay

Nuclear import was analysed at the single cell level using CLSM, as described in Jans *et al.* (Jans *et al.*, 1991), Efthymiadis *et al.* (1998) and Xiao *et al.* (1996a). HTC cells were used for the nuclear transport assay. Cells were grown on coverslips in 6-well tissue culture plates (Nunc) for 36 hours to 50 – 70 % confluence. In each well, DMEM media was replaced prior to use for the analysis of nuclear import with 2 ml of DMEM without phenol red and glutamine (ICN) containing 1 M HEPES/10% FCS. The cells grown on glass coverslips were rinsed with 1 × IB (see Table 2.7) and excess liquid was drained by gravity flow. This was followed by addition of 3 µl 1 × IB to the layer of cells, onto which a single layer of tissue paper was placed. After 3 seconds, cells were mechanically perforated by rapidly removing the tissue paper.

Slides were prepared as described above (Section 2.11.1). Reconstituted nuclear import mix was pipetted into the 'chamber' created on the slide. The nuclear import mix contained BSA (30 mg/ml) or cytosolic extract (untreated reticulocyte lysate, Promega), an ATP-regenerating system (0.125 mg/ml creatine kinase, 30 mM creatine phosphate, 2 mM ATP) and the transport substrate or a control sample (70-kDa fluorescein isothiocyanate- or Texas-red-labelled dextran; Sigma) to assess nuclear integrity. The total volume was 5 µl. The coverslip with perforated cells was placed with the cell-bearing surface face-down to the nuclear import mix and sealed with nail polish to prevent dehydration during the experiment. Experiments were performed at room temperature.

Cells were brought into focus using a 60 × magnification oil immersion lens (Radiance 2000, BioRad). Scans were performed using settings of 5 scans in Kalman filter mode, scan speed 166 ps, iris to 1.8 – 2.8 with offset 0 or 1. For each image, the laser power level, iris and offset were adjusted to achieve optimal resolution and brightness. Images were captured every 3 - 4 minutes over 15 - 45 minutes.

2.12. Statistical analyses

The Student's 2-tailed t-test for paired or unpaired experiments was used, as appropriate, for all statistical analyses (Microsoft Excel). The level of significance was set at $p \leq 0.05$.

CHAPTER 3

Importin binding properties of histones and chromatin assembly factors

3.1. INTRODUCTION

Histones are synthesised in the cytoplasm and, thus, must be translocated subsequently into the nucleus, where, once inside, they participate in an ordered sequential process of folding and compaction of DNA into chromatin. This process involves chromatin assembly factors such as NAP-1 (Ito *et al.*, 1996; Fujiinakata *et al.*, 1992) and N1/N2 (Chang *et al.*, 1997; Dilworth *et al.*, 1987). Acetylated histones and histone variants are often present in regions of chromatin that have higher transcriptional activity and are thought to play a role in the ordered disassembly of chromatin that enables gene transcription (Vermaak *et al.*, 2003; Wade and Wolffe, 1997). Other proteins associated with chromatin, such as the high mobility group (HMG) proteins HMG-14 and -17, also play a role in remodelling to a more transcriptionally active structure by binding the nucleosome directly in such a way that nucleosome stability and, potentially, chromatin folding is altered (Bustin *et al.*, 1995; Tremethick, 1994; Bustin *et al.*, 1991).

At the outset of this study, very little was known with respect to the mechanism for the nuclear transport of histones and other proteins associated with chromatin such as HMG-14, HMG-17, NAP-1 and N1/N2. Sequence motifs similar to the T-ag NLS had been identified in histones H1 (Schwamborn *et al.*, 1998) and H2B (Moreland *et al.*, 1987) only, while N1/N2, HMG-14 and -17 had been shown to harbour bipartite NLSs (Hu and Jans, 1999; Hock *et al.*, 1998; Table 3.2).

Generally, protein import into the nucleus is mediated via the conventional NLS-dependent nuclear import pathway by the nuclear import proteins (importins) which bind NLSs within the protein to be transported (see Section 1.3.3). The extensive requirement for histones in the assembly of new chromatin during DNA replication implies the necessity for efficient mechanisms of nuclear import. As a first step towards understanding the nuclear import of histones, nucleosome-associated proteins and chromatin assembly factors, a modified ELISA

method was used to determine their binding properties to importin α, importin β and the α/β heterodimer.

3.2. HISTONES ARE BOUND WITH HIGH AFFINITY BY IMPORTIN β

An assay based on the ELISA (described in detail in Section 2.10), previously used to quantitate the importin binding properties of a number of NLS-containing proteins that localise to the nucleus (Hubner *et al.*, 1997; Xiao *et al.*, 1997a), was used in this study also to the determine binding constants for histones.

Briefly, the assay involved adsorbing the protein of interest to a microtitre plate. The coated wells were incubated with importins over a series of concentrations, each in triplicate. The importins used were mouse importin α2 and importin β1, expressed as GST-fusion proteins (Section 2.4.1). Binding affinity was determined for importin α and β, individually, and also when associated into a heterodimer. The binding interaction was quantitated colourimetrically, based on alkaline phosphatase conversion of para-nitrophenyl phosphate, over a period of 90 minutes. Absorbance data in the linear range were selected and the change in absorbance plotted against time (KaleidaGraph 2.13, Macintosh). The values of each gradient were plotted against the importin concentration and the resulting curves were fitted to the function $B(x) = B_{max} (1 - e^{-kx})$, where x is the concentration of importin, B is the level of importin bound and k is the slope of the curve. The apparent dissociation constant (K_D) of the importin/protein interaction, representing the concentration of importin at which the level of binding is half-maximal, was calculated using from this function (0.693/k).

Peptide P101 (^{110}PGSDDEAAADAQHAAP**PKKKRKV**^{132}; Hubner *et al.*, 1997) which includes the archetypal T-ag-NLS (highlighted in bold type-face) was used as a positive control for importin α/β binding (Figure. 3.1). P101 demonstrated high affinity binding with importin α/β having a K_D of 3.2 ± 0.3 nM (n = 7). This binding occurred predominantly through the α subunit, which showed a K_D of 40.7 ± 11.2 nM (n = 3) compared to the K_D for the importin β subunit of 202.1 ± 28.9 nM (n = 2). The role of the α subunit was also apparent in the level of maximal binding. When expressed as a percentage of importin α/β, the α subunit showed maximal binding around 81 %, whereas that of the β subunit was 8 %.

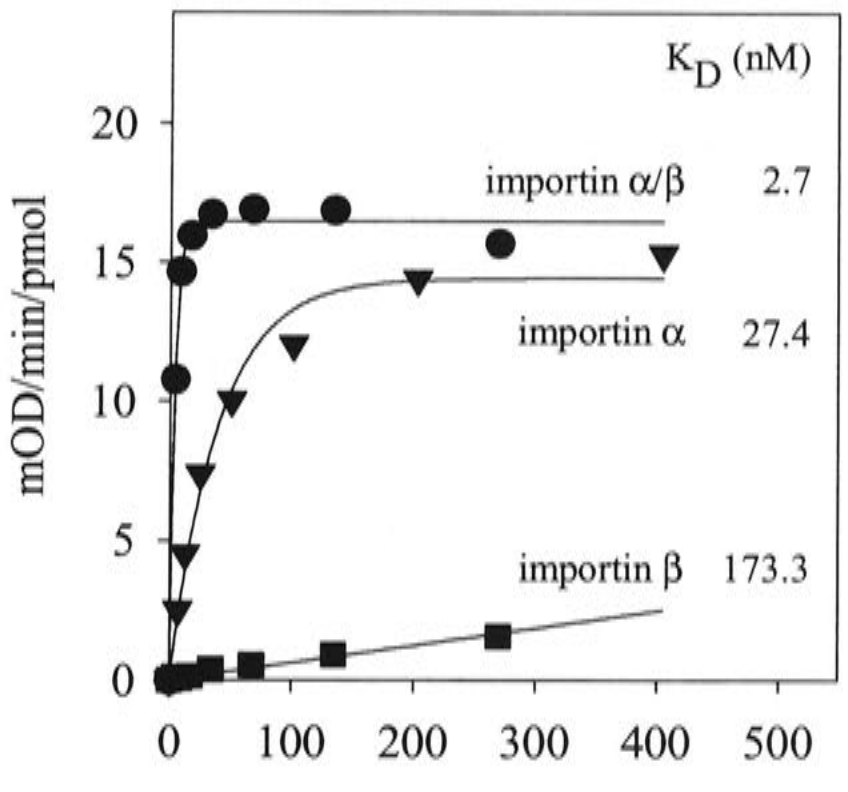

Figure. 3.1. The archetypal T-ag NLS is recognised with high affinity by importin α/β through importin α binding. Binding curves of P101, comprising the T-ag NLS, for importin α, β and the α/β heterodimer are shown. Data were generated using an ELISA, in which microtitre plates were coated with 1 µg of peptide P101 per well and incubated with increasing concentrations of importins (Section 2.10). Data were fitted using the function $B(x) = B_{max} (1 - e^{-kx})$, where x is the concentration of importin, B is the level of importin bound and k is the slope of the curve. The apparent dissociation constants (K_D) were calculated as 0.693/k and are indicated. Results shown are from a single typical experiment, performed in triplicate.

The histones analysed were H1 (calf thymus, Boehringer), the H2A/2B dimer (recombinant, *Xenopus laevis* sp., see Section 2.4.2), the H2AZ/2B dimer which contains the H2A variant histone, H2AZ (Faast *et al.*, 2001; Clarkson *et al.*, 1999; recombinant mouse histone; provided by M. Clarkson, Chromatin and Transcriptional Regulation Group, JCSMR) and the H3/4 tetramer (non-acetylated, isolated from chicken long chromatin, and acetylated, isolated from HeLa cells; provided by L. Hyman, Chromatin and Transcriptional Regulation Group, JCSMR). When these experiments were conducted, histones H2A and H2B had been proposed to be transported to the nucleus as heterodimers (Moreland *et al.*, 1987) and H3 and H4 as a heterotetramers (Chang *et al.*, 1997) and, hence, importin binding was determined for the dimeric and tetrameric forms of H2A/2B and H3/4, respectively.

All of the histones tested bound with high affinity to the importin α/β heterodimer and this interaction appeared to be mediated largely through importin β, since maximal binding by importin β was 85 to 100 % that of importin α/β (Figures 3.2 and 3.3; Table 3.1). Binding by importin α was low in all cases (K_Ds > 50 nM).

Table 3.1. Binding properties of importins to histones and chromatin associated proteins.

Protein	Importin α/β		Importin α			Importin β		
	K_D (nM)[A]	B_{max}[A]	K_D (nM)	B_{max}	Relative B_{max} (%)[B]	K_D (nM)	B_{max}	Relative B_{max} (%)[B]
H1	1.4 ± 0.6 (3)	10.7 ± 0.2	96.3 ± 11.4 (3)	5.2 ± 0.5	48	2.7 ± 0.2 (3)	10.6 ± 1.0	99
H2A/2B	9.2 ± 3.6 (4)	3.8 ± 0.8	207.2 ± 82.2 (3)	4.2 ± 1.2	109	5.5 ± 0.5 (3)	3.3 ± 1.3	87
H2AZ/2B	1.1 ± 0.4 (3)	8.0 ± 1.0	56.1 ± 13.1 (2)	5.7 ± 0.9	71	4.0 ± 1.6 (3)	8.9 ± 1.6	111
H3/4	3.7 ± 1.4 (3)	6.3 ± 0.3	152.7 ± 26.7 (3)	4.5 ± 1.0	72	8.2 ± 0.1 (3)	5.4 ± 0.3	86
H3/4-ac[C]	56.6 ± 10.4 (4)	2.6 ± 0.5	252.6 ± 43.6 (3)	3.5 ± 1.1	134	29.0 ± 3.4 (3)	1.1 ± 0.1	41
HMG-14	15.5 ± 4.0 (3)	8.8 ± 2.2	200.5 ± 6.1 (3)	3.1 ± 0.8	35	173.8 ± 38.0 (4)	2.5 ± 0.6	29
HMG-17	3.5 ± 1.2 (4)	9.7 ± 1.6	187.0 ± 29.4 (3)	4.2 ± 0.7	43	149.0 ± 2.0 (3)	2.5 ± 0.8	26
N1/N2	1.6 ± 0.1 (3)	10.7 ± 3.1	150.4 ± 32.5 (3)	2.9 ± 0.6	17	197.2 ± 31.4 (3)	3.9 ± 1.3	23
NAP-1	115.0 ± 29.0 (3)	1.5 ± 0.3	248.0 ± 23.4 (4)	2.8 ± 0.3	183	89.4 ± 8.7 (3)	1.0 ± 0.4	68

[A] Binding parameters were determined using an ELISA-based assay (see Figures 3.2 - 3.5), as described in the Materials and Methods (Section 2.10). Curves were fitted to experimental data using the function $B(x) = B_{max}(1-e^{-kx})$, where x is the concentration of importin, B is the level of importin bound and k is the slope of the curve. K_D, the apparent dissociation constant representing the importin concentration at which binding is half-maximal, was calculated as 0.693/k. B_{max} is the maximum level of importin binding. Results represent the mean ± SEM. Individual experiments were performed in triplicate, with the number of experiments indicated in parentheses.

[B] The relative B_{max} is expressed as a percentage of the B_{max} for α/β.

[C] Acetylated histone H3/4; see Table 3.2 for the sites of acetylation.

Of the histones, H1 showed the highest binding affinity for importin β with a K_D of 2.7 ± 0.2 nM (n = 3) (Table 3.1; Figure 3.2). The lack of a significant difference between the binding affinity for importin β and importin α/β (p = 0.1, n = 3) indicates the essential role of importin β in the binding of H1 to importin.

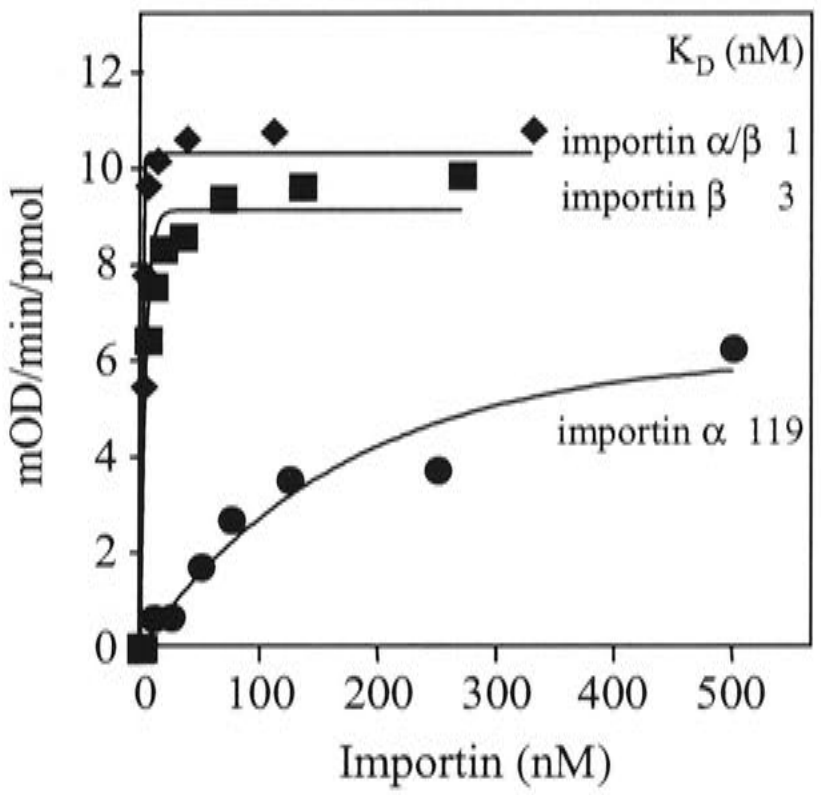

Figure 3.2. Histone H1 is recognised with higher affinity by importin β than importin α. Microtitre plates were coated with 4 pmol of histone H1, and binding affinity of importin α, β and the α/β heterodimer determined using an ELISA (Section 2.10). Binding curves for importin α, β and the α/β heterodimer are shown. The apparent dissociation constants (K_D) were calculated as 0.693/k from the function $B(x) = B_{max} (1 - e^{-kx})$ where x is the concentration of importin, B is the level of importin bound and k is the slope of the curve. Results represent a single typical experiment, performed in triplicate. Pooled data are shown in Table 3.1.

H2A/2B and H2AZ/2B displayed different importin binding affinities. Importin α, β and the α/β heterodimer all showed markedly higher binding to H2AZ/2B than to H2A/2B (p = 0.009 for importin α/β, Table 3.1; Figure 3.3a). This was indicated by both the lower K_D values and the higher maximal binding (greater than 50 %) by importin α/β and β to H2AZ/2B. For both H2A/2B and H2AZ/2B, however, importin binding occurred predominantly through importin β.

Binding of H3/4 tetramers, with and without acetylation, by importin subunits was compared also. The affinity of importins α/β and β for H3/4 was significantly diminished when H3/4 was acetylated (p = 0.01, n = 4 and p = 0.0009, n = 3, respectively), as was the level of maximal binding (by greater than 60%; Table 3.1; Figure 3.3b), although, binding remained predominantly mediated by the importin β rather than the α subunit.

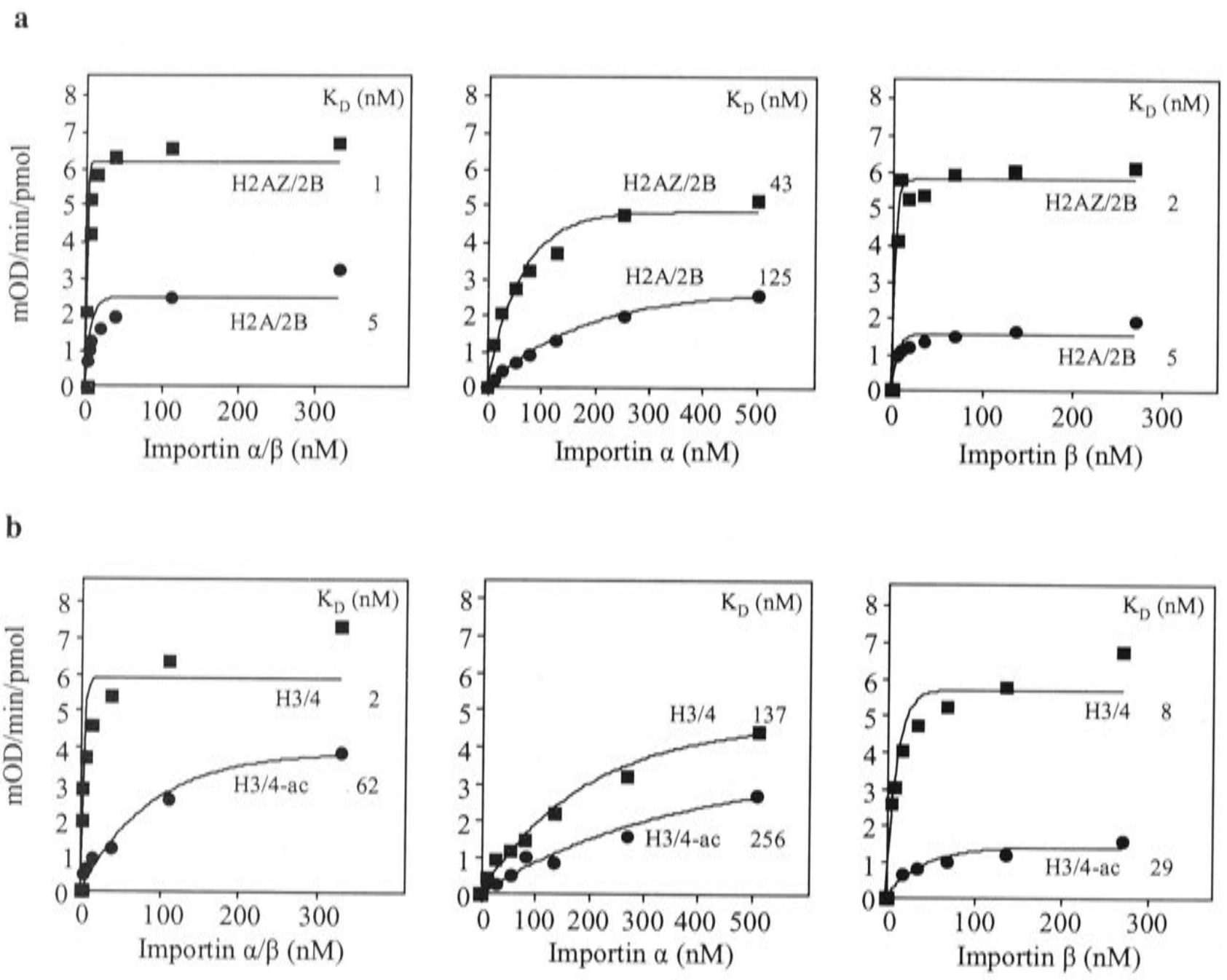

Figure 3.3. Importin β binds core histones with high affinity. Importin binding curves for H2A/2B and H2AZ/2B are shown in (**a**) and for acetylated and non-acetylated H3/4 are shown in (**b**). Microtitre plates were coated with 0.14 µg of histones (4 pmol) per well and binding affinity data for importin α, β and the α/β heterodimer was collected and analysed as described previously (Section 2.10). Results for importin α/β, α and β and are shown in the left, middle and right panels, respectively. The binding data were fitted to the function $B(x) = B_{max} (1 - e^{-kx})$, where x is the concentration of importin, B is the level of importin bound and k is the slope of the curve, from which the apparent dissociation constants (K_D) were calculated (0.693/k). The K_D values indicated represent the results from this single typical experiment, performed in triplicate. Pooled data are shown in Table 3.1.

3.3. IMPORTIN BINDING PROPERTIES OF THE CHROMATIN-ASSOCIATED PROTEINS HMG-14 AND -17

The ELISA was used to assess importin binding to the nucleosome associated proteins HMG-14 and -17 (provided by L. Hyman, Chromatin and Transcriptional Regulation Group, JCSMR). Unlike the observation for the core histones, the importin α/β heterodimer dominated HMG-14 and -17 binding. Importin α mediated binding in the context of the importin α/β heterodimer. This is reflected in the maximal level of binding by importin α being greater than that by importin β alone (Table 3.1; Figure 3.4). HMG-14 and -17 were bound with similar affinity by the importin α/β heterodimer and the individual subunits (Figure 3.4). This result may stem

from the high sequence conservation within the proposed NLS motifs of these proteins (Hock *et al.*, 1998).

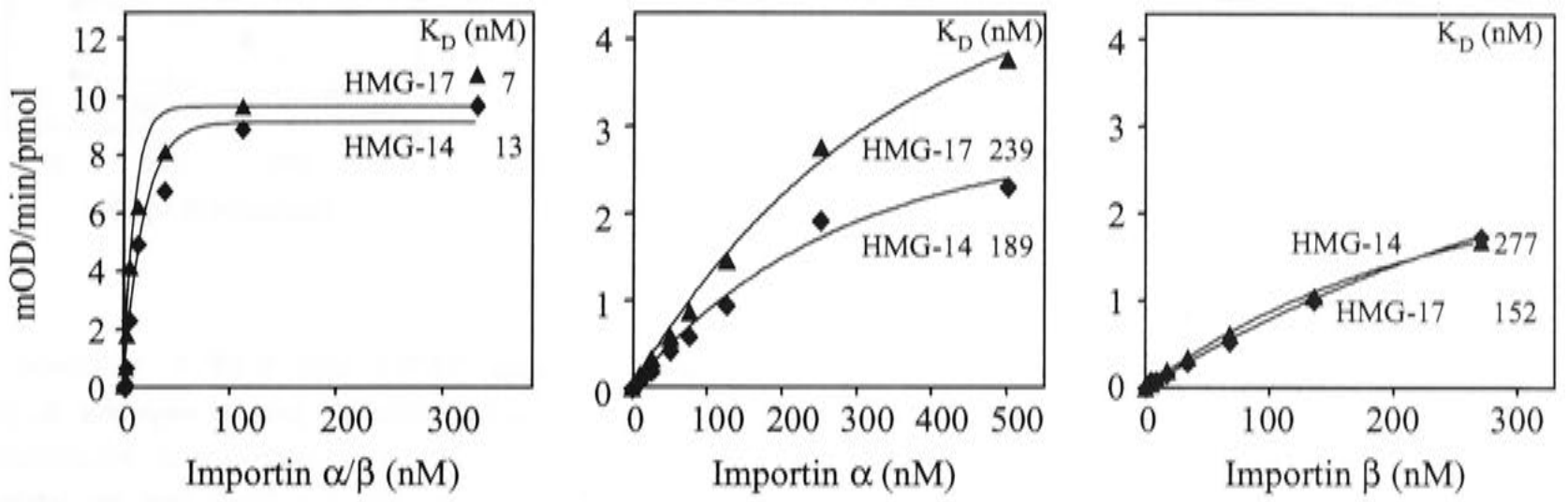

Figure 3.4. Importin binding to the chromatin-associated proteins HMG-14 and -17. Binding curves for both HMG-14 and -17 by importin α/β, α and β are shown in the left, middle and right panels, respectively. Experimental data were generated and analysed as described in the legend to Figure 3.3. Note that the scale of the y-axis is higher for the left panel. Results represent a single typical experiment, performed in triplicate, with pooled data shown in Table 3.1.

3.4. IMPORTIN BINDING PROPERTIES OF THE CHROMATIN ASSEMBLY FACTORS NAP-1 AND N1/N2

The affinity of importin for the chromatin assembly factors N1/N2 and NAP-1 (provided by N. Siddon, Chromatin and Transcriptional Regulation Group, JCSMR) was also assessed by the ELISA. Importin α/β demonstrated high binding affinity for N1/N2 (K_D = 1.6 ± 0.1 nM, n = 3), similar to that of the P101 positive control peptide which contains the T-ag-NLS (K_D = 3.2 ± 0.3 nM, n = 7; see Section 3.2). Separately, each of the importin subunits demonstrated similar binding affinities and levels of maximal binding (Table 3.1; Figure 3.5). Overall, these interactions were much weaker than importin α/β.

In contrast, NAP-1 was bound with low affinity by importin α/β (K_D = 115 ± 29 nM, n = 3) and this interaction appeared to be mediated through the β subunit, which contributed higher binding affinity than the α subunit (Table 3.1; Figure 3.5).

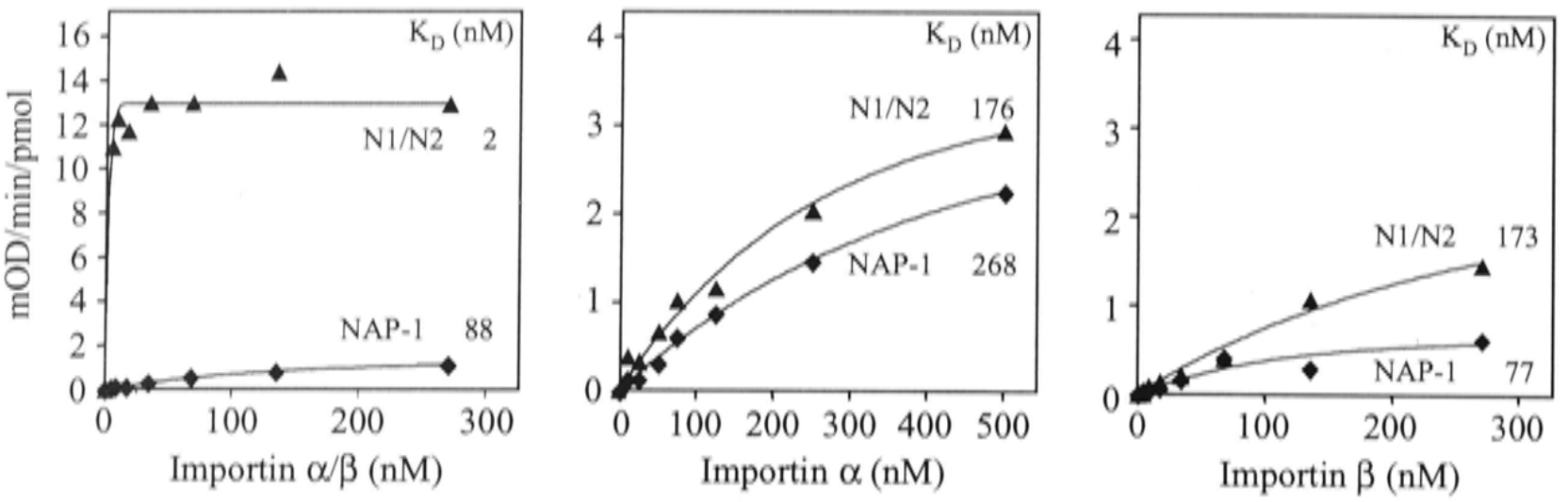

Figure 3.5. Importin binding to the chromatin assembly proteins N1/N2 and NAP-1. Microtitre plates were coated with 0.1 µg of N1/N2 and NAP-1 per well and binding affinity data of importin α, β and the α/β heterodimer were collected using an ELISA (Section 2.10). Data were analysed as described previously and binding curves for importin α, β and the α/β heterodimer are shown. Note that the scale of the y-axis is higher for the left panel. The apparent dissociation constants (K_D) indicated represent the results from this single typical experiment. Pooled data are shown are Table 3.1.

3.5. DISCUSSION

At the outset of this study, the nuclear import pathways for histones and other chromatin-associated proteins were ill-defined. The results presented in this chapter were the first quantitative data for the binding of histones, other chromatin-associated nuclear proteins and chromatin assembly factors by importins (Johnson-Saliba *et al.*, 2000). The results indicated that the import of histones into the nucleus may be mediated exclusively by importin β, whereas import of the chromatin-associated proteins and N1/N2 relies on the previously well-documented importin α/β pathway.

Despite the presence of multiple sequence elements in H1 resembling the T-ag NLS (see Table 3.2; Schwamborn *et al.*, 1998), which is recognised by importin α/β, H1 import into the nucleus had been shown (using an *in vitro* permeabilised cell system and fluorescence microscopy) to be mediated by importin β in a heterodimeric association with importin 7 (Jakel *et al.*, 1999). The data presented here are consistent with these findings. The ELISA method used also revealed a high affinity interaction between importin β and histone H1 (in the nM range, around 50-fold greater than that between importin α and H1 – see Table 3.1). While this is in contrast to the importin binding properties of conventional NLS-containing proteins, such as T-ag, where importin α mediates NLS recognition, importin β has been implicated as the sole mediator of nuclear import of several other proteins including HIV-1 Rev (Truant and Cullen, 1999; Henderson and Percipalle, 1997), GAL4 (Chan *et al.*, 1998), CREB, Fos, Jun (Forwood *et al.*, 2001a), SRY (Forwood *et al.*, 2001b) and TRF (Forwood and Jans, 2002). These proteins have in common with histones the fact that they all bind either DNA or RNA. High affinity

binding by importin β may therefore be an emerging feature of proteins which may be broadly classified as DNA/RNA-binding. Some proteins such as cyclin B1 (Moore *et al.*, 1999) and PTHrP (Lam *et al.*, 1999), which do not appear to bind DNA or RNA, however, also seem to be imported into the nucleus by this pathway.

Table 3.2. NLS sequences and acetylation sites in histones and other chromatin-associated proteins.

Protein	NLS [A]	References
H1°	**PVKKAKKKLAATPKKAKK**[159] **KTVKAKPVKASKPKKAKPVKPKAKSSAKRAGKKK**[193]	(Schwamborn *et al.*, 1998)
H2A	**SGRGKQGGKARAKAKSRSSRAGLQFPVGRVH RLLRKGNYAERVGAG**[46]	(Balicki *et al.*, 2002; Baake *et al.*, 2001a; Mosammaparast *et al.*, 2001)
H2AZ[B]	**AGGKAGKDSGKAKTKAVSRSQRAGLQFPVG RTHRHLKSRTT**[40]	Putative
H2B	↓ ↓ ↓ ↓ **PEPAKSAPAPKKGSKKALTKAQKKDGKKRKRM SRKESYSIYIYKVLKQVHPD**[52]	(Baake *et al.*, 2001a; Mosammaparast *et al.*, 2001; Moreland *et al.*, 1987)
H3	↓ ↓ ↓ ↓ ↓ **ARTKQTARKSTGGKAPRKQLATKAARKSAPATGGV KKPHRYRRPGTVALREIRRYQST**[58]	(Mosammaparast *et al.*, 2002b; Baake *et al.*, 2001a)
H4	↓ ↓ ↓ ↓ **SGRGKGGKGLGKGGAKRHRKVLRDNIQGITKPAIRR LARRGG**[42]	(Mosammaparast *et al.*, 2002b; Baake *et al.*, 2001a)
HMG-14	**PKRK**[4].....KPKK[32].....**KGKRG**[54]	(Hock *et al.*, 1998)
HMG-17	**PKRK**[4].....PKKKAPAKK[48].....**PKGKKG**[58]	(Hock *et al.*, 1998)
N1/N2	**RKKRK**TEEESPLKD**KAKKSK**[554]	(Hu and Jans, 1999)

[A] The NLSs are highlighted in bold type-face. The basic sequence is the amino acid consensus sequence for each histone, reported in Wells and McBride (1989).
[B] The H2AZ putative NLS is the N-terminal region, amino acids 1 – 40, based on NLS location within the other core histones. The sequence is from Suto *et al.* (2000). No studies have been performed defining the H2AZ NLS.
Acetylation sites are indicated by arrows (Siddon and Tremethick, 1999). These can be seen to occur at lysine residues in the histone N-termini, close to the putative NLSs.

At the time of this study, a conventional NLS-like motif had been identified only in H2B (yeast, GKKKRSKA[33]; Moreland *et al.*, 1987). Since this NLS closely resembled the T-ag NLS, it was believed that H2A/2B nuclear import would be mediated through the 'conventional importin α/β pathway'. The results presented in this chapter, however, are not consistent with this idea. While the H2A/2B dimer was found to bind importin α/β with high affinity, this interaction was not mediated by importin α, but rather by importin β. This was found to be true for the H3/4 tetramer also.

Since this section of the study was completed, distinct NLSs have been identified within the N-terminal domains of all the core histones in mammalian cells (Balicki *et al.*, 2002; Baake *et al.*, 2001b; Baake *et al.*, 2001a; Muhlhausser *et al.*, 2001) and yeast (Mosammaparast *et al.*, 2002a; Mosammaparast *et al.*, 2002b; Mosammaparast *et al.*, 2001). These studies are presented in detail in Section 1.5.2 but, briefly, fragments spanning the length of the core histones were generated as fusion proteins and nuclear import was reconstituted in permeabilised cells. While the minimal NLS-containing sequence in the H2B N-terminal was indeed found to localise the β-galactosidase fusion protein to the nucleus in an importin α/β-dependent manner, when in the context of the whole protein, it was indeed importin β that was shown to be the key mediator of nuclear import (Baake *et al.*, 2001b). The nuclear import of H2A, H3 and H4 were also shown to be importin β-mediated (Mosammaparast *et al.*, 2002a; Mosammaparast *et al.*, 2002b; Baake *et al.*, 2001b; Baake *et al.*, 2001a; Mosammaparast *et al.*, 2001; Muhlhausser *et al.*, 2001).

In addition to the N-terminal NLSs, the central globular domains of the histones were proposed to form 'topogenic NLSs' which played a fundamental role in the overall importin binding properties (Mosammaparast *et al.*, 2002b; Baake *et al.*, 2001b; Baake *et al.*, 2001a; Mosammaparast *et al.*, 2001). The globular domains of the histones are involved in inter-histone contacts, as revealed by analysis of the crystal structure of the nucleosome core particle (Luger *et al.*, 1997). This implies topological masking of the globular domain NLSs in the context of histone transport to the nucleus in the form of the H2A/2B dimer and H3/4 tetramer. It is therefore likely to be the NLS within the histone N-terminus that directs nuclear translocation (Baake *et al.*, 2001a). Given this, it is possible that the H2AZ NLS sequence may be more readily recognised by importins than that of H2A, accounting for the higher binding affinity observed for the H2AZ/2B dimer than the H2A/2B dimer to importins (Table 3.1).

Importin binding affinity for histones may be reduced by chemical masking of the NLSs. This may indeed be the case for the acetylated histones H3 and H4 as the sites of acetylation lie within the N-terminal NLS-containing regions (Table 3.2; Mosammaparast *et al.*, 2002b; Baake

et al., 2001a) and would explain the lower affinity binding of importin α/β and β to acetylated H3/4 compared to non-acetylated H3/4 (Figure 3.3b).

Although they also play a crucial role in nucleosome structure, the chromatin associated proteins differ from histones in that they do not bind DNA directly but instead interact with histones to mediate structural changes in chromatin (Bustin and Reeves, 1996). Importin α had been shown to be involved in the nuclear uptake of HMG-14 and HMG-17, which harbour bipartite NLSs (Hock *et al.*, 1998; Table 3.2). This was demonstrated by fluorescence microscopy in experiments conducted using reconstituted *Xenopus laevis* nuclei and permeabilised mammalian cells (Hock *et al.*, 1998). The ELISA results presented here demonstrate that HMG interacts primarily with importin α and provide a quantitative measure of this interaction. Similarly, N1/N2, which also has a functional bipartite NLS, participates in a high affinity interaction with importin α/β, with a preference for importin α, consistent with the findings of a previous kinetic study (Hu and Jans, 1999; see Table 3.2).

NAP-1 does not contain a typical NLS consensus motif (Fujiinakata *et al.*, 1992) but does undergo nuclear localisation during the S-phase of cell division (Moss *et al.*, 1976). Moreover, as it was found to be associated with H2A/2B in the cytoplasm (Ito *et al.*, 1996; Fujiinakata *et al.*, 1992), NAP-1 was assigned a role as the shuttle protein for H2A/2B translocation into the nucleus (Ito *et al.*, 1996). Recently, the dual function of NAP-1 in the nuclear import and deposition of the H2A/2B cargo onto newly assembling chromatin was delineated (Mosammaparast *et al.*, 2002a). This is presented in Section 1.5.2 and shown schematically in Figure 1.9. Briefly, Mosammaparast *et al.* (2002a) showed, using affinity chromatography and immunofluorescence studies in fixed cells, that yeast Nap1p simultaneously binds H2A/2B and Kap114 (corresponding to the mammalian importin β homologue importin 7), by which the entire complex is transported into the nucleus. Nap1p was not found to interact with the other importins. The ELISA data presented in this section of work is consistent with this finding, indicating, similarly, that of the importins tested, the highest affinity for NAP-1 was exhibited by importin β (Table 3.1). H2A/2B was shown to localise to the nucleus also in the absence of Nap1p, mediated by Kap114 (importin β) alone (Baake *et al.*, 2001b; Baake *et al.*, 2001a; Mosammaparast *et al.*, 2001). The ELISA used here demonstrated that this interaction was of greater affinity than the NAP-1/importin β interaction (see Table 3.1; Johnson-Saliba *et al.*, 2000). Together, these findings suggest that several pathways exist to ensure the nuclear import of H2A/2B.

The results presented here, together with those of others (Mosammaparast *et al.*, 2002b; Baake *et al.*, 2001b; Baake *et al.*, 2001a; Mosammaparast *et al.*, 2001; Muhlhausser *et al.*, 2001; Jakel

et al., 1999) suggest that histones are transported into the nucleus along distinct and efficient pathways. Despite falling well below the MWCO of the NPC (~ 45 kDa), which would permit nuclear uptake by passive diffusion, the existence of these pathways is consistent with the unconditional requirement for histones within the nucleus. Functionally, they may provide the cell with the means to regulate histone nuclear import, perhaps according to the changing requirements during the cell cycle. Practically, for the purposes of gene delivery, these pathways might provide an efficient route into the nucleus for a histone-mediated DNA-carrier system.

CHAPTER 4

In vitro assembly and transfection of chromatinised plasmid

4.1. INTRODUCTION

Given the high affinity interaction between histones and importins (see Section 3.2 and Johnson-Saliba *et al.*, 2000), the existence of importin-mediated nuclear import pathways (Mosammaparast *et al.*, 2002b; Baake *et al.*, 2001b; Baake *et al.*, 2001a; Mosammaparast *et al.*, 2001; Muhlhausser *et al.*, 2001) and the absolute requirement for histones in the nucleus, it is reasonable to propose that histones have potential as DNA-carrier proteins for gene delivery purposes. While the use of individual histones as DNA-carrier proteins for gene delivery has been described (reviewed in Section 1.5.3), their use in the form of histone octamers as found in chromatin has not. Gene delivery and expression might be enhanced by the assembly of plasmid DNA with histone octamers into chromatin, since the octameric structure may present multiple NLSs (see Table 3.2), thereby facilitating importin-mediated nuclear import. In addition, histone octamers provide a greater capacity to condense DNA than individual histones, thereby offering a greater degree of protection from cytosolic degradation; another key element to ensure efficient gene delivery.

Histone octamers were reconstituted from recombinant histones H2A, H2B, H3 and H4 (*Xenopus laevis*). The same recombinant histones were employed in solving the crystal structure of the nucleosome core particle (Luger *et al.*, 1997) and, furthermore, may be generated in large quantities using a bacterial expression system (Luger *et al.*, 1999). Histone octamers were assembled at various stoichiometries with a reporter plasmid. For the purposes of this work, this plasmid/histone octamer assembly is referred to as 'chromatin' and the different stoichiometries of octamers to plasmid as 'chromatin constructs'. Plasmid not assembled into chromatin is referred to as 'naked' while chromatin constructs are regarded as being 'more extensively chromatinised' or 'less extensively chromatinised' at high or low nucleosome densities, respectively, depending on the stoichiometry of the histone octamers. Each chromatin assembly was characterised using a variety of techniques, including sedimentation velocity ultracentrifugation, atomic force microscopy (AFM), a DNA supercoiling assay and

micrococcal nuclease (MNase) digestion. The chromatin constructs were introduced into cultured cells, using two different transfection methods (electroporation and lipofection) and their suitability as vectors for gene delivery was assessed by detection of reporter gene expression using FACS.

4.2. Construction of a reporter plasmid for gene expression and subcellular tracking studies

The pGeneGrip™ plasmid (Gene Therapy Systems; Table 2.9) was chosen as the core plasmid for this study. pGeneGrip™ contains a MCS for the insertion of a gene of interest, the expression of which is driven by the CMV promoter and enhancer sequence. The plasmid also harbours specific sites (Grip™) for the attachment of a 'peptide nucleic acid label', such as a fluorescent probe for gene tracking experiments. This technology enables analysis of gene expression and DNA tracking to be performed in the same transfection experiment and is described in more detail in Section 2.2.16. The 'peptide nucleic acid labels' are comprised of two identical repeated sequences of nucleotides, in which the deoxyribose-phosphate backbone has been substituted for a peptide backbone (hence peptide nucleic acid or 'PNA'), linked by a hairpin loop at one end. At one of the free ends, the peptide backbone is derivatised with a functional group, such as fluorescein (to enable DNA tracking) or maleimide (to enable the attachment of peptides by thiol alkylation chemistry). The Grip™ site and PNA labels have complementary sequences and hybridisation is thus able to occur initially by Watson-Crick bonding. Ultimately, a triple helix hairpin loop structure is formed through PNA-DNA-PNA hybridisation, which has been shown to be stronger than DNA-DNA hybridisation and, thus, extremely stable under conditions of varying temperature and pH (Zelphati *et al.*, 2000; Zelphati *et al.*, 1999).

Red fluorescent protein (RFP) was chosen as the reporter gene for this study. It permits the analysis of transgene expression by virtue of its fluorescence characteristics (excitation maximum at 558 nm and emission maximum at 583 nm). The Gateway™ cloning system (Life Technologies) was used to insert the coding region of RFP, from the pDsRed-C1 vector (Table 2.9), into the MCS of pGeneGrip™ (described in Section 2.2.15). Briefly, the cloning technology is based on site-specific recombination events of bateriophage λ. Complementary attenuation (*att*) sites within the vectors recombine in reactions mediated by proteins from phage λ and *E. coli*, which facilitate the exchange of DNA flanked by the sites. Cloning involved the generation of an Entry vector containing the RFP coding sequence, followed by recombination with a Destination vector engineered from pGeneGrip™. The product was the Expression vector pGeneGrip-RFP, comprising the coding RFP sequence inserted into the

pGeneGrip™ plasmid. These reaction schemes are presented in Figures 4.1 - 4.3 (all vectors and inserts are colour coded throughout the recombination reactions).

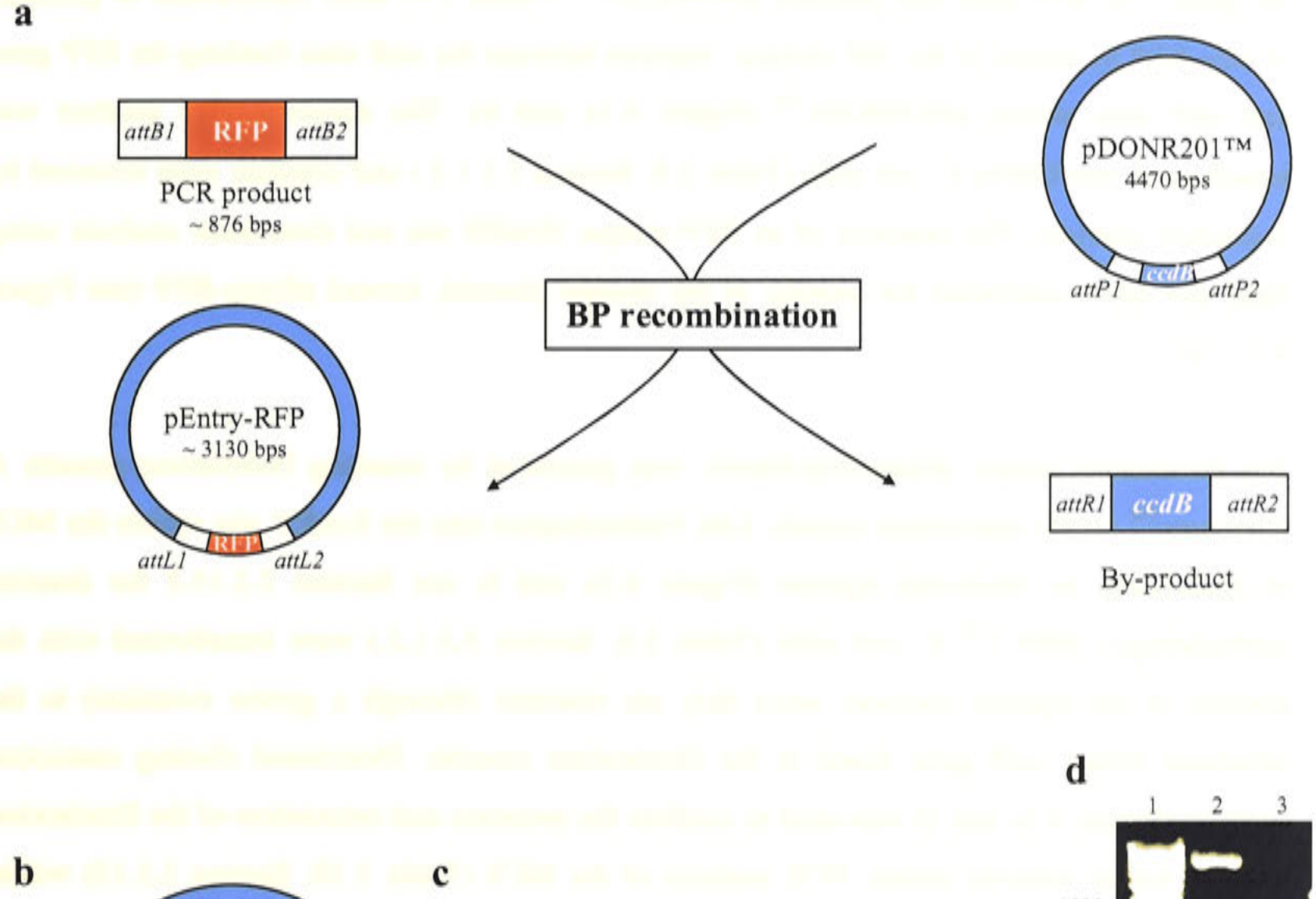

Figure 4.1. Generation of a Gateway™-compatible Entry vector containing the RFP coding sequence. The generation of pEntry-RFP using the BP recombination reaction (Section 2.2.15.1) is shown. The coding region of RFP from pDsRed-C1 was PCR-amplified using custom primers including *attB* sites flanking the RFP gene (Table 2.10). The 'BP recombination reaction' between the *attB*-flanked RFP gene and *attP*-flanked pDONR201™ vector cassette to produce the Entry clone containing the RFP gene flanked by *attL* sites is represented in (**a**), with the resultant plasmid restriction map shown in (**b**). The restriction analysis diagram (**c**), with the RFP insertion represented in red, shows the use of HindIII to verify the presence of an RFP-unique site, and HpaI and SacII to confirm directional cloning. A positive 'recombination' clone was confirmed by the presence of a unique HindIII site, shown in (**d**) lane 3. The release of a fragment between 750 and 1000 bps (~ 830 bps) upon HpaI/SacII digestion confirmed orientation is shown in (**e**) lane 3.

In order to generate the Entry vector (Figure 4.1; see Section 2.2.15.1 for detailed methodology), the coding region of RFP was PCR amplified from pDsRed-C1 (Clontech; Table 2.9) using custom primers (Life Technologies; Table 2.10) designed to insert *attB* sites flanking the gene. The RFP gene and plasmid pDONR201™ (Table 2.9) were recombined to generate pEntry-RFP by means of the 'BP clonase' reaction between the *attB* sites flanking the RFP gene and *attP* sites within pDONR201™ (Figure 4.1a and b). The recombination product was transformed into DH5α *E. coli* cells (Table 2.8; Section 2.2.1.2.) and colonies were screened by restriction analysis. The presence of an RFP-unique HindIII site and directional analysis using HpaI and SacII confirmed the identity of the desired plasmid, termed pEntry-RFP (see Figure 4.1c - e).

The Destination vector, pGeneGrip-DestA, was generated by inserting Destination cassette A (Gateway™ vector conversion system, Life Technologies) into the EcoRV site within the MCS of pGeneGrip by blunt-end ligation (Figure 4.2a and b; see Section 2.2.15.2 for detailed methodology). DB3.1™ *E. coli* cells (Table 2.8; Section 2.2.1.2.) were transformed with the product of the ligation reaction, since they are resistant (through a gyrase mutation) to the otherwise lethal *ccdB* gene found in the Destination cassette. Directional cloning restriction analysis (Figure 4.2c and d) was used to confirm the presence and orientation of the Destination cassette within selected clones. PCR analysis of the MCS (Table 2.10; Section 2.2.13) within the positive clones identified by restriction digestion (Figure 4.2d, lanes 3 and 7) confirmed the presence of the Destination cassette A (Figure 4.2e, lanes 2 and 3).

The pEntry-RFP plasmid was reacted with pGeneGrip-DestA (described in Section 2.2.15.3). 'LR clonase' was used to mediate recombination events between the *attL*-flanked RFP gene within pEntry-RFP and the *attR*-flanked Destination cassette A within pGeneGrip-DestA (Figure 4.3a and b). The product of the recombination reaction was transformed into DH5α *E. coli* cells (Table 2.8; Section 2.2.1.2.). Survival of DH5α *E. coli* colonies indicated loss of the lethal *ccdB* gene and hence successful recombination of the plasmids. The resulting clone, pGeneGrip-RFP, served as the reporter plasmid in this study. Colony PCR (5' and 3' pGeneGrip™ MCS primers, Gene Therapy Systems; Table 2.10; Section 2.2.13) was used to identify the presence and orientation of the inserted RFP gene within a number of colonies (Figure 4.3c). The positive colony was characterised by restriction digestion also with EcoRV, which released the inserted RFP gene and XhoI, which revealed the presence of a second restriction site due to the insertion of the RFP gene (Figure 4.3d and e).

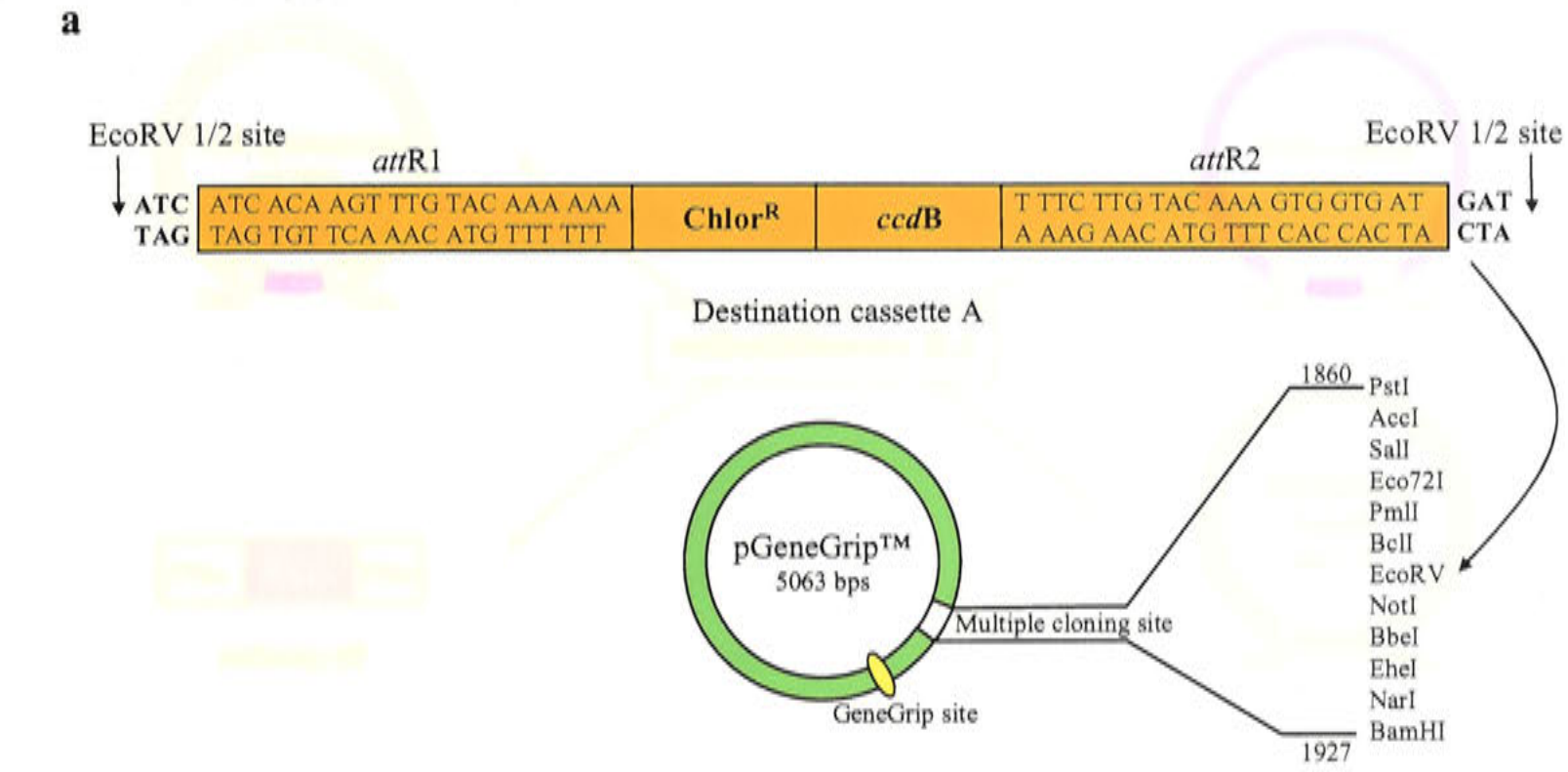

Figure 4.2. The production of the Destination vector, pGeneGrip-DestA. Destination cassette A (Life Technologies), flanked by *attR* sites, was blunt-end ligated into the EcoRV site within the MCS of pGeneGrip™ (**a**) to produce pGeneGrip-DestA, shown in (**b**) (see Section 2.2.15.2) as a restriction map The restriction analysis diagram in (**c**) shows the boundaries of the Destination cassette A (in orange) at EcoRV restriction sites. The use of SalI for orientation cloning analysis is indicated. SalI digestion produced two fragments of 1595 and 5158 bps, which can be seen in agarose gel insert in (**d**) (lanes 3 and 7). This was confirmed by PCR analysis across the MCS of the vector (5' and 3' pGeneGrip™ primers; see Table 2.10), shown in (**e**), where lanes 2 and 3 represent the positive clones corresponding to lanes 3 and 7 in (**d**). Lane 4 represents the pGeneGrip vector with the low molecular weight band corresponding to the MCS (61 bps). Controls included the ddH_2O blank for the PCR reaction (lane 5) and Destination cassette A (lane 6).

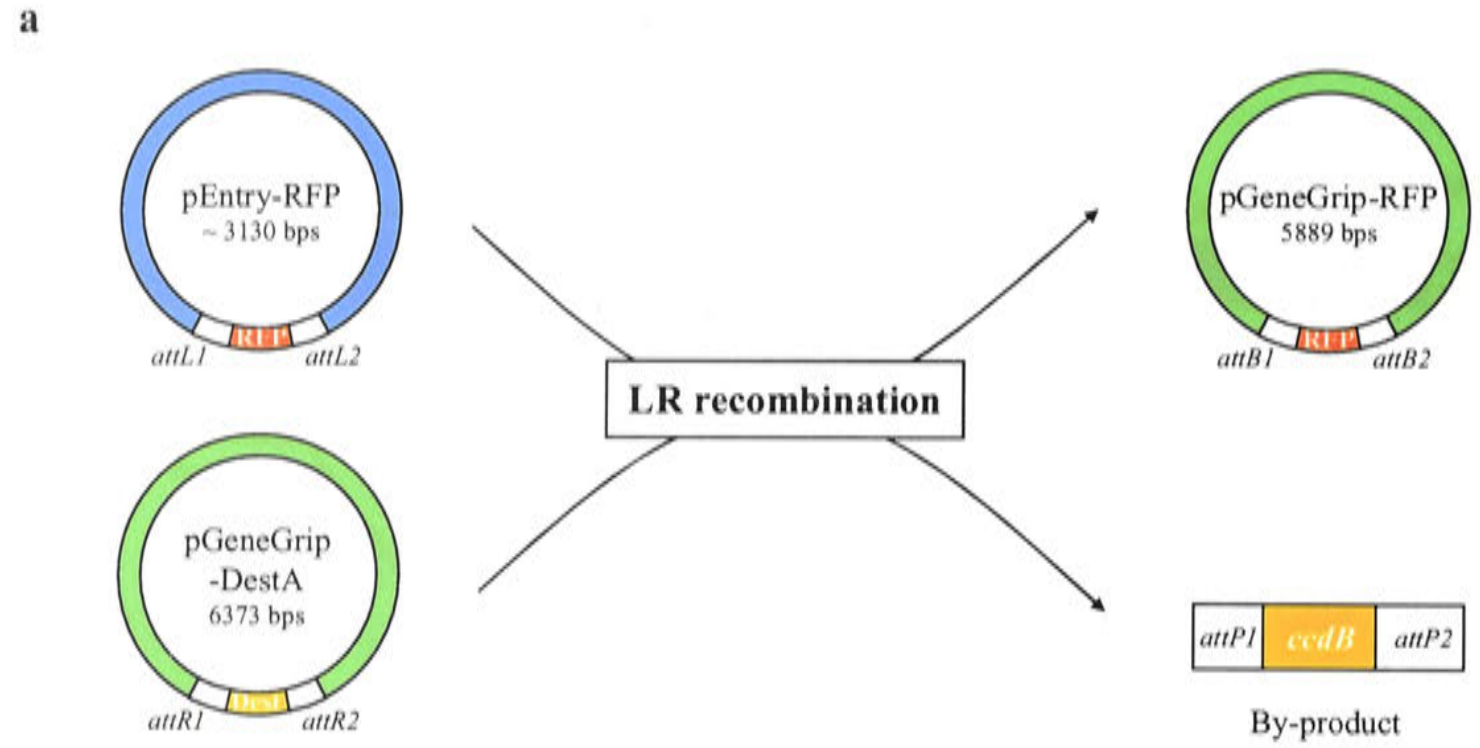

Figure 4.3. Recombination of the Entry vector pEntry-RFP with the Destination vector pGeneGrip-DestA produces the Expression vector pGeneGrip-RFP. The generation of pGeneGrip-RFP using the 'LR recombination reaction' between pEntry-RFP and pGeneGrip-DestA (see Section 2.2.15.3), is shown. LR clonase recombines the *attL* and *attR* sites in an 'LR recombination' (**a**) to produce the Expression vector, pGeneGrip-RFP, the restriction map of which is shown in (**b**). The agarose gel image in (**c**) shows the components of the LR reaction and PCR verification of the Expression vector. Lane 2 contains the pEntry-RFP and pGeneGrip-DestA mix before recombination. Lanes 3 - 5 contain 3 separate LR reactions. Disappearance of the band corresponding to pEntry-RFP and the appearance of higher molecular weight bands in lane 3 implies a successful recombination. Lanes 7 - 10 contain the PCR amplification products of 4 recombination colonies arising from LR reaction 1 (5' and 3' pGeneGrip™ primers; see Table 2.10). Lane 7 shows an insert corresponding in size to RFP (above 850 bps). A restriction analysis diagram in (**d**), with RFP coloured in red, shows the use of EcoRV (flanking the RFP insert) and XhoI (additional XhoI site due to RFP) to confirm the recombination reaction. Digestion products of the constituent recombination vectors can be seen in the agarose gel image in (**e**). XhoI has single restriction sites in both the RFP gene and in pGeneGrip, and therefore produces single cuts in pEntry-RFP and pGeneGrip-DestA, but releases 2 fragments of 2901 and 2926 bps from pGeneGrip-RFP. EcoRV does not digest pEntry-RFP, but releases the Destination cassette A (1700 bps) from pGeneGrip-DestA and releases RFP (864 bps) from pGeneGrip-RFP.

4.3. RECONSTITUTION OF THE HISTONE OCTAMER AND ASSEMBLY OF THE REPORTER PLASMID INTO CHROMATIN

Recombinant core histones H2A, H2B, H3 and H4 (*Xenopus laevis*) were purified from BL21DE3plysS *E. coli* cells (described in Sections 2.4.2.1 and 2.4.2.2) and were assembled into histone octamers (illustrated schematically in Figure 4.4a) according to the method described by Luger *et al.* (1999) (see Section 2.4.2.3).

Briefly, each lyophilised histone was solubilised in 1.5 ml of Unfolding buffer containing 7 M urea and the concentrations were determined spectrophotometrically by absorbance at 276 nm. The H2A and H2B solutions were adjusted to equimolar concentration using Unfolding buffer. The concentrations of H3 and H4 were adjusted similarly, but were 98 % that of H2A. The slight molar excess of H2A and H2B ensures maximal incorporation of H3 and H4 into the octamer, since under octamerisation conditions excess H3 and H4 form tetramers ($H3_2/H4_2$) that are difficult to purify away from the octamer (Luger *et al.*, 1999). The histone solutions were mixed, the final concentration was adjusted to 1 mg/ml of total protein using Unfolding buffer and the octamer assembly reaction was transferred into dialysis tubing (MWCO 6000 – 8000 Da, Spectra/Por® membrane, flat width 10 mm, Spectrum Laboratories).

The octamer assembly reaction was dialysed (overnight, at 4°C) against three changes of Refolding buffer (containing 2.2 M NaCl) and thereafter concentrated to around 1 ml (Centricon filter, YM-10, Amicon). The reconstituted octamers were purified using gel filtration (HiLoad 16/60 Superdex 200 prep grade column, Pharmacia) in the presence of Refolding buffer. Fractions corresponding to peaks on the chromatogram generated at 276 nm were analysed using SDS-PAGE (18 % polyacrylamide; Section 2.3.2). A typical chromatogram and gel analysis are presented in Figure 4.4b and c, respectively. Fractions containing the highest level of octamer (represented by an equimolar amount of each of the four constituent histones, as seen in Figure 4.4c fractions 64 - 70) were pooled and quantitated spectrophotometrically at 276 nm ($\varepsilon = 0.45$; Luger *et al.*, 1999) before use.

The number of histone octamers required to yield a physiological nucleosome density on the pGeneGrip-RFP reporter plasmid (5889 bps), based on the spacing of one histone octamer for every 230 bps (~150 bps per octamer plus ~80 bp of linker DNA), was calculated to be around 25. The purified octamers and pGeneGrip-RFP were assembled into chromatin constructs using the octamer transfer salt gradient method described by Thomas and Butler (Luger *et al.*, 1999; Richmond *et al.*, 1988; Thomas and Butler, 1977). The methodology, described in detail in Section 2.5.2, is based on the principle of progressively decreasing the salt concentration

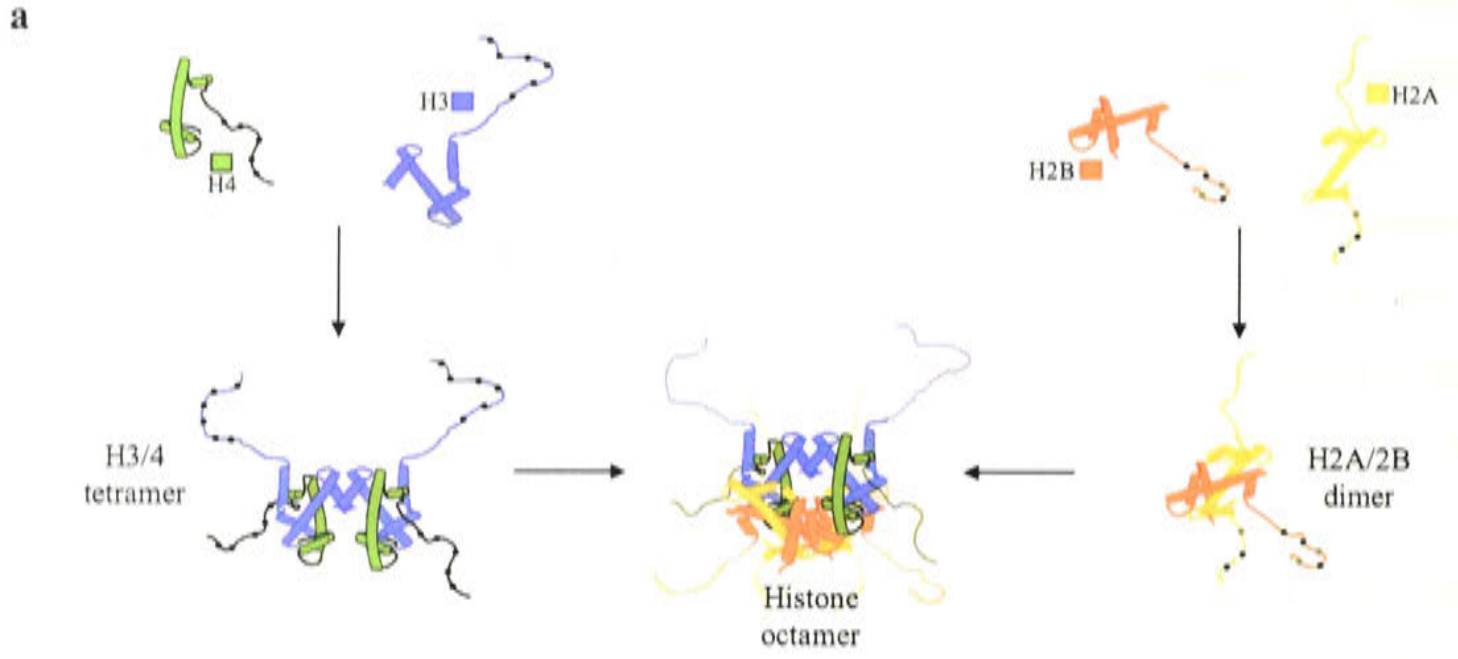

Figure 4.4. Histone octamer purification. Core histones H2A, H2B, H3 and H4 were reconstituted into octamers, shown schematically in (**a**). H2A and H2B form a dimer, two of which associate with the tetramer formed by H3 and H4 to form an octamer comprising [2(H2A/H2B)/($H3_2$/$H4_2$)]. Histone octamers were purified using gel filtration chromatography as described in Section 2.4.2.3 The chromatogram and corresponding SDS-PAGE analysis of fractions corresponding to peaks (indicated by arrows) on the chromatogram are shown in (**b**) and (**c**), respectively. Gel filtration was performed using a HiLoad 16/60 Superdex 200 prep grade column (Pharmacia) in Refolding buffer (see Table 2.4) at 4°C. The chromatogram was generated at 276 nm. The chart recording speed was 2 mm/minute. Fractions of 1 ml were collected every minute. The first peak (fractions 42 - 48) was comprised of high MW aggregation products. The second peak (fractions 62 - 75) was comprised of the reconstituted octamer as seen by equimolar amounts of the four constituent histones in the gel analysis (shown in **c**). The third peak contained excess H2A/2B (fractions 76 - 88), with traces of H3 and H4 (**c**). For this preparation, fractions 63 - 72 were pooled and the concentration of octamer determined spectrophotometrically at 276 nm. The control sample (boxed) was previously reconstituted H2A-octamer (with proven biological activity). The identity of the constituent histones is indicated; H2A and H2B co-migrate.

of the chromatin assembly buffer to facilitate DNA association with the octamers (Kunze and Netz, 2000). Lowering the initial salt concentration of the buffer from 2.2 M to physiological salt concentration (135 mM) would destabilise the octamer but interactions with DNA are able to substitute for the electrostatic stabilising effect of salt. DNA thus associates with the octamer to form a nucleosome, the basic structural unit of chromatin (see Figure 1.8). Typically, 50 µg of plasmid was assembled into chromatin to produce a range of constructs at stoichiometries of 0, 1, 2, 4, 10, 25 or 40 histone octamers per plasmid. The yield of chromatin was determined spectrophotometrically on the basis of DNA absorbance at 260 nm.

Before proceeding with the transfection studies, it was important to ensure that authentic chromatin had been assembled by using a variety of analytical approaches. These are described in the following section.

4.4. CHARACTERISATION OF THE CHROMATINISED REPORTER PLASMID

Sedimentation velocity ultracentrifugation, DNA supercoiling and atomic force microscopy (AFM) were used to characterise the nature of the chromatin structure formed upon the interaction of the plasmid DNA and histone octamers. However, as a definitive measure of chromatinisation of the pGeneGrip-RFP reporter plasmid, the formation of nucleosomes was verified using the micrococcal nuclease (MNase) digestion assay for each chromatin assembly reaction carried out for this study.

4.4.1. Sedimentation velocity ultracentrifugation reveals association of histone octamers with pGeneGrip-RFP

Analytical ultracentrifugation was used to determine the sedimentation coefficients (*s*-values; Svedberg units, *S*) of the various chromatin constructs, as described in Section 2.5.3. The rate of sedimentation depends on a number of factors, including the molecular mass, size and shape of the molecules of interest. Information may also be derived about sample purity, conformational changes, subunit stoichiometry and assembly or dissociation of multimeric macromolecular complexes. Macromolecules move in a characteristic formation, called a lamella or 'boundary', towards the bottom of the ultracentrifugation cell under the influence of a strong centrifugal field at a rate which is proportional to their *s*-value.

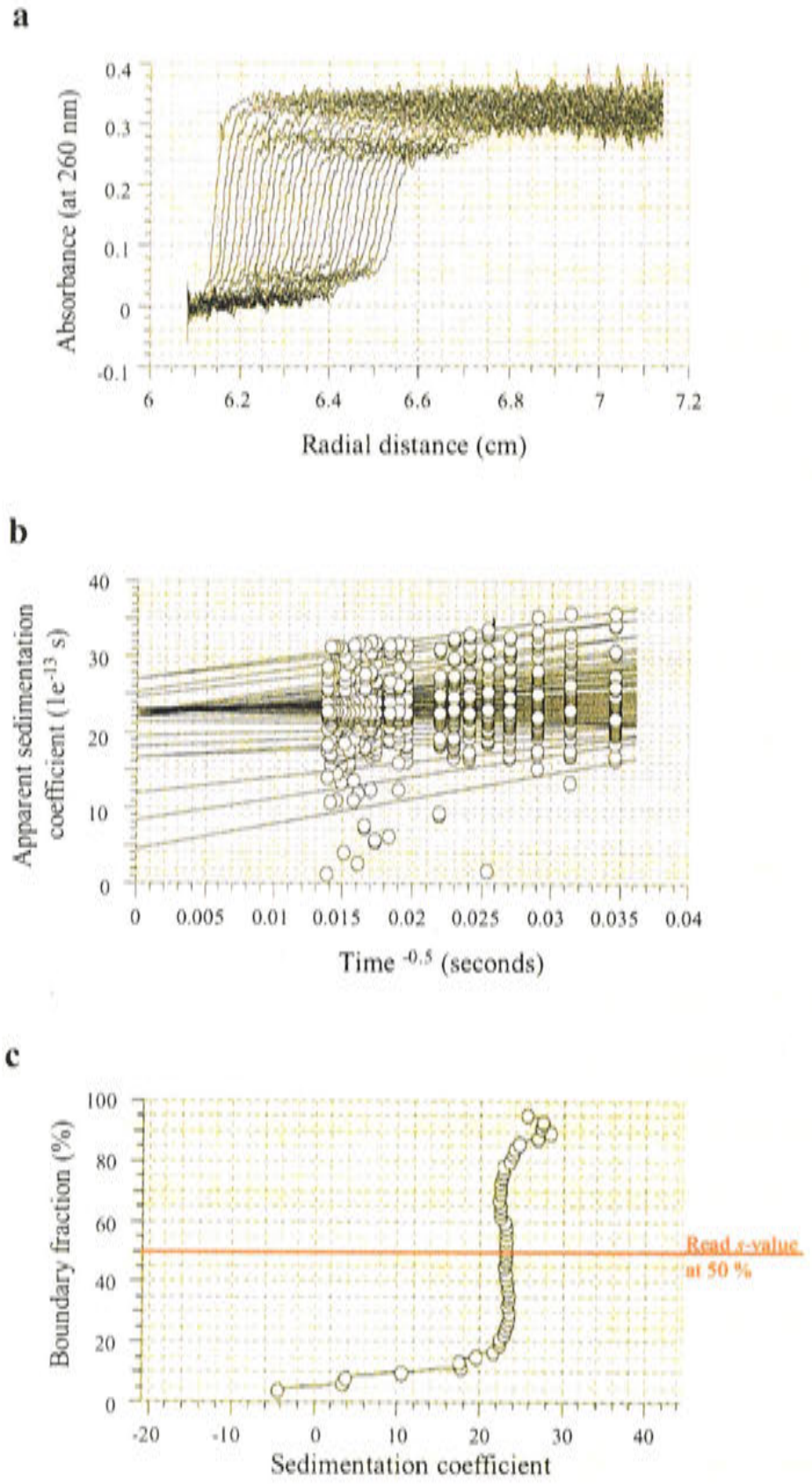

Figure 4.5. Sedimentation velocity ultracentrifugation analysis of the reporter plasmid, pGeneGrip-RFP. Sedimentation velocity ultracentrifugation was used to determine the sedimentation coefficient (*s*-value) of pGeneGrip-RFP, as described in Section 2.5.3. 6 µg of DNA were analysed in TE buffer, compared to a reference sample containing TE alone. Sedimentation was carried out overnight at 23000 rpm and 21°C. Typical ultracentrifugation-generated data analysed according to the method of van Holde and Weischet (1978) using Ultrascan software (Linux) is shown. The velocity plot, in (**a**), shows 30 absorbance scans at 260 nm of the DNA molecule boundary as it migrates towards the base of the centrifugation cell. The distance from the centre of rotation is represented on the x-axis; absorbance is represented on the y-axis. The van Holde and Weischet algorithm divides each boundary scan into 20 - 70 horizontal divisions and calculates an apparent *s*-value at each division. These are plotted against the inverse square root of time to produce an extrapolation plot, shown in (**b**). Linear extrapolations through each series of horizontal divisions intercept the y-axis, providing the true *s*-values for each boundary fraction. The boundary fraction is plotted against the *s*-values to obtain an integral distribution plot, shown in (**c**). Boundary fraction is represented on the y-axis expressed as a percentage; the sedimentation coefficient is represented on the x-axis. The sedimentation coefficient (*S*) is read at the 50 % boundary fraction, delineated in red.

Figure 4.5a is a typical example of a velocity plot of the unchromatinised reporter plasmid, pGeneGrip-RFP, showing a series of absorbance curves of the sample migrating towards the

bottom of the ultracentrifugation cell. This data was analysed using the UltraScan software (Linux) according to the method of van Holde and Weischet, in which the *s*-value is determined by measuring the rate of movement of the boundary midpoint (Hansen *et al.*, 1994; Van Holde and Weischet, 1978). An algorithm divides each scan into 20 - 70 horizontal divisions and calculates apparent *s*-values from the radial point of each division. The apparent *s*-values are plotted against the inverse square root of time to generate a van Holde and Weischet extrapolation plot (Figure 4.5b). Linear extrapolations are made through each series of horizontal divisions and intercept the Y-axis. These are the true *s*-values for each boundary fraction. Finally, the boundary fraction is plotted against the *s*-values to obtain a van Holde and Weischet integral distribution plot (Figure 4.5c). The sedimentation coefficient may then be read as the average *s*-value occurring at the 0.5 boundary fraction (50% on the distribution plot, Figure 4.5c). The sedimentation coefficient for pGeneGrip-RFP was found to be 23 ± 0 *S* (n = 2).

pGeneGrip-RFP was assembled into chromatin constructs at histone octamer stoichiometries of 1, 10, 25 and 40 per plasmid (described in Section 2.5.2), which were analysed similarly. Sedimentation velocity ultracentrifugation analysis revealed that as the number of octamers associated with the plasmid increased the sedimentation curves shifted towards the right compared to the reporter plasmid alone (0 octamers per plasmid), in accordance with increasing *s*-values (Figure 4.6a; Table 4.1). The number of octamers associated with the plasmid was found to be directly proportional to the sedimentation coefficient (Figure 4.6b; linear regression $R^2 = 0.995$). This confirmed that the octamers had assembled quantitatively onto the plasmid DNA.

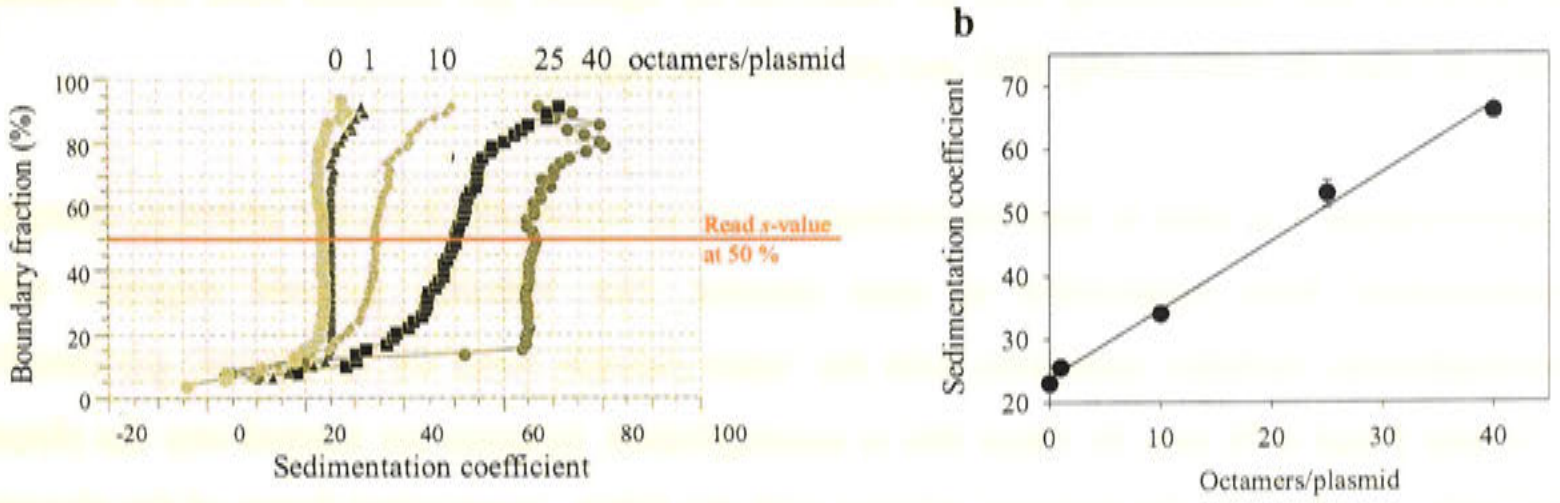

Figure 4.6. Sedimentation velocity ultracentrifugation analysis of the chromatin constructs. Chromatin constructs were assembled at 0, 1, 10, 25 and 40 molar ratios of octamers to DNA (pGeneGrip-RFP) using the octamer transfer salt dialysis method (Section 2.5.2) and sedimentation velocity ultracentrifugation was used to determine the sedimentation coefficients (*s*-values). Sedimentation data was captured and analysed as described in Section 2.5.3. Van Holde and Weischet distribution plots for each chromatin construct from a single experiment are shown in (**a**). The *s*-value is read at the midpoint of each curve, which is indicated in red. The sedimentation coefficients (*S*) were plotted against the number of octamers associated with the plasmid, shown in (**b**). Each point represents the average of two experiments, except for 10 octamers per plasmid which was performed once. Error bars represent the mean ± range/2 and where not shown fall within the symbols. See also Table 4.1.

Table 4.1. Sedimentation coefficients of the chromatin constructs.

Octamers/plasmid	Sedimentation coefficient (*S*)[A]	Calculated MW[B] (Da)
0	23 ± 0	3.89×10^6
1	25.5 ± 0.4	4.00×10^6
10	34	4.97×10^6
25	53 ± 2.1	6.60×10^6
40	66 ± 0	8.23×10^6

[A] Sedimentation coefficients (*s*-values, *S*) were determined using sedimentation velocity ultracentrifugation analysis, as described in Section 2.5.3 (see Figures 4.5 and 4.6). Results represent the mean ± range/2 for two separate estimations, with the exception of 10 octamers per plasmid which was performed once.
[B] The calculated molecular weight (MW) was based on the MW of the histone octamer (108486 Da) and pGeneGrip-RFP (5889 bps, which equates to 3886740 Da).

4.4.2. Assembly of pGeneGrip-RFP into chromatin *in vitro* induces supercoiling

The supercoiling assay was used in order to verify that the increase in *s*-values observed were due to nucleosome formation and not simply due to histones binding stochastically to the DNA. The degree of supercoiling of a plasmid following chromatin assembly provides a sensitive assay with which to examine nucleosome formation (see Section 2.5.4 for detailed method). One nucleosome introduces one negative supercoil in the plasmid DNA. The assay is based on the premise that supercoiling may be observed by agarose gel analysis once the histones are removed from the DNA using SDS and proteinase K digestion.

Topoisomerase I is used to remove intrinsic negative supercoils from the plasmid, changing its conformation from supercoiled to open circular. The 'relaxed' plasmid migrates with an electrophoretic mobility consistent with the 'open circular form' on an agarose gel (see Figure 4.7a lane 2 and 4.7b lane 2). Once this is accomplished, histones are titrated into the chromatin assembly reaction. As the histones interact with the DNA, supercoiled forms of the plasmid are induced due to nucleosome formation, even in the presence of Topoisomerase I (see Figure 4.7a lanes 2 - 5 and 7 - 8 and 4.7b lane 3).

This assay was used to demonstrate the feasibility of assembling a large plasmid into chromatin, as smaller plasmids such as the 3.4 kb pHBTS had been assembled into chromatin in the laboratory but larger plasmids such as the 5.9 kb pGeneGrip-RFP reporter plasmid, used in this

study, had not. A small scale chromatin assembly using the NAP-1-dependent method (Section 2.5.1) was carried out on the small pHBTS plasmid (Figure 4.7a lanes 1 - 5) and then on the larger pTRCA-GFP plasmid (5.1 kb) as a proof-of-principle (Figure 4.7a, lanes 6 - 8). Addition of only the H3/4 tetramer did not generate the supercoiled form (seen in Figure 4.7a, lanes 2 and 7). Topoisomers formed in the presence of the H3/4 tetramer with increasing amounts of the H2A/2B dimer and extended into the supercoiled form of the plasmid (Figure 4.7a, lanes 3 - 5 and 8). H2A/2B dimer titration beyond the optimal supercoiled state resulted in the reversion to more relaxed states of the plasmid (not shown).

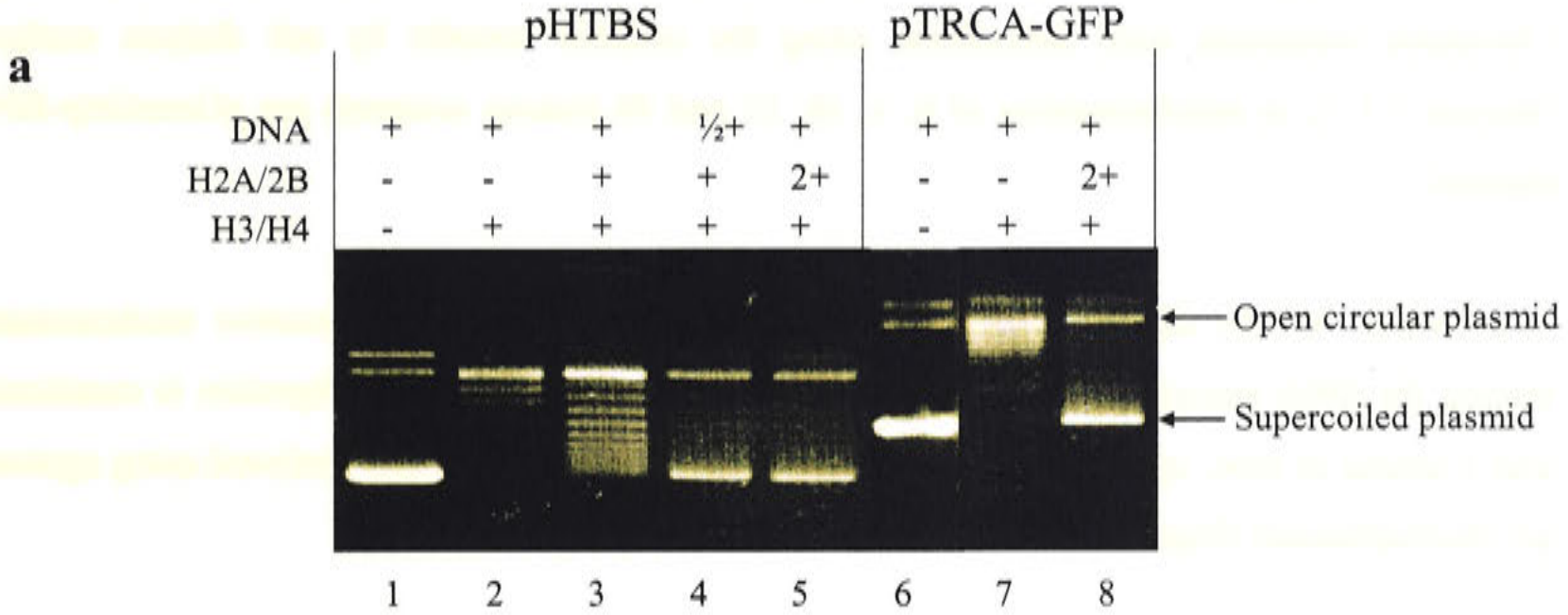

Figure 4.7. Supercoiling analysis of chromatinised pGeneGrip-RFP. Generation of the supercoiled form of the reporter plasmid, pGeneGrip-RFP, in the presence of core histones was monitored using the supercoiling assay (described in Section 2.5.4). The agarose gel analysis (1 %) is shown for pHBTS (3.4 kb) and pTRCA-GFP (5.1 kb) in (**a**), before the reaction was scaled up for the larger plasmid pGeneGrip-RFP (5.9 kb) shown in (**b**). Prior to the assay, plasmids were incubated with Topoisomerase I to induce a conformational change from the supercoiled state to open circular; (**a**) lanes 2 and 7 and (**b**) lane 2. Upon the further addition of increasing amounts of the H2A/2B dimer topoisomers are formed; (**a**) lanes 3 - 5 and lane 8. The optimal supercoiled state is shown in (**a**) lanes 5 and 8 and (**b**) lane 3. Molar ratios of DNA, H2A/2B and H3/4 are denoted.

Based on these results, the NAP-1 chromatin assembly reaction for pGeneGrip-RFP plasmid (5.9 kb) was scaled up accordingly. As seen in Figure 4.7b (lane 3), supercoiling was also induced in pGeneGrip-RFP. This demonstrated that the larger pGeneGrip-RFP plasmid could be efficiently assembled into chromatin also.

4.4.3. Micrococcal nuclease digestion reveals the presence of nucleosomes in chromatinised pGeneGrip-RFP

Resistance to digestion by MNase (see Section 2.5.5 for methodology) provides definitive proof of nucleosome formation upon reaction of plasmid DNA with histone octamers and, for this reason, was used to verify each chromatin assembly reaction carried out for this study. Chromatin constructs were assembled, using the octamer transfer by salt dialysis method (Section 2.5.2), at stoichiometries of 0, 1, 10, 25 and 40 histone octamers per pGeneGrip-RFP plasmid.

In principle, MNase digests the unprotected linker DNA between consecutive nucleosomes, leaving the DNA associated with nucleosomes intact (see Figure 4.8a). Digestion is monitored over a course of time, upon completion of which, DNA is recovered and analysed using agarose gel electrophoresis (Figure 4.8b).

The hallmark of chromatin is the generation of a ladder of bands following digestion with MNase. These bands correspond to DNA associated with a single nucleosome (mono-nucleosomal DNA), two tandem nucleosomes (di-nucleosomal DNA), three tandem nucleosomes (tri-nucleosomal DNA), and so on depending on the degree of accessibilty of the DNA during the time period of the experiment. The appearance of such a banding pattern demonstrates the formation of a nucleosomal array definitively (indicated with arrows in Figure 4.8), each protecting about 140 bps of DNA.

Apart from indicating the presence of nucleosomes, gel analysis also provides information on the degree of DNA protection since the rate of cutting is proportional to the degree of chromatinisation (or, in other words, the density of nucleosomes). For instance, the construct harbouring only one octamer was digested rapidly (similar to free DNA; not shown), with the appearance of the mono-nucleosomal band after only 10 minutes of incubation with MNase. As the incubation time with the enzyme increased to 20 and 60 minutes, this band migrated even further, indicating that over time the MNase gained access to and digested the free ends of the nucleosomal DNA as well. In contrast, plasmid assembled into chromatin with greater nucleosomal density took longer to be digested to the mono-nucleosome level, indicating greater MNase inaccessibility. Even after 60 minutes the extent of DNA protection was such

that di-nucleosomes and tri-nucleosomes could still clearly be seen to persist in the chromatin constructs containing 25 and 40 octamers per plasmid.

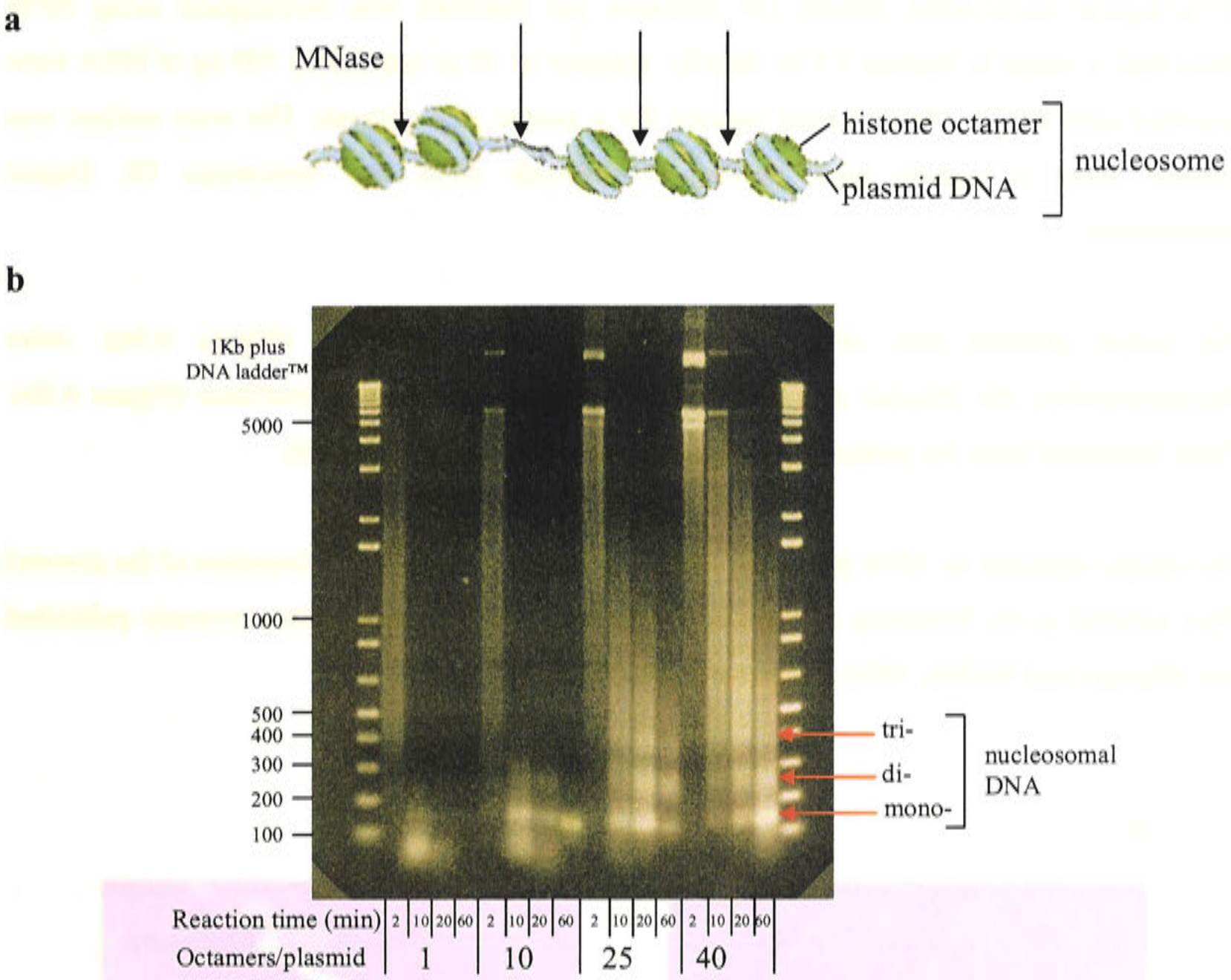

Figure 4.8. Micrococcal nuclease digestion of the chromatin constructs reveals the presence of nucleosomes. The principle of the MNase assay is based on digestion of unprotected linker DNA, while nucleosomal DNA remains intact, as illustrated in (**a**). An example of a typical MNase digestion of chromatinised plasmid analysed using agarose gel electrophoresis is shown in (**b**). Chromatin constructs containing 1, 10, 25 and 40 octamers per plasmid were incubated at room temperature for 2, 10, 20 and 60 minutes with MNase (25 mU/µg DNA), DNA recovered using 3M NaOAc precipitation and analysed on a 1.5 % agarose gel (described in Section 2.5.5). Each lane represents a different time point for the reaction (as indicated) and lanes are grouped according to the chromatin construct. The characteristic banding pattern corresponds to nucleosomal DNA (indicated by the red arrows).

Resistance to MNase digestion also has implications for the protection of DNA once transfected into cells. The observed resilience of the chromatin constructs to MNase digestion is an indication that within the cellular environment they should be more resistant to cytosolic nucleases (Pollard *et al.*, 2001; Lechardeur *et al.*, 1999).

4.4.4. Atomic force microscopy reveals compaction of chromatinised plasmid from open loops into extended rod-like structures

The topological structure of the pGeneGrip-RFP when naked and chromatinised at physiological nucleosome density (25 octamers per plasmid) was investigated using AFM (described in detail in Section 2.5.6). Briefly, samples of 10 µl containing 100 ng of DNA were adsorbed onto freshly cleaved mica squares for a period of 5 minutes. The mica surface was scanned using a tapping mode setting (MultiMode AFM and Nanoscope III, Digital Instruments).

The naked plasmid was observed in open loop conformations (Figure 4.9a). After chromatinisation, the plasmid appeared to be condensed into rod-like structures (Figure 4.9b). These structures were the predominant form for the chromatinised plasmid.

The images obtained by AFM provided visual confirmation that chromatinisation of the plasmid DNA resulted in the formation of rod-like condensates, in agreement with previously published data (Hansen and Wolffe, 1992; Simpson *et al.*, 1985).

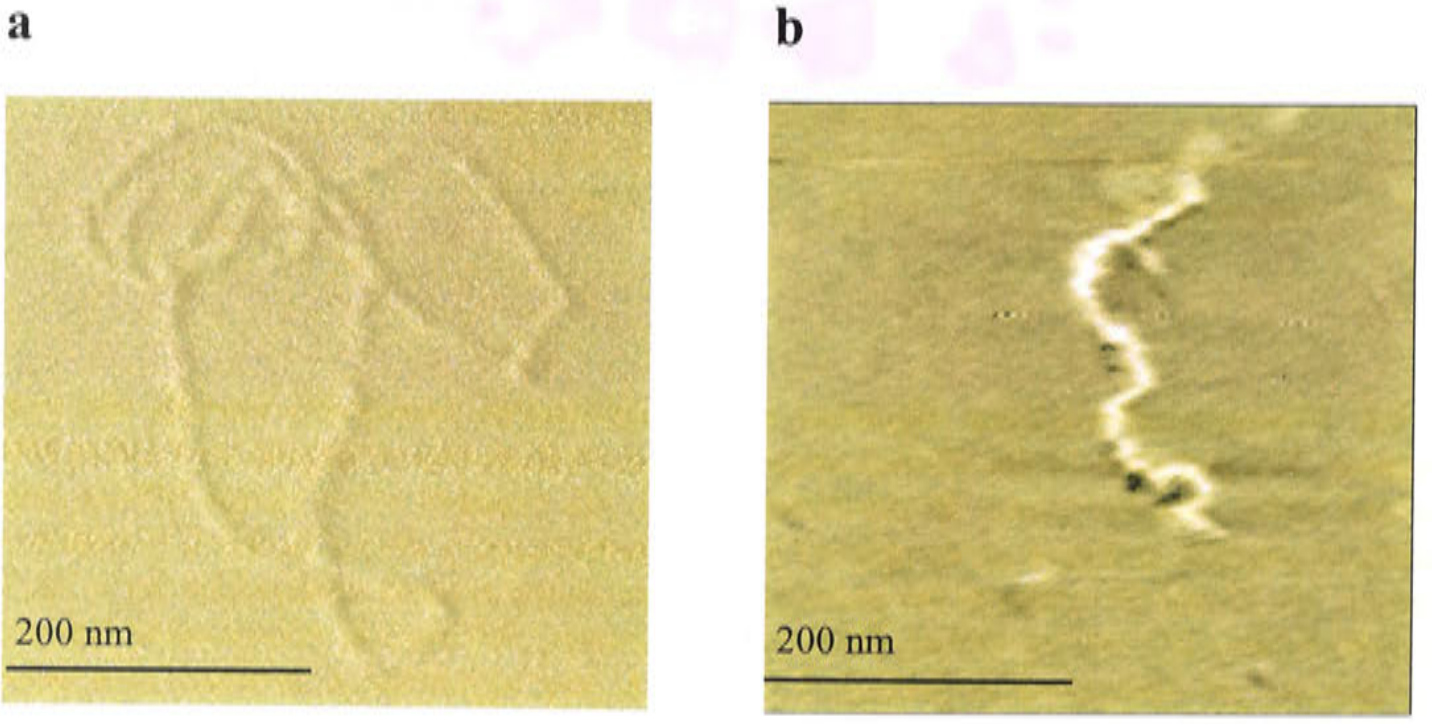

Figure 4.9. AFM images comparing naked and chromatinised plasmid DNA. pGeneGrip-RFP was subjected to chromatin assembly in the absence of histone octamers (naked plasmid) and at physiological nucleosome density (25 octamers per plasmid) (Section 2.5.2). Samples containing 100 ng of DNA were adsorbed onto freshly cleaved mica in a volume of 10 µl of chromatin buffer (135 mM NaCl/10 mM Tris-HCl). AFM was performed in tapping mode (MultiMode AFM and Nanoscope III, Digital Instruments) using a 125 µm silicon cantilever, with scanning rate 1 – 2 Hz and oscillation 400 kHz. Images were analysed using Nanoscope software (Digital Instruments). Images of the naked plasmid and extended structures formed upon chromatinisation at physiological nucleosome density of the plasmid (25 octamers per plasmid) are shown to scale 200 nm in (**a**) and (**b**), respectively.

4.5. Delivery of chromatinised reporter plasmid into cells in culture using electroporation

In order to test whether chromatinisation of plasmid DNA would enhance transfection efficiency *in vitro*, the chromatin constructs were introduced into cells in culture. Electroporation was chosen as the method for the first line of investigation of the potential of chromatin for gene delivery as it allows introduction of transfection constructs directly into the cytoplasm.

4.5.1. Optimisation of electroporation parameters for investigation of transport from the cytoplasm to the nucleus

4.5.1.1. Selecting an electroporation voltage which preserves the nuclear membrane

In order to be able to relate reporter gene expression directly to the efficiency of translocation into the nucleus, it was important to ensure that the transfection constructs were initially taken up into the cytoplasm exclusively and not into the nucleus. For this reason, a voltage for electroporation was sought that facilitated permeabilisation of the cell membrane but kept the NE intact.

HTC cells were selected as the cell type for the electroporation experiments because these cells were routinely used as the model cell type in a mechanically perforated cell system to investigate protein import into the nucleus *in vitro* (Chan *et al.*, 2000; Hu and Jans, 1999; Xiao and Jans, 1998), which had been established previously in the laboratory. In order to determine an optimal voltage that maximised electroporation but minimised NE damage, electroporation of HTC cells was carried out in PBS over a range of voltages, from 200 to 400 V, at a fixed capacitance of 500 μF in the presence of FITC-labelled dextrans of molecular masses 20 kDa and 70 kDa (see Sections 2.7.1 and 2.11.1 for detailed methods). FITC-dextran of MW 20 kDa is able to permeate the nucleus, being below the MWCO of the NPC (45 kDa); hence, fluorescence should be visible throughout the entire cell following electroporation. FITC-dextran with a MW of 70 kDa would, on the other hand, be excluded from the nucleus provided that the NE is intact. In this case, the resulting fluorescence would be localised to the cytoplasm. In the absence of electroporation, both dextrans should be excluded from the cell.

Following electroporation, FITC-dextran that had not been taken up by the cells was removed from the extracellular medium (PBS) by two rounds of centrifugation and washing in PBS (6000 rpm, Eppendorf centrifuge) before final resuspension of the cells in fresh PBS. Cells were divided into two aliquots. The resulting subcellular fluorescence was visualised in the first

aliquot of cells by confocal laser scanning microscopy (CLSM; described in Section 2.11.1). Cellular uptake of FITC-dextrans in the second aliquot of cells was analysed using fluorescence activated cell sorting (FACS). Prior to the analyses, these cells were incubated in propidium iodide (PI; Section 2.9.1.1) in order to assess the effect of electroporation on cell viability simultaneously (see Section 4.5.1.2). Dual FITC- and PI-fluorescence were detected (channels FL1 and FL2, respectively, FACScan, Becton Dickinson; see Section 2.9.1). FITC-fluorescence was quantitated relative to cells incubated in the presence of FITC-dextran but which had not been electroporated. For each test sample, 100000 events (cells) were recorded and analysed (CellQuest software, Macintosh). The FACS dot plots are shown in Figure 4.10, paired with the corresponding CLSM images. Qualitative results from the 70 kDa FITC-dextran optimisation are presented in Table 4.2.

Of the cells electroporated at 200 V with 70 kDa FITC-dextran 70.6 % were positive for FITC-fluorescence by FACS analysis but the geometric mean intensity within the cells was low. Due to the low fluorescence intensity, scoring the subcellular fluorescence in sufficient cells in the corresponding CLSM images could not be accomplished but, qualitatively, it appeared to be predominantly cytoplasmic (Figure 4.10b; Table 4.2). In contrast, almost all of the cells electroporated at 400 V had taken up the FITC-dextran and the geometric mean fluorescence was higher than in cells electroporated at 200 V (Figure 4.10b, FACS dot plot; Table 4.2). CLSM revealed that while some cells showed exclusively cytoplasmic fluorescence, in most of the cells fluorescence could be seen throughout the entire cell, including the nucleus, indicating that the NE had been permeabilised (Figure 4.10b, CLSM image; Table 4.2). This implied that 400 V was not suitable for the intended transfection experiments where transport from the cytoplasm to the nucleus was to be the parameter under investigation and thus required an intact nucleus. Electroporation at 300 V yielded levels of geometric mean fluorescence intensity greater than those seen with electroporation at 200 V and FACS analysis showed that almost all of the cells had taken up fluorescence (Table 4.2). Importantly, CLSM results for electroporation at 300 V indicated integrity of the NE, with fluorescence being exclusively cytoplasmic in 70 % of the cells and only 20 % not being permeabilised at the plasma membrane level (Figure 4.10b; Table 4.2). In order to show that the NE was still competent for passive transport after electroporation at 300 V, cells were electroporated in the presence of 20 kDa FITC-dextran. This dextran was found to distribute throughout the entire cell, demonstrating that the NE retained is passive permeability properties (Figure 4.10a).

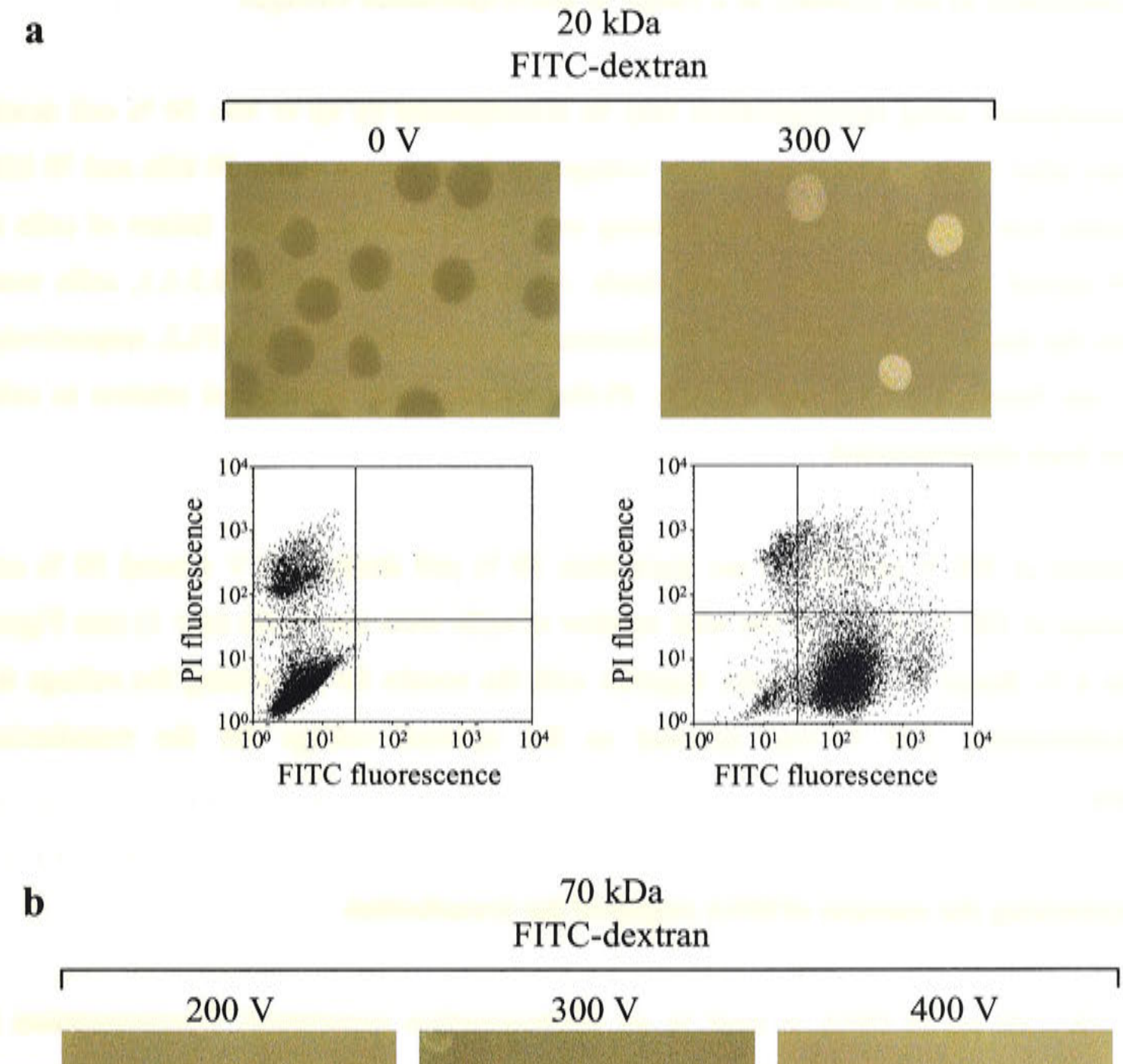

Figure 4.10. Determination of an optimal voltage for electroporation of HTC cells. Cells were electroporated in the presence of FITC-dextran of MW 20 kDa, shown in panel (**a**), or 70 kDa, shown in panel (**b**), at a range of voltages (2.5×10^7 cells/ml, total volume 400 µl, PBS buffer, BioRad 0.4cm gap cuvettes, 500 µF, BioRad GenePulser), and cellular uptake was monitored by CLSM and FACS (see Sections 2.11.1 and 2.9.1.3 for respective methods). Within each FITC-dextran group, the upper row of panels shows typical images captured using CLSM (BioRad, zoom 1, gain 900, Kalman 5) and the lower row of panels shows the corresponding FACS dot plot scans (FACScan, Becton Dickson). FITC was detected though channel FL1 and is represented on the x-axis; PI was detected though channel FL2 and is represented on the y-axis. The quadrants were set according to HTC cells which were incubated with FITC-dextran and PI, but not electroporated (**a**, 0 V). The results represent a single experiment. Collated data is presented in Table 4.2.

4.5.1.2. Assessment of cell viability at a range of electroporation voltages

Optimal transfection using electroporation may be accompanied by up to 30 - 50 % cell death. Cell viability after electroporation at various voltages in the presence of the 20 kDa and 70 kDa FITC-dextrans was determined using PI staining and FACS analysis, where failure of cells to exclude PI served as the indicator of cell death. As described in Section 4.5.1.1, cells were analysed on the basis of dual FITC- and PI-fluorescence (channels FL1 and FL2, respectively, FACScan; see Sections 2.9.1.1 and 2.9.1.3). PI-fluorescence was quantitated relative to cells that had not been electroporated.

Electroporation at 300 V resulted in not more than 30 % cell death, 400 V around 50 % cell death, whereas at 200 V 13.7 % of the total number of cells were not viable (n = 1) (see Figure 4.10; Table 4.2). Based on these results, together with the results for optimising the voltage for NE permeabilisation, 300 V was selected as the optimal voltage for the transfection experiments.

4.5.1.3. Optimising the amount of DNA required for transfection

Typically, 10 - 40 µg of DNA is used in an electroporation experiment. Electroporation is therefore a 'costly' transfection method in terms of the amount of DNA and histone octamer material used (50 µg of plasmid DNA was assembled into chromatin using 2 – 56 µg of histone octamers for each construct generated). In this context, it was important to determine the minimal dose of plasmid DNA for effective transfection. Moreover, this dose would have to be sufficient to yield detectable reporter gene expression but not be at the limit of saturation so that room for improvement with regard to gene transfer efficiency could be accommodated (through chromatinisation or other modifications).

Varying amounts of the pGeneGrip-RFP plasmid were electroporated at 300 V and 500 µF into HTC cells (see Section 2.7.1 for detailed method). Transfected cells were cultured for 48 hours, following which RFP expression was detected using FACS analysis, as described in Section 2.9.1.2. RFP positive cells were detected (channel FL2) relative to cells that had been subjected to the electroporation pulse in the absence of DNA.

Table 4.2. Uptake of 70 kDa FITC-dextran and cell viability at various electroporation voltages.

Voltage (V)	CLSM[A]				FACS[B]		
	Cells counted	Cyt FITC (% cells)	Nuc FITC (% cells)	Non-perm (% cells)	Fluorescent cells (%)[C]	Geo mean fluorescence[D]	Non-viable cells (%)[E]
0	ND[F]	ND	ND	ND	0.1 ± 0.1	4.3 ± 0.4	17.3 ± 4.6
200	ND	ND	ND	ND	70.6	156.8	13.7
300	177	69.5	10.7	19.8	96.6 ± 2.5	266.6 ± 31.5	29.5 ± 0.5
400	86	32.6	59.3	8.1	97.0 ± 2.0	341.5 ± 116.6	53.4 ± 5.7

Cells were electroporated in the presence of FITC-dextran of 70000 MW at voltages indicated and analysed by CLSM and FACS, as described in Sections 4.5.1.1 and 4.5.1.2.

[A] Cells were counted for at least 10 separate CLSM images per voltage. Cells were qualitatively assessed for cytoplasmic fluorescence (Cyt FITC), nuclear fluorescence (Nuc FITC) or not permeabilised (Non-perm) (see Figure 4.10). Results are presented as a percentage of total cells counted.

[B] FACS data were generated as described in Section 2.9.1, with 100000 cells analysed using CellQuest software (Macintosh). Results represent the mean ± range/2 of two experiments, with the exception of 200 V, which was performed once.

[C] FITC-positive cells were detected through channel FL1-H, relative to cells which had not been electroporated (see Figure 4.10). Results are presented as a percentage of total cells analysed.

[D] Geometric mean values of FITC fluorescence.

[E] Non-viable cells were assessed on the basis of PI fluorescence detected through channel FL2-H relative to cells which had not been electroporated (see Figure 4.10). Results are presented as a percentage of total cells analysed.

[F] Not determined. Cells could not be scored on the basis of no fluorescent signal in the 0 V samples and weak fluorescence in the 200 V samples.

The results obtained, shown in Figure 4.11, indicated that electroporation of 20 µg of plasmid DNA yielded the highest level of gene expression, with 4.5 ± 1.9 % of the cells positive for RFP fluorescence, followed by 10 µg with 1.9 ± 0.9 % RFP positive cells and 1 µg with 0.2 ± 0 % RFP positive cells (n = 2; see Figure 4.11a for typical FACS-generated profiles). Although the transfection efficiency was low (less than 10 % RFP positive cells), due mainly to the stringent transfection conditions, both the percentage of cells and fluorescence intensity were able to be analysed in terms of fluctuations in transgene expression levels (Figure 4.11b and c, respectively).

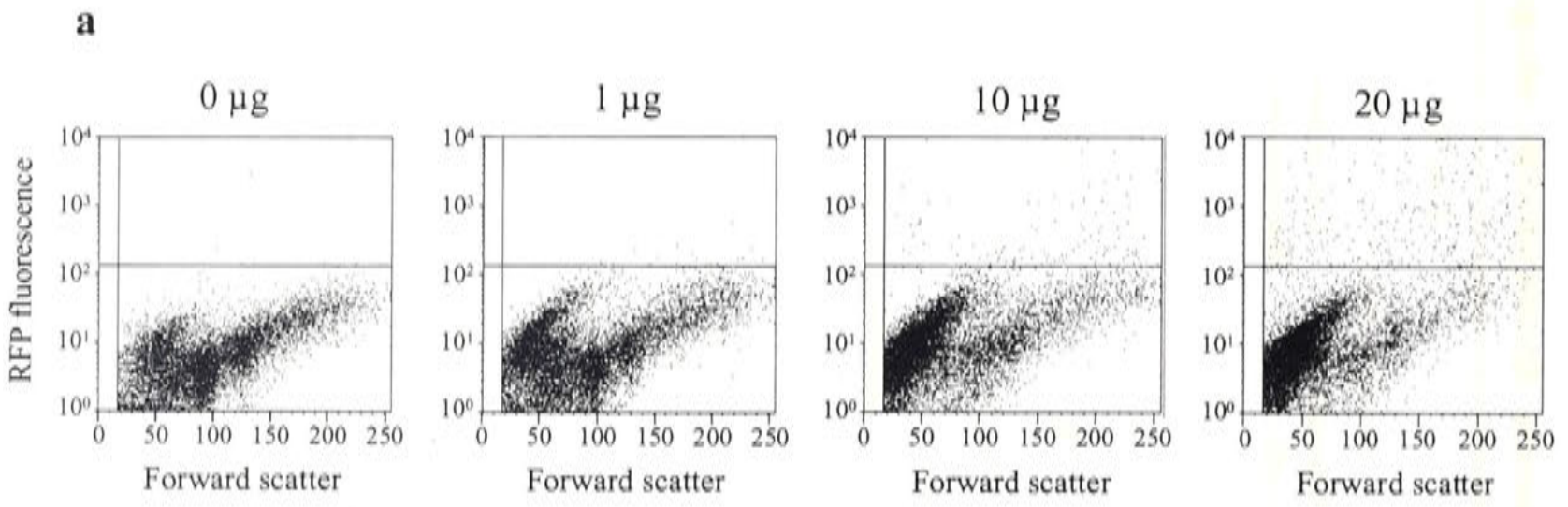

Figure 4.11. Titration of pGeneGrip-RFP for electroporation of HTC cells. 1, 10 and 20 µg of pGeneGrip-RFP were transfected into HTC cells by electroporation (5×10^6 cells, 400 µl total volume, PBS buffer, BioRad 0.4cm gap cuvettes, 500 µF, 300 V, BioRad GenePulser; Section 2.7.1). RFP expression was analysed by FACS 48 hours later (channel FL2; Section 2.9.1.2). The FACS dot plots shown in (**a**) represent the gene expression profiles from varying amounts of DNA, as indicated. Data from these were analysed using CellQuest software (Macintosh) and the percentage of cells expressing RFP and their corresponding geometric mean fluorescence values were plotted against the amount of DNA transfected, as shown in (**b**) and (**c**), respectively. Each point represents the mean ± range/2 of 2 separate experiments.

Based on these results, 10 µg of DNA were transfected in the subsequent electroporation experiments aimed at establishing the proof-of-principle of using a DNA delivery construct in the form of *in vitro* assembled chromatin.

4.5.2. Reporter gene expression in HTC cells electroporated with chromatinised plasmid

Chromatin constructs assembled at stoichiometries of 0, 2, 4, 25 and 40 octamers per pGeneGrip-RFP reporter plasmid were prepared using the histone octamer transfer salt dialysis method as described in Section 2.5.2. The DNA content was determined spectrophotometrically at 260 nm for each chromatin construct and 10 µg of DNA were aliquotted for electroporation.

HTC cells were electroporated in the presence of the chromatin constructs according to the parameters established in Section 4.5.1 (10 µg DNA, 300 V, 500 µF) and in a constant volume and salt concentration of 400 µl and 135 mM NaCl (PBS), respectively (Section 2.7.1). In order to establish if the relative level of gene expression was due to the presence of histones in the transfection mix or the effect of octamers in causing compaction of the plasmid, transfections were performed using 'associations' of pGeneGrip-RFP reporter plasmid and histones. Each 'association' contained the amount of octamer corresponding to that in the chromatinised constructs. These were assembled under conditions which would not permit chromatinisation. Histone octamers were transferred into chromatin buffer (CB, 135 mM NaCl/10 mM Tris-HCl); histone octamers are not stable below 2.2 M NaCl in the absence of DNA and therefore dissociation would occur. Plasmid was added subsequently and incubated for no longer than 10 minutes (5 minutes of which were on ice).

The percentages of cells expressing RFP from the range of chromatin constructs and 'DNA/histone associations' were determined by FACS 48 hours post-transfection (described in Section 2.9.1.2). As the density of octamers per plasmid increased, the percentage of cells showing RFP reporter gene expression decreased (Figure 4.12; Table 4.3). Relative to the naked plasmid (0 octamers per plasmid), a 2-fold decrease in the percentages of cells expressing RFP occurred with transfection of the 4 octamers per plasmid construct (although this did not reach statistical significance; $p = 0.09$, $n = 2$), as well as with the 25 and the 40 octamers per plasmid constructs ($p = 0.00001$ and 0.003, respectively). Similarly, but more dramatically, RFP expressing cells diminished to 14.3 ± 8.6 % ($p = 0.002$, $n = 3$) and 17.0 ± 7.4 % ($p = 0.002$, $n = 3$) when pGeneGrip-RFP had been 'associated' just prior to electroporation with the amount histones corresponding to the 25 and 40 octamers per plasmid constructs, respectively (see Table 4.3).

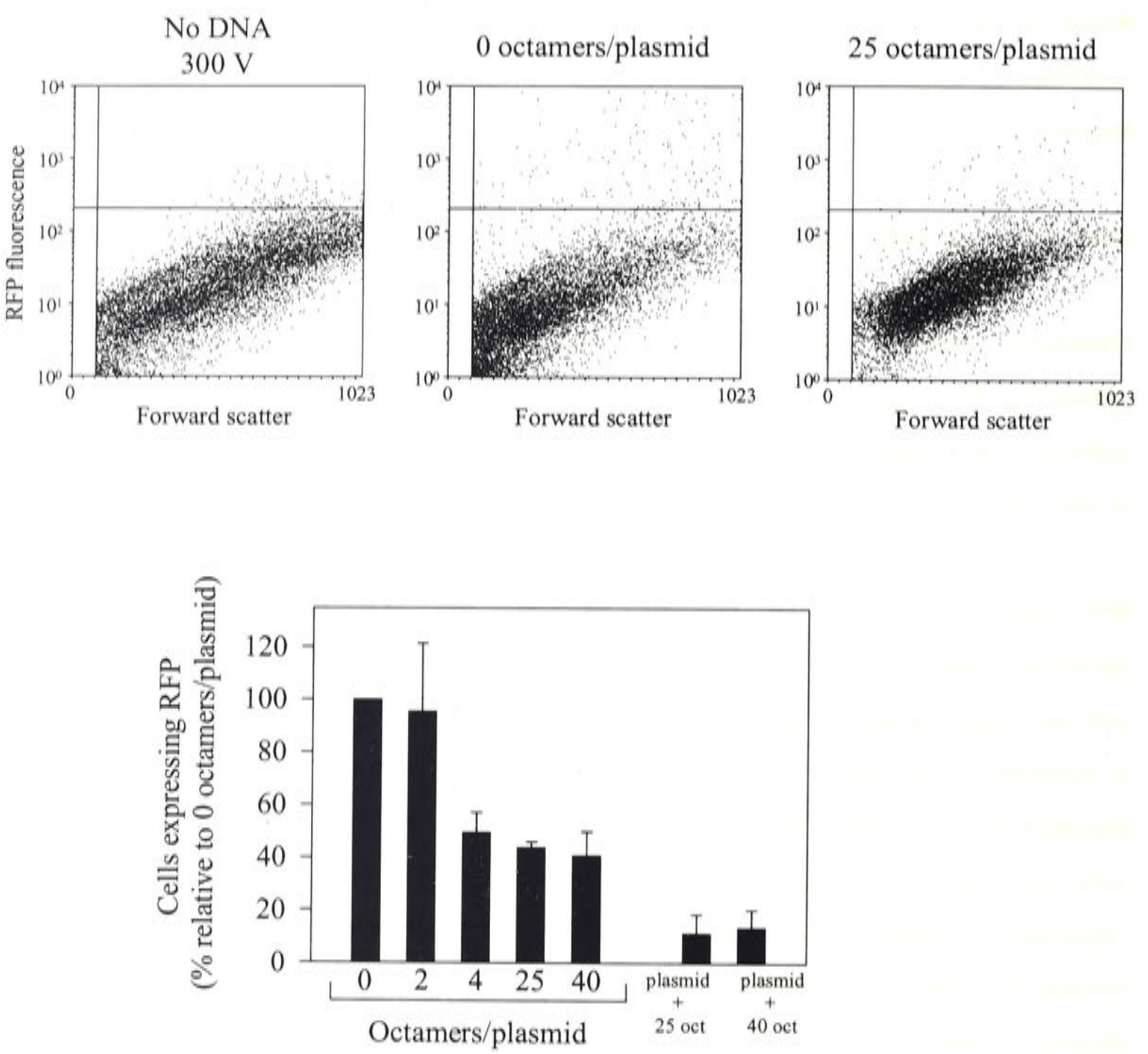

Figure 4.12. Gene expression in HTC cells transfected by electroporation with chromatinised pGeneGrip-RFP. HTC cells were transfected by electroporation (10 µg of DNA in chromatinised form, 300 V, 500 µF; Section 2.7.1) with chromatin constructs assembled at a range of histone octamer stoichiometries (Section 2.5.2). RFP expression was detected 48 hours post-transfection using FACS (channel FL2-H) (described in Section 2.9.1.2). Data were collected for 100000 events and analysed using CellQuest software (Macintosh). Representative FACS dotplots are shown in (**a**) for transfections with no DNA, 0 octamers per plasmid and 25 octamers per plasmid, as indicated. Cells expressing RFP were determined relative to the 'no DNA' control. Histogram analysis of pooled data is shown in (**b**). Results are presented as a percentage of RFP-expressing cells relative to the 0 octamers per plasmid transfections. Bars represent the means of 2 - 7 experiments, with the range/2 or SEM shown (see Table 4.3).

The results indicated, unexpectedly, that plasmid chromatinisation with histone octamers had inhibited transfection efficiency. As a similar pattern was observed upon transfection of the plasmid/octamer 'associations', this appeared to be an effect distinct from chromatin-induced plasmid condensation.

4.6. DELIVERY OF CHROMATINISED REPORTER PLASMID INTO CELLS IN CULTURE USING LIPOFECTION

In order to determine whether the decrease in transfection efficiency upon increasing chromatinisation of the reporter plasmid was specific to electroporation and to HTC cells, an alternative transfection method and cell type were investigated. Since electroporation consumed such a large amount of chromatinised material, lipofection was chosen as a material-saving alternative. This enabled smaller scale transfection experiments to be performed, requiring fewer cultured cells as well as a smaller amount of chromatinised DNA.

4.6.1. Assessing the effect of lipofection conditions on cell viability and reporter gene expression

The effects of the lipofection reagent and chromatin buffer conditions on cell viability and RFP reporter gene expression were assessed in a series of experiments similar to those conducted to assess parameters for transfection using electroporation.

Lipofectamine™ 2000 (Invitrogen) was used as the lipofection reagent, according to the manufacturer's instructions (Section 2.7.2). HTC and Cos-7 cells were plated into 6-well tissue culture plates at a density of 1×10^5 cells per well 24 hours prior to experimentation. In order to ensure that the transfection method would not adversely affect cell survival, as is typical for electroporation experiments, the effect of Lipofectamine™ 2000 on cell viability was assessed. Mock transfection experiments were conducted in which cells were transfected using Lipofectamine™ 2000 but in the absence of DNA. Cells were detached from the substratum 48 hours post-transfection and were resuspended in PBS (500 µl) for analysis by FACS. As PI and RFP are both detected through channel FL2, 7-amino-actinomycin D (7-AAD), which is detected though channel FL3, was chosen as an alternative cell viability indicator (see Section 2.9.1.1). 7-AAD was added to the cell suspension 10 minutes prior to FACS analysis. Fluorescent cells were detected relative to cells which had not been exposed to transfection reagent or 7-AAD. The data, analysed using CellQuest software (Macintosh), showed that neither of the cell lines tested experienced effects of toxicity due to Lipofectamine™ 2000 treatment, with cell viability consistently > 99 % (Figure 4.13a).

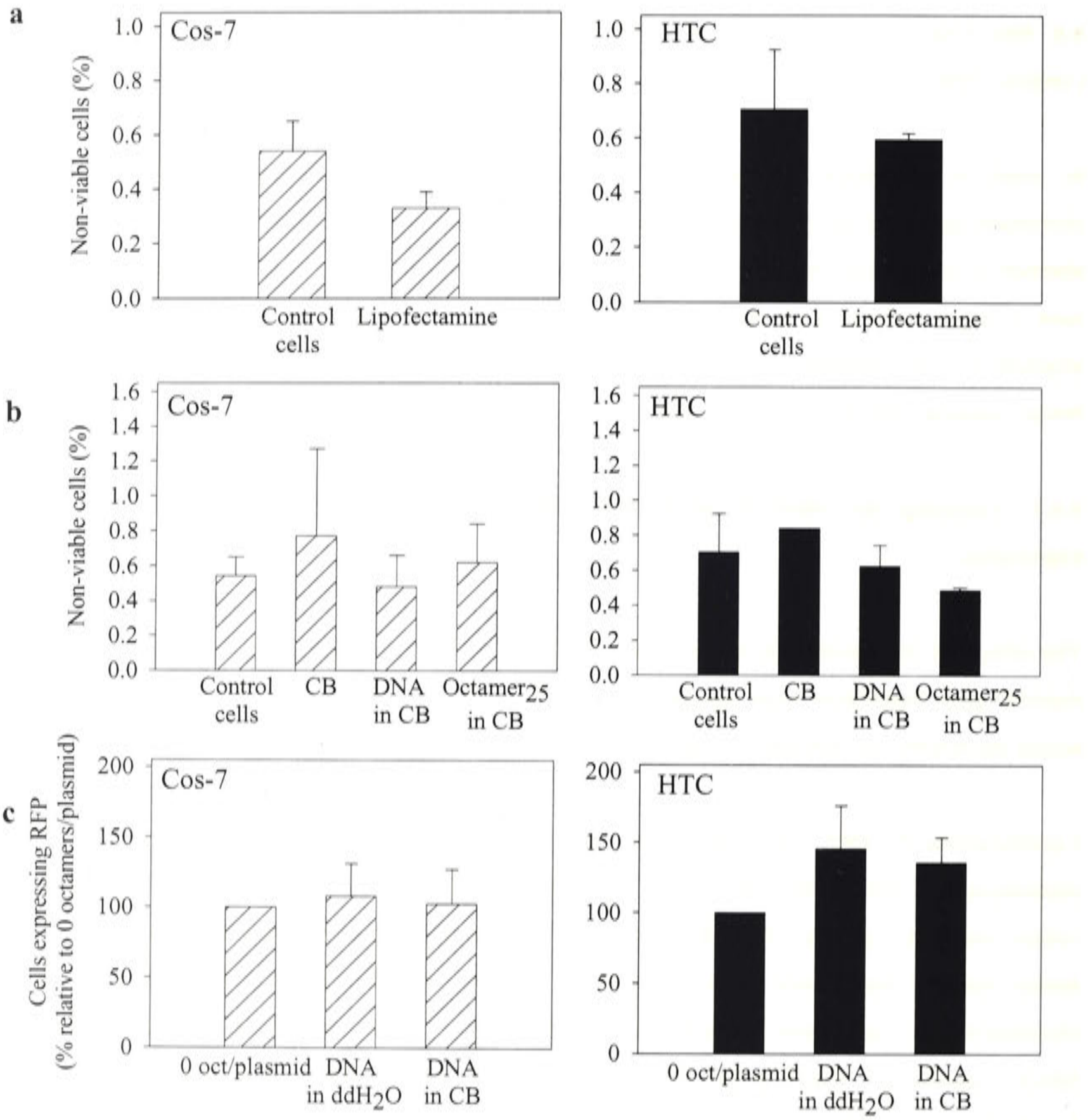

Figure 4.13. The effect of lipofection conditions on cell survival and reporter gene expression. Cos-7 (left panels) and HTC cells (right panels) were assessed for the effect on cell viability of Lipofectamine™ 2000, shown in panel (**a**) and chromatin buffer (CB; 135 mM NaCl/10 mM Tris, pH 7.4), shown in panel (**b**). The effect of chromatin buffer on RFP reporter gene expression is shown in panel (**c**). Lipofection was carried out as described in Section 2.7.2. The test transfection conditions are denoted on the x-axis of each histogram analysis. Control cells were not exposed to any of the test conditions. Cells were analysed 48 hours post-transfection using FACS. 100000 events (cells) were recorded and data were analysed using CellQuest software (Macintosh). For cell viability studies (panels **a**, **b**), 7-AAD fluorescence was detected through channel FL3 (see Section 2.9.1.1). Non-viable cells are represented as a percentage of total cells on the Y-axis. For reporter gene expression studies (panel **c**), RFP fluorescence was detected through channel FL2 (see Section 2.9.1.2). Cells expressing RFP are represented on the y-axis as a percentage relative to cells expressing RFP in the 0 octamers per plasmid transfections. All bars represent the mean of 4 experiments ± SEM.

In order to determine whether either the transfection material or buffer conditions of the experiment would have an effect on cell viability or reporter gene expression, chromatin buffer alone (CB, 135 mM NaCl/10 mM Tris, pH 7.4), pGeneGrip-RFP dialysed into CB or histone

octamers dialysed into CB were lipofected into cells. Cell viability and RFP reporter gene expression were assessed 48 hours post-transfection by FACS, as described previously (see Sections 2.9.1.1 and 2.9.1.2). The test conditions and control cells which had not been transfected produced similar cell viability profiles based on 7-AAD fluorescence (Figure 4.13b), indicating that neither the buffer conditions of transfection nor the transfection material adversely affected cell viability. In terms of reporter gene expression, FACS analysis of RFP-expressing cells revealed that the percentages of RFP expressing cells were not significantly different for the 0 octamers per plasmid chromatin construct, pGeneGrip-RFP solubilised in ddH_2O or pGeneGrip-RFP solubilised in chromatin buffer (HTC cells, $n = 4$, $p \geq 0.17$; Cos-7 cells, $n = 4$, $p \geq 0.53$; Figure 4.13c).

These experiments showed that Lipofectamine™ 2000, CB, histone octamers or the reporter plasmid did not adversely affect cell viability. Also, reporter gene expression was found to be similar when the pGeneGrip-RFP reporter plasmid was transfected in ddH_2O or CB, implying that the conditions under which chromatin assembly was carried out were compatible with transfection experiments. The absolute percentage of HTC cells transfected using Lipofectamine 2000 was similar to the percentage of cells transfected using electroporation, typically less that 10 % (data not shown). In contrast, around 20 % of Cos-7 cells were typically RFP-positive (see Figure 4.14).

4.6.2. Reporter gene expression in Cos-7 and HTC cells lipofected with chromatinised plasmid

Chromatin constructs for transfection assembled at stoichiometries of 0, 1, 2, 4, 25 and 40 histone octamers per pGeneGrip-RFP reporter plasmid were produced as described previously (Section 2.5.2). The concentration of DNA within the chromatin constructs was determined spectrophotometrically at 260 nm and aliquots containing 1 µg of DNA were prepared for lipofection in a constant volume of 50 µl/well. HTC and Cos-7 cells were plated into 6-well tissue culture plates at a density of 1×10^5 cells per well 24 hours prior to transfection. Cells were transfected as described in Section 2.7.2. RFP expression was quantitated by FACS 48 hours post-transfection, as described in Section 2.9.1.2.

Lipofection of the chromatin constructs (Figure 4.14) produced a pattern of relative reporter gene expression similar to that obtained by electroporation (summarised in Table 4.3). However, when lipofection was used, RFP expression observed upon transfection of the 4 octamers per plasmid construct was similar to that of the naked plasmid (0 octamers per plasmid), unlike electroporation which resulted in markedly reduced reporter gene expression (Figure 4.14; Table 4.3). This was followed by a 2-fold decrease in gene expression to the 25

octamers per plasmid level ($p = 0.007$, $n = 7$) and a 2.5-fold decrease to the 40 octamers per plasmid level ($p = 0.011$, $n = 4$) in Cos-7 cells. In HTC cells, the percentage of cells expressing RFP from the 25 and 40 octamers per constructs decreased 5-fold ($p < 0.0001$, $n = 7$ and 4, respectively) (see Figure 4.14; Table 4.3). Thus, in both cell types tested, the percentage of RFP expressing cells decreased with increasing molar ratio of histone octamers to DNA.

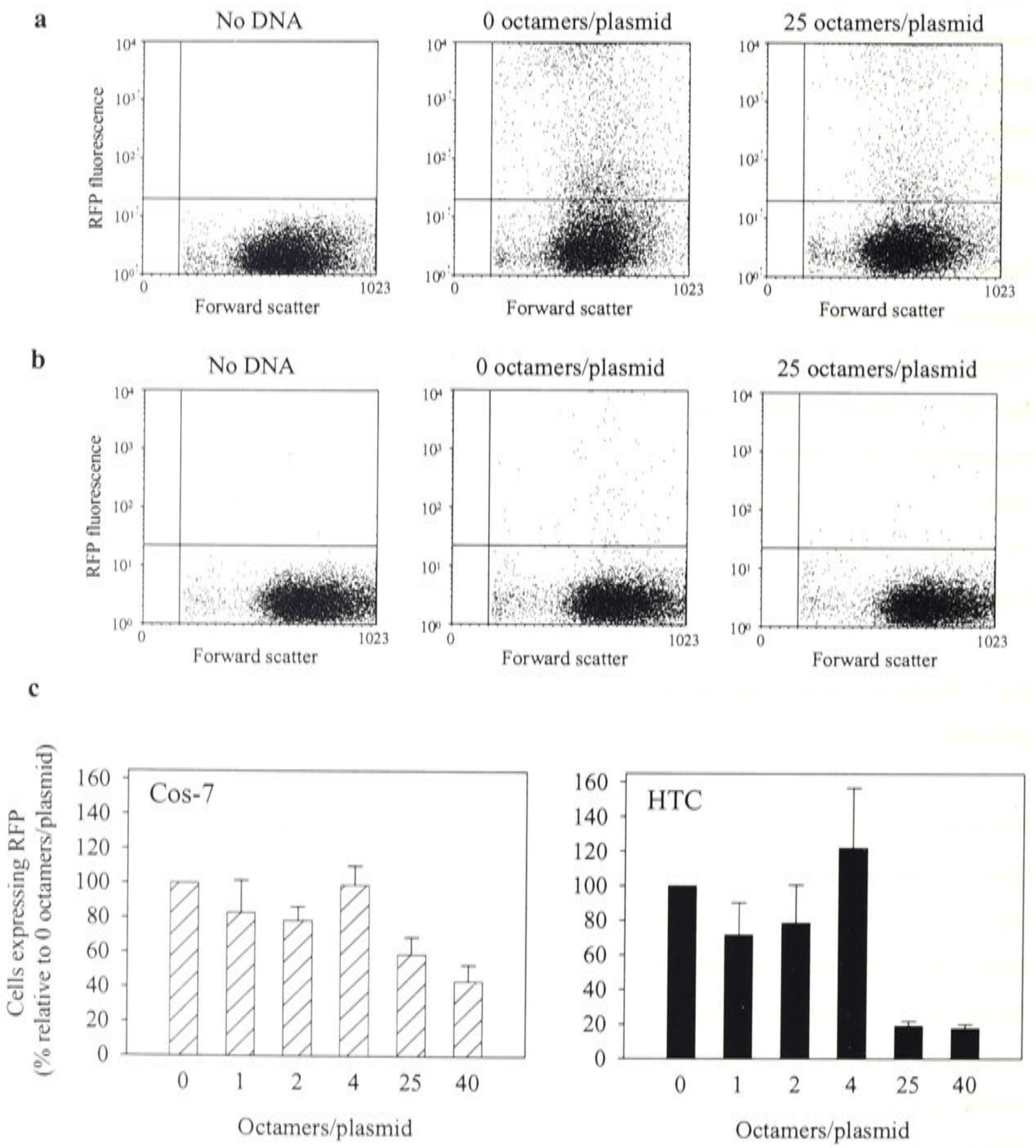

Figure 4.14. Expression of RFP in Cos-7 and HTC transfected by lipofection. Cos-7 and HTC cells were transfected using Lipofectamine™ 2000 (described in Section 2.7.2) with chromatin constructs assembled at a range of histone octamer stoichiometries (described in Section 2.5.2). Percentages of cells expressing RFP were determined by FACS (channel FL2, FACscan) 48 hours post-transfection (described in Section 2.9.1.2) and data for 100000 cells were analysed using CellQuest software (Macintosh). A typical series of FACS dot plots showing differential RFP expression for the no DNA control, 0 octamers per plasmid and 25 octamers per plasmid are shown in (**a**) for Cos-7 cells and in (**b**) for HTC cells. The RFP-positive quadrant was set relative to the no DNA control sample. Collated data is presented in histogram format in (**c**). Results are presented as a percentage relative to the number of cells expressing RFP in the 0 octamer per plasmid transfections, with each histogram representing the mean ± SEM of at least 3 independent experiments.

As described for the electroporation experiments (Section 4.5.2), pGeneGrip-RFP was incubated with the amounts of octamers corresponding to those in the chromatinised constructs under conditions which do not permit nucleosome formation, thus enabling assessment of an effect due to histones distinct from chromatinisation. These DNA/histone 'associations' were transfected into cells in a series of paired experiments with the chromatin constructs (Table 4.3). Similar to the chromatinised plasmid, in both cell lines, at low levels of histone density (corresponding to 1, 2 and 4 octamers per plasmid), the percentages of cells expressing RFP were similar to the naked plasmid (0 octamers per plasmid; Table 4.3). In Cos-7 cells, decreases in reporter gene expression relative to the naked plasmid were observed with the 25 and 40 octamer 'associations' ($p = 0.046$, $n = 7$ and $p = 0.011$, $n = 3$, respectively). While a similar trend appeared to have occurred in the HTC cells (Table 4.3), the difference between the DNA/histone associations and the naked plasmid were not statistically significant ($p > 0.068$).

Table 4.3. Relative percentages of cells expressing RFP upon transfection by electroporation or lipofection.

	Electroporation		Lipofection			
	HTC		Cos-7		HTC	
Octamers/plasmid	% cells[A]	n	% cells	n	% cells	n
0	100 ± 0	7	100 ± 0	7	100 ± 0	7
1	ND[B]		82.9 ± 18.6	7	71.6 ± 18.7	7
2	95.5 ± 25.9	2	78.4 ± 8.0	3	78.6 ± 22.2	3
4	49.6 ± 7.6	2	98.9 ± 11.1	3	122.1 ± 34.5	3
25	43.9 ± 2.1	5	58.8 ± 10.2	7	19.2 ± 2.4	7
40	40.8 ± 9.2	5	43.5 ± 9.3	4	17.8 ± 2.1	4
plasmid + 1 oct[C]	ND		97.8 ± 9.9	6	138.0 ± 23.8	7
plasmid + 2 oct	ND		97.3 ± 12.6	3	114.7 ± 53.2	3
plasmid + 4 oct	ND		92.3 ± 17.1	3	102.2 ± 45.8	3
plasmid + 25 oct	14.3 ± 8.6	4	60.1 ± 15.9	7	93.7 ± 15.8	7
plasmid + 40 oct	17.0 ± 7.4	4	49.9 ± 5.2	3	74.2 ± 6.2	4

Chromatin constructs assembled at differential histone octamer stoichiometries (Section 2.5.2) were transfected into HTC and Cos-7 cells by electroporation (Section 2.7.1) or lipofection (Section 2.7.2) and cells expressing RFP were detected by FACS (Section 2.9.1.2). FACS data were analysed using CellQuest software (Macintosh).

[A] Results are expressed as a percentage relative to RFP expressing cells transfected with 0 octamers per plasmid, and represent the mean ± SEM, with the number of times the experiment was performed indicated by n. Where n is 2, the mean ± range/2 is shown.

[B] Not done.

[C] Constructs comprising histones associated with plasmid DNA under non-chromatinising conditions at stoichiometries indicated.

These results indicated that chromatinisation of the plasmid resulted in diminished levels of reporter gene expression using both electroporation and lipofection transfection methods. The similar trends observed in transgene expression for the range of chromatin constructs and corresponding 'DNA/histone associations' suggested that the presence of histones alone was a contributing factor to reduced reporter gene expression, distinct from chromatinisation.

4.7. Discussion

The first use of chromatin as a vehicle for gene delivery is reported in this chapter. Despite potentially having properties considered advantageous for the purpose of gene delivery, chromatinisation of the reporter plasmid at increasing nucleosome densities appeared to be associated with decreased transfection efficiency of the reporter gene.

The reporter plasmid used in this study was generated by recombination events between two plasmids, pGeneGrip™ and pDsRed-C1, using the Gateway™ cloning system (Life Technologies, see Section 2.2.15 for a detailed description). This involved constructing several intermediate Gateway™-compatible vectors before pGeneGrip-RFP was generated through the final recombination reaction (Figures 4.1 – 4.3). pGeneGrip-RFP was able to be assembled into chromatin by incubation with pre-formed histone octamers, using a method based on the principle of decreasing the salt concentration of the reaction buffer to facilitate transfer of the histone octamers onto the DNA (Kunze and Netz, 2000; Thomas and Butler, 1977). Since this method had been described originally for the association of histone octamers with a defined sequence of linear DNA in order to assemble a regularly spaced array of nucleosomes (Luger *et al.*, 1997; Richmond *et al.*, 1988), it was imperative to verify chromatin formation when using a large plasmid as the DNA template.

Data from analytical ultracentrifugation studies showed increasing *s*-coefficients upon increasing the molar ratio of histone octamers to DNA, demonstrating that the octamers had associated with DNA (Figure 4.6). The existence of nucleosomes was verified using the supercoiling- and MNase digestion assays. In addition, the MNase assay indicated that chromatinised plasmid assembled with stoichiometries of 25 and 40 octamers was more resistant to digestion (di- and tri-nucleosomes, as well as higher molecular weight smearing were still evident after 60 minutes of digestion, see Figure 4.8) than plasmid assembled with fewer octamers. Since it has been shown that naked plasmid DNA degrades rapidly when introduced into the cytoplasm (Lechardeur *et al.*, 1999), this is an important observation with implications for protection of the chromatin constructs against cytosolic degradation.

The chromatin constructs were transfected into cells in culture using electroporation. Unexpectedly, upon electroporation into HTC cells chromatinised plasmids assembled at increasing molar ratios of octamers were found to yield 2-fold fewer cells that expressed the reporter gene compared to the naked plasmid (Figure 4.12; Table 4.3). Briefly incubating the reporter plasmid with histone octamers under conditions of low salt and low temperature, to produce DNA/histone 'associations' that would lack higher order chromatin structures, resulted in a more marked decrease of around 5-fold in the number of cells expressing RFP (Figure 4.12; Table 4.3). This suggested that reduced gene expression may have been a result of the association of histone octamers, distinct from any condensation effect on the reporter plasmid.

In order to ensure that these observations were not a consequence of the transfection method or cell type, transfections were performed using lipofection and Cos-7 cells also. Consistent with the trend observed using electroporation, progressively fewer cells expressing RFP ensued upon increasing the stoichiometry of octamers assembled onto the reporter plasmid (Figure 4.14; Table 4.3). However, unlike the data obtained from electroporation where RFP expression diminished to around 50 % at low levels of nucleosome density (see 4 octamers per plasmid, Table 4.3), lipofection resulted in diminished RFP expression at the higher levels of nucleosome density, which were obtained with 25 and 40 octamers per plasmid (Table 4.3). While lipofection of DNA/histone 'associations', resulted similarly in a pattern of decreased RFP expression, the dramatic decrease that had been observed when the amount of histones associated with the plasmid was increased was specific to electroporation (see Table 4.3).

The composition of the liposome/DNA transfection complex would undoubtedly change as the ratio of octamers to plasmid is increased; however, sufficient internucleosomal DNA remains to enable association with the cationic lipid. The rate limiting step in lipofection is endosomal escape, which is primarily mediated by the interaction of the cationic transfection lipids with the anionic endosomal lipids (Zabner et al., 1995; Xu and Szoka, 1996). The contribution arising from the presence of histone octamers in the lipoplex to the processes of endosomal escape is unknown but given the overwhelming excess of cationic lipid is likely to be negligible. The presence of histone octamers is, similarly, unlikely to have an effect on other processes important for lipofection, such as cell association and internalisation. Compromised lipofection is therefore unlikely to account for the diminished RFP expression.

The size and hence MW of the plasmid DNA may play a role in gene transfer efficiency. Fluorescently-labelled DNA of similar size to the pGeneGrip-RFP reporter plasmid used in this study (6000 bps) was reported to have markedly diminished mobility in the cytoplasm (Lukacs *et al.*, 2000). Using spot photobleaching measurements (fluorescence recovery after photobleaching, FRAP), a 20-fold reduction in the diffusion coefficient was found for a > 2000

bp DNA fragment compared to a 100 bp DNA fragment. Beyond 2000 bp, DNA was essentially immobile in the cytoplasm. This was in contrast to the smaller DNA fragments (<500 bps) which distributed throughout the cytoplasm and nucleus within a few minutes of cytoplasmic microinjection (Lukacs *et al.*, 2000).

Increasing the cytoplasmic mobility by compaction of plasmid DNA might provide one mechanism by which to enhance gene delivery efficiency. While no quantitative information exists on the cytoplasmic diffusion coefficients of compacted DNA, evidence from studies of *in vitro* reconstituted nuclear import suggest that transfection constructs compacted using pLy may accumulate in the nucleus more readily (Chan *et al.*, 2000). No consensus has yet been reached on a relationship between transfection efficiency and DNA condensation, however, a bias towards a positive correlation seems to exist in the literature (for reviews see Vijayanathan *et al.*, 2002; Bloomfield, 1996). Upon chromatinisation, at the first level of compaction, DNA is condensed in length by a factor of 5. This involves the formation of nucleosomes and results in the canonical 'beads-on-a-string' fibre (Van Holde *et al.*, 1980; see Figure 1.8). Further compaction into structures resembling the '30 nm fibre' is facilitated by the N-terminal tails of the core histones which participate in inter-nucleosome contacts (Tse and Hansen, 1997; Fletcher and Hansen, 1995; Schwarz and Hansen, 1994). H1 linker histones serve to stabilise this structure (Carruthers *et al.*, 1998; Leuba *et al.*, 1998). AFM revealed that the super-structure of the plasmid used in this study when chromatinised at physiological nucleosome density (25 octamers per plasmid) was an extended rod shape (Figure 4.9). This was consistent with previously published data which suggested that circular chromatin constructs led to the generation of compacted extended structures (Ladoux *et al.*, 2000; Hansen and Wolffe, 1992; Simpson *et al.*, 1985), most likely caused by inter-nucleosomal interactions (Luger *et al.*, 1997; Tse and Hansen, 1997; Fletcher and Hansen, 1995; Schwarz and Hansen, 1994; Yao *et al.*, 1991; Simpson *et al.*, 1985). In this study, however, despite chromatin-induced plasmid condensation, overall transfection efficiency was diminished as reflected in the decreased percentages of cells expressing RFP with increased chromatinisation.

While chromatinisation at physiological nucleosome density (25 octamers per pGeneGrip-RFP) caused compaction of the plasmid, it simultaneously increased the relative molecular weight by ~2-fold (see Table 4.1). According to Seksek *et al.* (1997) and Lukacs *et al.* (2000), diffusion of molecules of this MW (6.6×10^6 Da; Table 4.1) is very slow through the cytoplasm, implying that the more extensively chromatinised constructs should have progressively lower diffusion rates. Indeed, decreased RFP expression from both the extensively chromatinised plasmids and the plasmids 'associated' with the corresponding amount of histone octamers (Table 4.3) may be as a result of decreased cytoplasmic mobility due to increased MW. This would, in turn, reduce the probability of plasmid entry into the nucleus.

It is apparent, nonetheless, that the chromatin constructs do reach the nucleus since reporter gene expression is observed. The reduced numbers of cells that were positive for transgene expression, observed in association with increased chromatinisation of the reporter plasmid, may be a reflection of the encumbering molecular weight of the constructs. This brings into question the degree of translocation of the chromatin constructs from the cytoplasm into the nucleus. In this context, the role of importin binding to the histones within the *in vitro* assembled chromatin constructs becomes important in facilitating nuclear import of the transfection constructs as a whole. These central issues concerning nuclear translocation are addressed in the experiments described in the following chapter.

CHAPTER 5

Limitations of chromatin as a gene delivery vehicle

5.1. INTRODUCTION

Translocation into the nucleus is a limiting process for non-viral gene delivery methods. The driving hypothesis of this study was that chromatin has several features that might enhance nuclear translocation, thus potentiating transgene delivery. DNA compaction had been reported previously by a number of groups to enhance transfection efficiency (Deas *et al.*, 2002; Dauty *et al.*, 2001; Fritz *et al.*, 1996; Gao and Huang, 1996; Wagner *et al.*, 1991), an effect almost certainly attributable to improved nuclear uptake. This was reflected in a study by Chan and Jans (Chan *et al.*, 2000) who reported that during the course of plasmid DNA condensation induced by pLy, plasmid morphology passed through several structural intermediates to finally adopt a fully compacted spheroid structure, which could be correlated with a corresponding 7-fold increase in nuclear uptake of the plasmid. Chromatinisation was seen to induce plasmid compaction from open loop into rod-like structures (see Section 4.4.4) and, therefore, could be expected to facilitate enhance nuclear uptake.

Another important feature of *in vitro* assembled chromatin, according to the initial hypothesis of this study, is the presentation of multiple histone NLSs which, in principle, should increase the potential for nuclear uptake. The MWCO of the NPC (~ 45 kDa) dictates that the large chromatinised constructs would require importin-facilitated nuclear uptake, mediated by NLSs. In theory, this requirement for NLSs should be met by the histone octamers which, in addition to the high importin β-binding affinity exhibited individually by its constituent histones (see Section 3.2), should present a total of 8 NLSs (one from each histone).

Despite these potentially positive contributions to transgene delivery, the data presented in Chapter 4 revealed that chromatinisation of the model plasmid, pGeneGrip-RFP, resulted in diminished transfection efficiency of the reporter plasmid. In this chapter, experiments aimed at elucidating the mechanisms for the reduced reporter gene expression are described, with a focus on nuclear uptake as a limiting factor. Determining the reasons for reduced transfection efficiency was important in order to be able to design strategies that circumvent these shortcomings, as chromatinisation of DNA still has potentially useful properties such as the

ability to accommodate large lengths of DNA, protect the DNA from cytoplasmic nucleases and the potential to couple targeting signals, such as additional NLSs.

In order to determine the degree of nuclear accumulation of the chromatin constructs in an *in vitro* reconstituted nuclear import system comprising permeabilised cells (Chan and Jans, 1999; Hu and Jans, 1999; Xiao *et al.*, 1998), the reporter plasmid was labelled fluorescently with a DNA-sequence-specific PNA probe to which FITC had been conjugated. However, using CLSM, the fluorescence signal could not be detected above cellular autofluorescence. An alternative method was therefore used to assay the nuclear uptake in transfected cells. This was based on FACS analysis of nuclei that were isolated from the transfected cells. Importantly, this method allowed determination of reporter gene expression and nuclear accumulation of the chromatin constructs from the same pool of transfected cells.

Since, contrary to the working hypothesis of this study, chromatinisation of the reporter plasmid did not enhance transgene expression, the assumption that histone octamers assembled into chromatin would retain their ability to bind importins and, therefore, increase the probability of nuclear uptake of the chromatinised plasmids was tested using the modified ELISA method.

While electroporation and lipofection are widely employed as methods for transfection, the possibility of transfection-induced damage to the chromatinised constructs had not been excluded as a reason for the decreased transfection efficiency observed. This possibility was investigated first.

5.2. The effect of electroporation and lipofectamine transfection conditions on chromatin structure

In order to determine whether either electroporation or lipofection had any effect on chromatin structure, the supercoiling and MNase assays were used to investigate the stability of chromatin under the transfection conditions.

For the supercoiling assay (described in Section 2.5.4), pGeneGrip-RFP was incubated with Topoisomerase I in order to induce the open, circular form of the plasmid. Following this, a range of chromatin constructs were assembled at histone octamer stoichiometries of 0, 1, 25 and 40, using the octamer transfer by salt dialysis method (Section 2.5.2). Each chromatin construct was quantitated spectrophotometrically based on DNA content and apportioned for either electroporation (10 µg DNA) or lipofection (1 µg DNA) treatment.

Electroporation conditions were as described in Section 2.7.1, except that cells were absent; the cell-containing aliquot being replaced by an equivalent volume of PBS. The supercoiled status of the chromatin constructs was determined before and after electroporation. While the supercoiled form of the plasmid was still evident after electroporation, higher molecular weight smearing can be seen in the agarose gel analysis (Figure 5.1a, lanes 7 - 10). This implied that the conditions of electroporation had induced aggregation of the constructs.

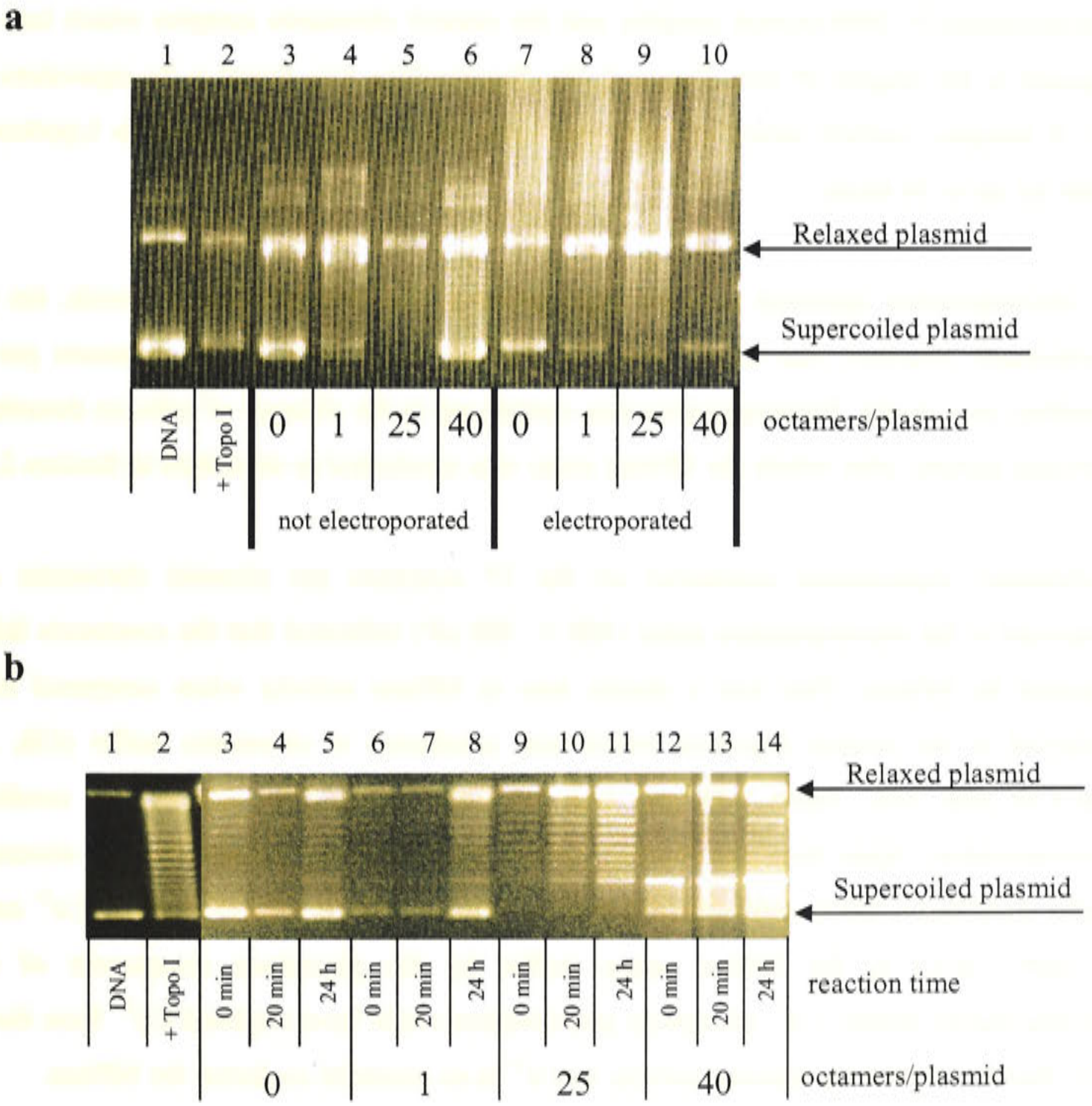

Figure 5.1. The effect of electroporation and lipofection on the supercoiled structure of the chromatinised plasmids. Agarose gel (1 %) images of supercoiling within chromatin constructs are shown after electroporation in (**a**) and after incubation with Lipofectamine™ 2000 in (**b**). The supercoiling assay was carried out as described in Section 2.5.4. After incubating with Topoisomerase I, pGeneGrip-RFP was assembled into a range of chromatin constructs using the octamer transfer salt dialysis method (Section 2.5.2), as denoted. Chromatin constructs were subjected to electroporation in the absence of cells (PBS buffer, 300 V, 500 µF, 10 µg DNA, final volume 400 µl; Section 2.7.1) or incorporated into liposomes using Lipofectamine™ 2000 (1:50 v/v serum-free media, 1 µg DNA, final volume 100 µl; Section 2.7.2). Relaxed and supercoiled forms of the plasmid are labelled. Note the presence of extensive smearing at high molecular weight in samples that were subjected to electroporation (**a**, lanes 7 - 10). Incubation times with Lipofectamine™ 2000 are indicated. Liposomal lipids were dissociated from the plasmid DNA by SDS (Section 2.5.4).

Lipofection conditions were as described in Section 2.7.2, except that cells were absent. Chromatin constructs were prepared with Lipofectamine™ 2000 and were incubated at room temperature for 20 minutes before aliquots were removed for assaying, as these are the conditions recommended by the manufacturer (Invitrogen) to allow liposome/DNA complexes to form prior to addition to cells (see Section 2.7.2). Liposome/chromatin complexes were incubated for an additional 24 hours at 37°C to simulate conditions of the post-transfection cell culture (except in the absence of cells). Supercoiled status was compared for the Lipofectamine™ 2000-treated samples and the control chromatin samples which had not been exposed to the reagent (0 min; Figure 5.1b). Supercoiling was found to be equivalent between the '0 minutes' control constructs and constructs that had been incubated in Lipofectamine™ 2000 for up to 24 hours.

As electroporation appeared to cause aggregation of the chromatinised plasmids, the effect on nucleosome structure was tested using the MNase assay with the 25 octamers per plasmid construct as a model. Electroporation was carried out in the absence of cells, as described in the previous section, after which the MNase assay was conducted as described in Section 2.5.5.

Preliminary experiments conducted on the 25 octamers per plasmid chromatin construct subjected to the electroporation pulse (300 V, 500 µF) indicated that the constructs failed to be digested by MNase. This was a drastic loss in MNase activity when compared to activity observed in the control digestion which was conducted in chromatin buffer (CB, 135 mM NaCl/10 mM Tris; Table 2.5) and had not been exposed to any of the conditions for electroporation. Apart from the electric current, the possibility existed that the electroporation buffer itself had a detrimental effect. It may be that possible precipitation of the Ca^{2+} component (2 mM $CaCl_2$) in the MNase assay buffer by the phosphate component of the PBS electroporation buffer. Ca^{2+}-phosphate precipitation could have depleted Ca^{2+} from the reaction mix, thereby abolishing enzyme activity as Ca^{2+} is an essential co-factor for MNase.

In order to exclude this possibility, the electroporation and non-electroporation test-samples were dialysed from the PBS electroporation buffer into CB prior to MNase digestion. A control sample of chromatinised plasmid (25 octamers per plasmid) in CB that had not been exposed to PBS was included, as described above, to verify the activity of the MNase enzyme. Using the recommended amount of 25 mU of MNase per µg of DNA (for 4 µg of DNA; 100 mU), the characteristic MNase digestion banding pattern indicating the presence of nucleosomes was seen in the control and the 'non-electroporated' samples, whereas the sample that had been subjected to electroporation conditions still appeared to be resistant to digestion (Figure 5.2a). Only when 3 times more MNase was added was the 'electroporated' sample digested to the extent that enabled nucleosomes to be clearly identified (Figure 5.2b).

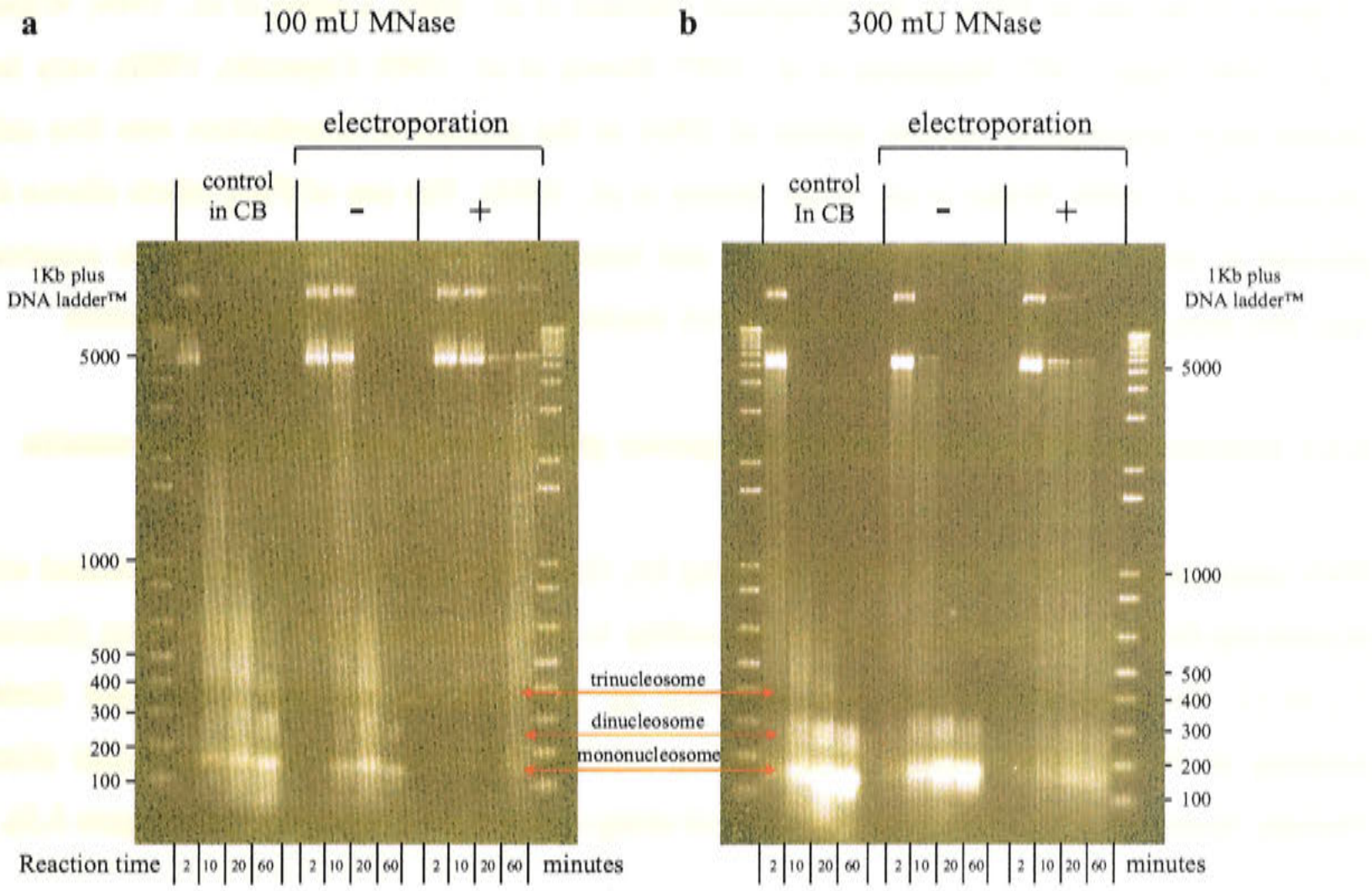

Figure 5.2. Electroporation increases the resistance of chromatin to MNase digestion. Agarose gel electrophoresis of MNase digestion of chromatin constructs after electroporation is shown (1.5 % agarose). Chromatin samples comprising 25 octamers per plasmid were subjected to electroporation (10 µg DNA, PBS buffer, 0.4 cm gap BioRad electroporation cuvettes, 300 V, 500 µF) in the absence of cells, essentially as described in Section 2.7.1 Samples were dialysed overnight into chromatin buffer (CB, 135 mM NaCl/10 mM Tris) and the MNase assay conducted as described using an aliquot of 4 µg of chromatinised DNA (Section 2.5.5). The control sample was maintained in CB and had not been exposed to PBS or electroporation. Digestions using a total of 100 mU and 300 mU of MNase are shown in (**a**) and (**b**), respectively. Bands corresponding to nucleosomal DNA are denoted in red.

Collectively, these results suggested that electroporation had a detrimental effect on chromatin structure by inducing the formation of MNase-resistant, aggregated structures which migrated in an agarose gel at higher molecular weight that non-electroporated chromatin. As the chromatin structure appeared to be retained in the presence of Lipofectamine™ 2000, lipofection was employed as the method of transfection for the remainder of the study.

5.3. Determination of the efficiency of chromatinised plasmid uptake into the nucleus

In order to visualise the subcellular distribution properties of the chromatin constructs *in situ*, pGeneGrip-RFP was labelled with FITC. Labelling was achieved using the GeneGrip™ site (Gene Therapy Systems) within the pGeneGrip-RFP reporter plasmid, which contains a sequence comprising 8 consecutive binding sites to which short, linear FITC-PNA molecules were hybridised (see Section 4.2 for a description of PNA chemistry). While reconstituted

permeabilised cell systems and studies involving microinjection have provided valuable evidence of the fate of DNA in the cytoplasm (Salman *et al.*, 2001; Ludtke *et al.*, 1999; Wilson *et al.*, 1999; Dean, 1997; Hagstrom *et al.*, 1997; Dowty *et al.*, 1995; Capecchi, 1980), very few studies have investigated nuclear uptake of DNA in the context of transfection into live cells (Brisson *et al.*, 1999; Wilke *et al.*, 1996; Dowty *et al.*, 1995). The use of PNA labels allows the plasmid to retain its transcriptional activity and hence the functional activity of the construct may also assessed in conjunction with the DNA tracking studies (Gene Therapy Systems).

5.3.1. Generation of fluorescein-labelled reporter plasmid and assembly into chromatin

PNA conjugated to FITC (PNA-FITC labelling kit, Gene Therapy Systems) was incubated with pGeneGrip-RFP in a labelling reaction according to the manufacturer's instructions (Section 2.2.16.1). Unbound PNA-FITC was removed by precipitating labelled DNA and further washing in 70 % EtOH, before resuspending labelled DNA in 1 × labelling buffer (Gene Therapy Systems). FITC-labelling was verified using agarose gel electrophoresis (Figure 5.3).

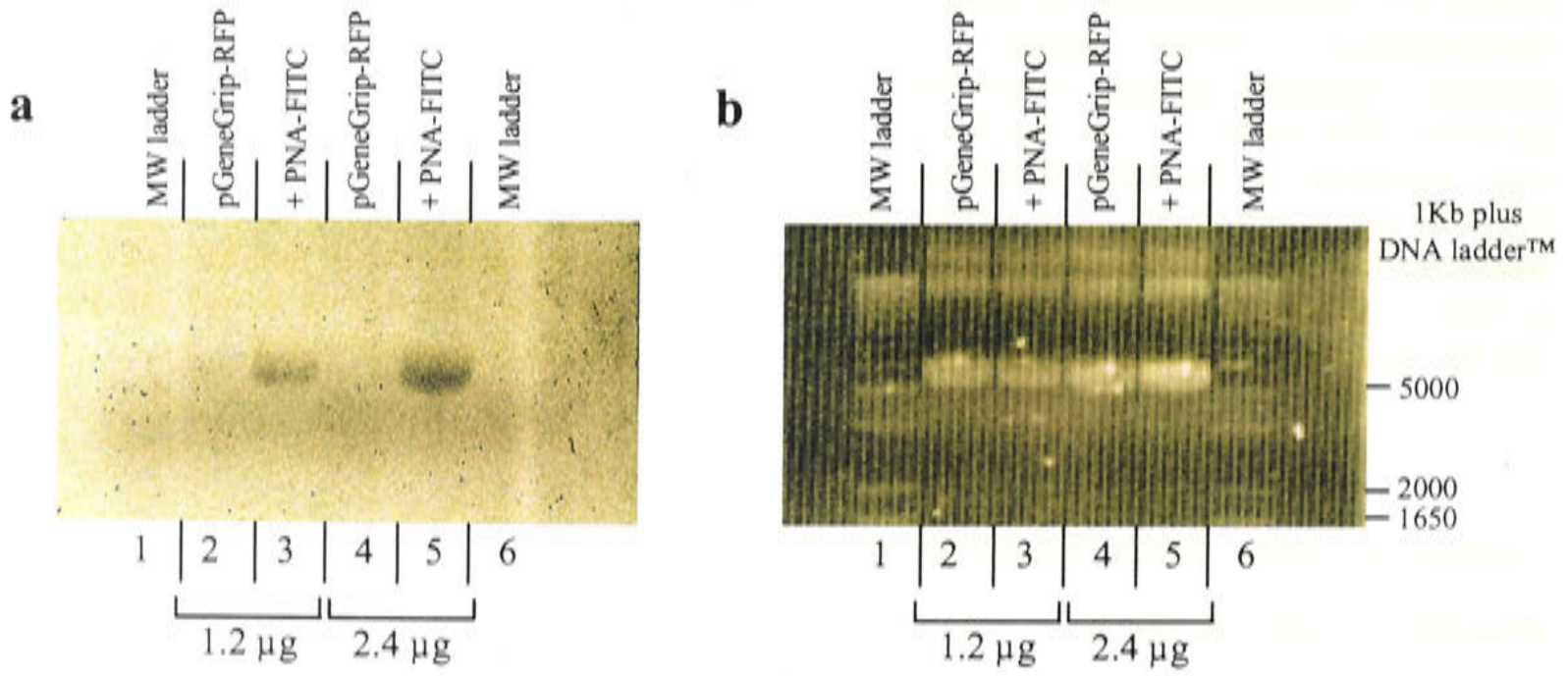

Figure 5.3. FITC-PNA labelling of pGeneGrip-RFP. pGeneGrip-RFP (100 µg) was labelled with FITC at the GeneGrip™ site using PNA-FITC (8 PNA-FITC labels/plasmid, Gene Therapy Systems; Section 2.2.16.1). Labelling was carried out at 37°C for 2 hours, after which unbound label was removed by precipitating the labelled DNA in 3M NaOAC and isopropanol, followed by washing in 70 % EtOH. Labelled DNA was resuspended in 1 × labelling buffer (Gene Therapy Systems). Labelling was verified using agarose gel electrophoresis (1 %, 100 V for 90 minutes). The presence of FITC was visualised using a Fluorimager (FLA-3000, Fuji, excitation 473 nm; emission 538 nm), shown in (**a**). DNA was visualised by EtBr staining under UV illumination (FLA-3000, Fuji, excitation 473 nm; emission 580 nm), shown in (**b**). FITC-labelled pGeneGrip-RFP can be seen in lanes 3 and 5.

The FITC-label was visualised in the gel using a Fluorimager (FLA-3000, Fuji), with parameters of excitation at 473 nm and emission at 538nm for FITC (Figure 5.3a). Fluorescence can be seen in lanes 3 and 5 in Figure 5.3a. EtBr staining of the DNA (visualised using the

FLA-3000, Fuji, excitation at 473 nm and emission at 580nm for EtBr) confirmed the source of fluorescence to be the FITC-labelled pGeneGrip-RFP plasmid (Figure 5.3b, lanes 3 and 5), as the unlabelled plasmid control (Figure 5.3b, lanes 2 and 4) did not produce a fluorescent signal (Figure 5.3a, lanes 2 and 4).

PNA-FITC-labelled pGeneGrip-RFP (pGeneGrip-RFP-FITC) was assembled into chromatin containing a 0, 1, 2, 4, 25 or 40 molar ratios of histone octamers to DNA using the octamer transfer salt dialysis method (Section 2.5.2). The MNase digestion assay (Section 2.5.5) was used to verify chromatinisation by monitoring the formation of nucleosomes. In order to serve as a control reaction, unlabelled pGeneGrip-RFP, which was previously shown to form nucleosomes upon chromatinisation (see Figure 4.8), was assembled into chromatin in parallel (Figure 5.4).

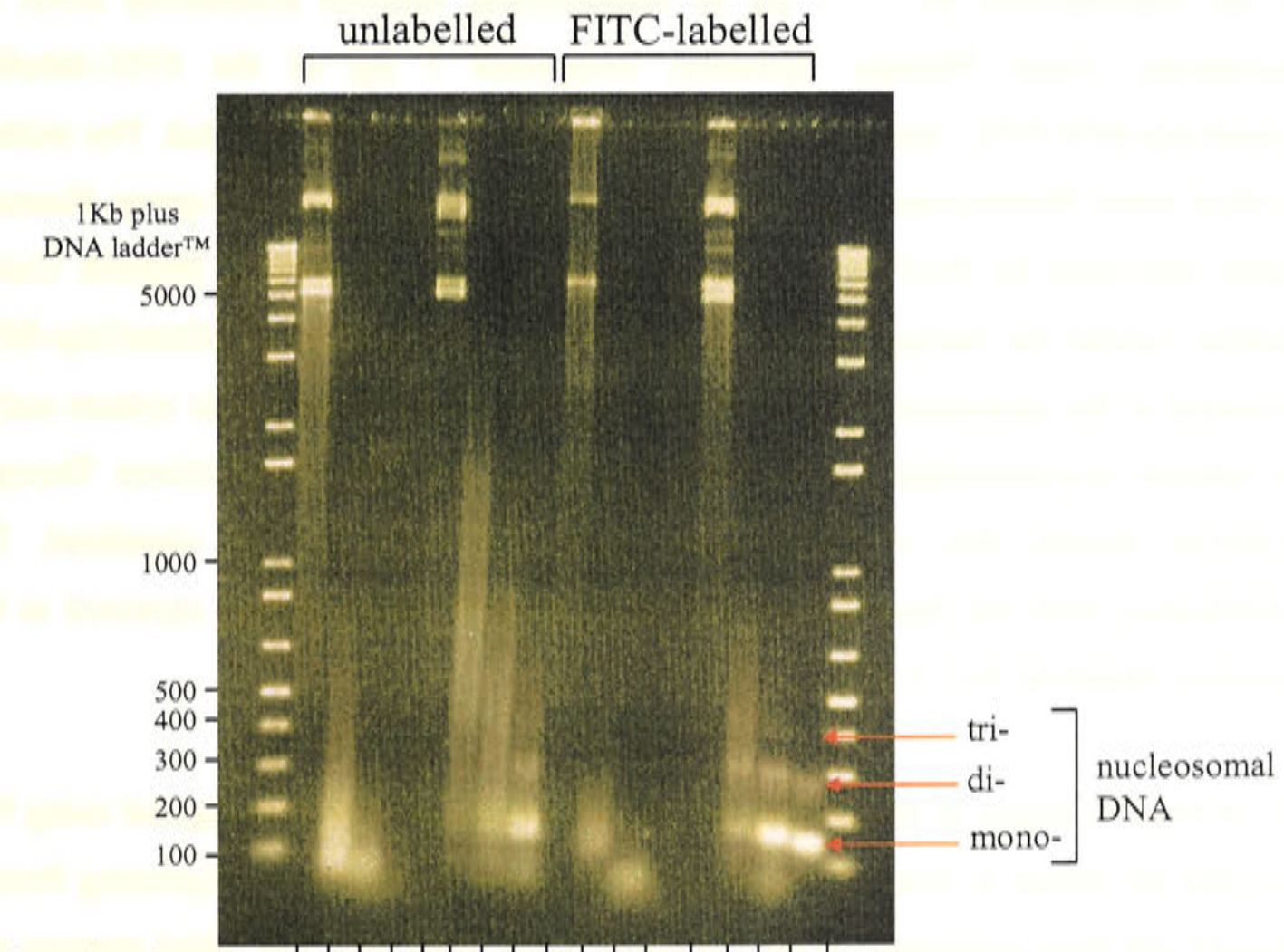

Figure 5.4. Nucleosome formation confirms chromatinisation of pGeneGrip-RFP-FITC. PNA-FITC-labelled pGeneGrip-RFP was assembled into a range of chromatin constructs by the octamer transfer salt dialysis method, in parallel with the unlabelled plasmid (Section 2.5.2). MNase digestion of unlabelled and labelled chromatin constructs containing 1 and 25 octamers per plasmid is shown. 4 µg of chromatinised plasmid constructs were incubated for 2, 10, 20 and 60 minutes with MNase (100 mU), DNA was recovered by NaOAc precipitation overnight and electrophoresed through 1.5 % agarose at 90 V (described in Section 2.5.5). The gel was stained in EtBr for 20 minutes, destained in ddH_2O for half of that time and visualised under UV illumination. Bands corresponding to nucleosomal DNA are indicated with red arrows.

Chromatinisation of pGeneGrip-RFP-FITC generated MNase digestion products that were consistent with the presence of nucleosomes and identical to the digestion pattern of unlabelled chromatinised pGeneGrip-RFP. This confirmed that chromatin assembly was not inhibited in the presence of the PNA-FITC label.

5.3.2. Gene expression and nuclear accumulation of fluorescein-labelled chromatinised reporter plasmid

The *in vitro* nuclear transport assay, described in detail in Section 2.11.2 was investigated as a means to determine the kinetic parameters of nuclear uptake using the fluoresceinated chromatin constructs. HTC cells grown on coverslips were permeabilised mechanically and cytosolic extract and an ATP-regenerating system, required for protein import into the nucleus, were added together with the test sample to a final volume of 5 µl. The test sample, as recommended by the manufacturer (0.1 – 1 µg of fluorescently labelled pGeneGrip DNA for confocal microscopy, Gene Therapy Systems), comprised 1 µg of the FITC-labelled plasmid, pGeneGrip-RFP-FITC, but the fluorescence signal could not be detected. The methodology was verified when fluorescence was visualised easily using a T-ag NLS-green fluorescent protein fusion (provided by Prof D. Jans, Nuclear Signalling Laboratory, Monash University) as a positive control for nuclear uptake in this system. The amount of pGeneGrip-RFP-FITC was increased to the maximum volume that could be accommodated in the system and was 3 times the amount recommended by the manufacturer of the FITC label (Gene Therapy Systems). However, despite this, a fluorescence signal still could not be visualised. The level of fluorescence from the fluoresceinated pGeneGrip-RFP plasmid thus appeared to be below the detection threshold for CLSM.

An alternative means of monitoring nuclear accumulation was investigated using FACS. FACS provides the means to simultaneously detect both the fluorescence originating from the labelled plamsid and from expression of the transgene in the same cell. The initial strategy was therefore to determine the percentage of cells in the transfected population that were positive for both FITC-fluorescence originating from the transfected plasmids and RFP fluorescence originating from their expression. Following this, isolation of nuclei and analysis by FACS would indicate the proportion of nuclei that had accumulated the FITC-labelled chromatin constructs. Collation of these results with the proportion of RFP positive cells could provide the means to establish a relationship between nuclear accumulation of the transfection constructs and transgene expression.

HTC and Cos-7 cells were transfected using lipofection (Section 2.7.2) with the range of differentially chromatinised constructs assembled using FITC-labelled pGeneGrip-RFP (see

Section 5.3.1). Cells were analysed by FACS 48 hours post-transfection for both RFP fluorescence, detected through channel FL2, relative to cells which had been transfected in the absence of DNA (Lipofectamine™ 2000 only), and FITC fluorescence, detected through channel FL1 relative to cells which had been transfected with unlabelled plasmid (see Sections 2.9.1.2 and 2.9.1.3, respectively). Representative FACS dot plots for Cos-7 cells are shown in Figure 5.5.

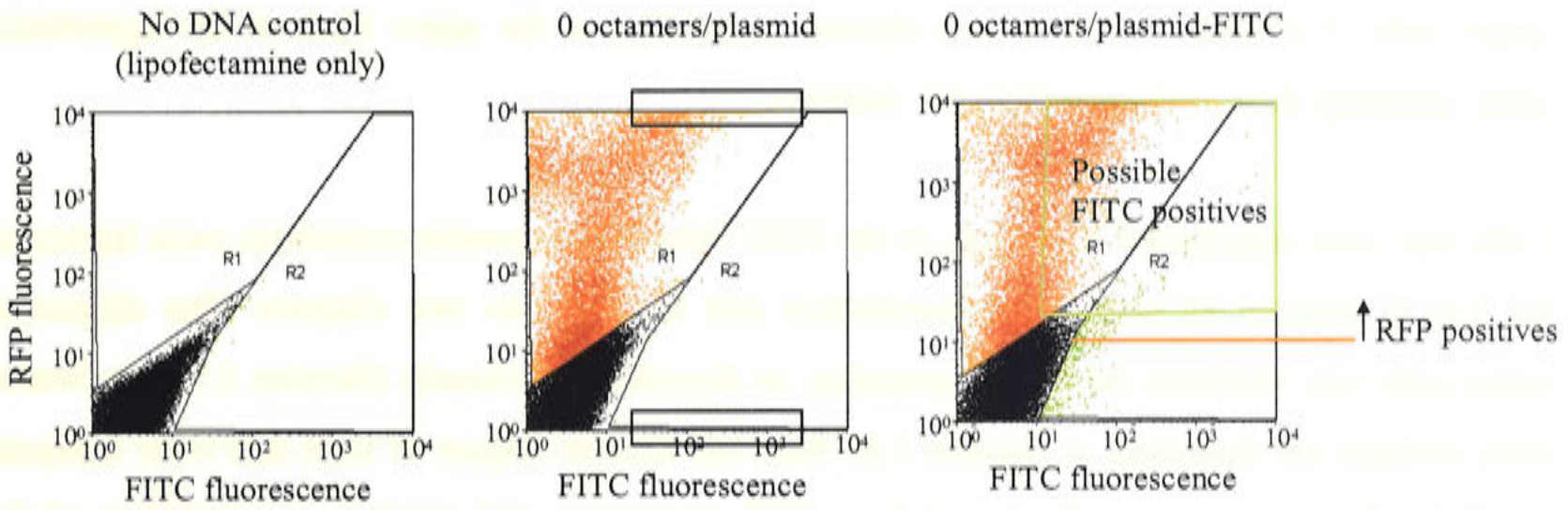

Figure 5.5. Highly fluorescent RFP is also detected in channel FL1 and masks the detection of FITC. Cos-7 cells were transfected with a range of fluorescein-conjugated pGeneGrip-RFP chromatin constructs (see Sections 2.2.16.1, 2.5.2 and 2.7.2). 48 hours post-transfection dual detection of RFP expression and FITC-fluorescence was determined by FACS (channels FL2 and FL1, respectively; Section 2.9.1). Typical FACS dot plots are shown for the no DNA control, unlabelled pGeneGrip-RFP 0 octamers per plasmid and FITC-labelled pGeneGrip-RFP 0 octamers per plasmid transfections. RFP fluorescence is represented on the y-axis, in region 1 (R1) and FITC-fluorescence on the x-axis, in region 2 (R2). R1 was set according to the distribution of RFP expressing cells using the unlabelled 0 octamers per plasmid construct. R2 was set, thereafter, according to the distribution of FITC-positive cells using the FITC-labelled 0 octamers per plasmid construct. RFP-positive cells in the unlabelled (no FITC) 0 octamers per plasmid dot plot accumulate at the upper end of the detection limit of channel FL2 (boxed) and score highly on the FITC-fluorescence scale (boxed). Other possible FITC-positive cells are demarcated in the green square and all possible RFP-positive cells may lie above the red line.

Cells that were FITC-positive could not be detected with confidence because RFP expression from the unlabelled (no FITC) transfections could be detected ('bleed-through') in the FITC channel, FL1 (Figure 5.5). The FITC signal appeared to be weak, consistent with the difficulties experienced using CLSM (see above), with fluorescence intensity ranging from 10^1 - 10^2 units. In comparison, fluorescence originating from cells electroporated in the presence of FITC-dextran was between 10^2 – 10^3 fluorescence units (compare Figure 4.10). The problem thus was therefore one of very high RFP fluorescence and low FITC fluorescence, such that reliable identification of true RFP/FITC double-positive cells above the background of RFP-positive cells was deemed to be not possible in the whole cell context and for this reason had to be abandoned. However, quantitation of RFP-positive intact cells (analysed as illustrated in Figures 4.14a and b) and quantitation of FITC-positive isolated nuclei was pursued, separately. This method still provided a basis from which to investigate the parameter of interest - nuclear accumulation of the differentially chromatinised plasmids. It also permitted the levels of nuclear

accumulation of the chromatin constructs in a population of nuclei to be related to the level of RFP transgene expression observed in the same population of cells.

With appropriate size detection settings (forward scatter), subcellular components, such as nuclei, may be investigated by flow cytometry (Petersen, 1986). For the detection of whole cells, the forward scatter parameter was set on a linear scale due to the large size of the particles, while for the detection of nuclei, the forward scatter was set on a logarithmic scale. This meant that the comparatively smaller nuclei appeared between the first and second decades and the larger cells, if present, would form a distinct population at the upper limit of the logarithmic scale, enabling their exclusion from the analysis.

Cells that were transfected with each of the FITC-labelled chromatin constructs were harvested for FACS analysis 48 hours post-transfection and divided into two aliquots. One aliquot of intact cells was analysed for RFP expression, as described previously (Section 2.9.1.2). Nuclei were isolated (as described in Section 2.8) from the second aliquot of cells and were analysed for FITC-fluorescence (see Section 2.9.1). RFP expression and nuclear accumulation of the transfection constructs were thus determined separately but from the same transfection experiment, enabling a direct comparison of these parameters. A total of 30000 cells were recorded for the RFP analysis, while 5000 nuclei were analysed. The majority of nuclei events fell between 10 and 100 units on the forward scatter, compared to forward scatter of intact cells which fell between 400 and 1000 units (Figure 5.6). The absence of a distinct population of events at the upper end of the forward scatter scale of the nuclei implied a homogeneous population had been isolated.

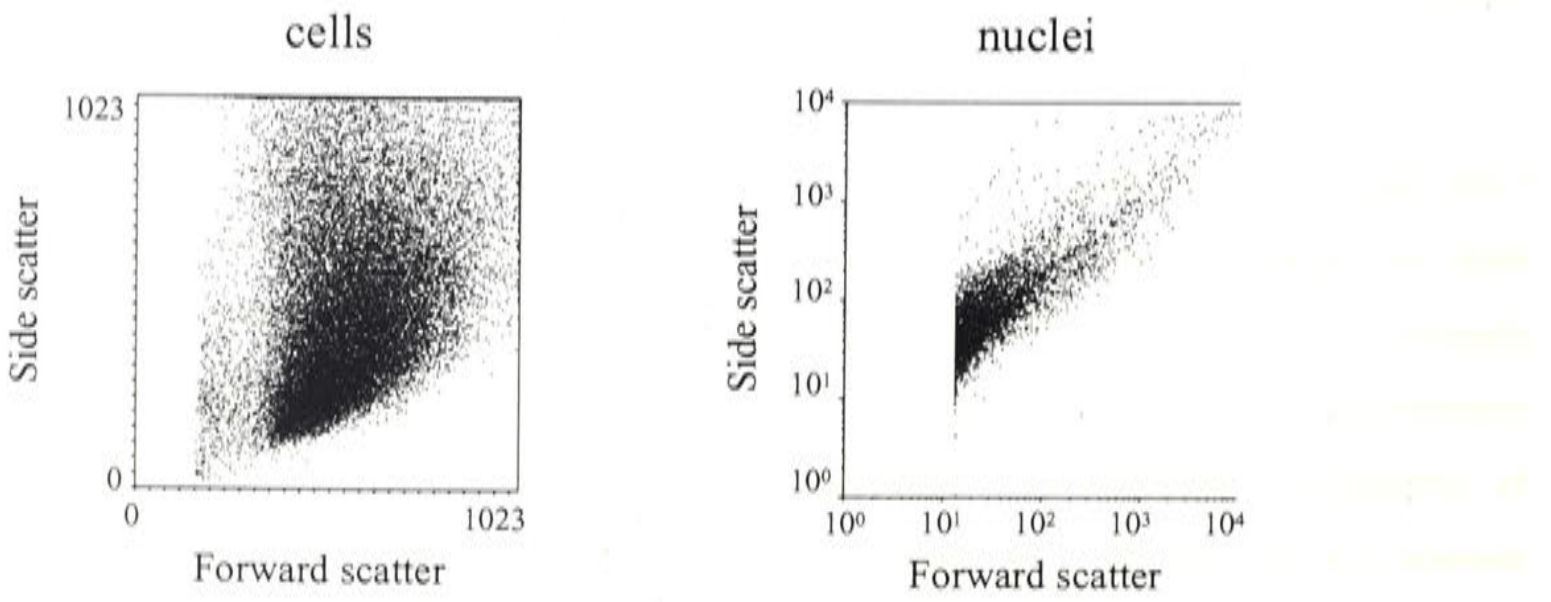

Figure 5.6. Qualitative analysis by FACS reveals a homogenous population of intact isolated nuclei. FACS analyses of whole cells (Cos-7) and nuclei isolated using NE-PER™ cell extraction reagents, as described in Section 2.8, are shown. Cells and nuclei were analysed on the basis of forward light scatter (x-axis) and side light scatter (y-axis). Forward scatter settings were on a linear scale for whole cells and on a logarithmic scale for nuclei. The majority of nuclear events fall between the first and second decades of log (10 – 100 units Forward scatter), whereas cellular events fall between the second and third decades of log (500 – 1000 units Forward scatter).

Nuclear FITC fluorescence originating from the FITC-labelled chromatin constructs was quantitated relative to nuclei isolated from cells transfected with either no construct (no DNA control) or unlabelled construct (0 octamers per plasmid). Channel FL1 was set so that FITC-negative events fell within the first decade of log on the FITC fluorescence axis. Figure 5.7a shows typical series of FACS dot plots obtained from nuclear accumulation analyses for a range of FITC-labelled chromatin constructs in Cos-7 cells. Collated data comparing RFP expression from the whole-cell analyses and FITC accumulation from the isolated nuclei analyses of Cos-7 cells are presented in Figure 5.7b and Table 5.1. Data obtained from an identical series of experiments performed using HTC cells are also presented in Table 5.1.

In both Cos-7 and HTC cells, the percentage of nuclei that took up the constructs chromatinised at lower nucleosome densities (1, 2 and 4 octamers per plasmid) were not significantly different from the naked plasmid (0 octamers per plasmid) ($p \geq 0.31$ for Cos-7 cells; $p \geq 0.09$ for HTC cells; see Table 5.1). In contrast, the constructs more extensively chromatinised at higher nucleosome densities, 25 and 40 octamers per plasmid, accumulated in significantly fewer nuclei in Cos-7 cells when compared to the naked plasmid ($p = 0.038$ and 0.041, respectively; see Table 5.1). Similarly, fewer HTC nuclei accumulated the 25 octamers per plasmid construct than naked plasmid ($p = 0.04$; see Table 5.1).

The tendency for RFP expression to be reduced upon increasing the chromatinisation of the reporter plasmid was consistent with the results observed previously (see Table 4.3). The relative percentages of cells expressing RFP from the less densely chromatinised constructs (1, 2 and 4 octamers per plasmid) were not significantly different from the percentages of nuclei that showed their accumulation, in both Cos-7 ($p \geq 0.562$; Figure 5.7b; Table 5.1) and HTC cells ($p \geq 0.192$; see Table 5.1). This suggested that of the nuclei that took up transfection constructs, a similar proportion had facilitated RFP expression. This was in contrast to the relationship between nuclear accumulation and transgene expression observed with more extensive chromatinisation at 25 octamers per plasmid (Table 5.1). Here, 3-fold fewer Cos-7 cells expressed RFP than nuclei that took up the construct ($p = 0.032$) and around 8-fold fewer in HTC cells ($p = 0.041$). A similar trend was observed for the 40 octamers per plasmid construct in Cos-7 cells. These results suggested that, in addition to decreased nuclear accumulation, the greater the degree of chromatinisation of the constructs the greater the inhibition of gene expression.

a

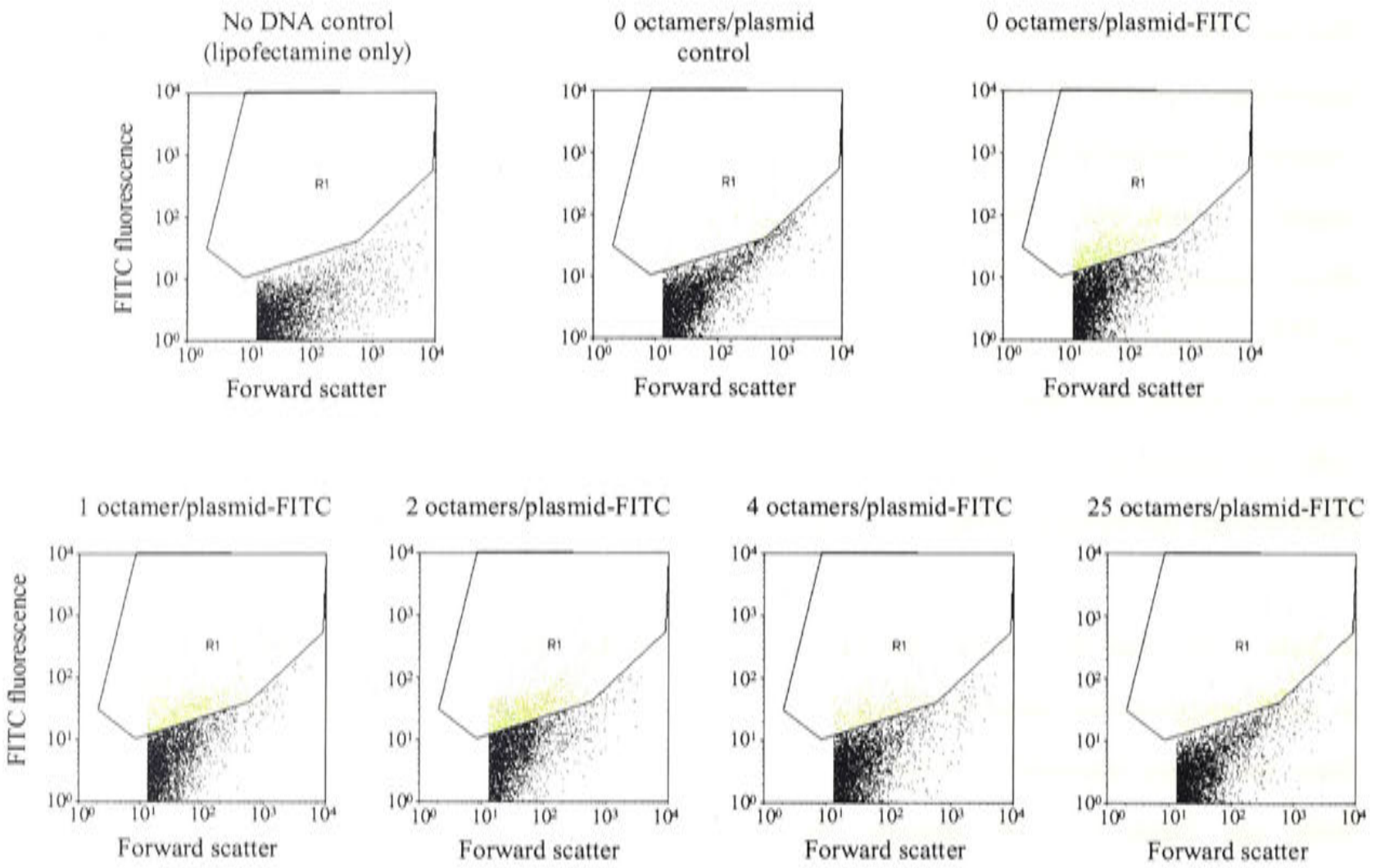

b

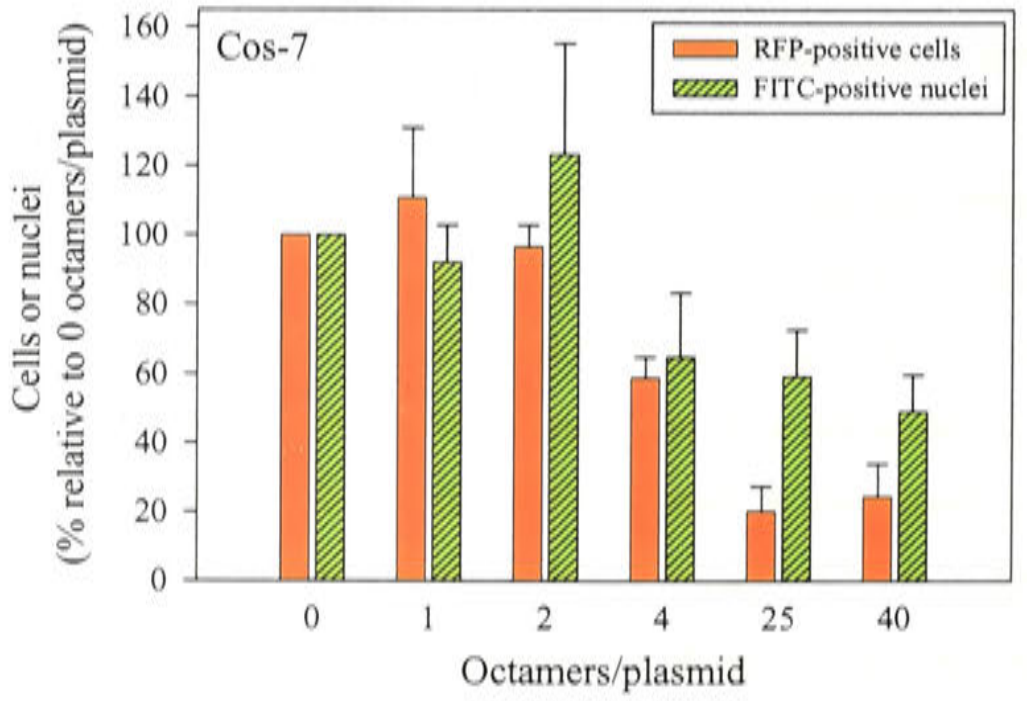

Figure 5.7. Nuclear accumulation of fluorescein-labelled chromatin constructs and corresponding RFP reporter gene expression in whole cells. Cos-7 cells were transfected with a range of differentially chromatinised fluorescein-labelled pGeneGrip-RFP constructs as described in Section 2.7.2. RFP expression was determined by FACS 48 hours post-transfection (channel FL2; Section 2.9.1.2). Nuclei were isolated (Section 2.8) and FITC-positive nuclei quantified also by FACS (channel FL1; Section 2.9.1.3). A typical series of FACS dot plots showing differential nuclear accumulation for a range of chromatin constructs can be seen in (**a**), with FITC-positive events represented within the polygon labelled R1 and coloured in green. Histogram analysis of pooled data is shown in (**b**). Red bars represent RFP-positive cells and the shaded green bars represent FITC-positive nuclei. The results are expressed as the percentage of cells or nuclei relative to the 0 octamers per FITC-labelled plasmid transfections and represent the mean ± SEM of 2 - 5 experiments. Experiments performed twice are represented by the mean ± range/2.

Table 5.1. Relative percentages of cells expressing RFP and nuclei positive for FITC.

	Cos-7 cells			HTC cells		
Octamers/plasmid	% RFP positive cells*	% FITC positive nuclei	n	% RFP positive cells*	% FITC positive nuclei	n
0	100 ± 0	100 ± 0	5	100 ± 0	100 ± 0	3
1	110.8 ± 20.2	92.2 ± 10.7	5	100.1 ± 7.1	60.6 ± 18.4	3
2	96.5 ± 6.2	123.3 ± 31.9	2	87.4 ± 15.6	66.9 ± 21.3	3
4	58.8 ± 5.9	64.7 ± 18.6	2	52.1 ± 5.7	65.9 ± 10.9	3
25	20.2 ± 7.2	59.3 ± 13.4	5	4.9 ± 2.8	40.8 ± 11.8	3
40	24.3 ± 9.5	48.9 ± 10.7	3	ND[A]	ND	
plasmid + 25 octamers[B]	54.3 ± 15.3	109.1 ± 18.6	5	24.9 ± 6.2	66.1 ± 18.7	3

Cos-7 and HTC cells were transfected (see Section 2.7.2) with fluorescein-labelled pGeneGrip-RFP (PNA-FITC labelling kit, Gene Therapy Systems; see Section 2.2.16.1) assembled into chromatin constructs at a range of histone octamer stoichiometries (Section 2.5.3). Cells were harvested 48 hours post-transfection and divided into two aliquots. In one of the aliquots of cells, RFP expression was determined by FACS (channel FL2; Section 2.9.1.2). Nuclei were isolated from the other aliquot (Section 2.8) and FITC-positive nuclei detected by FACS (channel FL1; Section 2.9.1.3). Data were analysed using CellQuest software (Macintosh). Results represent the mean ± SEM, expressed as the percentage of RFP-positive cells or FITC-positive nuclei relative to the 0 octamers per FITC-labelled plasmid transfections. The number of times the experiment was performed is indicated by n. For experiments performed twice, the mean ± range/2 is shown. Only experiments in which RFP-expressing cells and FITC-nuclei were determined in the same pool of transfected cells are presented.

[A] Not done.

[B] Construct comprising histones associated with pGeneGrip-RFP under non-chromatinising conditions at stoichiometry 25 octamers per plasmid.

* Note that the differences between the percentages of RFP-positive cells reported in Tables 5.1 and 4.3 are attributable to the presence of the PNA-FITC label.

In order to separate the specific effect of chromatinisation from the histone binding effect, the reporter plasmid was 'associated' with histones at a stoichiometry corresponding to 25 octamers per plasmid (plasmid + 25 octamers; see Table 5.1). As described in Sections 4.5.2 and 4.6.2, this was achieved by an initial incubation of the octamers in 135 mM NaCl/10 mM Tris (CB), followed by addition of pGeneGrip-RFP and then a further incubation for 10 minutes on ice, under which conditions chromatin cannot form. Unlike the observation for the chromatinised constructs, the levels of nuclear accumulation were not significantly lower than those of the naked plasmid, in Cos-7 ($p = 0.67$) or HTC cells ($p = 0.21$). This suggested that the decrease in nuclear accumulation observed when the reporter plasmid was loaded with high densities of histone octamers was specific to chromatinisation. However, as the relative percentages of RFP positive cells were significantly lower than the relative percentages of FITC-positive nuclei in

both Cos-7 ($p = 0.03$) and HTC cells ($p = 0.05$) for transfection with the 25 octamers per plasmid 'association', it appeared that the inhibition of gene expression at high densities of histone octamers was not specific to chromatinisation.

These results demonstrated that chromatinisation resulted in reduced nuclear uptake of the transfection constructs. Furthermore, the presence of histones either as chromatin or stochastically bound appeared to result in inhibition of gene expression. The trend of reduced RFP expression observed upon increasing chromatinisation of the reporter plasmid could thus be related both to reduced nuclear uptake and to inhibition of gene expression.

5.4. THE IMPORTIN BINDING PROPERTIES OF CHROMATIN

Given that importin β binds core histones with high affinity (see Section 3.2; Johnson-Saliba *et al.*, 2000), effective regulated transport of histones into the nucleus is implied (see also Section 1.5.2). One of the potential benefits of using an *in vitro* assembled chromatin system for the purposes of gene delivery was the possibility to exploit the nuclear import pathways of histones. This relied on the accessibility of importins to the histone NLSs in the context of a chromatinised plasmid. Since increasing the density of nucleosomes on the chromatinised reporter plasmid resulted in decreased levels of nuclear accumulation, it was important to verify whether the histones retained their importin binding affinity in the presence of DNA and were therefore able to contribute to the nuclear import of the chromatin constructs. The ELISA method, described in Chapter 3 to determine the importin binding affinities of histones (and other chromatin-associated proteins), was used here to determine importin binding to the histone octamer in the presence of DNA.

5.4.1. Importin binding to the core histone H3/4 is reduced in the presence of DNA

Importin binding to the core histone H3/4 tetramer in the absence and presence of DNA was investigated as a first step towards elucidating the importin binding properties of chromatin. This was because the H3/4 tetramers associate with DNA to induce the initial formation of topoisomers, but do not form the compacted, chromatinised structure.

Using the NAP-1 method of chromatin assembly (Section 2.5.1), H3/4 tetramers (isolated from chicken long chromatin; provided by L. Hyman, Chromatin and Transcriptional Regulation Group, JCSMR) were associated with plasmid DNA (in the absence of H2A/2B) and the supercoiling assay was used to determine plasmid conformation (Section 2.5.4). Agarose gel electrophoretic analysis of the supercoiled status revealed that plasmid DNA associated with H3/4 formed topoisomers, but occurred predominantly in the open circular (relaxed)

conformation of DNA (Figure 5.8a, lane 1), consistent with the absence of nucleosomes. The topoisomers tended towards the supercoiled conformation of the plasmid (Figure 5.8a, lane 2) only when H2A/2B dimers (recombinant *Xenopus laevis*, see Section 2.4.2.4) were added to H3/4 in the assembly reaction. The supercoiled state was reached at a stoichiometry of H2A/2B dimer to H3/4 tetramer of 2:1, mimicking that within the histone octamer (Figure 5.8a, lane 3).

Using the ELISA method (see Section 2.10 for method), the binding properties of the importin α/β heterodimer and importin β were determined for the H3/4-DNA association (seen in Figure 5.8a lane 1) and compared to that of the H3/4 tetramer alone.

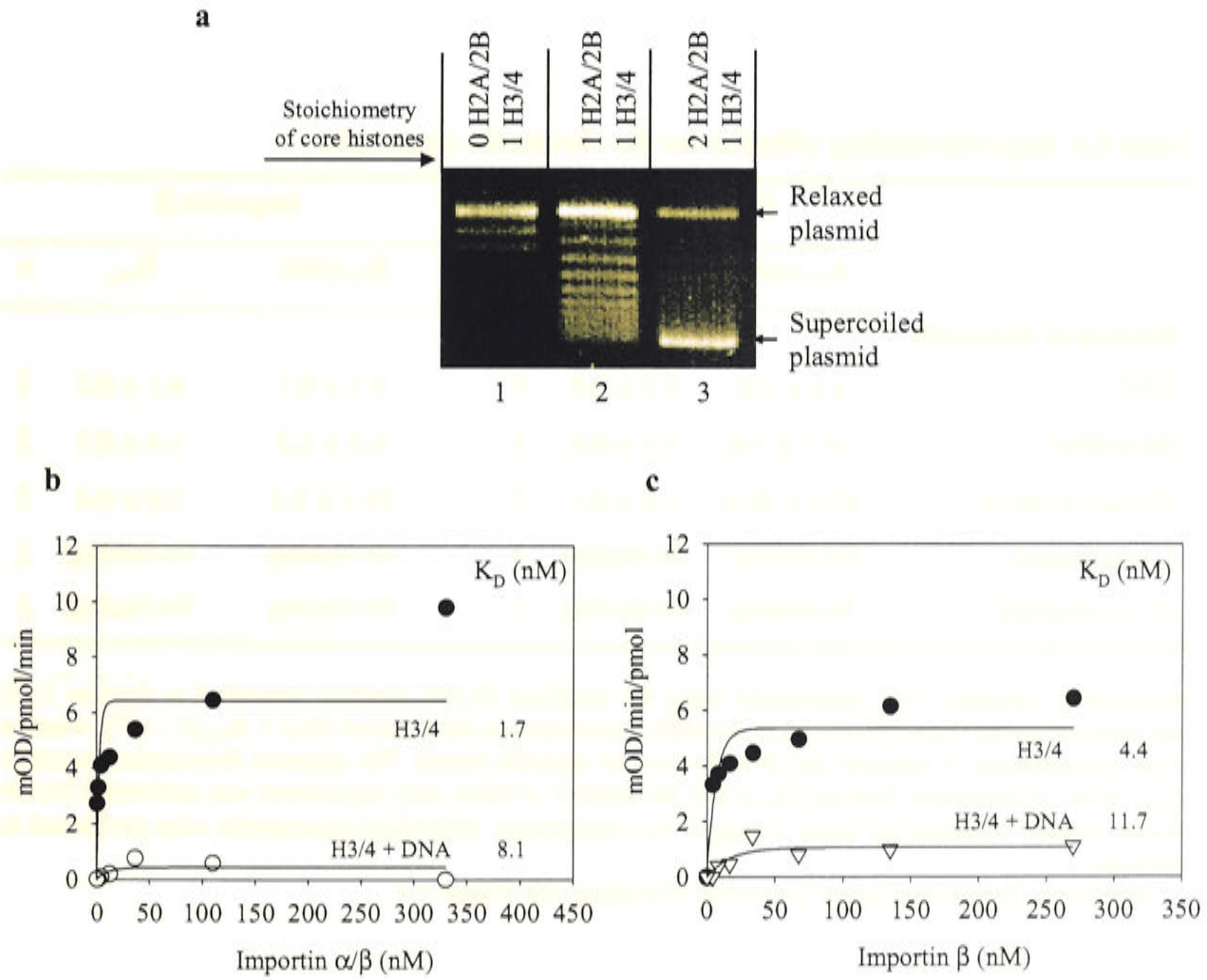

Figure 5.8. Importin binding properties of the core histone H3/4 in the presence of DNA. H3/4 was associated with DNA using the NAP-1 chromatin assembly method (see Section 2.5.1) and importin binding properties were determined using the ELISA method (see Section 2.10). The supercoiling assay following the H3/4-DNA association is shown in (**a**). The plasmid was relaxed using Topoisomerase I, and H3/4 added. A band corresponding to the relaxed form of the plasmid can be seen in Lane 1. Successive lanes (2 and 3) represent titration of H2A/2B onto the H3/4-DNA association, with topoisomers seen to tend towards the supercoiled form, evident at a stoichiometry of H2A/2B to H3/4 of 2:1 (lane 3). Importin binding of the H3/4-DNA association represented in (**a**) lane 1 was compared to that of H3/4 alone. The binding curves, corrected for the presence of DNA alone, are shown for the importin α/β heterodimer in (**b**) and for importin β in (**c**). Results represent a typical experiment, performed in triplicate. Curves were fitted in Sigma Plot (Jandel Scientific) using the function $B(x) = B_{max}(1 - e^{-kx})$, where x is the concentration of importin and B is the level of importin bound. The apparent dissociation constants (K_D) were calculated from k, the slope of the curve, using 0.693/k. See Table 5.2 for pooled data.

To remove the contribution from the importin/DNA binding component, the H3/4-DNA binding data was corrected using binding data for an equivalent amount of DNA, which had been subjected to the NAP-1 chromatin assembly process in the absence of histones. The corrected data showed that the effect of DNA was to lower the maximum level of importin α/β binding to H3/4 tetramers by 4-fold ($p = 0.001$) (Figure 5.8b; Table 5.2), consistent with occlusion of importin binding sites. The K_D values were not significantly different in the presence of DNA, indicating that the affinity of the available importin binding sites in H3/4 was unchanged. Similarly, the maximal level of importin β binding to H3/4 was reduced in the presence of DNA, up to 4-fold ($p = 0.004$), with no significant difference in the K_D values (Figure 5.8c; Table 5.2).

Table 5.2. Importin binding affinities for the chromatin constructs.

	Importin α/β			Importin β		
	K_D (nM)	B_{max}	n	K_D (nM)	B_{max}	n
Histones or chromatin						
H3/4	4.5 ± 2.8	7.3 ± 0.8	2	5.1 ± 0.7	6.1 ± 0.8	2
H3/4/DNA	15.7 ± 7.6	1.3 ± 0.9	2	9.5 ± 2.2	1.4 ± 0.3	2
Histone octamer	59.0 ± 26.6	3.4 ± 0.1	2	39.3 ± 9.5	3.8 ± 0.4	2
1 oct/plasmid	No binding[A]	No binding	2	No binding	No binding	2
25 oct/plasmid	No binding	No binding	2	No binding	No binding	2

Dissociation constants were determined using the modified ELISA method (described in Section 2.10) and analysed using Sigma Plot (Jandel Scientific) according to the function $B(x) = B_{max}(1 - e^{-kx})$, where x is the concentration of importin and B is the level of importin bound. The apparent dissociation constants (K_D), levels of maximum binding (B_{max}) and the number of times each experiment was performed (n) are shown. Results represent the mean ± range/2 for experiments. Individual experiments were performed in triplicate.

[A] Could not be determined due to low levels of binding. See Figure 5.9.

5.4.2. Importin binding to the core histone octamer is abolished in the presence of DNA

The importin binding properties of chromatin constructs assembled at stoichiometries of 1 and 25 histone octamers per pGeneGrip-RFP plasmid were determined using the ELISA method (Section 2.10) and compared to those of the histone octamer alone (Table 5.2). The amount of histone octamers was kept constant in each well of the ELISA microtitre plate at 4 pmol. Importin binding to pGeneGrip-RFP plasmid DNA corresponding to the amount in each of the

chromatin constructs was determined in order to correct for non-specific binding of importins to DNA.

A peptide comprising residues 67 – 94 of PTHrP was used as a positive control for importin β binding (Lam *et al.*, 1999) and demonstrated a high binding affinity, having a K_D of 0.8 ± 0.3 nM (n = 2) and maximal binding level of 24.2 ± 1.3 (n = 2) (data not shown). The histone octamer alone exhibited binding to the importin α/β heterodimer (K_D = 59.0 ± 26.6 nM) and to importin β (K_D = 39.3 ± 9.5 nM) (Figure 5.9; Table 5.2), although this was of lower affinity than that of its components – the H2A/2B dimer and the H3/4 tetramer (a reduction of around 10-fold; see Table 3.1). Unlike H3/4/DNA, however, which still exhibited an importin binding component in the presence of DNA (Figure 5.8b and c; Table 5.2), no binding could be attributed to the histone octamer after chromatinisation at neither 1 nor 25 octamers per plasmid, as the binding curves for pGeneGrip-RFP DNA and the chromatin constructs were superimposable (Figure 5.9).

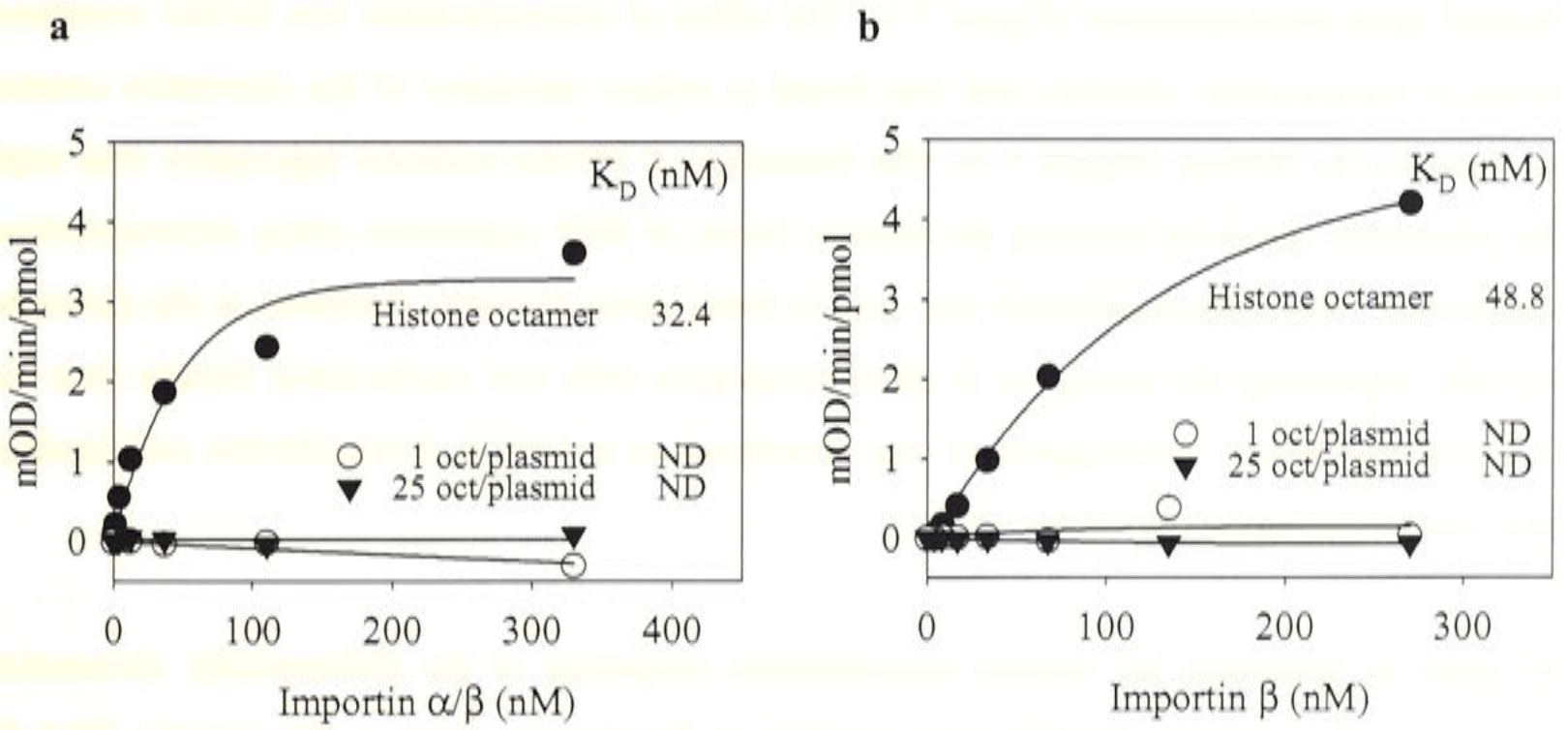

Figure 5.9. Assembly of the core histone octamer into chromatin abolishes importin binding. Importin binding curves of the histone octamer alone and chromatin constructs containing 1 and 25 octamers per plasmid are shown. Microtitre plates were coated with 4 pmol per well of octamer, irrespective of the stoichiometry of the chromatin samples. The amount of plasmid DNA corresponding to that in the 1 and 25 octamers per plasmid samples served as the control for non-specific binding to the chromatin constructs. Data were determined using the modified ELISA method (Section 2.10). Comparative binding curves for the octamer, 1 octamer/plasmid and 25 octamers/plasmid are shown in (**a**) for importin α/β and in (**b**) for importin β. Data were analysed using Sigma Plot (Jandel Scientific) according to the function $B(x) = B_{max}(1 - e^{-kx})$, where x is the concentration of importin and B is the level of importin bound. The apparent dissociation constants (K_D) were calculated from k, the slope of the curve as 0.693/k. The K_D values are denoted for the histone octamer but binding was too low to allow their determination for the chromatin constructs. These results represent a single typical experiment, performed in triplicate. Pooled data is presented in Table 5.2.

Overall, these results demonstrated that the association of DNA with the histone octamer in the context of chromatin abrogated binding by importins. Contrary to the original prediction, it is therefore highly improbable that nuclear import of the chromatinised constructs could be mediated by the importin α/β or importin β pathways.

5.5. Discussion

Some of the possible mechanisms for the reduction observed in transgene expression upon increasing the chromatinisation of the reporter plasmid were examined in this chapter, specifically the degree of nuclear accumulation of the chromatin constructs and the importin/histone binding properties.

The transfection methods used in this study, namely electroporation and lipofection, were assessed in terms of their effects on the structure of the chromatinised plasmid constructs. While the supercoiled conformation of the chromatin constructs was maintained in the presence of the lipofection reagent, the agarose gel analysis revealed that high molecular weight aggregates had formed upon electroporation (Figure 5.1). The effect of electroporation was further examined in terms of nucleosomal structure and was found to induce resistance of the chromatin constructs to digestion by MNase (Figure 5.2). The formation of MNase-resistant aggregates may explain the anomalies observed between the relative levels of RFP expression using electroporation or lipofection, where electroporation was seen to bring about dramatic decreases in the percentages of cells expressing the transgene at chromatinisation with low nucleosome density (see Table 4.3). For this reason, electroporation was abandoned as a method of transfection and lipofection was used in the remainder of the study.

In order to determine the nuclear accumulation properties of the differentially chromatinised constructs, the reporter plasmid was coupled to fluorescein using a site-specific PNA-FITC hybridisation label. The presence of the FITC label did not hinder assembly of the plasmid into chromatin (Figure 5.4). The visualisation of fluorescein-labelled chromatin constructs in an *in vitro* permeabilised cell system using CLSM was not possible due to the limiting sensitivity against the background of cellular autofluorescence. Flow cytometry was adopted as an alternative method. However, the reliable detection in whole cells of transfected FITC-labelled chromatin constructs was also not possible in tandem with detection of RFP-expressing cells due to RFP 'bleed through' into the FITC detector. FITC-fluorescence could be detected in isolated nuclei. Consequently, RFP reporter gene expression was detected in whole cells and the FITC-fluorescence originating from the labelled chromatinised plasmids was detected in the isolated nuclei from pools of cells within the same transfection experiment.

Compared to the naked construct (0 octamers per plasmid), nuclear accumulation of the constructs chromatinised at lower nucleosome densities (1, 2 and 4 octamers per plasmid) was unchanged. In contrast, significantly fewer nuclei accumulated the transfection constructs chromatinised at higher nucleosome densities (25 and 40 octamers per plasmid; ~50 % fewer; Table 5.1). As discussed in Section 4.7, the findings of Lukacs *et al.* (2000) suggest that the high MW of the chromatin complexes (6.6×10^6 Da for the 25 octamers per plasmid construct compared to 3.9×10^6 Da for the naked plasmid; see Table 4.1) may hinder diffusion through the cytoplasm and, consequently, reduce the amount of transfection constructs presenting at the NPC for import into the nucleus. Interestingly, a construct harbouring the theoretical MW equivalent to the 25 octamers per plasmid construct (but non-chromatinised) accumulated to a similar degree as the naked plasmid (Table 5.1). This suggests that MW *per se* was not an issue in this case and that it was in fact chromatinisation that inhibited nuclear uptake. This will be discussed in detail in Chapter 7 in the context of DNA compaction and nuclear accumulation efficiency.

Of the cells transfected with the constructs chromatinised at higher nucleosome densities (25 and 40 octamers per plasmid), markedly fewer showed RFP expression compared to the percentage of nuclei which had accumulated FITC fluorescence (Figure 5.7 and Table 5.1). This may indicate that gene expression was repressed at higher molar ratios of histone octamers to plasmid and raises the important issue of the transcription efficiency of the transgene. When using 'non-physiological' vehicles for non-viral gene delivery, such as pLy or PEI, it is crucial that DNA is released from the carrier once in the nucleus so that it may be transcribed. A proposed advantage of using a chromatinised plasmid for gene delivery was that this mimics the physiological 'packing' of the DNA template, for which endogenous processes exist to facilitate 'unpacking' prior to transcription. Chromatin assembly (using the method employed here) at high levels of nucleosome density has been shown to be transcriptionally repressive *in vitro* (Sandaltzopoulos *et al.*, 1994; Hansen and Wolffe, 1992; Izban and Luse, 1992). However, addition of appropriate chromatin remodelling enzymes can overcome this repression (Logie and Peterson, 1997; Ng *et al.*, 1997). *In vivo*, cells have specialised transcription complexes that re-model localised regions of chromatin by inducing sliding of the nucleosome away from the promoter region of the gene in order to facilitate transcription (for reviews see Luger, 2003; Orphanides and Reinberg, 2000; Kadonaga, 1998). In this study, pGeneGrip-RFP was expressed in fewer cells, when chromatinised at high nucleosome density. One possible explanation for this may be that the *in vitro* assembled chromatin could not be re-modelled efficiently *in vivo* in order for transcription to have occurred unhindered.

The data presented in this chapter suggests that reduced nuclear uptake and inhibition of transcription were pivotal factors leading to reduced transgene expression. While some nuclear entry of the chromatinised plasmids would have occured during the process of cell division

(Escriou *et al.*, 2001; Wilke *et al.*, 1996), as the duration of the reporter gene assay was 48 hours, it is assumed that this nuclear accumulation would be equivalent for the different constructs. Nuclear import at other times would occur only through the NPC, as this is the established route for all transport into the nucleus (see Section 1.3.3.1). The reduced nuclear import observed in conjunction with increased chromatinisation may therefore be considered to arise from inhibition of this component of nuclear uptake.

The accumulation of low molecular weight nucleic acids is well documented (Zelphati and Szoka, 1996) and the possibility that some of the nuclear fluorescence quantitated in the experiments reported here (Table 5.1) may be due to accumulation of degraded chromatinised constructs cannot be excluded. This degradation may result from the action of nucleases. Firstly, DNase I, which was added to the isolated nuclei in order to prevent their aggregation, may act on any plasmids should they may remain associated with the outside of the nucleus. Nuclear 'adherent' plasmids, however, seem unlikely as the nuclei underwent various wash steps during the isolation procedure (Section 2.8). Secomdly, cytosolic nucleases may degrade the cytoplasmically-localised transfected plasmids (Pollard *et al.*, 2001; Leuchardeur *et al.*, 1999). Since association with histone octamers protects the DNA from degradation (Section 4.4.3), it may therefore be argued that the low frequency of FITC-positive nuclei is simply due to the lowered incidence of fluorescently labelled degradation products accumulating in the nucleus. Conversely, in the event of high levels of degradation of the plasmid, as may occur in the absence of histone octamers (the low nucleosome density constructs), a high frequency of FITC-positive nuclei would occur. In this case, expression of the transgene would be abrogated. On the contrary, the frequency of RFP-expressing cells tracks the frequency of FITC-positive nuclei. This indicates that degraded plasmid as the source of nuclear fluorescence is highly improbable and the levels of nuclear fluorescence observed are indeed representative of the accumulation (or lack thereof) of the series of chromatin constructs.

The possibility exists that a proportion of the chromatin constructs remained bound at the NPC and never entered the nucleus to allow transcription and gene expression to occur. The source of some of the nuclear-associated fluorescence could possibly, therefore, have been at the nuclear envelope, rather than the nucleoplasm. Although this possibility cannot be excluded, the fact that transcriptional repression occurs at high levels of histone octamer density, both *in vitro* (Sandaltzopoulos *et al.*, 1994; Hansen and Wolffe, 1992; Izban and Luse, 1992) and *in vivo* (Luger, 2003; Orphanides and Reinberg, 2000; Kadonaga, 1998), makes a more likely explanation that some nuclear transport did occur and that transcription of these constructs was repressed. Further evidence for this stems from the observation that despite uninhibited nuclear accumulation of the 25 octamers per plasmid 'association', only half that proportion of cells expressed the reporter gene (Table 5.1).

At the outset of this study, it was proposed that the importin-mediated uptake of histones would be extended to chromatin nuclear import. In light of both the decreased levels of cells expressing RFP and nuclear accumulation of the constructs with increasing plasmid chromatinisation, the ability of histones to retain their importin binding affinity (Section 3.2) when simultaneously bound to DNA was investigated. Results generated using the modified ELISA method indicated that the core histone octamer was bound by importins with reduced affinity and at 2-fold lower levels of maximal binding when compared to the binding affinity of its constituent H2A/2B dimers and H3/4 tetramer (compare Tables 3.1 and 5.2). In crystal structure studies of a single nucleosome, amino acids 16 – 24 of H4 have been shown to bind to a specific domain of the H2A/2B dimer on the surface of the histone octamer (Luger *et al.*, 1997). As this region of H4 has also been shown to contain an NLS (see Table 3.2; Mosammaparast *et al.*, 2002b; Baake *et al.*, 2001a; Muhlhausser *et al.*, 2001), it may be postulated that this intra-octamer contact may preclude the NLS from importin-binding, thus reducing the level of maximal binding by importins. Moreover, the level of maximal importin binding to H3/4 was observed to be reduced in the presence of DNA, suggesting further occlusion of available importin binding sites (Figure 5.8a). When associated with DNA, the H3/4 tetramer was able to contribute to importin binding, possibly as a more open form of the plasmid was predominant which may have allowed importin accessibility. In contrast, when associated with DNA through chromatinisation there was no measurable binding contributed by the octamer. Thus, in chromatinised plasmids, DNA may mask the histone NLSs and abrogate importin binding. This finding is consistent with those of others showing that some proteins are mutually exclusive for DNA and importin binding (Forwood *et al.*, 2001b; Chan *et al.*, 1998).

The results presented in this chapter suggest that key limiting steps for the success of using *in vitro* assembled chromatin for gene delivery purposes are the efficiency of nuclear uptake and transcription of the reporter plasmid. Strategies to overcome these limitations are explored in the next chapter.

CHAPTER 6

Strategies to enhance transgene expression from the chromatinised plasmids

6.1. INTRODUCTION

The results presented in Chapter 5 indicated that the trend of decreased transfection efficiency observed with increasing levels of plasmid chromatinisation may be partly attributed to reduced nuclear uptake. It was also apparent that not all of the plasmid-containing nuclei supported transcription of the reporter gene from the plasmids chromatinised at high nucleosome densities, as reflected in the marked decrease in the proportion of cells expressing the reporter gene compared to the proportion of cells that showed nuclear accumulation of the transfection constructs (Figure 5.7; Table 5.1). Therefore, the impairment of transcriptional activity concomitant with increasing chromatinisation was implicated as another contributor to decreased reporter gene expression (Section 5.3.2). In this chapter, the approaches undertaken to address the problems of reduced nuclear import and inhibited transcription are described.

Several studies have described the inclusion of NLSs in the transfection constructs in order to enhance nuclear import (reviewed in Escriou *et al.*, 2003; Cartier and Reszka, 2002; Bremner *et al.*, 2001). Since importin binding to the intrinsic NLSs of the histone octamer was found to be abrogated in the context of DNA-induced nucleosome formation (Section 5.4), NLSs additional to those present in the histones were incorporated into the chromatin constructs. Enhanced uptake of the transfection constructs by the nucleus should increase the probability for transcription and, ultimately, expression levels of the reporter gene. Inclusion of the NLS in the chromatin transfection constructs was explored at two levels. Firstly, at the level of the DNA-carrier protein, a histone-NLS fusion protein was generated for assembly into histone octamers and, secondly, at the level of the DNA, by directly coupling a NLS to specific sites within the reporter plasmid. The NLS that was employed was a peptide sequence derived from the SV40 T-ag, which had been optimised with the inclusion of a nuclear-import-enhancing site previously (P101; Hubner *et al.*, 1997). The use of this peptide allowed the possibility for the nuclear entry of the chromatinised constructs by the 'conventional' importin α/β-mediated

pathway (see Section 3.2). This strategy of switching to an alternative nuclear import pathway was first employed by Chan *et al.* (2001), who found that the DNA binding protein used (GAL4) in their gene delivery construct was mutually exclusive for importin β- and DNA-binding (Chan *et al.*, 1998). Inclusion of an SV40 T-ag peptide in the GAL4-based gene delivery construct restored nuclear import via the importin α/β-mediated pathway and transgene expression was shown to be enhanced.

Comparison of the relative levels of nuclear accumulation and the reporter gene expression of the chromatin constructs reported in Section 5.3.2 suggested that impairment of gene expression may have arisen also as a result of inefficient transcription of the more extensively chromatinised constructs that had entered the nucleus. One of the reasons for introducing transfection constructs into cells in the form of *in vitro* assembled chromatin was that chromatin is the physiological form in which DNA exists in the cell. While it is known that regions of chromatin heavily associated with nucleosomes are generally refractory to transcription *in vitro* (Sandaltzopoulos *et al.*, 1994; Hansen and Wolffe, 1992; Izban and Luse, 1992), mechanisms exist in the cell to re-model nucleosome density, moving nucleosomes away from the promoter regions of the genes so that transcription can occur (Orphanides and Reinberg, 2000; Kadonaga, 1998). It was expected that the CMV promoter and enhancer region, which is constitutively active (pGeneGrip™, Gene Therapy Systems), would drive expression of the reporter gene when transfected into cells in culture, even when the reporter plasmid was chromatinised. The discrepancy between the proportion of nuclei that had accumulated the chromatinised plasmids and cells that had expressed the reporter gene suggests that this may not have been the case and that chromatinisation had inhibited transcription of the transgene.

In order to test the hypothesis that chromatinisation inhibited transgene expression, two strategies were adopted to determine if the putative transcriptional block could be overcome and if the transcriptional permissiveness of the chromatinised constructs could be potentiated. In the first approach, chromatinisation of the reporter plasmid with histone octamers that incorporated the H2AZ variant histone instead of H2A was investigated. Fan *et al.* demonstrated that H2AZ-octamers inhibited the formation of highly condensed chromatin fibres (Fan *et al.*, 2002). The presence of H2AZ might therefore facilitate the formation of transcriptionally competent chromatin domains. In addition, it had been demonstrated that H2AZ/2B dimers had greater affinity for importin β than H2A/2B dimers in the ELISA-based binding studies (Section 3.2). This may be extrapolated to mean that H2AZ-containing chromatin may be transported to the nucleus more efficiently than H2A-containing chromatin (provided that the NLSs are not masked to the same extent as in H2A-chromatin; Section 5.4).

In the second approach, an alternative transgene expression system was investigated. This approach was based upon the premise that regions of condensed chromatin, which are refractory to transcription, undergo 're-modelling' *in vivo* to become transcriptionally active when targeted by appropriate re-modelling complexes (Orphanides and Reinberg, 2000; Kadonaga, 1998). The ability of the T-cell specific GMCSF promoter, which can recruit transcription complexes in the model T-cell line, Jurkat (Rao *et al.*, 2001; Himes *et al.*, 1993), was tested for its potential to drive reporter gene expression when in the context of *in vitro* assembled chromatin.

6.2. INCLUSION OF EXTRINSIC NLSS IN THE CHROMATIN TRANSFECTION CONSTRUCTS

The *in vitro* binding studies reported in Section 5.3.2 showed that when DNA was associated with the histone octamers in nucleosomes, the intrinsic importin β-specific NLSs within the histones no longer mediated high affinity binding. This implied that the importin β-mediated pathway was unlikely to facilitate efficient nuclear import of the chromatin constructs. Consequently, extrinsic SV40 T-ag optimised NLS peptide sequences (GPGSDDEAAADAQHAAP**PKKKRKV**GY; the NLS is highlighted in bold type-face) which target the importin α/β-mediated nuclear import pathway and had been shown previously to enhance nuclear delivery of plasmid DNA (Chan and Jans, 2001; Chan *et al.*, 2000; Akhlynina *et al.*, 1999; Chan and Jans, 1999; Akhlynina *et al.*, 1997) were incorporated into the chromatin constructs.

6.2.1. Generation of a histone-NLS fusion protein and its incorporation into histone octamers

6.2.1.1. Construction of an H2A-NLS expression plasmid

The coding region of H2A (*Xenopus laevis*) was subcloned from the plasmid pET3a-H2A (Table 2.9), together with the SV40 T-ag NLS subcloned from plasmid pPR28 (Table 2.9) which contains the optimised T-ag NLS, into the pET5a vector by Dr M. Lam (Nuclear Signalling Laboratory, JCSMR; see Figure 6.1a - c for the ligation strategy). A candidate clone, containing H2A fused at the C-terminal to the NLS, was identified by restriction analysis using the restriction endonuclease SpeI, which would digest at a unique site present as a consequence of the NLS PCR product insertion. The candidate clone, termed pET5a-H2A-NLS (Figure 6.1d) was sequenced (described in Section 2.2.14) using the 'forward sense' sequencing primer H2A5' (Table 2.10). This confirmed the presence of the H2A coding region and the C-terminal insertion of the NLS coding region (denoted in Figure 6.1d).

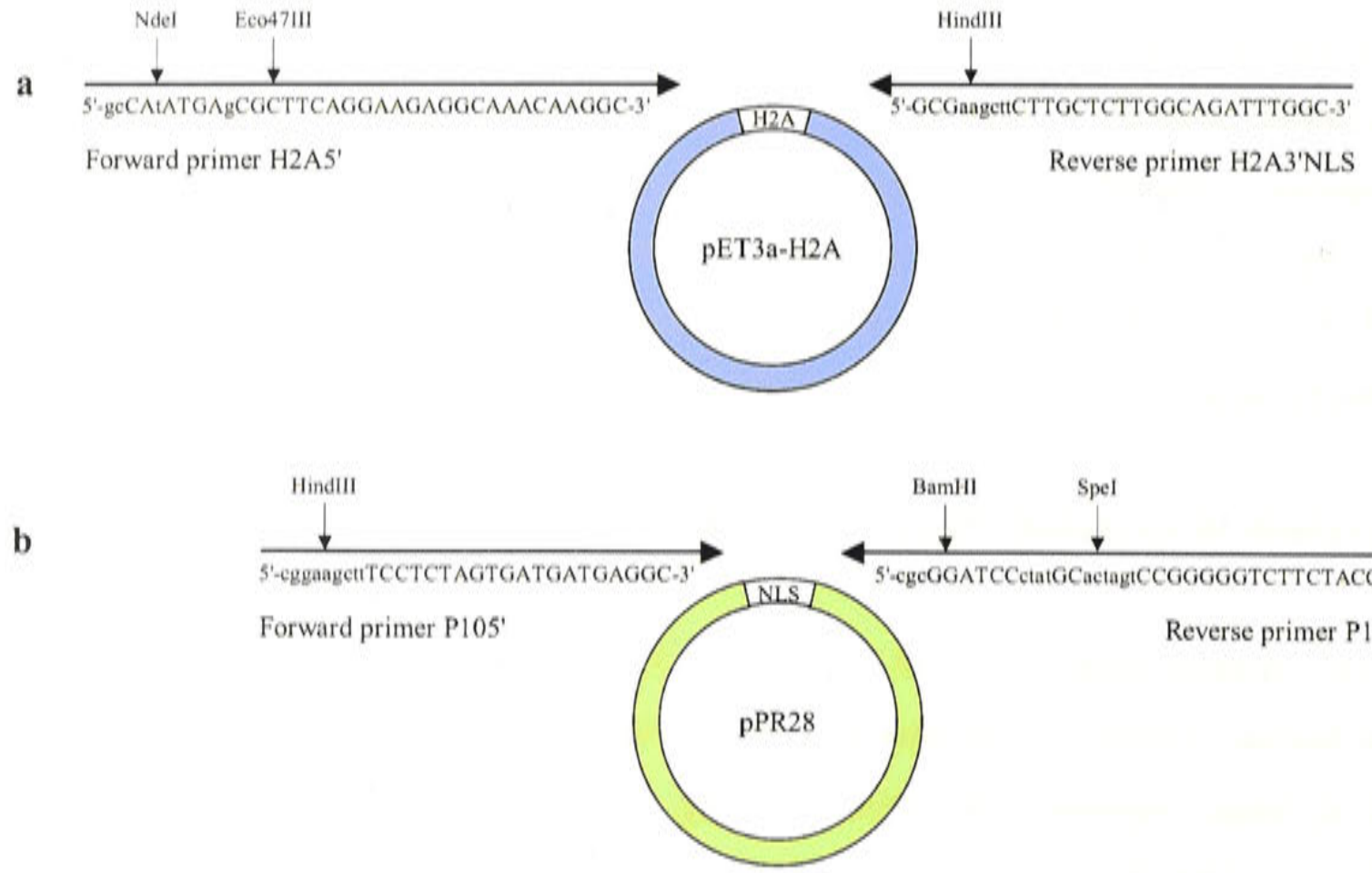

Figure 6.1. Generation of an H2A-NLS expression plasmid. A schematic representation of the strategy employed to clone a plasmid for the expression of the H2A-NLS fusion protein is shown in (**a** – **c**). H2A was PCR amplified from pET3a-H2A (**a**) and the NLS was PCR amplified from pPR28 (**b**) using custom primers designed to introduce restriction sites (shown in lower case font) (see Tables 2.9 and 2.10; Section 2.2.12). Cloning of both PCR products into pET5a was carried out simultaneously, using 'sticky-end' ligation of the restriction sites indicated in (**c**) by Dr M. Lam (Nuclear Signalling Laboratory, JCSMR). A clone identified by restriction digest analysis with SpeI was sequenced ('forward' primer H2A5', see Table 2.10 and Section 2.2.14; Perkin Elmer ABI Prism 377 DNA sequencer) to confirm the presence of the H2A-NLS fusion. The nucleotide profile is shown in (**d**). The NLS coding sequence is boxed in red, with the single letter amino acid code translation shown. The H2A coding sequence is indicated by the black arrow.

6.2.1.2. Expression of H2A-NLS in BL21DE3lysS *E. coli* cells

For protein expression, pET5a-H2A-NLS was transformed into BL21DE3lysS *E. coli* cells using the heat shock method (Section 2.2.1.2; Table 2.8). A detailed description of H2A-NLS expression is set out in Section 2.4.2.1 but, briefly, an overnight starter culture was established from an H2A-NLS bacterial colony selected on the basis of ampicillin and chloramphenicol resistance on solid agar medium. This was used the following morning to inoculate a larger culture of 800 ml. This culture was incubated at 37°C with agitation until an OD_{600nm} of between 0.6 and 0.8 was reached, at which point IPTG was added to a final concentration of 0.5 mM. The culture was incubated for a further 2 hours at 37°C and thereafter agitated gently overnight at room temperature. Samples of culture, removed before the addition of IPTG and 24 hours later, were analysed by 18 % SDS-PAGE and Coomassie staining. Induced expression of a protein of MW between 14.9 and 19.6 kDa was evident, in accordance with the predicted value for H2A-NLS of 16.7 kDa (H2A, 13960 Da; NLS, 2760 Da; see Figure 6.2a).

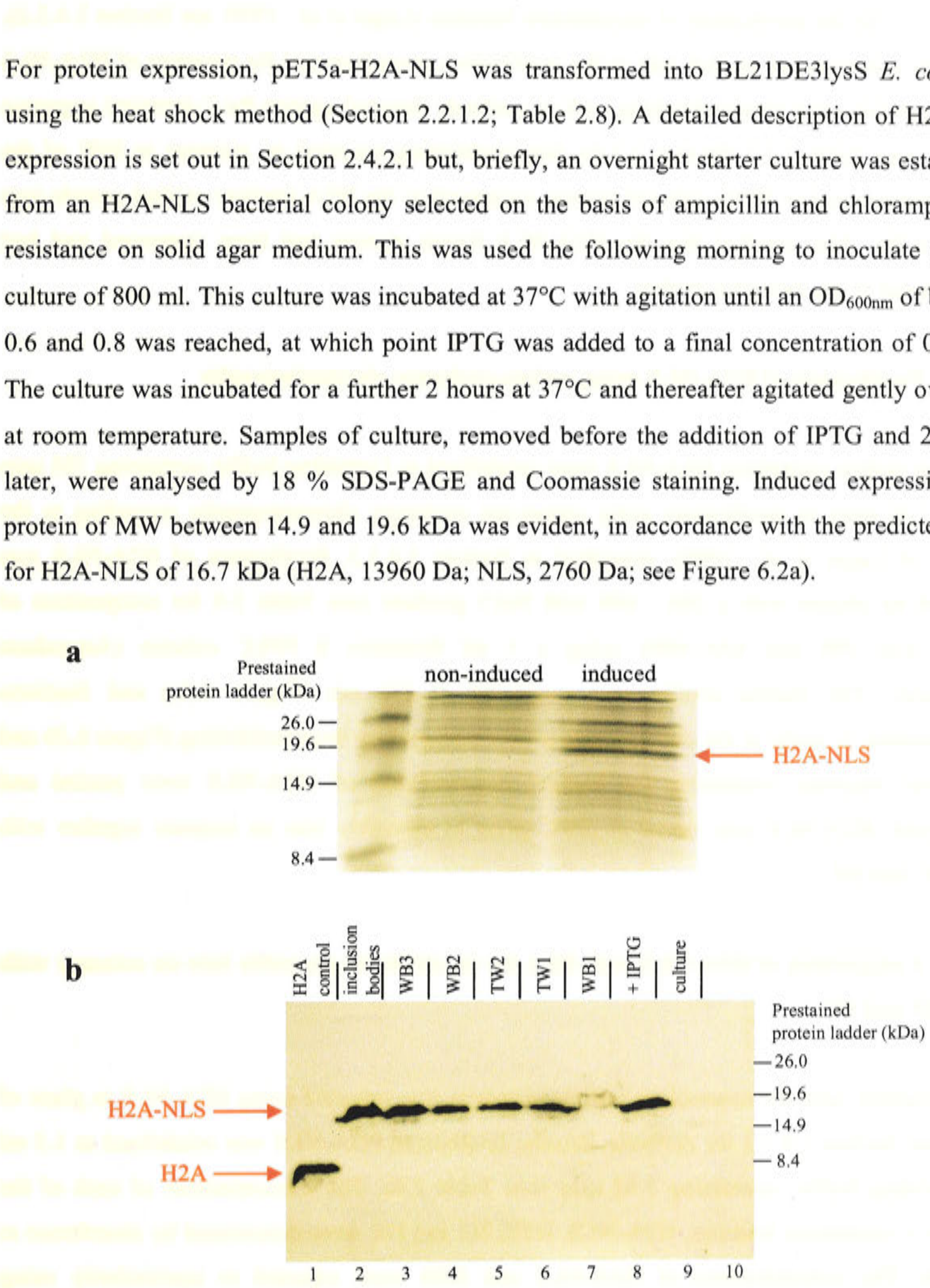

Figure 6.2. Expression of H2A-NLS in BL21DE3lysS *E. coli* cells and isolation of inclusion bodies. BL21DE3lysS *E. coli* cells were transformed by heat shock with pET5a-H2A-NLS (see Section 2.2.1.2). Samples of culture, removed before addition of IPTG and 24 hours later, analysed by 18 % SDS-PAGE and Coomassie staining, are shown in (**a**). An overexpressed protein between 14.9 and 19.6 kDa, corresponding in MW to H2A-NLS (16.7 kDa) is indicated by the red arrow. Inclusion bodies were purified (Section 2.4.2.2) and samples removed at each stage. Samples were electrophoresed through 18 % SDS-polyacrylamide. Protein transfer onto a nitrocellulose membrane was carried out overnight at 10 V in the presence of Transfer buffer (Section 2.3.4; Table 2.3). The nitrocellulose membrane was probed for the presence of H2A-NLS using an H2A-antibody (Table 2.13; Section 2.3.4). Antibody reactivity visualised by chemiluminesence (Pierce, see Table 2.14) is shown in (**b**). Inclusion bodies purification steps are denoted (+ IPTG is 24 hours post induction, WB is Wash buffer; TW is Wash buffer/1 % Triton X-100; Table 2.4). The H2A positive control and H2A-NLS are indicated by red arrows.

Inclusion bodies were prepared from the IPTG-induced cultures by following the protocol of Luger *et al.* for the purification of recombinant histones (Luger *et al.*, 1999; see Section 2.4.2.2). A sample was removed at each step in the purification procedure and the presence of H2A-NLS was monitored using immunoblotting with an antibody directed against the C-terminal sequence of H2A (see Table 2.12; Section 2.3.4). Immunoblotting revealed an increase in MW of the H2A-immunorecative IPTG-induced protein compared to the H2A positive control sample (see Figure 6.2b). This verified that the H2A-NLS fusion protein had been expressed and had accumulated in the inclusion bodies.

6.2.1.3. Purification of H2A-NLS using cation-exchange chromatography

Inclusion bodies containing H2A-NLS were solubilised in Unfolding buffer containing 7M urea (Table 2.4) prior to purification using cation-ion exchange chromatography according to the method of Luger *et al.* (1999), described in Section 2.4.2.2. Purification of H2A-NLS was achieved by elution with a 200 - 600 mM NaCl gradient (see Table 2.4 for composition of buffers SAU-200 and SAU-600) using a 1 ml Resource S FPLC column (Amersham Pharmacia). The elution profile was monitored at 276 nm (Figure 6.3a) and fractions corresponding to peaks in the chromatogram were analysed by immunoblotting (Figure 6.3b and c). Those fractions containing the highest concentration of H2A-NLS were pooled and lyophilised. H2A-NLS was stored at -20°C prior to assembly into an octamer together with H2B, H3 and H4.

6.2.1.4. Comparison of H2A-NLS with H2A for its ability to assemble into an octamer with H2B, H3 and H4

The procedure used for assembling histone octamers was repeated using H2A-NLS in place of H2A (see Section 2.4.2.3 for method). Briefly, lyophilised H2A-NLS was solubilised in 1.5 ml of Unfolding buffer, containing 7 M urea (see Table 2.4). The concentrations of each of the octamer's constituent histones, H2A-NLS, H2B, H3 and H4, were determined by absorbance at 276 nm. The concentrations of H2A-NLS and H2B were adjusted to equimolarity using Unfolding buffer (Table 2.4). Similarly, the concentrations of H3 and H4 were adjusted to equimolarity but were 98 % that of H2A-NLS to ensure maximal incorporation of H3 and H4 into the octamer (Luger *et al.*, 1999). The final concentration of the histone mix was determined by measuring the absorbance at 276 nm and was adjusted to 1 mg/ml using Unfolding buffer (final volume ~ 2 ml). For comparison, H2A-containing octamers were assembled in parallel with H2A-NLS containing octamers in an identical manner.

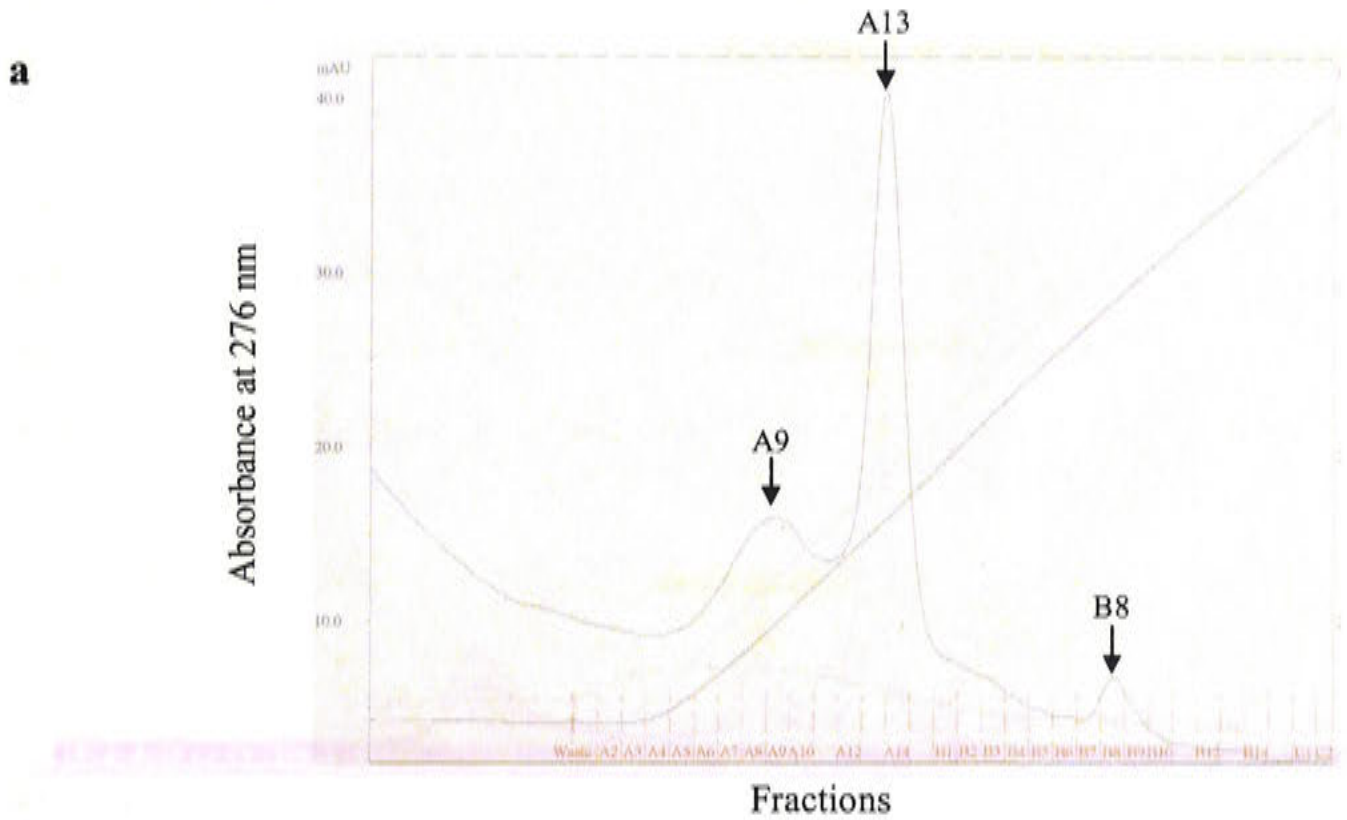

Figure 6.3. Purification of H2A-NLS. H2A-NLS was purified from isolated inclusion bodies using cationic exchange chromatography (1 ml Resource S column, Amersham Pharmacia) eluting in 1 ml fractions with a linear NaCl gradient (200 - 600 mM) at a flow rate of 1 ml/min. The chromatographic trace captured at 276 nm is shown in (**a**). 10 µl samples of the loading material, column flowthrough and peak fractions A9, A13 and B8 (indicated by arrows) were electrophoresed through duplicate 18 % SDS-polyacrylamide gels and transferred onto nitrocellulose, overnight at 10V (Section 2.3.4). One nitrocellulose membrane was stained using Ponceau-S and imaged digitally using the LAS-1000 imaging system (Fuji), shown in (**b**). The other nitrocellulose membrane was immunoblotted using an H2A antibody (Section 2.3.4; Table 2.12). This identified H2A-NLS in the loading material and peak fraction A9. Chemiluminescence was used for visualisation (Pierce, Table 2.14) and the image captured digitally using 'chemiluminescence' settings on the LAS-1000 imaging system (Fuji) is shown in (**c**). Fractions A7 – A10 were pooled and lyophilised for assembly into octamers.

The octamer assembly reactions were dialysed (MWCO 6000 – 8000 Da, Spectra/Por® membrane, flat width 10 mm, Spectrum Laboratories) overnight against three changes of Refolding buffer (containing 2.2 M NaCl; see Table 2.4 and Section 2.4.2.3) and thereafter concentrated to a volume around 1 ml (Centricon filter, YM-10, Amicon). Histone octamers were purified using gel filtration chromatography (HiLoad 16/60 Superdex 200 prep grade column, Pharmacia) in Refolding buffer, as described before (Section 2.4.2.3; Table 2.4). The

eluate was monitored at 276 nm and the chromatograms for both H2A-containing octamers and H2A-NLS-containing octamers are shown in Figure 6.4.

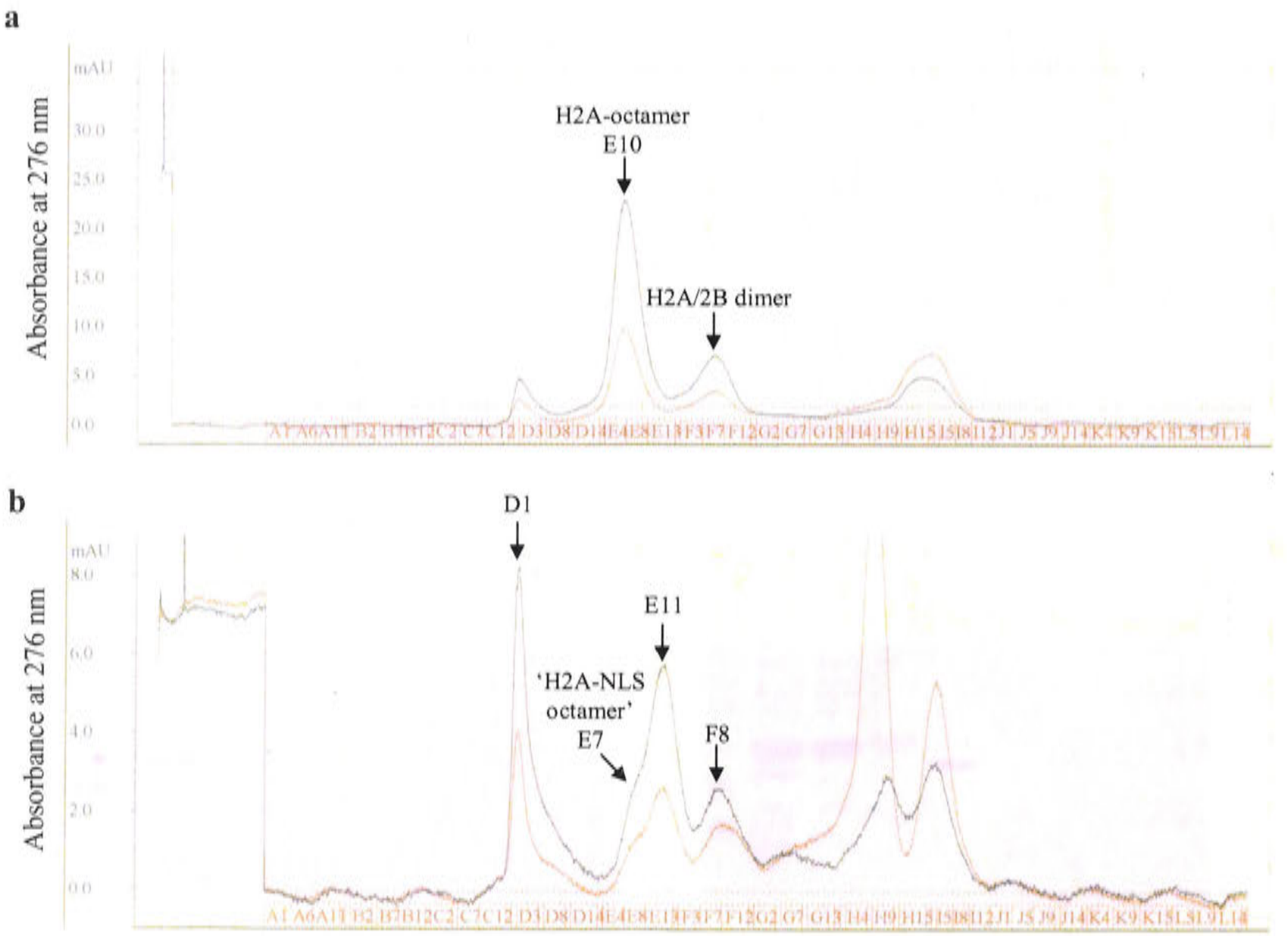

Figure 6.4. Analysis of H2A- and H2A-NLS-octamer assembly reactions by gel filtration chromatography. Product profiles from H2A- and H2A-NLS-octamer assemblies (see text and Section 2.4.2.3 for details) are shown in (**a**) and (**b**), respectively. Chromatography was performed using a HiLoad 16/60 Superdex 200 prep grade column (Pharmacia) in Refolding buffer (see Table 2.4) at 4°C. Chromatograms were generated at absorbance 276 nm and fractions of 1 ml were collected every minute. Peaks corresponding to the octamer and excess H2A/2B are labelled on the chromatogram. Fraction for analysis by SDS-PAGE are also labelled.

The chromatogram representing H2A-octamer assembly was typical of previously assembled H2A-containing octamers, displaying the characteristic peaks corresponding to the octamer and excess H2A/2B dimer (Figure 6.4a; compare Figure 4.4b and c). The peak corresponding to H2A-containing octamer was symmetrical. This indicated the absence of excess H3/4 tetramer and that an equimolar association of the constituent histones had occurred. The chromatogram of the H2A-NLS-octamer assembly product differed greatly from that of the H2A-octamer. Based on the elution volume of the H2A-octamer, the peak corresponding to the H2A-NLS-containing octamer was a leading shoulder (indicated in Figure 6.4b). This suggested that a small amount of H2A-NLS-octamer may have formed, but the main peak would comprise excess H3/4 tetramer.

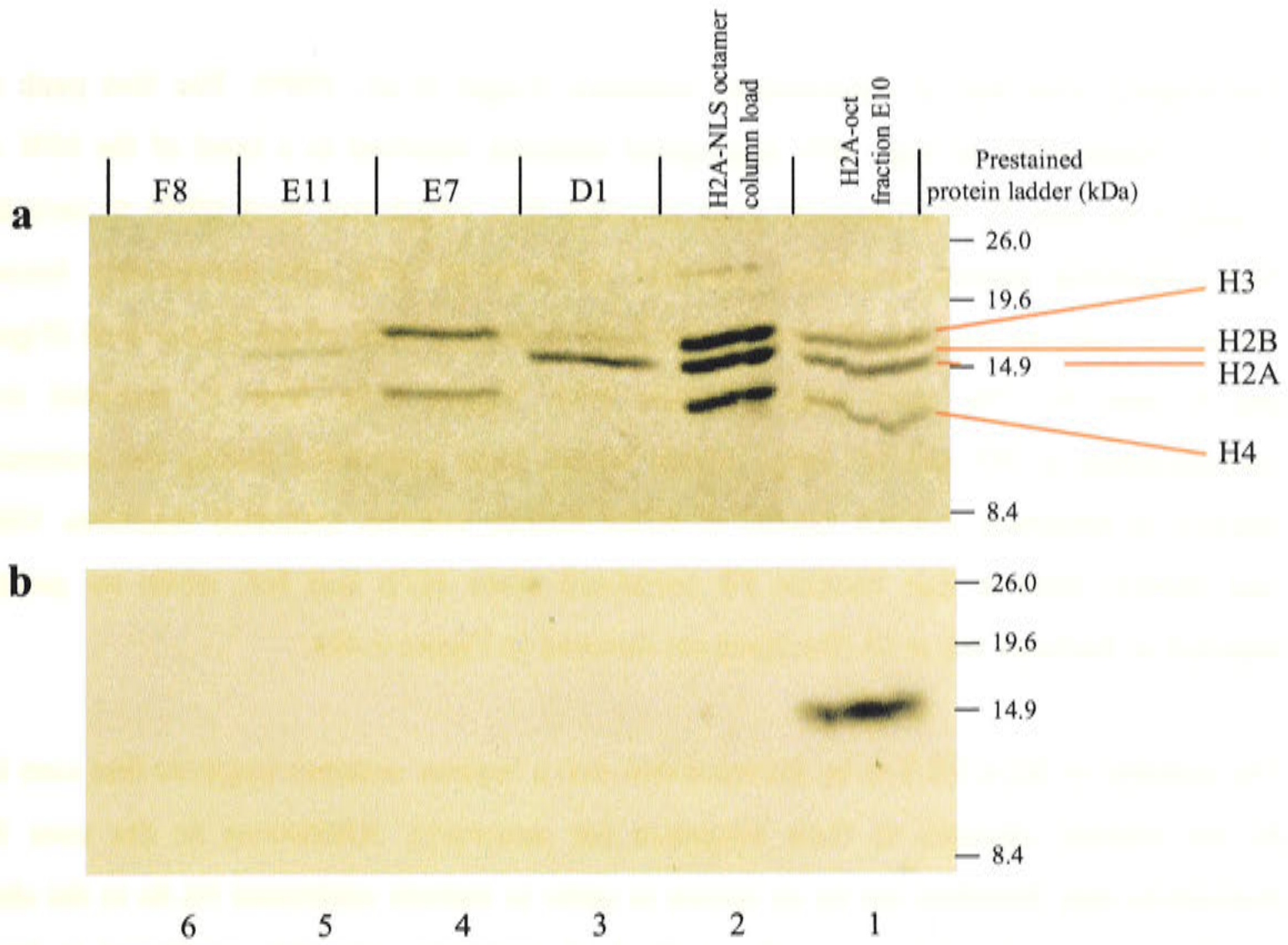

Figure 6.5. SDS-PAGE analysis of the H2A-NLS octamer purification. Fractions D1, E7, E11 and F8 corresponding to peaks on the H2A-NLS chromatogram were analysed by 18 % SDS-PAGE and immunoblotting using an antibody directed against H2A, essentially as described in the legend to Figure 6.3. The Coomassie blue stained SDS-PAGE analysis and corresponding chemiluminescent visualisation of antibody reactivity are shown in (**a**) and (**b**), respectively. The antibody positive control was H2A-containing octamer from fraction E10 of the parallel H2A-octamer reconstitution (Figure 6.4a). The FPLC fractions are denoted according to the chromatographic trace in Figure 6.4b.

The 18 % SDS-PAGE analysis revealed that the peak corresponding to fraction E10 of the chromatographic trace shown in Figure 6.4a contained equimolar amounts of the constituent histones (Figure 6.5a, lane 1), implying assembly of the H2A-containing octamer. The presence of H2A in the purified H2A-containing octamer fraction was confirmed by immunoblotting using an antibody directed against H2A (Figure 6.5b, lane 2). Indeed, immunoblotting analysis of the fractions corresponding to peaks on the H2A-NLS chromatogram revealed that the H2A-NLS-containing octamer had not formed in a quantity greater than the detection limit of the analysis procedure (Figure 6.5b). The immunoblot analysis failed to detect H2A-NLS in any of the fractions analysed from the H2A-NLS-containing octamer assembly (Figure 6.5b, lanes 3 – 6). Furthermore, the SDS-PAGE analysis showed that the material loaded onto the gel filtration column containing the post-dialysis assembly reaction of the H2A-NLS-octamer appeared to comprise H2B, H3 and H4, with only a faint band corresponding in MW to H2A-NLS (Figure 6.5a, lane 2). This anomaly was unexpected since all the constituent histones in the assembly reaction were measured to equimolarity by absorbance at 276 nm prior to dialysis. Since H2B, H3 and H4 were clearly present, it appears that H2A-NLS may have precipitated out of solution during the dialysis or subsequent concentration procedures rather than incorporate into an octamer. Perusal of the H2A-NLS octamer assembly reaction chromatographic profile revealed

concordance with that of unassembled octamers (Luger *et al.*, 1999). The first peak fraction (D1), corresponding to high MW aggregated material, resolved to a band of the MW of H2B (Figure 6.5a, lane 3). The shoulder peak (fraction E7), which was most likely to include H2A-NLS-containing histone octamers, revealed no material. This was presumably because the amount of material was insufficient to reach the detection limit of the stains used (Figure 6.5a and b, lane 4). The next peak (fraction E11; Figure 6.5a, lane 5) resolved to bands corresponding to H3 and H4 only, which would have associated during the octamerisation reaction as tetramers; a result typical of failed histone octamer assembly reactions. Other gels (not shown) showed that fraction F8 contained some H2B and H4, while no protein was detected in fractions H6 or I3 (fractions are denoted in Figure 6.4b).

The inability of H2A-NLS to be incorporated into a histone octamer suggests that core histones do not tolerate changes to their sequence (or structure). Alterations to the core histones themselves may therefore not be an option in order to include additional NLSs in the chromatin constructs using the octamer transfer method of chromatin assembly employed in this study. However, this may still be a viable option if the NLS-modified histones are to be used as DNA-carriers in their own right (Fritz *et al.*, 1996).

6.2.2. The effect on transfection efficiency of direct coupling of NLSs to the reporter plasmid

6.2.2.1. Coupling of the NLS peptide to pGeneGrip-RFP using a PNA-maleimide linker

In an alternative approach to enhance the nuclear uptake properties of the chromatin constructs, the pGeneGrip-RFP plasmid was coupled to the optimised T-ag NLS peptide. The NLS peptide was synthesised with and without an FITC group by K.N. McAndrew (Biomolecular Resource Facility, JCSMR) (see amino acid sequence in Figure 6.6a).

The NLS coupling procedure was achieved through exploitation of the GeneGrip™ site in pGeneGrip-RFP in two steps; firstly, attachment of a chemically reactive maleimide moiety to the plasmid and, secondly, reaction of maleimide with the N-terminal cysteine residue of the NLS peptide. The first step involved hybridisation of PNA-maleimide (PNA-maleimide labelling kit, Gene Therapy Systems) to the GeneGrip™ site, in a manner similar to the PNA-FITC labelling reaction described in Section 5.3.1 (see also Section 2.2.16.2.). Immediately following this reaction, cross-linking of the peptide to maleimide was carried out, following the manufacturer's instructions. The NLS peptide was incubated, at around 30-fold molar excess, with the PNA-maleimide labelled plasmid at 4°C overnight in 1 × Labelling buffer (provided in the PNA-maleimide labelling kit, Gene Therapy Systems). The molar excess of NLS results in

the formation of a covalent thioether bond between the PNA-maleimide and the free sulphydryl group of the terminal cysteine residue of the NLS peptide (Figure 6.6b). The bond formed is stable and irreversible. Unbound PNA-maleimide and peptide were removed by isopropanol precipitation of the plasmid DNA and washing in 70 % EtOH. Plasmid was resuspended in 1 × Labelling buffer (Gene Therapy Systems). This procedure was repeated to ensure removal of excess label. The modified plasmid was termed pGeneGrip-RFP-NLS. As the pGeneGrip™ plasmid has 8 binding sites within the GeneGrip™ region for the hybridisation of PNA labels, potentially 8 NLS peptides may be coupled to the plasmid. The fluorescein-conjugated NLS peptide was coupled to pGeneGrip-RFP in exactly the same manner.

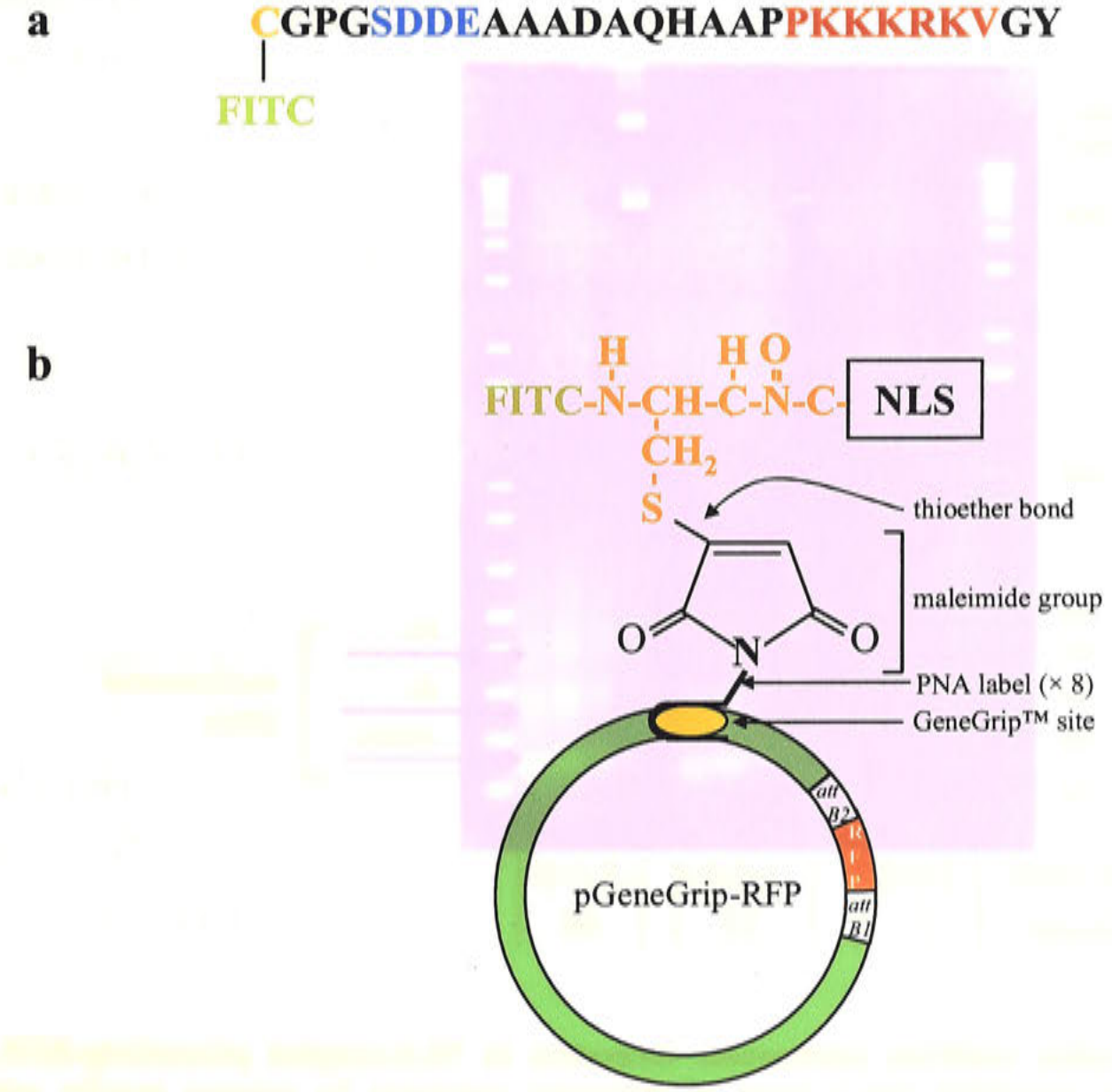

Figure 6.6. Conjugation of an NLS peptide to pGeneGrip-RFP. An optimised SV40 T-ag NLS-containing peptide was coupled to pGeneGrip-RFP using PNA-maleimide as a linker. The optimised T-ag NLS peptide, in single-letter amino acid code is shown in (**a**), with the T-ag NLS coloured in red, the nuclear-import-enhancing protein kinase CK2 site in blue and the terminal cysteine residue which through its free sulphydryl group facilitates binding to the maleimide-PNA molecule in orange. An FITC group (in green) was attached to the N-terminal amine of the cysteine residue within the NLS peptide to form NLS-FITC. The conjugate, pGeneGrip-RFP-NLS is shown in (**b**). PNA-maleimide was hybridised to the GeneGrip™ site of pGeneGrip-RFP (PNA-maleimide labelling kit, Gene Therapy Systems; Section 2.2.16.2.). Reaction between the sulphydryl group of the terminal cysteine residue (in orange) of the NLS peptide and the reactive maleimide group facilitates the formation of a stable thioether bond. Note that the GeneGrip™ sequence contains 8 consecutive sites for the hybridisation of PNA-labels; only one label is represented.

6.2.2.2. Assembly of pGeneGrip-RFP-NLS into chromatin constructs

The plasmid, pGeneGrip-RFP-NLS (± FITC), was reconstituted into chromatin with H2A-containing histone octamers. Chromatin constructs comprising 0, 1, 4, 25 and 40 molar ratios of octamer to DNA were generated using the octamer transfer salt dialysis procedure (described in Section 2.5.2). Digestion of the chromatinised constructs with MNase (Section 2.5.5) revealed the characteristic digestion-resistance pattern corresponding to the formation of nucleosomes (see Figure 6.7 for chromatinised pGeneGrip-RFP-NLS MNase digestion; identical results were obtained in the presence of the NLS-FITC label). This demonstrated that attachment of the PNA-maleimide-NLS (± FITC) did not hinder chromatinisation of the plasmids.

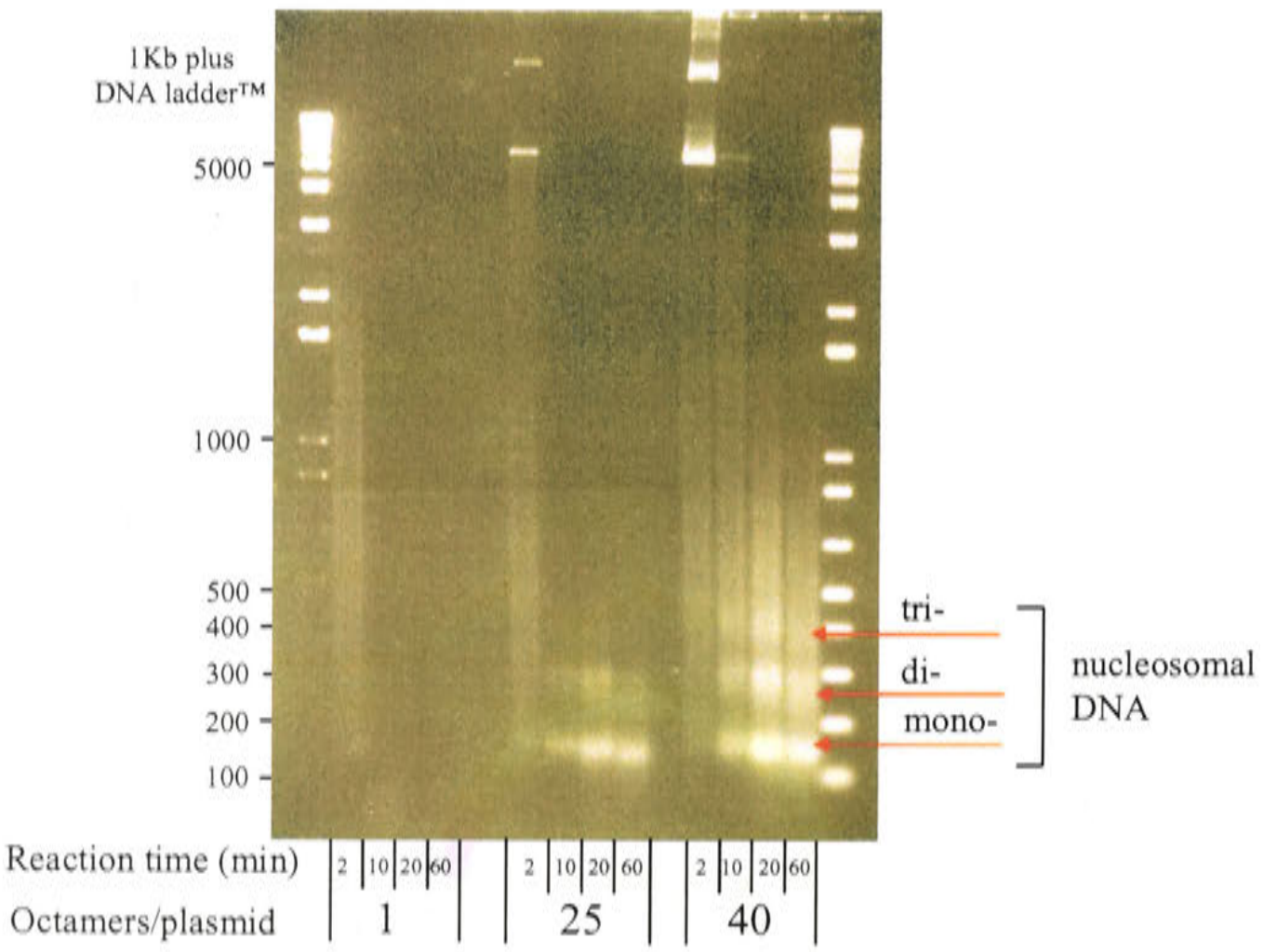

Figure 6.7. MNase digestion confirms nucleosome formation in NLS-coupled pGeneGrip-RFP. pGeneGrip-RFP-NLS was assembled into a range of chromatin constructs by octamer transfer salt dialysis (Section 2.5.2) and subjected to MNase digestion (Section 2.5.5) to verify chromatinisation. Agarose gel electrophoresis analysis (1.5 % agarose; 100 V) of the MNase reaction is shown. The stoichiometries of histone octamers to plasmid DNA are denoted for each of the chromatin constructs. Bands corresponding to nucleosomal DNA are indicated in red.

6.2.2.3. Transfection efficiency of chromatinised pGeneGrip-RFP is altered in the presence of NLSs

Aliquots of the differentially chromatinised NLS-coupled constructs containing 1 µg of plasmid DNA were prepared for transfection using Lipofectamine™ 2000 into cultured HTC and Cos-7

cells, along with non-NLS coupled pGeneGrip-RFP, as described previously (Section 2.7.2). Flow cytometry was used to detect RFP-expressing cells (channel FL2) 48 hours post-transfection (Section 2.9.1.2). FACS dot plot analysis quadrants were set relative to 'negative' transfections performed with no DNA and to cells which had been transfected with pGeneGrip-RFP only (0 octamers/plasmid, non-NLS), known to express RFP. The FACS dot plots for Cos-7 transfected cells are shown in Figure 6.8a. Data were analysed in two ways. In order to ascertain the effect of chromatinisation on the transfection efficiency of the reporter plasmid, data were analysed relative to the 0 octamers/plasmid-NLS transfections. Collated data for Cos-7 and HTC cells are presented in histogram format in Figure 6.8b. In order to ascertain the effect of the NLSs on the transfection efficiency of the chromatin constructs *per se*, data were analysed relative to control transfections with 0 octamers per plasmid (non-NLS). This data is presented in Table 6.1.

Table 6.1. Comparison of the relative percentages of cells expressing RFP from chromatin constructs in the absence and presence of coupled NLS peptides.

Octamers /plasmid	Cos-7 (relative % RFP expressing cells) [A]				HTC (relative % RFP expressing cells) [A]			
	No NLS [B]	n	NLS	n	No NLS [B]	n	NLS	n
0	100 ± 0	9	44.4 ± 6.6	6	100 ± 0	8	45.1 ± 20.1	3
1	89.5 ± 15.1	9	71.3 ± 11.0	3	71.6 ± 18.7	7	ND[C]	3
4	98.9 ± 11.1	3	39.9 ± 8.3	3	122.1 ± 34.5	3	42.1 ± 22.1	3
25	53.1 ± 8.7	9	54.2 ± 11.0	6	19.2 ± 2.4	7	27.4 ± 4.7	3
40	36.7 ± 7.4	6	34.6 ± 4.9	3	17.8 ± 2.1	4	ND	3

pGeneGrip-RFP-NLS was assembled into chromatin constructs at the stoichiometries indicated in the table using the octamer transfer salt dialysis method (Section 2.5.2). Constructs were transfected into Cos-7 and HTC cells by lipofection (Section 2.7.2). RFP-expressing cells were determined by FACS (channel FL2) relative to RFP-negative 'no DNA' transfections (Section 2.9.1.2). Data were analysed using CellQuest software (Macintosh).
[A] Results are expressed relative to the percentage RFP-expressing cells in the 0 octamers/plasmid control transfections (no NLS) as the mean ± SEM. n indicates the number of times experiments were performed.
[B] Results for 'no NLS' are from the series of experiments reported in Table 4.3.
[C] Not done.

Unexpectedly, the proportion of RFP expressing cells from the NLS-coupled 0 octamers per plasmid transfections decreased significantly to around 50% that of transfections with the non-NLS 0 octamers per plasmid (Table 6.1; Cos-7 cells, $p < 0.001$; HTC cells, $p = 0.002$). However, there was no significant difference in the percentages of cells expressing RFP within

the series of differentially chromatinised NLS-coupled constructs in Cos-7 or HTC cells (Figure 6.8). The reduction in percentages of cells expressing RFP that had been observed with increasing plasmid chromatinisation to the level of 40 octamers per plasmid in the absence of the extrinsic NLSs (Table 4.3) appeared to be abrogated in the presence of the NLS peptides (Figure 6.8b; Table 6.1).

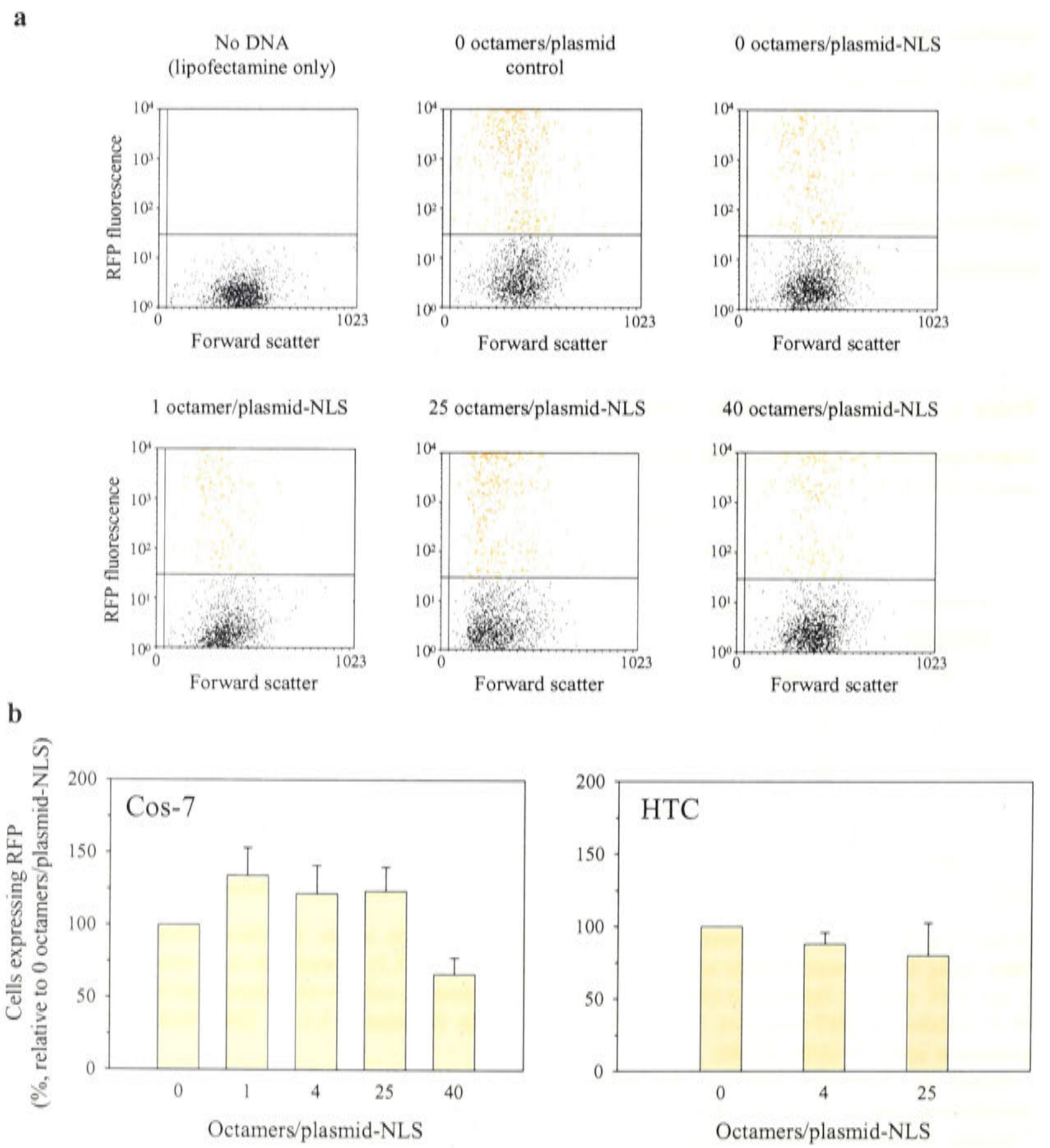

Figure 6.8. RFP expression is insensitive to increasing degrees of chromatinisation of the reporter plasmid when coupled to NLSs. Cos-7 and HTC cells were transfected with a range of chromatinised NLS-coupled pGeneGrip-RFP constructs, as indicated, using Lipofectamine™ 2000 (Section 2.7.2). Cells expressing RFP were quantitated by FACS (channel FL2) 48 hours post-transfection and data were analysed using CellQuest software (Macintosh) (Section 2.9.1.2). Typical FACS dot plots of Cos-7 cells showing the density of RFP-expressing cells for transfection of a range of NLS-coupled chromatin constructs is shown in (**a**). Quadrants were set relative to the 'no DNA' transfection and the known RFP-positive control, 0 octamers/plasmid. RFP-positive cells are represented within the upper right quadrant, coloured in red. Collated data for Cos-7 and HTC cells are represented in histogram format in (**b**). Each bar represents the mean of at least 3 experiments ± SEM. Data is presented relative to the NLS-coupled non-chromatinised reporter plasmid (0 octamers/plasmid-NLS). See also Table 6.1.

Thus, while the incorporation of NLSs via the GeneGrip™ site did not enhance the number of cells expressing the reporter gene relative to the non-NLS chromatinised plasmids *per se*, transfection efficiency in Cos-7 and HTC cells did, however, appear to be rendered insensitive to the degree of chromatinisation.

6.2.2.4. Nuclear accumulation of the chromatinised pGeneGrip-RFP-NLS-FITC constructs

Experiments analogous to those described in Section 5.3.2 were performed with fluorescein-conjugated T-ag NLS peptide in order to relate the proportion of RFP expressing cells to the proportion of nuclei that had taken up the NLS-coupled chromatin constructs. Briefly, NLS-FITC-coupled pGeneGrip-RFP that had been assembled into chromatin constructs at stoichiometries of 0, 4 or 25 histone octamers per plasmid (see Section 6.2.2.2) were prepared in equivalent aliquots containing 1 µg of plasmid DNA for each transfection into Cos-7 and HTC cells (Lipofectamine™ 2000; Section 2.7.2). Transfected cells were incubated for 48 hours for optimum expression of RFP, as carried out previously. Following this, cells for each transfection were divided into two aliquots for separate analysis of whole cell RFP fluorescence and nuclear FITC-fluorescence using FACS (Section 2.9.1).

The number of whole cells expressing RFP were quantitated (channel FL2, as described in Section 2.9.1.2; Figure 6.9a) in the first aliquot of cells, relative to 'negative control' cells transfected with no DNA (Lipofectamine only) and to 'positive control' cells which had been transfected with pGeneGrip-RFP (0 octamers/plasmid, non-NLS).

Nuclei were isolated from the second aliquot of cells (see Section 2.8 for detailed methodology). The number of nuclei positive for FITC fluorescence were determined (channel FL1, as described in Section 2.9.1.3; Figure 6.9b) relative to isolated nuclei from 'FITC-negative control cells' transfected with the NLS-coupled non-chromatinised construct (0 octamers per plasmid-NLS; prepared as described in Sections 6.2.2.1 and 6.2.2.2) and to isolated nuclei from 'FITC-positive control cells' transfected with the FITC-coupled non-chromatinised construct (0 octamers per plasmid-FITC; prepared as described in Section 5.3.1). Representative FACS dot plot are shown in Figure 6.9b.

Nuclei data were analysed in two ways, as described in the previous section. Data were normalised relative to cells transfected with 0 octamers per plasmid-NLS-FITC in order to ascertain the effect of increasing degrees of chromatinisation on the nuclear accumulation of the reporter plasmid with coupled T-ag NLSs (Figure 6.9c). Data were also normalised relative to cells transfected with FITC-coupled 0 octamers per plasmid (non-NLS, naked) in order to

ascertain the effect of the NLSs on nuclear accumulation of the chromatin constructs *per se* (presented in Table 6.2).

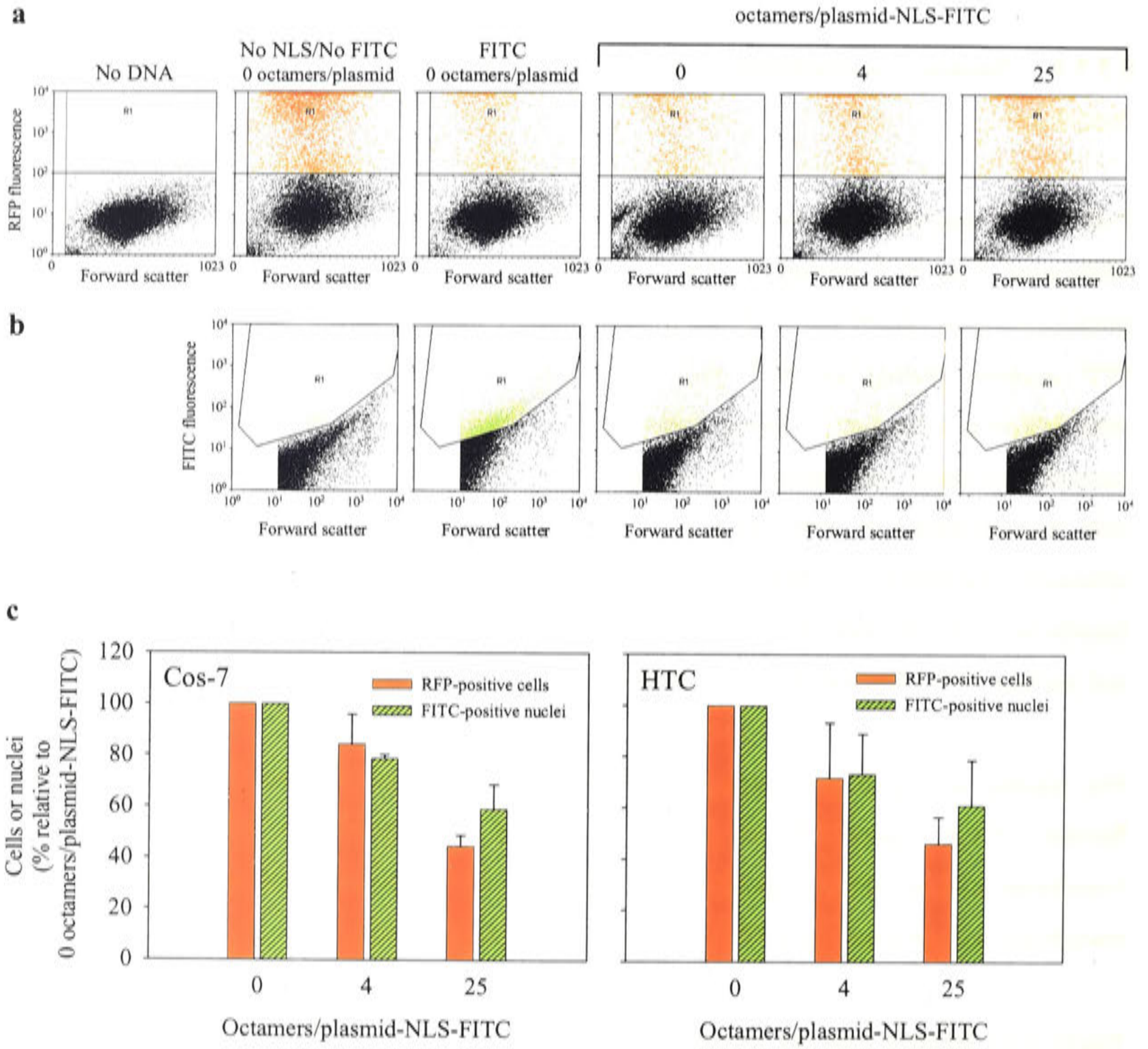

Figure 6.9. Nuclear accumulation of NLS-coupled chromatin transfection constructs and corresponding RFP expression. Cos-7 and HTC cells were transfected with fluorescein-conjugated NLS-coupled pGeneGrip-RFP assembled into chromatin at stoichiometries of 0, 4 and 25 histone octamers per plasmid (see Sections 2.7.2, 2.2.16.2 and 2.5.2, respectively). Cells were harvested 48 hours post-transfection and were divided into 2 aliquots for whole cell analysis of RFP expression and isolated nuclei analysis of FITC by FACS (Section 2.9.1; channels FL2 and FL1, respectively). FACS dot plots of Cos-7 cell transfections are shown. Whole cells analysed for RFP expression are shown in panel (**a**). Quantitation was relative to the 'no DNA negative control' transfection and to the 0 octamers/plasmid (No NLS/No FITC) 'RFP-positive control transfection'. RFP-positive events are represented within the upper right quadrant, R1, coloured in red. Isolated nuclei analysed for FITC are shown in panel (**b**). Quantitation was relative to the 'No NLS/No FITC' 0 octamers/plasmid 'FITC-negative control' transfection and to the 'FITC' 0 octamers/plasmid 'FITC-positive control' transfection. FITC-positive events are represented within the region marked, R1, coloured in green. Collated data for Cos-7 and HTC cells are represented in histogram format in (**c**). Red bars represent RFP-positive cells; shaded green bars represent FITC-positive nuclei. Data is presented as a percentage of cells or nuclei relative to transfections with the FITC-NLS-coupled plasmid (0 octamers/plasmid-NLS-FITC). Each bar represents the mean of 3 experiments ± SEM. See also Table 6.2.

Table 6.2. Comparison of the relative percentages of cells expressing RFP and nuclei accumulating the FITC-labelled chromatin constructs with and without coupled NLSs.

	Cos-7							
	Relative % RFP-positive cells[A]				Relative % FITC-positive nuclei[B]			
Octamers /plasmid	No NLS[D]	n	NLS	n	No NLS	n	NLS	n
0	100 ± 0[C]	5	57.5 ± 10.9[C]	2	100 ± 0	5	43.4 ± 17.5	3
4	58.8 ± 5.9	2	41.5 ± 6.2	2	64.7 ± 18.6	2	33.9 ± 14.7	3
25	20.2 ± 7.2	5	23.4 ± 5.9	2	59.3 ± 13.4	5	28.3 ± 9.8	3
	HTC							
	% RFP-positive cells				**% FITC-positive nuclei**			
Octamers /plasmid	No NLS	n	NLS	n	No NLS	n	NLS	n
0	100 ± 0	3	49.7 ± 7.2	3	100 ± 0	3	47.7 ± 17.5	3
4	52.1 ± 5.7	3	33.3 ± 6.1	3	65.9 ± 10.9	3	46.4 ± 11.3	3
25	4.9 ± 2.8	3	21.9 ± 3.2	3	40.8 ± 11.8	3	36.1 ± 8.8	3

The table shows data for two sets of chromatin constructs. Data marked 'No NLS' represents chromatin constructs reconstituted using the FITC-coupled pGeneGrip-RFP plasmid. Data marked 'NLS' represents chromatin constructs reconstituted using the FITC-NLS-coupled pGeneGrip-RFP plasmid.

Cos-7 and HTC cells were transfected by lipofection as described in Section 2.7.2. 48 hours post-transfection, cells were divided into two aliquots for analysis by FACS (see Section 2.9.1) of whole cells and isolated nuclei (see Section 2.8).

[A] % RFP-positive cells were quantitated by FACS (channel FL2) relative to RFP-negative transfections in the absence of DNA (lipofectamine only).

[B] % FITC-positive nuclei were quantitated by FACS (channel FL1) relative to FITC-negative '0 octamers per plasmid' transfections.

[C] All results are expressed relative to FITC-coupled 0 octamers per plasmid transfections (no NLS, non-chromatinised). The number of times the experiment was performed is represented by n. Results represent the mean ± SEM. Where n is 2, the mean ± range/2 is shown.

[D] Results for 'no NLS' are from experiments reported in Table 5.1.

Compared to the FITC-labelled naked plasmid (0 octamers per plasmid-FITC) 60 % fewer nuclei accumulated the FITC-NLS-coupled naked plasmid (0 octamers per plasmid-NLS-FITC) (Table 6.2). The reduction was significant in HTC nuclei ($p = 0.046$, $n = 3$) and approaching significance in Cos-7 nuclei ($p = 0.085$, $n = 3$). This might explain the reduced levels of cells expressing RFP observed in transfections with the FITC-NLS-coupled 0 octamers per plasmid control construct relative to transfections with the non-NLS FITC-labelled 0 octamers per plasmid control construct in both Cos-7 (57.5 ± 10.9 %, $n = 2$) and HTC cells (49.7 ± 7.2 % $n = 2$) (Table 6.2; see also Table 6.1). Comparison of the relative percentages of nuclei that had accumulated the chromatin constructs in the presence of the NLSs revealed no statistically significant difference between the 0 and 25 octamers per plasmid constructs in Cos-7 ($p =$

0.149) nor HTC cells (p = 0.597; Figure 6.9; Table 6.2). This was in contrast to the nuclear accumulation data for the non-NLS reporter plasmid constructs, where a significant reduction (Cos-7, p = 0.038; HTC, p = 0.04) was seen upon increased chromatinisation of the reporter plasmid (see Table 5.1; Table 6.2).

At the level of more extensive chromatinisation with a nucleosome density of 25 octamers per plasmid, although there appeared to be a ~ 2-fold difference between the relative percentages of nuclei that had accumulated the non-NLS and NLS-coupled constructs, this difference was not statistically significant. At this level of chromatinisation (25 octamers per plasmid), the relative percentages of RFP-positive cells and FITC-positive nuclei were similar in the presence of coupled NLSs (Cos-7, p = 0.74; HTC, p = 0.2; Table 6.2; Figure 6.10). This was in contrast to the results obtained from cells transfected without coupled NLSs, where greater percentages of nuclei accumulated the constructs than cells that expressed RFP (Cos-7, p = 0.032; HTC, p = 0.041; see Table 5.1; Figure 6.10).

These results suggest that the presence of the NLSs coupled to the plasmid did not enhance nuclear import of the chromatin constructs and, in fact, appeared to have reduced transfection efficiency overall.

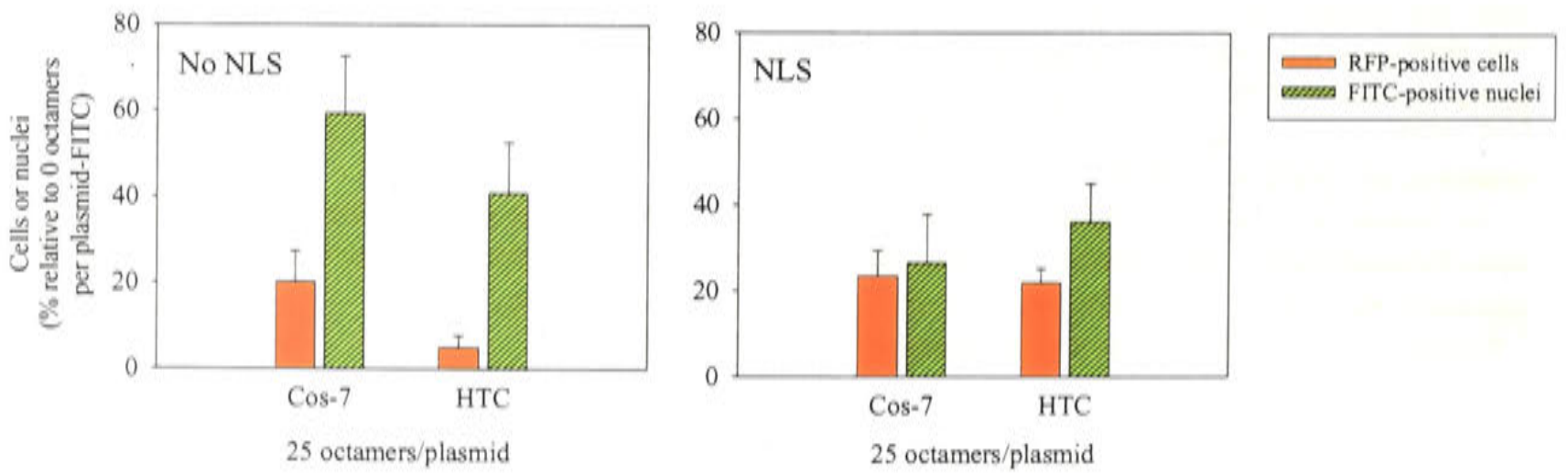

Figure 6.10. The proportion of cells expressing RFP relative to the proportion of nuclei accumulating the 25 octamers per plasmid construct are similar in the presence of coupled NLSs. Relative percentages of whole cells expressing RFP and isolated nuclei accumulating the 25 octamers per plasmid construct are compared in the absence and presence of coupled NLS peptides in Cos-7 and HTC cells, as indicated. The red bars represent RFP-positive cells and the shaded green bars represent FITC-positive nuclei. Results are expressed as the percentage of cells or nuclei relative to 0 octamers per pGeneGrip-RFP-FITC transfections. Bars represent 5 experiments in the 'No NLS' and 2 - 3 experiments in the 'NLS' group. Results are tabulated in Tables 5.1 and 6.2.

6.3. INVESTIGATING MEANS TO ENHANCE THE TRANSCRIPTIONAL PERMISSIVENESS OF THE CHROMATINISED REPORTER PLASMID

Two approaches having the aim of enhancing transgene expression by facilitating transcription of the chromatinised reporter plasmids are described in this section. Firstly, chromatin was assembled using H2AZ-containing histone octamers, which might create transcriptionally primed regions of chromatin (Fan *et al.*, 2002). Secondly, since the pGeneGrip-RFP model may not be a universal indicator of transfection efficiency using chromatinised plasmids, a different expression system containing an endogenous promoter, namely GMCSF, able to recruit transcription complexes in GMCSF-specific Jurkat cells (Himes *et al.*, 1993) was investigated.

6.3.1. Transfection of chromatin constructs assembled with octamers containing the variant histone H2AZ

6.3.1.1. Assembly of pGeneGrip-RFP into chromatin with H2AZ-containing histone octamers

H2AZ-containing octamers, in which recombinant H2AZ (mouse) had been substituted for H2A within the reconstituted histone core particle [2(H2AZ/H2B)/($H3_2$/$H4_2$)], were provided by Dr J-Y. Fan (Chromatin and Transcriptional Regulation Group, JCSMR). The pGeneGrip-RFP plasmid was assembled into chromatin constructs with stoichiometries of 1, 4, 25 and 40 H2AZ-octamers per plasmid (using the octamer transfer by salt dialysis method; see Section 2.5.2). As done previously, sample containing only pGeneGrip-RFP was included also to serve as the naked plasmid control (0 octamers per plasmid) in the transfection experiments. The formation of chromatin was verified using the MNase digestion assay (described in Section 2.5.5), which revealed the presence of nucleosomal DNA fragments (Figure 6.11; see Figure 4.8 for comparison with H2A-containing chromatin constructs).

6.3.1.2. Reporter gene expression in Cos-7 and HTC cells transfected with H2AZ-chromatin constructs

Chromatin constructed using the H2AZ-containing histone octamer at stoichiometries of 0, 1, 4, 25 and 40 octamers per plasmid were prepared for lipofection in 1 µg DNA aliquots (Section 2.7.2). In addition, aliquots of 1 µg of pGeneGrip-RFP were prepared under non-chromatinising conditions (as described previously; Section 4.5.2) with the amount of H2AZ-containing histone octamer corresponding to that in each of the chromatin constructs. The resulting H2AZ-octamer/DNA 'associations' were a means to determine the role of the histone octamers on gene expression independent of a chromatinisation effect (as had been determined for the chromatin

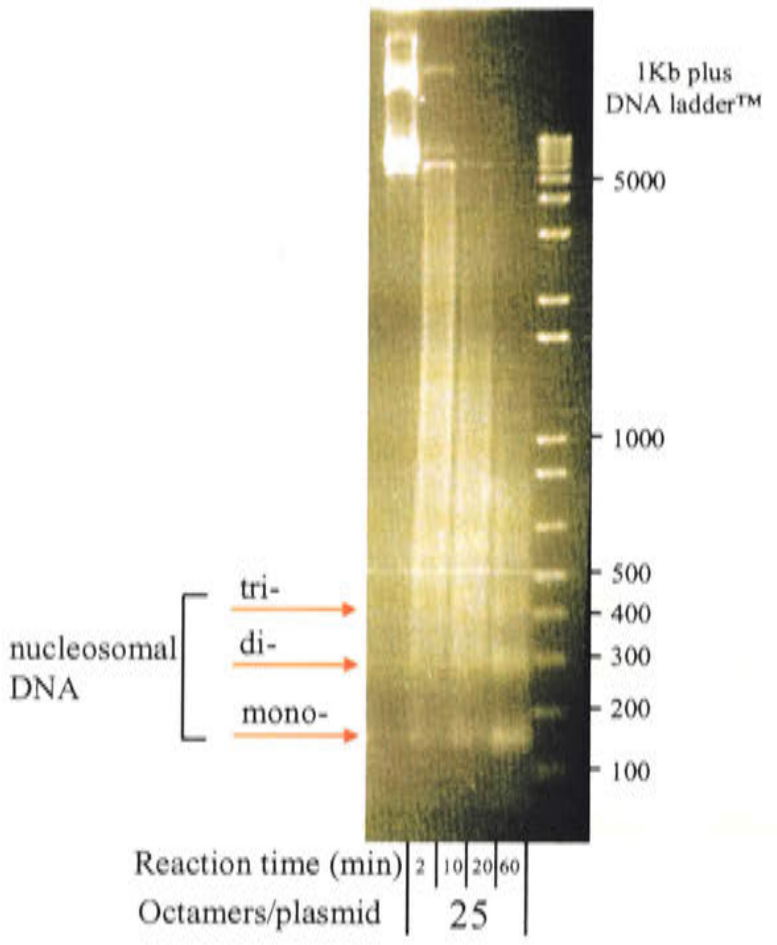

Figure 6.11. MNase digestion of chromatin constructs assembled with H2AZ-octamers. pGeneGrip-RFP was reconstituted into chromatin with H2AZ-containing histone octamers at various stoichiometries using the octamer transfer salt dialysis method, as described in Section 2.5.2. MNase digestion was carried out (100 mU/DNA sample; Section 2.5.5) and samples were electrophoresed through 1.5 % agarose at 90 V, followed by EtBr staining and destaining in ddH_2O, before visualisation under UV light. MNase digestion is shown for the H2AZ-containing construct reconstituted at a stoichiometry of 25 octamers per plasmid. The presence of bands corresponding to nucleosomal DNA (indicated in red) confirmed the formation of chromatin using the H2AZ-containing octamer.

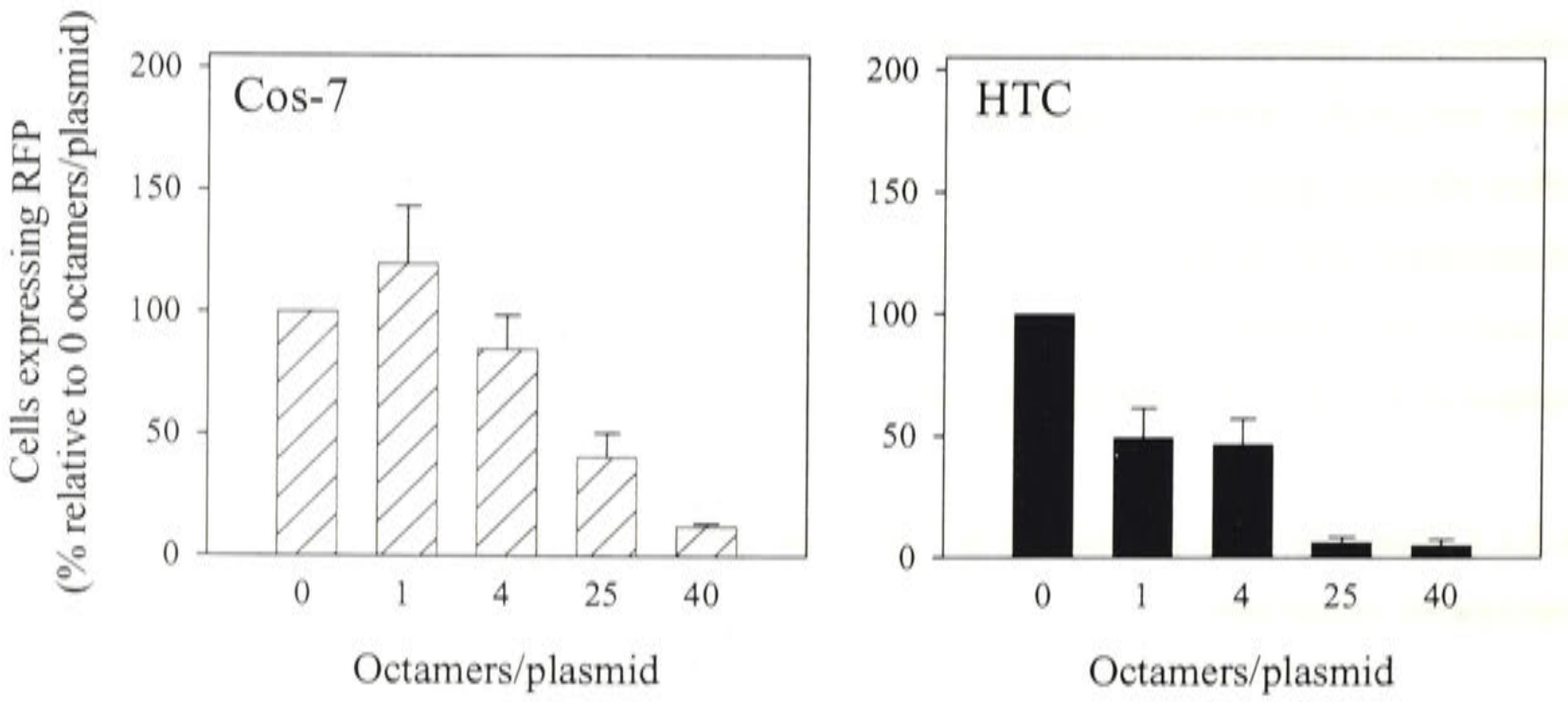

Figure 6.12. RFP expression in Cos-7 and HTC cells transfected with chromatinised constructs containing H2AZ-octamers. Chromatin constructs comprising 0, 1, 4, 25 and 40 H2AZ-octamers per plasmid (assembled as described in Section 2.5.2) were transfected into Cos-7 and HTC cells using Lipofectamine™ 2000 (Section 2.7.2). RFP expression was determined by FACS 48 hours after transfection (channel FL2) and raw data were analysed using CellQuest software for Macintosh (Section 2.9.1.2). Percentages of cells expressing RFP are presented relative to cells transfected with the 0 octamers per plasmid control construct. Each histogram represents the mean of at least 3 experiments with SEM, except for the 4 octamers per plasmid construct in Cos-7 cells which represents the mean ± range/2. Collated data is presented in Table 6.3

constructs comprising histone octamers containing H2A; Sections 4.5.2 and 4.6.2). HTC and Cos-7 cells (plated into 6-well tissue culture plates at a density of 1×10^5 cells per well 24 hours prior to transfection) were transfected using Lipofectamine™ 2000 (see Section 2.7.2 for methodology). The number of cells expressing RFP was determined by FACS 48 post-transfection, as described previously (Section 2.9.1.2).

Consistent with the trend observed using the chromatin constructs prepared from H2A-containing octamers, the percentage of RFP-expressing cells decreased concomitantly with increasing nucleosome densities in the H2AZ-containing chromatin constructs in both of the cell lines tested (Figure 6.12; Table 6.3).

In Cos-7 cells, a 2-fold reduction in RFP positive cells was observed when transfected with the 25 octamers per plasmid construct relative to the 0 octamers per plasmid naked construct ($p = 0.004$, $n = 5$). The relative percentages of RFP-expressing cells were reduced a further 3-fold when the 40 octamers per plasmid construct was transfected ($p = 0.03$, $n = 3$). Chromatin-induced suppression of transfection efficiency was more pronounced in HTC than in Cos-7 cells. A 2-fold reduction in the percentage of HTC cells expressing RFP was observed upon transfection of 1 octamer per plasmid chromatinised construct ($p = 0.05$, $n = 2$). The percentages of RFP positive cells were significantly reduced for all of the remaining stoichiometries of H2AZ-containing octamers relative to the naked plasmid ($p \leq 0.05$).

Transfection of the DNA/H2AZ-octamer-associated plasmids produced a pattern of RFP-expressing cells, relative to the extent of octamer density, similar to that seen for the DNA/H2A-octamer 'associations' (Figure 6.12; Table 6.3). In Cos-7 cells, a statistically significant reduction in the proportion of cells expressing RFP relative to the naked plasmid (0 octamers per plasmid) was observed at the level of association of 40 octamers per plasmid ($p = 0.04$, $n = 2$). In HTC cells the relative number of RFP-expressing cells was reduced significantly when both 25 and 40 octamers were associated per reporter plasmid ($p = 0.01$, $n = 3$; $p = 0.05$, $n = 3$, respectively). The DNA/H2AZ-octamer 'associations' corresponding to lower levels of octamer density yielded populations of RFP-expressing cells not significantly different from those obtained upon transfection of the naked plasmid.

The relative percentages of RFP-expressing cells when transfecting chromatin assembled with H2A-containing octamers are compared to when transfecting chromatin assembled with H2AZ-containing octamers in Table 6.3. In Cos-7 cells, the proportion of RFP-positive cells was significantly different only at the level of the 40 octamers per plasmid, with the H2AZ-chromatin transfection being significantly lower than H2A-chromatin ($p = 0.004$). In HTC cells, transfections with H2AZ-chromatin constructs yielded significantly fewer relative numbers of

Table 6.3. Relative percentages of cells expressing RFP transfected with H2A and H2AZ-chromatin constructs.

	H2A-containing chromatin constructs [A]				H2AZ-containing chromatin constructs			
	Cos-7	n	HTC	n	Cos-7	n	HTC	n
Octamers/plasmid								
0	100 ± 0	7	100 ± 0	7	100 ± 0	5	100 ± 0	3
1	82.9 ± 18.6	7	71.6 ± 18.7	7	119.8 ± 23.5	5	49.3 ± 12.1	3
2	78.4 ± 8	3	78.6 ± 22.2	3	ND[C]		ND	
4	98.9 ± 11.1	3	122.1 ± 34.5	3	84.8 ± 14.0	2	46.4 ± 10.7	3
25	58.8 ± 10.2	7	19.2 ± 2.4	7	40.4 ± 10.2	5	6.3 ± 2.3	3
40	43.5 ± 9.3	4	17.8 ± 2.1	4	12.2 ± 1.2	3	5.2 ± 2.5	3
plasmid + 1 oct[B]	97.8 ± 9.9	6	138.0 ± 23.8	7	109.8 ± 5.1	4	114.4 ± 14.9	3
plasmid + 2 oct	97.3 ± 12.6	3	114.7 ± 53.2	3	ND		ND	
plasmid + 4 oct	92.3 ± 17.1	3	102.2 ± 45.8	3	119.1 ± 3.6	2	91.6 ± 8.6	3
plasmid + 25 oct	60.1 ± 15.9	7	93.7 ± 15.8	7	82.4 ± 11.6	5	31.7 ± 8.0	3
plasmid + 40 oct	49.9 ± 5.2	3	74.2 ± 6.2	4	15.6 ± 11.6	2	34.2 ± 15.4	3

Chromatin constructs assembled with either H2A-containing or H2AZ-containing histone octamers (see Section 2.5.2 for method) were transfected into Cos-7 and HTC cells using lipofection (see Section 2.7.2). Cells expressing RFP were detected by FACS 48 hours post transfection (channel FL2H, see Section 2.9.1.2) and analysed using CellQuest software (Macintosh). The number of times the experiment was performed is represented by n. Values shown reflect the percentage of RFP positive cells, expressed relative to 0 octamers per plasmid, and represent the mean ± SEM. Where n is 2 the mean ± range/2 is shown.

[A] Data presented was taken from Table 4.3.

[B] Constructs comprising histones associated with plasmid DNA were generated under non-chromatinising conditions at the stoichiometries indicated. Transfections using the plasmid/histone octamer 'associations' were performed in paired experiments with the chromatinised constructs.

[C] Not done.

RFP-expressing cells than transfections with H2A-chromatin for the 25 - ($p = 0.01$) and the 40 octamers per plasmid chromatinised constructs ($p = 0.01$).

The results showed that, overall, the trend of transfection efficiency was similar when the reporter plasmid was chromatinised or 'associated' with either H2A-containing histone octamers or H2AZ-containing histone octamers. At higher levels of nucleosome density (25 and 40 octamers per plasmid, see Table 6.3) H2AZ-octamer chromatinisation and 'association' appeared to reduce the pool of RFP-positive cells even further than that observed with transfections comprising the H2A-containing octamers.

6.3.2. Investigation of the effect of plasmid chromatinisation in a transgene expression system driven by an endogenous promoter

6.3.2.1. Assembly of pGMCSF-1(2)TK-luc+ into chromatin

The plasmid pGMCSF-1(2)TK-luc+ (referred to as pGMLuc, see Table 2.9; Himes *et al.*, 1993), which includes a luciferase reporter gene under the control of a fragment of the human GMCSF promoter region (– 620 to + 37; Figure 6.13a), was kindly provided by K. Bunting (Cytokine Gene Expression Laboratory, JCSMR). A large scale bacterial culture was prepared and plasmid was purified (Qiagen MaxiPrep kit, see Section 2.2.2).

On the basis of physiological nucleosome density, pGMLuc was calculated to be saturated with 26 histone octamers (6.1 kb, at 1 nucleosome per 230 bps). Chromatin constructs comprising 1, 2, 4 and 26 octamers per plasmid were thus generated, as described previously (with H2A-containing histone octamers, using the octamer transfer salt dialysis method; see Section 2.5.2). The pLuc plasmid was also subjected the dialysis procedure but in the absence of histone octamers in order to generate the naked plasmid (0 octamers per plasmid), used as the reference construct from which to determine the baseline expression of luciferase. Assembly into chromatin was verified by the appearance of nucleosomal DNA using the MNase digestion assay (Figure 6.13b, see Section 2.5.5 for methodology).

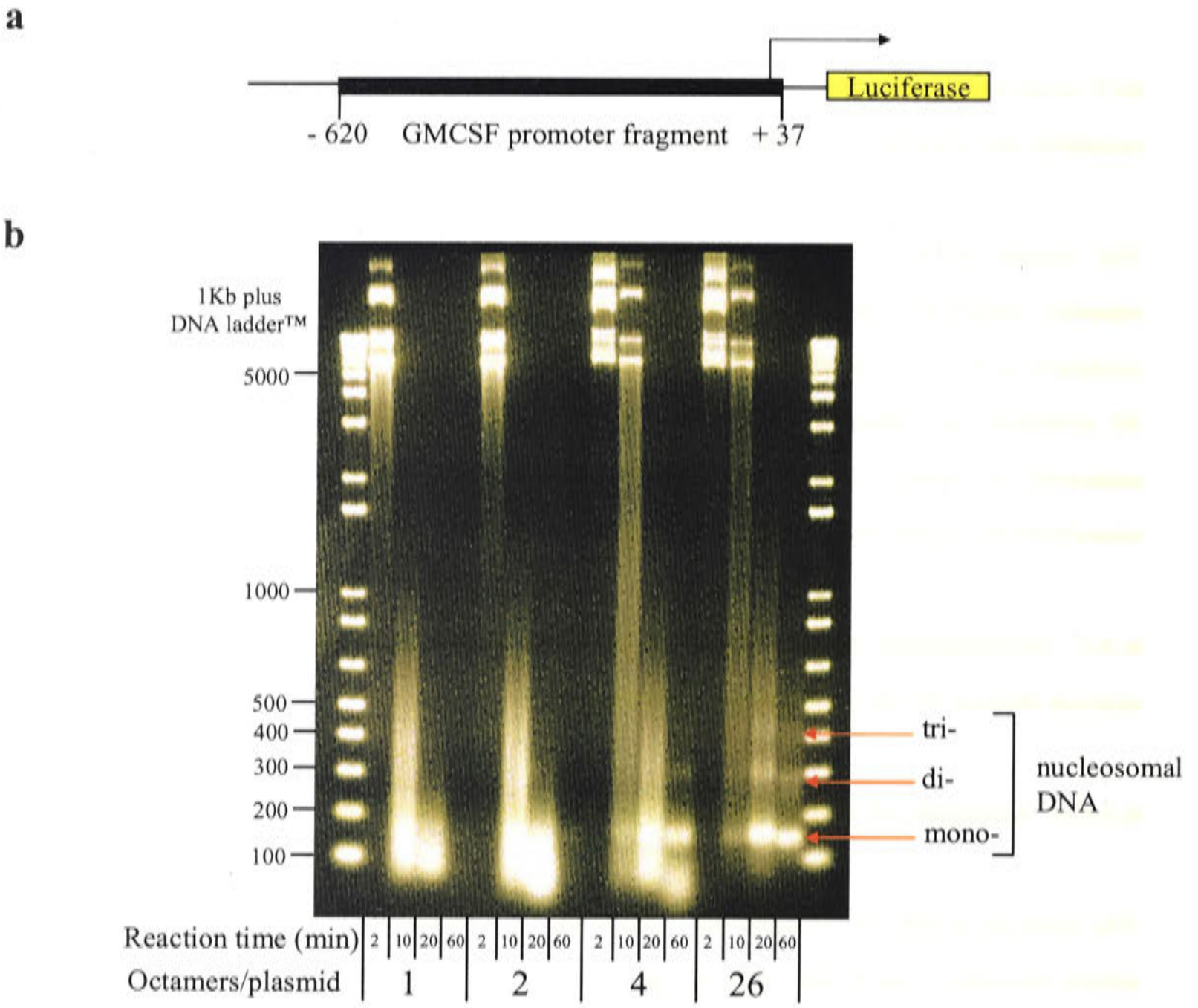

Figure 6.13 Assembly of the luciferase reporter plasmid pGMCSF-1(2)TK-luc+ into chromatin. The promoter and reporter gene region of pGMCSF-1(2)TK-luc+ is shown in (**a**), comprising the – 620 to + 37 fragment of the human GMCSF promoter region and the luciferase reporter gene. pGMLuc was assembled into chromatin at stoichiometries of 1, 2, 4 and 26 histone octamers per plasmid using the octamer transfer salt dialysis method (described in Section 2.5.2). Samples of 4 µg of DNA were digested with MNase (100 mU per sample; Section 2.5.5) and analysed by gel electrophoresis through 1.5 % agarose at 90 V. The EtBr-stained agarose gel visualised under UV light is shown in (**b**). Bands corresponding to nucleosomal DNA are denoted in red.

6.3.2.2. A preliminary comparison of the effect of chromatinisation on transgene expression from different expression systems

Jurkat cells were prepared on the day of transfection by seeding at 5×10^5 cells per well in 24-well tissue culture plates and were transfected with the naked (0 octamers per plasmid) and chromatinised pGMLuc constructs (containing 1 µg of DNA) using Lipofectamine™ 2000 (see Sections 2.7.2 and 2.9.2). The pharmacological stimuli phorbol-12-myristate-13-acetate (PMA) and calcium ionophore were added to the cells to final concentrations of 20 ng/ml and 1 µM, respectively, between 30 and 34 hours post-transfection. Cells were incubated for a further 8 hours before quantitation of luciferase reporter gene expression. Luciferase activity was determined using the luciferase assay (described in Section 2.9.2), conducted according to the

method of Himes and Shannon (2000). The results were normalised relative to the luminescence produced from transfection of the naked plasmid (0 octamers per pGMLuc).

The pGeneGrip-RFP plasmid was assembled in parallel into chromatin constructs with stoichiometries of 0, 1, 4 and 25 histone octamers per plasmid (Section 2.5.2). These were transfected into Jurkat cells under the same conditions as described above, in the absence and presence of the pharmacological stimuli. RFP-expressing cells were analysed 48 hours post transfection, as described in Section 2.9.1.2. In order to facilitate the comparison of transgene expression between the pGeneGrip-RFP and pGMLuc plasmids, the total RFP fluorescence was determined from the FACS-generated data (rather than the percentage of cells expressing RFP as had been determined previously; CellQuest software, Macintosh). Results were normalised relative to the total fluorescence observed from transfection with the naked plasmid (0 octamers per pGeneGrip-RFP).

Transfection of the chromatinised pGMLuc contstructs yielded a pattern of luciferase activity (luciferin conversion) that was insensitive to the degree of chromatinisation as, relative to the naked reference plasmid (0 octamers per pGMLuc), no significant difference was observed in transgene expression for any of the pGMLuc chromatin constructs (Figure 6.14, Table 6.4).

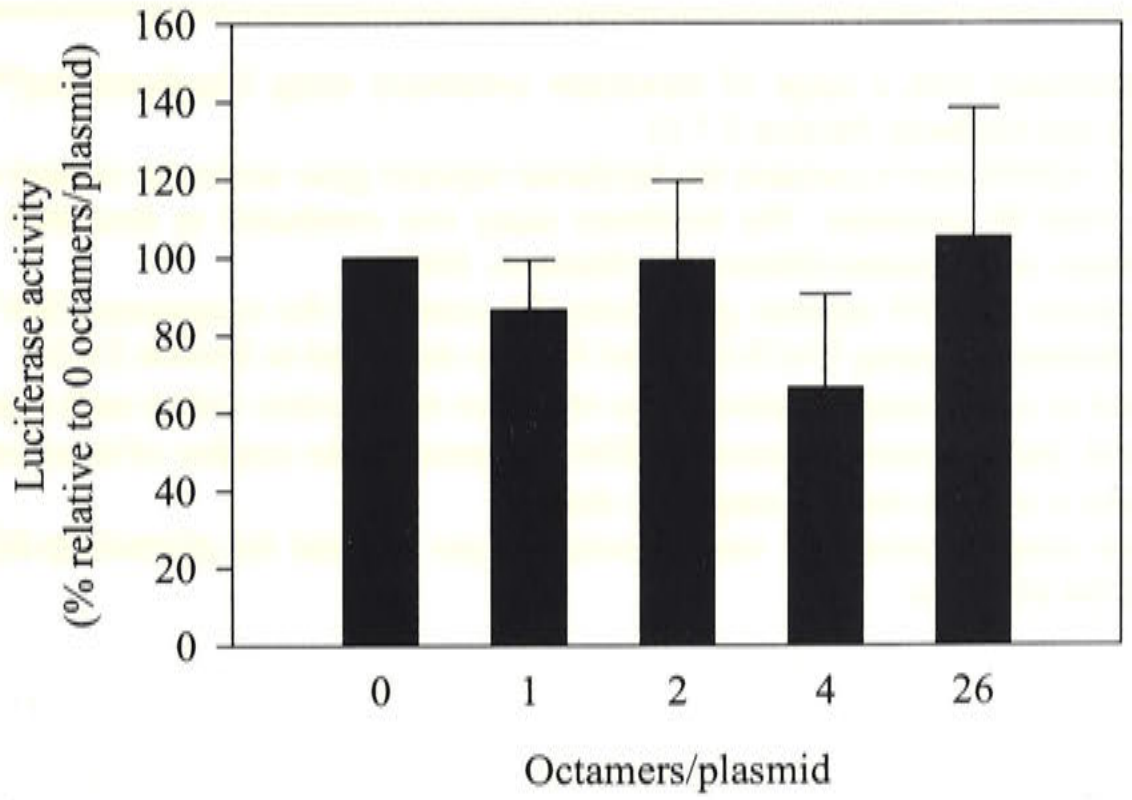

Figure 6.14. Transgene expression under the control of a tissue-specific promoter is resistant to chromatinisation. pGMLuc constructs, chromatinised at the stoichiometries indictated, were transfected into Jurkat cells using Lipofectamine™ 2000 (see Sections 2.5.2 and 2.7.2 for the respective methods). The luciferase assay was performed as described in Section 2.9.2. Luciferase activity was determined 40 hours post-transfection. Results are normalised relative to 0 octamers per pGMLuc plasmid. Each histogram represents the mean ± SEM of at least 3 experiments, except for the 4 octamers/plasmid transfection which was performed twice and represents the mean ± range/2.

In contrast, the total fluorescence output of RFP in Jurkat cells was reduced 2-fold with transfection of pGeneGrip-RFP which had been chromatinised at the higher level of nucleosome density (25 octamers per plasmid, $p = 0.006$, $n = 4$) compared to the naked plasmid (Table 6.4). This was in the absence of the pharmacological stimuli for transcription, PMA and calcium ionophore (Table 6.4). This trend was observed also in the presence of the pharmacological stimuli (Table 6.4). These results were consistent with the results that had been obtained with transfection of the chromatinised pGeneGrip-RFP constructs in Cos-7 and HTC cells (Table 4.3).

Table 6.4. Comparison of reporter gene expression in Jurkat cells transfected with chromatin constructs comprising of different transgene expression systems.

	pGMLuc [A]		pGeneGrip-RFP [B]			
Octamers/plasmid	% Luciferase activity [C]	n	Unstimulated % total RFP fluorescence [C]	n	Stimulated % total RFP fluorescence [C]	n
0	100.0 ± 0.0	4	100 ± 0	5	100	1
1	86.5 ± 12.8	4	84.2 ± 9.3	5	101.6	1
2	99.3 ± 20.2	3	122.1 ± 16.5	2	ND [E]	1
4	66.5 ± 24.0	2	158.6 ± 20.3	2	ND	1
25/26 [D]	105.2 ± 33.1	4	46.8 ± 7.6	4	21.3	1

Jurkat cells were transfected with a range of chromatin constructs using Lipofectamine™ 2000 (as described in Materials and Methods, Section 2.7.2).

[A] pGMLuc (pGMCSF-1(2)TK-luc+) contains the luciferase reporter gene under the control of the cell-specific endogenous GMCSF promoter. The luciferase assay was conducted as described in Section 2.9.2, according to Himes and Shannon (Himes and Shannon, 2000).

[B] pGeneGrip-RFP contains the RFP reporter gene under the control of the exogenous CMV promoter. RFP expression was determined using FACS (channel FL2) as described in Section 2.9.1.2.

[C] Results are presented as a percentage relative to the reference transfection within each experiment of 0 octamers per plasmid, and represent the mean ± SEM. n represents the number of times experiments were performed. Where n is 2, the mean ± range/2 is shown.

[D] The level of histone octamer saturation was 25 octamers per plasmid for pGeneGrip-RFP and 26 octamers per plasmid for pGMLuc.

[E] Not done.

Transgene expression using the pGMLuc plasmid was not hindered even by high levels of chromatinisation, whereas transgene expression using the pGeneGrip-RFP plasmid was significantly hindered at similar degrees of chromatinisation. One main difference between the two expression constructs is that transgene expression using pGMLuc is under the control of the Jurkat cell-specific GMCSF promoter, while transgene expression using pGeneGrip-RFP is

under the control of the exogenous viral CMV promoter. These results may imply, therefore, that gene expression under the control of an endogenous cell-specific promoter is not encumbered by increased levels of chromatinisation.

6.4. DISCUSSION

In this chapter, the two strategies investigated with the aim to enhance the transfection efficiency of the chromatinised plasmids, namely the incorporation of additional NLSs and the potentiation of transcription, are described.

Conjugation of extrinsic NLS to the chromatinised plasmid has the potential to improve nuclear uptake efficiency and, hence, transgene expression. Consequently, the aim was to incorporate the SV40 T-ag-derived optimised NLS peptide into the delivery vehicle as a fusion with the DNA-binding component of the chromatin transfection construct (the histone octamer) and coupled to the DNA itself. Of the NLSs documented to date, the SV40 T-ag NLS has been the most extensively investigated and, in the context of enhancing nuclear import of gene delivery constructs, the most frequently used (Escriou *et al.*, 2003; Cartier and Reszka, 2002; Bremner *et al.*, 2001).

In order to incorporate the NLS into the histone octamers, a C-terminal H2A-T-ag NLS fusion protein was generated. The expression and purification of H2A-NLS proved to be highly problematical due to frequent failure of the *E. coli* strain to express the protein in sufficient quantities. Moreover, the H2A-NLS fusion protein did not incorporate together with H2B, H3 and H4 into an octamer under the standard octamerisation conditions used and came out of solution during the dialysis step of the procedure (Section 6.2.1.4). Other recombinant histones with modifications to either their N- or C-termini, or variant forms of histones such as the H2A variant H2A-Bbd, have not only been found to be problematic to purify but, also, frequently do to not form octamers readily using the method of chromatin assembly described in this thesis (see Luger *et al.*, 1997; personal communications, Drs J-Y. Fan and J. Zhou, Chromatin and Transcription Regulational Group, JCSMR). This may be attributed to the critical functionality of the histone tail regions in nucleosome stability, reflected in the high sequence conservation across species (Luger and Richmond, 1998). In order to reconstitute chromatin using histones that will not form octamers *in vitro*, more intricate methods of assembly into chromatin are required which involve titration of the H2A/2B dimers and H3/4 tetramers onto the assembling DNA template (similar to the NAP-1 based method described in Section 2.5.1). These methods are better suited to small scale reconstitution of DNA into chromatin, in the order of less than 1

µg, but become cumbersome in the large scale reconstitutions required for this study (~ 50 µg DNA).

Using the GeneGrip™ technology (Gene Therapy Systems), the T-ag NLS peptide was coupled to pGeneGrip-RFP via a PNA-maleimide linker (Figure 6.6). Surprisingly, compared to transfections with the non-NLS-coupled plasmid, the conjugated NLSs appeared to reduce the proportion of cells expressing the reporter gene to around 60 %. While several studies have reported little or no enhancement of gene expression upon covalent attachment of exogenous NLSs to the plasmid (Roulon *et al.*, 2002; Ciolina *et al.*, 1999; Neves *et al.*, 1999a; Sebestyen *et al.*, 1998), one other study has also reported a similar decrease in expression (50 - 60 %; Ciolina *et al.*, 1999). This result, however, was obtained upon conjugation of 43 NLSs to the plasmid (6 NLSs/1 kb); the authors suggesting that the covalent association of so many peptides at random sites throughout the plasmid might have inhibited gene transcription. In the experiments described in this Chapter, the number of RFP-expressing cells was not reduced in the presence of the PNA-maleimide linker at the GeneGrip™ site (83.3 ± 6.8 %, n = 2, relative to non-maleimide-coupled pGeneGrip-RFP; Cos-7 cells; data not shown). This suggests that the reduction in the proportion of RFP-positive cells was not due to inhibition of gene expression as a result of the labelling process. Moreover, the use of fluorescein-conjugated NLS-coupled plasmids to monitor nuclear uptake demonstrated that the number of nuclei that took up the NLS-coupled plasmid was reduced to around 50 % relative to that of the non-NLS plasmid. This could indeed account for the reduction in reporter gene expression observed.

Interestingly, in the presence of NLSs, the relative proportions of cells expressing RFP were similar upon transfection of the differentially chromatinised constructs (Tables 6.1 and 6.2). This was in contrast to the pattern observed in the absence of NLSs, where the relative proportions of RFP-expressing cells decreased upon increasing chromatinisation of pGeneGrip-RFP (Tables 4.3). The relative number of nuclei that took up the transfection constructs chromatinised at higher nucleosome densities (25 octamers per plasmid) was not enhanced by the exogenous T-ag NLSs. Contrary to the findings in the absence of the NLS (Table 5.1), similar percentages of isolated nuclei showed FITC fluorescence as cells that showed RFP fluorescence. One possible reason for this effect may derive from the proximity of the GeneGrip™ site to the reporter gene (the PNA-labelling site lies ~ 400 bps upstream of the RFP reporter gene). While pGeneGrip-RFP-NLS assembly into chromatin was verified by the presence of nucleosomes (Figure 6.7), the positioning of those nucleosomes is not controlled using the octamer transfer by salt dialysis method. It may be possible that the binding of multiple PNA-maleimide-NLS (± FITC) moieties at the GeneGrip™ site disrupted the pattern of nucleosome positioning at or near the reporter gene. This might, consequently, have

increased the transcriptional permissiveness of the transgene region (Ng *et al.*, 1997; Hansen and Wolffe, 1992; Izban and Luse, 1992). In order to investigate whether the conjugated NLS peptides indeed brought about alteration of nucleosome positioning at the reporter gene, further studies involving DNA footprinting and *in vitro* transcription assays (Ng *et al.*, 1997; Hansen and Wolffe, 1992; Izban and Luse, 1992) would be required. A mutated or reversed form of the NLS peptide, known to be devoid of nuclear import functionality, was not included in this study as the sequence specificity of this NLS had been demonstrated previously (Chan and Jans, 2001; Chan *et al.*, 2000; Chan and Jans, 1999). In hindsight, inclusion of this peptide in the chromatin constructs might have been able to elucidate whether the (unexpected) reduction in the number of nuclei that took up the constructs was specific to the NLS peptide sequence or simply due to conjugation of a peptide *per se*.

In light of the results, the degree of accessibility of the coupled NLSs to importin α/β within the chromatin constructs is difficult to assess. Due to prohibitive amounts of the NLS-coupled constructs required to quantitate importin binding affinity using the ELISA method employed in this study, this could not be determined and transfection efficiency was employed instead as a measure of NLS functionality. By deduction, if the NLSs were not accessible, patterns of nuclear accumulation and reporter gene expression similar to those observed in the absence of NLSs could be expected (Table 5.1). Due to the similar nuclear accumulation levels of the differentially chromatinised NLS-coupled constructs (Table 6.2), it is tempting to suggest that the NLSs were equally accessible to importins in all the constructs. Importin-mediated nuclear import is non-restrictive to size and would therefore allow the naked and chromatinised plasmids to accumulate to similar degrees. The fact that 50 % fewer nuclei accumulated the naked NLS-coupled plasmid compared to the naked non-NLS plasmid suggests that nuclear uptake may have been inhibited by the presence of the conjugated peptide. The reason for this is unclear.

Based on the postulate that H2AZ-chromatin would generate a more transcriptionally permissive DNA template (Fan *et al.*, 2002), the reporter plasmid was assembled into chromatin with histone octamers that included H2AZ (in place of the usual H2A). Reporter gene expression from the constructs chromatinised at higher nucleosome densities (25 and 40 octamers per plasmid) appeared to be even more inhibited with H2AZ-chromatin than with H2A-chromatin (Table 6.3). This implied that the use of H2AZ-containing histone octamers did not improve the transcriptional permissiveness of the chromatinised reporter plasmid to a significant degree. In an attempt to explain these results in light of the approaches used in the Fan study (Fan *et al.*, 2002), sedimentation velocity ultracentrifugation was carried out (as described in Section 4.4.1). The H2AZ-containing chromatin construct assembled at 25

octamers per plasmid yielded an *s*-value of 64 *S* (not shown). Interestingly, this *s*-value was similar to that of the H2A-containing chromatin construct assembled at 40 octamers per plasmid (66 *S*; see Table 4.1). Indeed, perusal of Table 6.3 shows that similar proportions of cells express RFP for the 25 H2AZ-octamers per plasmid and 40 H2A-octamers per plasmid transfections. The *s*-value suggests, amongst other properties, a high nucleosome density, which in turn has been associated with transcriptional repression *in vitro* (Sandaltzopoulos *et al.*, 1994; Hansen and Wolffe, 1992). This may account for the comparatively lower levels of RFP expression observed for the 25 H2AZ-octamers per plasmid construct compared to the 25 H2A-octamers per plasmid construct.

It was considered possible that the results obtained with the pGeneGrip-RFP transgene expression system used might not be typical and hence another expression system was investigated. Luciferase activity was similar for the GMCSF promoter-containing reporter constructs chromatinised at low and high nucleosome densities. In contrast, the expression of the RFP transgene in Jurkat cells from the differentially chromatinised pGeneGrip-RFP reporter constructs replicated the trends observed in Cos-7 and HTC cells (Table 4.3). The GMCSF promoter/Jurkat cell system was chosen because the GMCSF promoter has the ability to recruit appropriate chromatin remodelling complexes in Jurkat cells which overcome transcriptional repression that occurs due to the presence of nucleosomes occluding the reporter gene region (Rao *et al.*, 2001; Himes *et al.*, 1993). The level of transgene activity observed using the pGMLuc plasmid may be a reflection of this ability. The poor level of RFP transgene expression using the pGeneGrip-RFP plasmid may be a reflection of its inability to recruit transcription complexes efficiently in the cell lines tested. These results may implicate a transcriptional block as a likely contributor to the poor level of RFP reporter gene expression observed upon chromatinisation of the pGeneGrip-RFP plasmid.

These comparisons between the two gene expression systems, however, are made cautiously as two different assays for reporter gene expression and two different reporter plasmids were used (even though the plasmids were of similar size and expression of the reporter genes was determined after similar durations). Nonetheless, this preliminary result may provide the basis from which to initiate a future study which may prove to have exciting implications for promoter-driven cell-specific expression of transfection constructs. Future work may involve constructing the pGeneGrip-RFP plasmid containing the GMCSF promoter and, conversely, the pGMLuc plasmid containing the CMV promoter. Transfection into Jurkat cells would enable the direct comparison of the effect of chromatinisation on transgene expression between the different plasmids. Another interesting series of experiments would be to investigate the importance of cell-specificity; for instance, transfection of the proposed GMCSF-containing

pGeneGrip-RFP into non-GMCSF-specific cells, such as Cos-7 and HTC. This might also address the question of whether the GMCSF promoter may be more active than the CMV promoter. Using fluorescein-labelled plasmids, the relationship between nuclear accumulation and reporter gene expression may be determined also. Furthermore, microinjection of the chromatinised GMCSF promoter-containing and CMV promoter-containing constructs directly into the nucleus would enable assessment of the ability of each promoter to recruit transcription complexes and may be a first step towards investigating whether the promoter region plays an important role in transgene expression.

CHAPTER 7

General Discussion

The ability to cure human disease at the genetic level is undeniably tantalising and, arguably, makes gene therapy one of the most exciting areas of experimental therapeutic research. The use of non-viral gene delivery vectors is not marred by the safety issues associated with the use of viral vectors, however viral-mediated gene delivery still represents the largest proportion of gene therapy trials. This is largely due to the superior transfection efficiency of viral vectors compared to non-viral vectors. One of the most significant hurdles in non-viral gene delivery is the efficient transfer of transfection constructs into the nucleus. The design of efficient non-viral gene delivery vectors with improved nuclear transfer capacity is therefore of paramount importance. With this in mind, the use of individual histones, which have inherent nuclear import properties, as DNA-carrier vehicles for gene delivery purposes has been evaluated previously (see Section 1.5.3). Although no real consensus was reached regarding the efficiency of each individual histone, as transfection outcomes appeared to be dependant on the cell types tested, results overall indicated that histones showed promise as gene transfer vehicles. The novel use of histones in the form of the histone core octamer assembled with plasmid DNA into chromatin to facilitate gene transfer is described in this thesis.

The fundamental hypothesis at the outset of this thesis was that chromatinisation of the gene delivery plasmid might have several features that could enhance the potential for gene transfer applications. It was proposed that the feature of DNA compaction would shield the DNA from degradation in the cytoplasm, accommodate the transfer of large plasmids and facilitate passage through the NE. In addition, histones were shown to be bound by the importin β nuclear transport protein with high affinity (see Section 3.2) and were subsequently shown to be transported into the nucleus along this importin-facilitated pathway (see Section 1.5.2). These findings suggested a definite basis for a gene delivery construct coupled to the nuclear import of histones as the nuclear import pathway could provide a conduit into the nucleus for DNA assembled with histones into chromatin. Furthermore, chromatin is the physiological form in which condensed DNA occurs *in vivo*. As mechanisms exist within the nucleus to de-condense chromatin into a readily transcribable form, the problems related to the inhibition of gene

expression when plasmid DNA is complexed with artificial compacting agents (Bielinska *et al.*, 1997; Zabner *et al.*, 1995) might be circumvented when the transfected plasmid is presented in a form recognisable by the nuclear transcription machinery.

The findings presented in this thesis suggest that chromatinisation of the reporter plasmid used in this study, pGeneGrip-RFP, does not provide a superior gene delivery vehicle. Chromatinisation of pGeneGrip-RFP was demonstrated using several analytical techniques, including sedimentation velocity ultracentrifugation (that demonstrated quantitative association of histone octamers with the plasmid), a supercoiling assay (that demonstrated plasmid topology) and digestion with MNase (that demonstrated nucleosome formation). The assembled chromatin constructs were indeed expressed upon transfection into Cos-7 and HTC cells but increasing the levels of chromatinisation of the reporter plasmid reduced the proportion of cells that expressed the transgene. This observation could be related in part to reduced nuclear accumulation of the transfection constructs that was observed at the more extensive levels of chromatinisation (see Section 5.3.2). Furthermore, the nuclear accumulation data suggested that gene expression was repressed at higher levels of chromatinisation (Section 5.3.2).

Several strategies were tested with the aim of improving the poor outcome transfection efficiency. As the DNA-induced structure within the chromatin constructs abolished binding of importins to the intrinsic NLSs in the histones (see Section 5.4), these NLSs were unable to contribute to facilitated nuclear transport. The SV40 T-ag NLS peptide had been shown previously in a number of studies to enhance nuclear import and, hence, reporter gene expression when coupled to the transfection construct (for reviews see Escriou *et al.*, 2003; Cartier and Reszka, 2002; Bremner *et al.*, 2001). SV40 T-ag NLS peptides were therefore included as additional extrinsic NLSs in the chromatin constructs by coupling to the plasmid. Transfection efficiency of the chromatin transfection constructs was not enhanced with the inclusion of these NLS peptides (see Section 6.2.2.3 and 6.2.2.4).

In order to facilitate the transcriptional permissiveness of the chromatinised plasmid, pGeneGrip-RFP was assembled into chromatin using H2AZ-containing histone octamers since H2AZ-chromatin has been associated with less compact, transcriptionally poised chromatin fibres (Fan *et al.*, 2002). The suppression of reporter gene expression observed with extensive H2A-chromatinisation, however, persisted with H2AZ-chromatin.

In this study, reporter gene expression had been investigated principally using the pGeneGrip-RFP plasmid, under control of the CMV promoter. As the discrepancy between the proportions of nuclei that had accumulated the transfected constructs at high levels of chromatinisation and

cells that expressed the transgene had brought to light the possibility of transcriptional repression, an interesting prospect was the use of an endogenous promoter known to recruit transcription complexes in the context of cell-specific transgene expression. Interestingly, transgene expression using the GMCSF promoter in Jurkat cells was insensitive to chromatinisation. This was in contrast to transgene expression using the pGeneGrip-RFP plasmid in Jurkat cells. This result may have interesting implications for cell-specific gene delivery and may provide the basis for a new study.

In addition to previously documented limitations of non-viral gene delivery, including cytoplasmic degradation of the transfected DNA, endosomal sequestration and impaired nuclear import, the results of this thesis highlighted another limitation - the transcriptional permissiveness of the transfection constructs.

7.1. HITCHING A RIDE INTO THE NUCLEUS ALONG THE NUCLEAR IMPORT PATHWAYS OF HISTONES

The results presented in Chapter 3 were the first binding affinity data for importins and histones and suggested for the first time the primary role of importin β1 in the nuclear transport of the core histones (Johnson-Saliba *et al.*, 2000) as, previously, the 'conventional' importin α/β pathway had been predicted to mediate in the nuclear uptake of histones (Moreland *et al.*, 1987). The importin β1 binding affinities determined for various histones where high (in the range of 3 - 8 nM; Table 3.1) and were comparable to those reported for other importin β1 'substrates', such as PTHrP (2 nM, Lam *et al.*, 1999) and GAL4 (12 nM; Chan *et al.*, 1998). The high binding affinities were therefore not surprising considering that importin β1 is the subject of stringent competition, not only from conventionally α/β-translocated proteins, but also from the growing list of other importin β1-bound 'substrates' (Forwood and Jans, 2002; Forwood *et al.*, 2001a) and may also reflect the demand for histones in the nucleus.

Subsequent to the publication of the importin-histone binding affinity data (Johnson-Saliba *et al.*, 2000), several members of the importin β family were indeed shown to play a role in the nuclear transport of the core histones. The identity of these importins in vertebrate cells was established by affinity chromatography and subsequent gel analysis as importin β1, transportin, importin 5, importin 7 and importin 9 (Baake *et al.*, 2001b; Baake *et al.*, 2001a; Muhlhausser *et al.*, 2001). In yeast, transport of core histones was attributed primarily to Kap114p but also to 121p, 123p and 95p, which correspond to the mammalian importins importin 9, importin β3, importin β4 and importin β1, respectively (Mosammaparast *et al.*, 2002b; Mosammaparast *et al.*, 2001). In these studies, NLSs were identified in the amino-terminal tails of the histones.

The overall globular structure of the histones was also found to play a role in conferring nuclear localisation (Mosammaparast *et al.*, 2002b; Baake *et al.*, 2001a; Mosammaparast *et al.*, 2001; Muhlhausser *et al.*, 2001). Thus, the high affinity binding of importin β1 for the core histones and the efficient nuclear transport processes suggested that this nuclear translocation pathway might also provide an efficient route into the nucleus for plasmid DNA when associated with histones.

The crystal structure of a single nucleosome revealed that the NLS-containing N-terminal tails of the histones protrude from the core histone octamer (Luger *et al.*, 1997; Figure 7.1). This suggested that the core histone NLSs were likely to be accessible to importins.

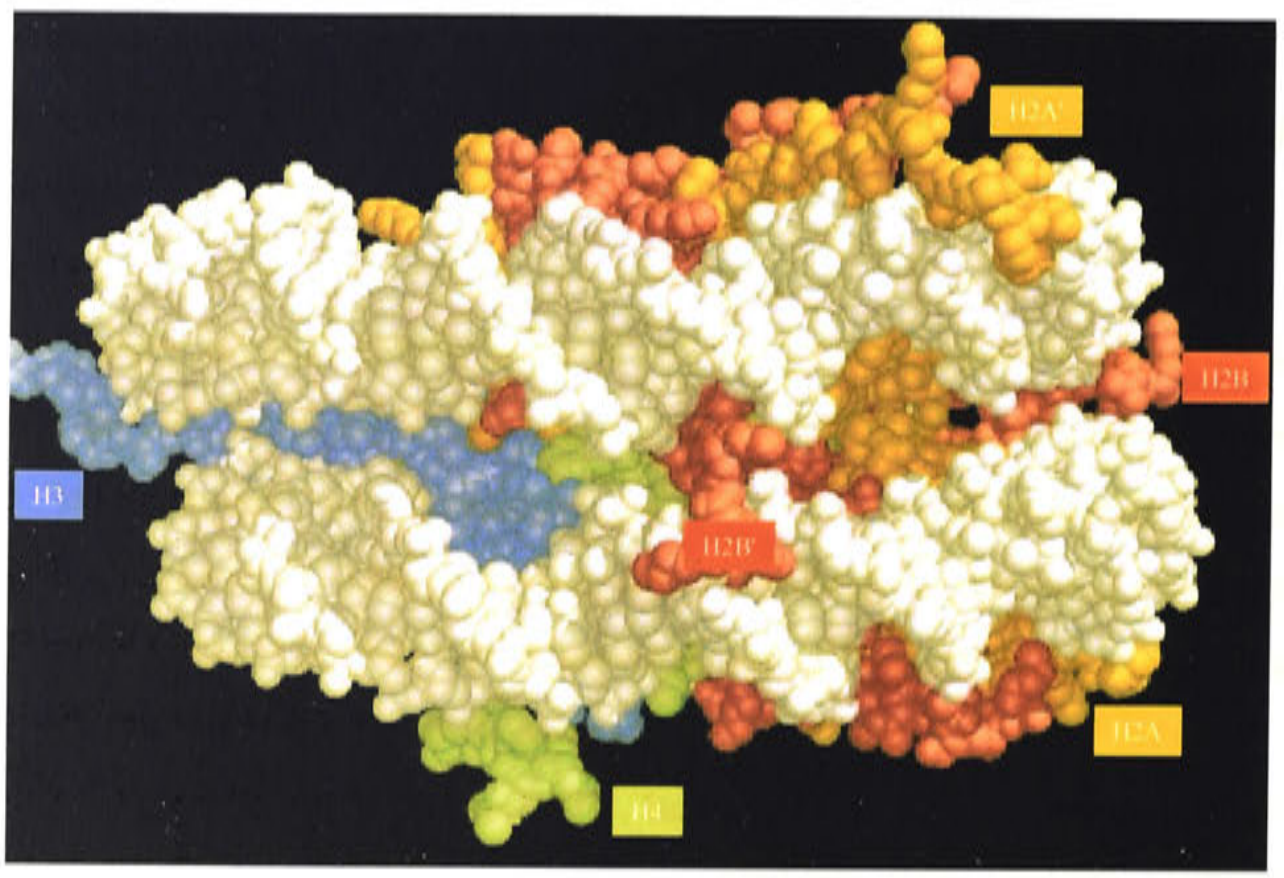

Figure 7.1. A single nucleosome. DNA is represented in white and surrounds the core histone octamer, each histone of which is represented in a different colour. The NLS-containing N-terminal tails of histones H2A', H2B' and H3' can be seen to protrude from the core. In the context of a multi-nucleosomal structure, the state of compaction may obscure the NLSs from access by nuclear import proteins. From Luger *et al.* (1997).

However, the association of core histones into an octamer resulted in reduced binding affinity for importin β1, compared to the H2A/2B dimer and H3/4 tetramer alone (Table 5.2). It is conceivable that when histones are associated into an octamer, their globular domains, believed to present topological NLSs, would be engaged in inter-histone contacts (Luger *et al.*, 1997) and therefore would not be able to bind importin. In addition, while the crystal structure studies of a single nucleosome revealed that the tail domains of the histones exit the plane of the core octamer, contacts on the surface of the histone octamer between the N-terminal tail of H4 and

an acidic domain of the H2A/2B dimer were shown (Luger *et al.*, 1997). This intra-octamer contact may diminish the capacity for importin-binding of the N-terminal H4 NLS and contribute also to the overall reduced binding affinity observed (see Table 3.2).

Similarly, importin β binding was markedly reduced when the core histone H3/4 tetramer and the histone octamer were associated with the pGeneGrip-RFP plasmid by the chromatin assembly process (Section 5.4). As importin binding was effectively abolished for the chromatin constructs, occlusion of the N-terminal NLSs through the process of nucleosome formation was implied. This was observed in the context of a single nucleosome (1 octamer per plasmid; see Table 5.2) and may be extrapolated to the chromatin constructs generated at higher nucleosome density (25 octamers per plasmid). Here nucleosomes would be serially arranged initially and compacted further into a higher order chromatin structure (Figure 1.10; Figure 4.9). Even though the organisation of the histone tail regions in higher order chromatin structures has yet to be elucidated (Luger, 2003), the tails have been shown to be engaged in the process of higher order chromatin folding (Carruthers *et al.*, 1998; Leuba *et al.*, 1998). Thus, in the context of the chromatinised plasmids, it may be postulated that these NLSs may have been occluded, which would account for the abolition of importin binding that was observed (see Section 5.4.2). Interestingly, as pGeneGrip-RFP assembled at histone octamer stoichiometry corresponding to the fully chromatinised plasmid (25 octamers per plasmid) but under non-chromatinising conditions appeared to yield a degree of nuclear accumulation similar to the naked plasmid (see Table 5.1), the continued accessibility of importins may be implied.

The apparent enhancement in transfection efficiency reported by others using the individual core histones as DNA carrier proteins (presented in Section 1.5.3) may well be due to the continued accessibility of the histone NLSs, since the individual core histones do not induce higher orders of DNA folding into compacted structures. Furthermore, single histones remain in an unfolded state unless associated with their partner histones, in the form of the H2A/2B dimer or H3/4 tetramer (Luger *et al.*, 1997). Balicki *et al.* (2002) were able to localise the gene transfer activity of H2A to a 37-amino acid peptide within the N-terminus. The secondary structure and positively charged residues (NLS) of the 37-mer were shown to play a vital role in nuclear localisation, suggesting importin accessibility.

As the MW of the chromatinised plasmids exceeds the MWCO of the NPC for passive diffusion into the nucleus (40 – 60 kDa), efficient translocation must be facilitated by the importins. However, occlusion of the histone NLSs when in a nucleosomal format precluded importin-mediated nuclear transport of the chromatin constructs. This would instead force entry into the nucleus using the highly inefficient mechanisms associated with the nuclear uptake of

high MW plasmids (Ludtke *et al.*, 1999; Wilson *et al.*, 1999; Hagstrom *et al.*, 1997). This may account for the decreased nuclear accumulation observed for the more extensively chromatinised, higher MW constructs.

7.2. MOLECULAR WEIGHT AS A RATE-LIMITING BARRIER IN NON-VIRAL GENE DELIVERY

In addition to the MW restrictions imposed by the NPC, diffusion through the cytoplasm to the nucleus has emerged as a highly significant issue impacting upon non-viral mediated gene delivery. Large linear DNA fragments were found to remain mostly perinuclear and did not enter the nucleus, in contrast to DNA fragments less than 1 kb in length which were found in the nucleus within 4 hours after cytoplasmic microinjection (Ludtke *et al.*, 1999; Wilson *et al.*, 1999; Hagstrom *et al.*, 1997). Large plasmid DNAs were found to behave similarly, with no detectable diffusion away from the site of cytoplasmic microinjection observed during the duration of the experiment (6 hours; Ciolina *et al.*, 1999; Neves *et al.*, 1999b; Sebestyen *et al.*, 1998).

Two properties of molecules have been found to limit diffusion through the cytoplasm; dimension and MW. In a seminal study, Seksek *et al.* (1997) showed using spot photobleaching that macromolecules (fluoresceinated dextrans) with a gyration radius larger than 300 Å had reduced mobility in the cytoplasm. Lukacs *et al.* (2000) widened this study to investigate the diffusion capacity of DNA fragments in the cytoplasm. Similarly, spot photobleaching was used to determine that the diffusion coefficients of various sized fluorescein-labelled DNA fragments (21 - 6000 bps), which were microinjected into the cytoplasm, became markedly reduced for fragments greater than 1000 bps (equates to 660 kDa).

Similar in size to the largest DNA fragment used in the Lukacs study, the pGeneGrip-RFP plasmid used in this study was 5889 bps (equates to 3960 kDa). When chromatinised using histone octamers (108486 Da per octamer), the constructs yielded a range of molecular masses between ~ 4069 - 6672 kDa (corresponding to the 1 octamer per plasmid - 25 octamers per plasmid constructs, see Table 4.1). This was up to 10-fold greater than the critical molecular weight of the 1000 bp construct in the Lukacs study. While the findings of the Lukacs study may be used only cautiously to explain some of the findings of this study, as DNA used by Lukacs *et al.* (2000) were naked linear fragments and the transfection constructs used in this study were closed circular plasmids compacted with histone octamers, it may be reasonable to suggest that the more extensively chromatinised constructs experienced hindered cytoplasmic diffusibility. Indeed, the decrease in the relative proportion of nuclei that had accumulated the

chromatin constructs with increasing levels of chromatinisation (increasing stoichiometry of histone octamers) lends support to this hypothesis (Section 5.3.2).

The Lukacs model (Lukacs *et al.*, 2000) and observations of the diminished cytoplasmic mobility of large DNA fragments (Ludtke *et al.*, 1999; Wilson *et al.*, 1999; Hagstrom *et al.*, 1997) predict that nuclear accumulation of DNA greater than 3000 bps would be abolished. Despite this, nuclear accumulation of the pGeneGrip-RFP plasmid and expression of the reporter gene were observed (Section 5.3.2). This may be due in part to the tendency of the chromatinised plasmid towards compaction.

An important feature of the hypothesis tested in this study was that reconstituted chromatin would make the transfection of large plasmids possible by inducing compaction of the DNA. Compaction of plasmid DNA has been postulated previously to facilitate passage through the various membrane barriers presented by the transfected cell on the way to the nucleus and, experimentally, has been associated with enhanced transfection efficiency (Lucius *et al.*, 2001; Chan *et al.*, 2000; Chan and Jans, 1999; Fritz *et al.*, 1996; Wagner *et al.*, 1990). Atomic force and electron microscopy revealed that the plasmids used in these studies were compacted typically to diameters less than 100 nm (16 – 60 nm, Chan *et al.*, 2000; 80 – 100 nm, Wagner *et al.*, 1991).

In the context of this work, the compacted state of the fully nucleosome-saturated pGeneGrip-RFP chromatin construct (25 octamers per plasmid construct) was important. The image of the fully chromatinised plasmid using surface AFM, shown in Figure 4.9, provided visual confirmation of compaction into an extended rod shape (compared with the open structure of the naked plasmid). This image was consistent with the model proposed for circular chromatin molecules (Ladoux *et al.*, 2000; Hansen and Wolffe, 1992; Simpson *et al.*, 1985) where compaction into structures resembling the canonical '30 nm chromatin fibre' is facilitated by the N-terminal tails of the core histones which participate in inter-nucleosome contacts (Tse and Hansen, 1997; Fletcher and Hansen, 1995; Schwarz and Hansen, 1994; Yao *et al.*, 1991). The AFM of adsorbed chromatinised DNA may be somewhat distorted due to contacts made with the surface of the imaging 'slide' (mica). Techniques such as dynamic light scattering or AFM performed in solution would allow the super-structure of the chromatin constructs to be determined with greater assurance and facilitate accurate physical measurements of the structural properties. Nonetheless, MNase digestion patterns and AFM revealed that chromatinisation of the plasmid at physiological nucleosome density (25 octamers per pGeneGrip-RFP) induced compaction through nucleosome formation, in the first instance, and through internucleosomal contacts, in the second instance.

Despite compaction, the extensively chromatinised constructs at higher nucleosome densities were less effective than the constructs assembled at lower nucleosome densities in nuclear accumulation (see Section 5.3.2). One could argue that the higher MW of the extensively chromatinised constructs may well have counteracted any positive effect conferred by compaction but the fact that the plasmid/histone octamer 'association' with comparable MW (25 octamers per plasmid) accumulated in nuclei to a similar degree as the naked plasmid suggests that MW *per se* was not prohibitive. As discussed in Section 7.1, these observations may be reconciled by the continued accessibility of the histone NLSs in the plasmid/histone octamer 'association', unlike in the chromatinised constructs (where importin binding was abolished). Therefore, in the absence of NLS accessibility, the chromatin constructs may have succumbed to MW-dependent nuclear uptake.

7.3. INCORPORATION OF NLS PEPTIDES IN THE GENE DELIVERY VEHICLE

Non-viral-mediated gene delivery is characterised by inefficient nuclear entry, as fewer than 10 % of transfected DNA molecules have been shown to reach the nucleus (Zabner *et al.*, 1995; Chu *et al.*, 1990; Capecchi, 1980). Transport into the nucleus of molecules exceeding the MWCO of the NPC (40 – 60 kDa) is facilitated by the interaction between importins and an NLS in the 'transport substrate' (see Section 1.3.3). Since the size of most transfection constructs exceeds the MWCO of the NPC, in the absence of importin binding, entry into the nucleus becomes highly inefficient. In order to enhance the efficiency of nuclear uptake, a number of particular NLSs (of which the SV40 T-ag NLS has been the most widely studied) have been incorporated into the transfection constructs (for reviews see Escriou *et al.*, 2003; Cartier and Reszka, 2002; Bremner *et al.*, 2001).

In this study, two approaches were taken to include a peptide derived from the SV40 T-ag NLS in the chromatin transfection constructs. An H2A-NLS fusion protein was generated in order to incorporate the NLS at the level of the DNA carrier protein as an H2A-NLS-containing histone octamer. However, the fusion of the NLS inhibited histone octamer formation under the standard octamerisation conditions used (Section 6.2.1). The tails of the core histones are important in the formation of intra-nucleosomal contacts (for review see Luger and Richmond, 1998) and therefore modifications to the C-terminal regions may indeed translate into nucleosome instability. An alternative approach involved coupling of NLSs to the reporter plasmid directly. T-ag NLS peptides were linked to the reporter plasmid by means of maleimide-PNA (Section 6.2.2). The N-terminal cysteine residue in the NLS peptide provided the means for conjugation to PNA via a chemically stable thioether bond (Figure 6.6). The nucleophilic addition of a thiolate to maleimide derivatives occurs rapidly and in very high

yield. The site-specific hybridisation of the PNA moiety to pGeneGrip™ proceeds via 8 concatameric sites which are engineered into the plasmid (Gene Therapy Systems).

The reporter gene was expressed following transfection of the chromatinised NLS-coupled plasmids into HTC and Cos-7 cells, which demonstrated that the coupling strategy permitted transcription. However, a 50 - 60 % decrease in expression of the reporter gene from non-chromatinised NLS-coupled plasmid relative to the non-chromatinised non-NLS plasmid was observed (Table 6.1). Interestingly though, the proportion of cells expressing the reporter gene were not reduced further in accordance with increasing chromatinisation (Figure 6.8), as had been the previously observed pattern in the absence of the additional NLS peptides (Figure 4.14).

The strategy of including NLSs in the gene delivery vector as a means to improve transfection efficiency through increased nuclear uptake of the transfection constructs has been reviewed recently; inclusion of NLSs, it seems, does not always lead to an enhancement in gene expression (Escriou *et al.*, 2003; Cartier and Reszka, 2002; Bremner *et al.*, 2001). Of the 10 studies reviewed by Cartier and Reszka (2002) in which an NLS was conjugated directly to the DNA, only 3 demonstrated a significant (10-fold or greater) enhancement of gene expression (Branden *et al.*, 1999; Subramanian *et al.*, 1999; Zanta *et al.*, 1999).

Zanta *et al.* achieved a 10 - 1000-fold increase in luciferase reporter gene expression using a T-ag NLS covalently attached to a linear DNA fragment via a hairpin oligonucleotide linker molecule (Zanta *et al.*, 1999). However, when this NLS-coupling technology was applied to a closed circular plasmid, no increase in transgene expression was observed, with the non-NLS control, NLS-conjugated and mutated, non-functional NLS-conjugated plasmids demonstrating similar levels of gene expression (Roulon *et al.*, 2002). The authors suggested that the discrepancy between the two groups of published data lay in the ability of a linearised NLS-coupled DNA fragment to negotiate through the NPC. The circular plasmid may present different challenges to translocation through the NPC and may have required additional NLSs.

Indeed, the number of NLSs conjugated to the plasmid DNA appears to play an important role in transfection efficiency. Concatameric attachment of 2 NLSs directly to the plasmid had no effect on transfection efficiency, whereas 11 NLSs resulted in an 8-fold increase in gene expression (Branden *et al.*, 1999). In contrast, other studies reported that the attachment of up to 115 NLSs throughout the plasmid did not improve gene expression compared to the non-NLS plasmid (Ciolina *et al.*, 1999; Neves *et al.*, 1999b; Sebestyen *et al.*, 1998).

Detailed comparison of these studies reveals that the distribution of the NLS peptides may be an important factor. In most of the studies the NLSs were generally distributed throughout the plasmid (Ciolina *et al.*, 1999; Neves *et al.*, 1999b; Sebestyen *et al.*, 1998), whereas Branden *et al.* (1999) studied the effect of concatameric NLS peptides. Random distribution of NLSs had been proposed previously to inhibit transcription of the reporter gene; specifically with the covalent attachment of 43 NLSs (6 NLSs/1 kb) being shown to decrease transgene expression by 60 % in one study (Ciolina *et al.*, 1999).

In the present study, the concatameric nature of the PNA hybridisation site, downstream of the reporter gene, precluded the possibility that the decreased transfection efficiency of the non-chromatinised NLS-coupled pGeneGrip-RFP plasmid (0 octamers per plasmid; see Section 6.2.2.3) was due to inhibited transcription. Furthermore, the percentage of cells expressing the reporter gene from the plasmid coupled to PNA-maleimide was similar to the non-PNA-coupled plasmid (relative to non-maleimide labelled pGeneGrip-RFP; Cos-7 cells; data not shown). The nuclear accumulation studies (Table 6.2) revealed that the non-chromatinised fluoresceinated NLS-coupled construct entered 50 % fewer nuclei than in cells transfected with the equivalent non-NLS construct. This alone may be sufficient to account for the relative decrease in the percentage of cells expressing the reporter gene but why inhibited nuclear uptake had occurred remains unclear.

Interaction of the NLS-coupled chromatinised constructs with the importin α/β heterodimer was not demonstrated directly in this work. However, since NLS-regulated importin-mediated nuclear import is independent of MW, the ability of the highly chromatinised NLS-coupled constructs to accumulate in a similar proportion of nuclei as the naked NLS-coupled constructs, suggests that nuclear uptake had indeed been facilitated by the additional coupled NLSs.

Interaction of SV40 T-ag NLS-coupled plasmids with importin α could be shown formally only when at least 10 NLS peptides were coupled to the plasmid DNA (Ciolina *et al.*, 1999; Neves *et al.*, 1999b). While this demonstrated the competency of the NLS-coupled plasmid to be transported into the nucleus via the importin α/β-mediated pathway, no enhancement in gene expression was observed in any of these studies. The Branden study, which did show enhancement of gene expression, however, did not investigate whether this was due to enhanced nuclear accumulation of the NLS-coupled plasmids (Branden *et al.*, 1999). The lack of consensus on the use of NLS peptides to enhance transgene expression due to improved nuclear import of the NLS-coupled plasmid is evident from the literature (for reviews see Cartier and Reszka, 2002; Bremner *et al.*, 2001; Escriou *et al.*, 2001), with a number of questions remaining unanswered. Which of linear or plasmid DNA is more compentent for

NLS-mediated nuclear uptake? Is the site of NLS coupling crucial? How many NLSs are required to mediate nuclear import and would gene expression still be supported under intensive NLS coupling?

While the work presented here did not demonstrate an NLS-induced improvement in transfection efficiency, it did demonstrate the appeal of the PNA-labelling procedure. Its simplicity, ability to preserve gene expression and potential to enhance plasmid nuclear uptake (Branden *et al.*, 1999) appear to be superior compared to other highly cumbersome procedures involving complex chemical reactions with molecules which are difficult to produce in practical quantities (Neves *et al.*, 1999a; Zanta *et al.*, 1999).

7.4. Transcriptional permissiveness and repression of transcription as a means to control transgene expression

Despite the diffusional restrictions associated with macromolecular movement both in the cytoplasm and across the nuclear membrane, discussed in Section 7.2, expression of the reporter gene demonstrated that a sufficient proportion of the chromatin constructs were able to enter the nucleus in the cell types tested. Dissociation of the condensing agent from the transfecting plasmid DNA is necessary for transcription and subsequent gene expression (Zabner *et al.*, 1995). It had been proposed that gene expression should not be adversely affected by chromatinisation as this the physiological form in which DNA is found in the nucleus. However, the discrepancy between the proportion of cells expressing the reporter gene and the proportion of nuclei that took up the more extensively chromatinised transfection constructs suggested otherwise.

The most likely explanation for this discrepancy is that transcription had been inhibited at the higher levels of chromatinisation (Hebbes *et al.*, 1994 and for reviews see Luger, 2003; Horn and Peterson, 2002). Studies of reconstituted chromatin models *in vitro* have revealed that the presence of nucleosomes, nucleosome residence on the gene promoter region and compaction of chromatin, with increasing levels of nucleosome density towards those approximating physiological density, results in greater than 90 % repression of transcription (Sandaltzopoulos *et al.*, 1994; Hansen and Wolffe, 1992).

Similarly, compaction of genomic DNA in chromatin within the nucleus *in vivo* (Figure 7.2) is intrinsically refractory to transcription. Here, however, recruitment of chromatin re-modelling complexes functions to 'prime' DNA for transcription by initiating the decompaction of chromatin and subsequent translocation of nucleosomes from the promoter region of the gene

(for reviews see Horn and Peterson, 2002; Kadonaga, 1998). This facilitates the binding of the basal transcription machinery. Only when DNA is naked do the rates of *in vitro* transcription approximate those seen *in vivo* (Izban and Luse, 1992 and for review see Orphanides and Reinberg, 2000).

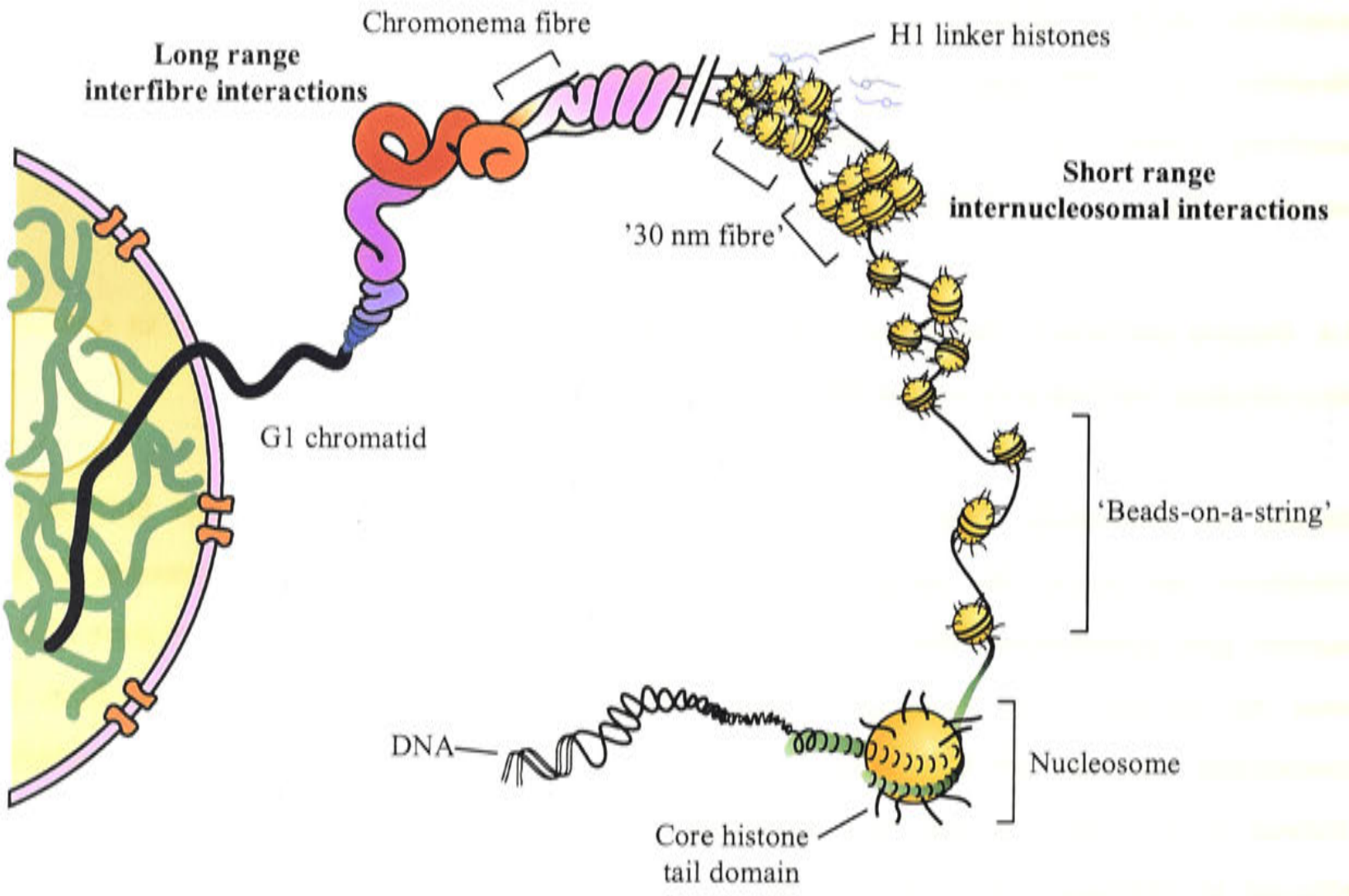

Figure 7.2. Chromatin folding *in vivo*. Cartoon showing the multiple levels of chromatin folding *in vivo* in the interphase nucleus, represented on the left. DNA folding proceeds through an ordered series of primary ('beads-on-a-string'), secondary ('30 nm fibre') and tertiary (chromonema fibre) structures, mediated predominantly through the histone tail interactions. Original figure from Horn and Peterson (2002).

The pGeneGrip™ plasmid was chosen for use in this study as it enabled both gene tracking and expression analyses to be performed in the same experiment. However, since the RFP reporter gene did not seem to be readily expressed from the chromatinised pGeneGrip-RFP plasmid in HTC or Cos-7 cells, an alternative approach was sought. A transgene expression system in which the promoter, when matched to the cell type, had been shown to recruit chromatin re-modelling and transcription complexes and thus facilitate transgene expression (Rao *et al.*, 2001; Himes *et al.*, 1993) was investigated. When chromatinised pGMLuc constructs harbouring the T-cell-specific GMCSF promoter were transfected into Jurkat cells (Section 6.3.2), luciferase reporter gene expression was not significantly different from that of the naked

construct (0 octamers per pGMLuc; Figure 6.14). Contrary to pGMLuc, when the chromatinised pGeneGrip-RFP constructs were transfected into Jurkat cells, reporter gene expression decreased upon increasing the degree of nucleosome density (Table 6.4), consistent with the pattern observed in Cos-7 and HTC cell transfections. This data may suggest that chromatin re-modelling of pGeneGrip-RFP was inefficient in the cell lines tested. The observation that gene expression driven by the GMCSF promoter was insensitive to chromatinisation in Jurkat cells suggests that recruitment of the appropriate transcriptional complexes had occurred.

The role of the promoter and enhancer region in cellular gene expression from chromatinised plasmids merits further testing. In order to confirm this proposal, an interesting future study would be to compare the abilities of the full length GMCSF promoter region, the active GMCSF promoter region (– 620 to + 37 fragment, used in this study) and a non-functional mutated form of the GMCSF promoter with the ability of the CMV promoter (and others) to drive gene expression from a chromatinised reporter plasmid in a cell-specific manner. 'Promoter-customised' chromatin constructs may very well prove to be valuable in the context of cell-specific gene expression.

In addition to the re-modelling complexes which induce changes in chromatin architecture (for reviews see Luger, 2003; Horn and Peterson, 2002; Orphanides and Reinberg, 2000; Kadonaga, 1998), histone variants, such as H2AZ, are believed to alter the condensation state of chromatin and, thus, also play a role in gene regulation. The presence of H2AZ has been shown to inhibit the formation of highly condensed chromatin *in vitro*, suggesting that H2AZ creates localised areas of chromatin that are primed for transcription (Fan *et al.*, 2002). The possibility that chromatin composed of H2AZ histone octamers would be more transcriptionally viable than chromatin comprised of H2A histone octamers and should yield higher levels of gene expression was tested. The results presented in Section 6.3.1.2 indicated that the relative percentage of cells expressing the RFP reporter gene following transfection with H2AZ-containing chromatin constructs was actually lower than that from transfection with H2A-containing chromatin constructs (Table 6.3).

As discussed in Section 6.4, the sedimentation velocity profile of H2AZ-containing chromatin assembled at a density of 25 octamers per plasmid (64 *S*, data not shown) resembled that of H2A-containing chromatin at 40 octamers per plasmid (66 *S*; Table 4.1). These high sedimentation coefficients (>> 55 *S*) are similar to those obtained when intermolecular association of reconstituted nucleosomal arrays has been demonstrated (Schwarz and Hansen, 1994). Both the apparent increase in nucleosome density (saturated H2AZ-chromatin is

comparable to super-saturated H2A-chromatin) and possible formation of oligomers may account for the relative inhibition of reporter gene expression at high levels of chromatinisation with H2AZ-octamers when compared to H2A-octamers.

The results obtained using H2AZ-containing chromatin were contrary to expectation in light of the findings of Fan *et al.* (2002). However, as the Fan study was conducted strictly *in vitro* using a linear DNA template which assembled a defined array of nucleosomes to demonstrate structural differences between H2A-containing chromatin and H2AZ-containing chromatin, these findings may not extend to a closed circular plasmid. Interestingly, *in vivo*, H2AZ has been shown to be associated with both activation (Adam *et al.*, 2001) and repression (Dhillon and Kamakaka, 2000) of transcription. Thus, the finding that *in vitro* assembled H2AZ-chromatin appears to be more repressive to gene expression than H2A-chromatin is an important new discovery and the role of H2AZ in relating chromatin super-structure to transcriptional permissiveness awaits further elucidation. Of course, the possibility that the H2AZ-chromatin constructs accumulated in the nucleus to a lesser extent than H2A-chromatin constructs cannot be excluded but seems to be the less likely explanation.

In addition to the presence of variant histones, modifications to the linker histones, core histones or the DNA itself also play a part in transcriptional viability. Acetylated histones, for instance, are generally associated with areas of transcriptionally active chromatin (Vermaak *et al.*, 2003; Luger and Richmond, 1998). In this light, a future line of investigation may involve the assembly of chromatin using histone octamers containing the acetylated core histone H3/4 tetramer (although, it was found that acetylation masks the NLS site in H3/4 (Section 3.2), it could be argued that the NLSs would be non-functional in any case (see Section 7.1) in a nucleosomal array).

The results presented in Section 6.3 indicate that the transcriptional permissiveness of the transfection constructs appears to be another significant factor in the efficiency of non-viral gene delivery. The *in vitro* assembled chromatin system forms an ideal basis from which to investigate the potential to achieve transgene expression in a cell-specific manner by using different endogenous promoters. Furthermore, transgene expression has the potential to be regulated by the use of agents which can mediate reversible inhibition of promoter function (Burcin *et al.*, 1999). The chromatin system also provides for the additional possibility of regulating transgene transcription on a more global level through the incorporation of variant histones or modifications, such as acetylation, that alter chromatin super-structure.

7.5. LESSONS FROM NATURE – VIRUSES AND CHROMOSOMES

The factors essential for optimising non-viral gene delivery relate strongly to ensuring cell-specific delivery, overcoming various barriers to the passage of DNA to the nucleus and, ultimately, being able to regulate expression of the therapeutic gene (Zabner *et al.*, 1995). In this context, there are lessons to be learned from nature. Viruses are able to overcome all of the membrane barriers on the way to the nucleus. Adenovirus, for instance, uses specialised cell-surface binding proteins, a pH-sensitive endosomal escape peptide and recruits histone H1 to facilitate nuclear entry of its genome (see Figure 1.3). Viruses are therefore excellent models for the rational design of more efficient gene delivery systems in which the efficient processes of viral infection are combined with the advantageous properties of synthetic delivery vectors.

An example of a hybrid viral/non-viral system is the 'virosome' approach. Here, viral capsid proteins have been incorporated into liposomes in order to facilitate fusion with the target cell membrane so that the liposomal contents are introduced directly into the cytoplasm (Ramani, 1998; Ramani, 1997) While the majority of work has been conducted using the membrane fusion protein of the haemagglutinating virus of Japan (HVJ or Sendai virus; for review see Kaneda, 2000), other viruses investigated include vesicular stomatitis virus (Imazu *et al.*, 2000), HIV (Larsen *et al.*, 1993), HSV (Rouse *et al.*, 2000) and influenza virus (Schoen *et al.*, 1999; Maeda *et al.*, 1981). Fusion of 'virosomes' with target cells has been shown to occur rapidly (within 10 to 30 minutes of introduction) and fluorescently-labelled DNA could be detected in the nucleus 5 minutes later (Morishita *et al.*, 1994). In contrast, cationic liposomes required 5 to 20 hours for membrane fusion and 24 hours after the introduction of labelled DNA, fluorescence could be detected in endosomal compartments, but not yet in the nucleus (Morishita *et al.*, 1994).

The ability to regulate therapeutic gene expression so that it is consistent with the normal physiological pattern remains a critical limitation of gene therapy. This is further complicated because physiological gene expression is regulated at several levels, from cell signalling pathways to chromatin structure. Recently, artificial chromosomes have been promoted as a potential solution to this problem (Lipps *et al.*, 2003). Artificial chromosomes have been constructed from a centromere, telomeres and the genomic DNA harbouring the gene of interest, derived from the fragmentation of natural chromosomes. These 'chromosomes' are still highly experimental, but the idea that they would mimic the natural state of DNA and have an essentially unlimited cloning capacity is comparable to the idea of the *in vitro* assembled chromatin system presented in this thesis. The presence of regulatory elements for gene expression and the potential to segregate and replicate presents a distinct advantage over the *in*

vitro assembled chromatin system, however, production, manipulation, and achieving transfection and nuclear import of artificial chromosomes may prove highly challenging. In this framework, the *in vitro* assembled chromatin system has the potential to provide a manageable basis for the transfection of large DNA constructs, once the limitations of reduced nuclear import and transcription repression are overcome.

Reduced nuclear import may be addressed by optimising parameters such as the level of compaction of the chromatinised plasmids and the degree of accessibility of NLSs. As a first step towards investigating the potential of the *in vitro* assembled chromatin system for gene delivery, the first stage of chromatin compaction was used; the assembly of nucleosomes. The second stage of compaction involves the linker histone H1. Histone H1 facilitates stabilisation of the '30 nm chromatin fibre' and further compaction into 100 nm fibres (see Figure 7.2; for review see Hansen, 2002), however, the structure and function of higher order chromatin organisation remain largely undefined both *in vitro* (Luger, 2003) and *in vivo* (Horn and Peterson, 2002). Interestingly, histone H1 showed the highest affinity for importin β1 amongst the histones tested (see Section 3.2; Johnson-Saliba *et al.*, 2000). Furthermore, there appears to be a consensus in the literature that of the histones trialed as DNA carrier proteins for gene delivery purposes, H1 consistently enhanced gene transfer (Section 1.5.3). These points suggest that the inclusion of H1 in a gene delivery vector based on the *in vitro* assembled chromatin system would warrant investigation. Firstly, because H1 nucleosome-compacted plasmid DNA may be condensed to higher order structures beyond the '30 nm chromatin fibre' mode, processes such as passage through cellular membranes and diffusion through the cytoplasm may be potentiated. Secondly, because H1 may be able to direct nuclear import by means of intrinsic NLSs and since H1 binds to DNA outside of the nucleosome structure, it may not be subject to the same chromatin-induced masking effect as was observed for the core histones.

The results presented in this study indicate that the accessibility of NLSs within the transfection constructs is vital in order to ensure importin-mediated nuclear import. While the future challenge in NLS-mediated nuclear import of transfection constructs is to delineate the fine balance required for the promotion of nuclear import with the preservation of gene expression, the *in vitro* assembled chromatin system has the potential for nuclear import enhancing elements to be incorporated.

The chromatin-induced transcriptional repression may be overcome by the use of optimised promoter and enhancer regions to recruit the appropriate chromatin re-modelling complexes and drive transcription of the reporter gene. This could provide the basis for tissue-specific expression of the therapeutic gene. Inclusion of gene regulatory elements would provide

another level of control. Furthermore, incorporation of origins of replication (Jenke *et al.*, 2002; Baiker *et al.*, 2000) into the *in vitro* assembled chromatin system might provide a means for the maintenance of the transfection construct through multiple rounds of cell division, thus addressing another limiting factor of non-viral gene delivery systems, that of long-term expression of the therapeutic gene.

It seems that nature has provided the scaffolding for an exciting collaboration with biotechnology that may enable the development of that, as yet elusive, 'ideal vector' and finally bring gene therapy out of the realm of experimental therapeutics and into everyday medicine.

REFERENCES

Abdallah, B., Hassan, A., Benoist, C., Goula, D., Behr, J.P. and Demeneix, B.A. (1996) A powerful nonviral vector for in vivo gene transfer into the adult mammalian brain: Polyethylenimine. *Human Gene Therapy*. **7**: 1947-1954.

Adam, M., Robert, F., Larochelle, M. and Gaudreau, L. (2001) H2A.Z is required for global chromatin integrity and for recruitment of RNA polymerase II under specific conditions. *Molecular and Cellular Biology*. **21**: 6270-6279.

Akey, C.W. (1990) Visualization of transport-related configurations of the nuclear pore transporter. *Biophysical Journal*. **58**: 341-355.

Akey, C.W. and Luger, K. (2003) Histone chaperones and nucleosome assembly. *Current Opinion in Structural Biology*. **13**: 6-14.

Akhlynina, T.V., Rosenkranz, A.A., Jans, D.A. and Sobolev, A.S. (1995) Insulin-mediated intracellular targeting enhances the photodynamic activity of chlorin e(6). *Cancer Research*. **55**: 1014-1019.

Akhlynina, T.V., Rosenkranz, A.A., Jans, D.A., Gulak, P.V., Serebryakova, N.V. and Sobolev, A.S. (1993) The use of internalizable derivatives of chlorin-e(6) for increasing its photosensitizing activity. *Photochemistry and Photobiology*. **58**: 45-48.

Akhlynina, T.V., Jans, D.A., Rosenkranz, A.A., Statsyuk, N.V., Balashova, I.Y., Toth, G., *et al* (1997) Nuclear targeting of chlorin e(6) enhances its photosensitizing activity. *Journal of Biological Chemistry*. **272**: 20328-20331.

Akhlynina, T.V., Jans, D.A., Statsyuk, N.V., Balashova, I.Y., Toth, G., Pavo, I., *et al* (1999) Adenoviruses synergize with nuclear localization signals to enhance nuclear delivery and photodynamic action of internalizable conjugates containing chlorin e(6). *International Journal of Cancer*. **81**: 734-740.

Akkaraju, G.R., Huard, J., Hoffman, E.P., Goins, W.F., Pruchnic, R., Watkins, S.C., *et al* (1999) Herpes simplex virus vector-mediated dystrophin gene transfer and expression in MDX mouse skeletal muscle. *Journal of Gene Medicine*. **1**: 280-289.

Albert, M.J. (1986) Enteric Adenoviruses - Brief Review. *Archives of Virology*. **88**: 1-17.

Alemany, R., Balague, C. and Curiel, D.T. (2000) Replicative adenoviruses for cancer therapy. *Nature Biotechnology*. **18**: 723-727.

Allan, J., Hartman, P.G., Crane-Robinson, C. and Aviles, F.X. (1980) The structure of histone H1 and its location in chromatin. *Nature*. **288**: 675-679.

Allen, T.M., Hansen, C. and Rutledge, J. (1989) Liposomes with prolonged circulation times - factors affecting uptake by reticuloendothelial and other tissues. *Biochimica et Biophysica Acta*. **981**: 27-35.

Allen, T.M., Hansen, C., Martin, F., Redemann, C. and Yauyoung, A. (1991) Liposomes containing synthetic lipid derivatives of polyethylene glycol show prolonged circulation half-lives Invivo. *Biochimica et Biophysica Acta*. **1066**: 29-36.

Anderson, D.B., Laquerre, S., Goins, W.F., Cohen, J.B. and Glorioso, J.C. (2000) Pseudotyping of glycoprotein D-deficient herpes simplex virus type 1 with vesicular stomatitis virus glycoprotein G enables mutant virus attachment and entry. *Journal of Virology*. **74**: 2481-2487.

Athanasopoulos, T., Fabb, S. and Dickson, G. (2000) Gene therapy vectors based on adeno-associated virus: characteristics and applications to acquired and inherited diseases. *International Journal of Molecular Medicine*. **6**: 363-375.

Baake, M., Doenecke, D. and Albig, W. (2001a) Characterisation of nuclear localisation signals of the four human core histones. *Journal of Cellular Biochemistry*. **81**: 333-346.

Baake, M., Bauerle, M., Doenecke, D. and Albig, W. (2001b) Core histones and linker histones are imported into the nucleus by different pathways. *European Journal of Cell Biology*. **80**: 669-677.

Baeza, I., Gariglio, P., Rangel, L.M., Chavez, P., Cervantes, L., Arguello, C., *et al* (1987) Electron-microscopy and biochemical-properties of polyamine-compacted DNA. *Biochemistry*. **26**: 6387-6392.

Baiker, A., Maercker, C., Piechaczek, C., Schmidt, S.B., Bode, J., Benham, C. and Lipps, H.J. (2000) Mitotic stability of an episomal vector containing a human scaffold/matrix-attached region is provided by association with nuclear matrix. *Nature Cell Biology*. **2**: 182-184.

Balicki, D. and Beutler, E. (1997) Histone H2A significantly enhances in vitro DNA transfection. *Molecular Medicine*. **3**: 782-787.

Balicki, D., Putnam, C.D., Scaria, P.V. and Beutler, E. (2002) Structure and function correlation in histone H2A peptide-mediated gene transfer. *Proceedings of the National Academy of Sciences of the United States of America*. **99**: 7467-7471.

Balicki, D., Reisfeld, R.A., Pertl, U., Beutler, E. and Lode, H.N. (2000) Histone H2A-mediated transient cytokine gene delivery induces efficient antitumor responses in murine neuroblastoma. *Proceedings of the National Academy of Sciences of the United States of America*. **97**: 11500-11504.

Barkats, M., Bilang-Bleuel, A., Buc-Caron, M.H., Castel-Barthe, M.N., Corti, O., Finiels, F., *et al* (1998) Adenovirus in the brain: Recent advances of gene therapy for neurodegenerative diseases. *Progress in Neurobiology*. **55**: 333-341.

Battersby, B.J., Grimm, R., Huebner, S. and Cevc, G. (1998) Evidence for three-dimensional interlayer correlations in cationic lipid-DNA complexes as observed by cryo-electron microscopy. *Biochimica et Biophysica Acta-Biomembranes*. **1372**: 379-383.

Bauerle, M., Doenecke, D. and Albig, W. (2002) The requirement of H1 histones for a heterodimeric nuclear import receptor. *Journal of Biological Chemistry*. **277**: 32480-32489.

Bayliss, R., Littlewood, T. and Stewart, M. (2000) Structural basis for the interaction between FxFG nucleoporin repeats and importin-beta in nuclear trafficking. *Cell*. **102**: 99-108.

Beg, A.A., Ruben, S.M., Scheinman, R.I., Haskill, S., Rosen, C.A. and Baldwin, A.S. (1992) I-Kappa-B Interacts with the nuclear-localization sequences of the subunits of Nf-Kappa-B - a mechanism for cytoplasmic retention. *Genes & Development*. **6**: 1899-1913.

Behr, J.P. (1994) Gene transfer with synthetic cationic amphiphiles: prospects for gene therapy. *Bioconjugate Chemistry*. **5**: 382-389.

Bergelson, J.M., Cunningham, J.A., Droguett, G., KurtJones, E.A., Krithivas, A., Hong, J.S., *et al* (1997) Isolation of a common receptor for coxsackie B viruses and adenoviruses 2 and 5. *Science*. **275**: 1320-1323.

Bestman-Smith, J., Gourde, P., Desormeaux, A., Tremblay, M.J. and Bergeron, M.G. (2000) Sterically stabilized liposomes bearing anti-HLA-DR antibodies for targeting the primary cellular reservoirs of HIV-1. *Biochimica et Biophysica Acta-Biomembranes*. **1468**: 161-174.

Bett, A.J., Haddara, W., Prevec, L. and Graham, F.L. (1994) An efficient and flexible system for construction of adenovirus vectors with insertions or deletions in early region-1 and region-3. *Proceedings of the National Academy of Sciences of the United States of America*. **91**: 8802-8806.

Bielinska, A.U., Kukowska-Latallo, J.F. and Baker, J.R., Jr. (1997) The interaction of plasmid DNA with polyamidoamine dendrimers: mechanism of complex formation and analysis of alterations induced in nuclease sensitivity and transcriptional activity of the complexed DNA. *Biochimica et Biophysica Acta*. **1353**: 180-190.

Blair-Parks, K., Weston, B.C. and Dean, D.A. (2002) High-level gene transfer to the cornea using electroporation. *Journal of Gene Medicine*. **4**: 92-100.

Blessing, T., Remy, J.S. and Behr, J.P. (1998) Monomolecular collapse of plasmid DNA into stable virus-like particles. *Proceedings of the National Academy of Sciences of the United States of America*. **95**: 1427-1431.

Blobel, G. and Wozniak, R.W. (2000) Proteomics for the pore. *Nature*. **403**: 835-836.

Bloomfield, V.A. (1996) DNA condensation. *Current Opinion in Structural Biology*. **6**: 334-341.

Bordignon, C., Notarangelo, L.D., Nobili, N., Ferrari, G., Casorati, G., Panina, P., *et al* (1995) Gene-Therapy in Peripheral-Blood Lymphocytes and Bone-Marrow for Ada(-) Immunodeficient Patients. *Science*. **270**: 470-475.

Bottger, M., Zaitsev, S.V., Otto, A., Haberland, A. and Vorob'ev, V.I. (1998) Acid nuclear extracts as mediators of gene transfer and expression. *Biochimica et Biophysica Acta*. **1395**: 78-87.

Branden, L.J., Mohamed, A.J. and Smith, C.I. (1999) A peptide nucleic acid-nuclear localization signal fusion that mediates nuclear transport of DNA. *Nature Biotechnology*. **17**: 784-787.

Breeuwer, M. and Goldfarb, D.S. (1990) Facilitated nuclear transport of histone H1 and other small nucleophilic proteins. *Cell*. **60**: 999-1008.

Bremner, K.H., Seymour, L.W. and Pouton, C.W. (2001) Harnessing nuclear localization pathways for transgene delivery. *Current Opinion in Molecular Therapeutics*. **3**: 170-177.

Briggs, L.J., Stein, D., Goltz, J., Corrigan, V.C., Efthymiadis, A., Hubner, S. and Jans, D.A. (1998) The cAMP-dependent protein kinase site (Ser(312)) enhances dorsal nuclear import through facilitating nuclear localization sequence/importin interaction. *Journal of Biological Chemistry*. **273**: 22745-22752.

Brisson, M., Tseng, W.C., Almonte, C., Watkins, S. and Huang, L. (1999) Subcellular trafficking of the cytoplasmic expression system. *Human Gene Therapy*. **10**: 2601-2613.

Budker, V., Gurevich, V., Hagstrom, J.E., Bortzov, F. and Wolff, J.A. (1996) pH-sensitive, cationic liposomes: A new synthetic virus-like vector. *Nature Biotechnology*. **14**: 760-764.

Buller, R.M.L., Janik, J.E., Sebring, E.D. and Rose, J.A. (1981) Herpes-simplex virus type-1 and type-2 completely help adenovirus-associated virus-replication. *Journal of Virology*. **40**: 241-247.

Burcin, M.M., Schiedner, G., Kochanek, S., Tsai, S.Y. and O'Malley, B.W. (1999) Adenovirus-mediated regulable target gene expression in vivo. *Proceedings of the National Academy of Sciences of the United States of America*. **96**: 355-360.

Bustamante, C., Zuccheri, G., Leuba, S.H., Yang, G. and Samori, B. (1997) Visualization and analysis of chromatin by scanning force microscopy. *Methods*. **12**: 73-83.

Bustin, M. and Reeves, R. (1996) High-mobility-group chromosomal proteins: architectural components that facilitate chromatin function. *Progress in Nucleic Acid Research and Molecular Biology*. **54**: 35-100.

Bustin, M., Trieschmann, L. and Postnikov, Y.V. (1995) The Hmg-14/-17 chromosomal protein family - architectural elements that enhance transcription from chromatin templates. *Seminars in Cell Biology*. **6**: 247-255.

Bustin, M., Becerra, P.S., Crippa, M.P., Lehn, D.A., Pash, J.M. and Shiloach, J. (1991) Recombinant human chromosomal-proteins Hmg-14 and Hmg-17. *Nucleic Acids Research*. **19**: 3115-3121.

Cao, Y. and Suresh, M.R. (2000) Bispecific MAb aided liposomal drug delivery. *Journal of Drug Targeting*. **8**: 257-266.

Capecchi, M.R. (1980) High-efficiency transformation by direct micro-injection of DNA into cultured mammalian-cells. *Cell*. **22**: 479-488.

Carruthers, L.M., Bednar, J., Woodcock, C.L. and Hansen, J.C. (1998) Linker histones stabilize the intrinsic salt-dependent folding of nucleosomal arrays: mechanistic ramifications for higher-order chromatin folding. *Biochemistry*. **37**: 14776-14787.

Cartier, R. and Reszka, R. (2002) Utilization of synthetic peptides containing nuclear localization signals for nonviral gene transfer systems. *Gene Therapy*. **9**: 157-167.

Cavazzana-Calvo, M., Hacein-Bey, S., Basile, C.D., Gross, F., Yvon, E., Nusbaum, P., *et al* (2000) Gene therapy of human severe combined immunodeficiency (SCID)-X1 disease. *Science*. **288**: 669-672.

Chan, C.K. and Jans, D.A. (1999) Enhancement of polylysine-mediated transferrinfection by nuclear localization sequences: Polylysine does not function as a nuclear localization sequence. *Human Gene Therapy*. **10**: 1695-1702.

Chan, C.K. and Jans, D.A. (2001) Enhancement of MSH receptor- and GAL4-mediated gene transfer by switching the nuclear import pathway. *Gene Therapy*. **8**: 166-171.

Chan, C.K., Senden, T. and Jans, D.A. (2000) Supramolecular structure and nuclear targeting efficiency determine the enhancement of transfection by modified polylysines. *Gene Therapy*. **7**: 1690-1697.

Chan, C.K., Hubner, S., Hu, W. and Jans, D.A. (1998) Mutual exclusivity of DNA binding and nuclear localization signal recognition by the yeast transcription factor GAL4: implications for nonviral DNA delivery. *Gene Therapy*. **5**: 1204-1212.

Chandler, L.A., Doukas, J., Gonzalez, A.M., Hoganson, D.K., Gu, D.L., Ma, C.L., *et al* (2000) FGF2-targeted adenovirus encoding platelet-derived growth factor-B enhances de Novo tissue formation. *Molecular Therapy*. **2**: 153-160.

Chang, L., Loranger, S.S., Mizzen, C., Ernst, S.G., Allis, C.D. and Annunziato, A.T. (1997) Histones in transit: cytosolic histone complexes and diacetylation of H4 during nucleosome assembly in human cells. *Biochemistry*. **36**: 469-480.

Chen, J., Stickles, R.J. and Daichendt, K.A. (1994a) Galactosylated histone-mediated gene-transfer and expression. *Human Gene Therapy*. **5**: 429-435.

Chen, J.B., Gamou, S., Takayanagi, A. and Shimizu, N. (1994b) A novel gene delivery system using EGF receptor-mediated endocytosis. *FEBS Letters*. **338**: 167-169.

Chen, J.B., Gamou, S., Takayanagi, A., Ohtake, Y., Ohtsubo, M. and Shimizu, N. (1998) Targeted in vivo delivery of therapeutic gene into experimental squamous cell carcinomas using anti-epidermal growth factor receptor antibody: Immunogene approach. *Human Gene Therapy*. **9**: 2673-2681.

Chen, S.Y., Zani, C., Khouri, Y. and Marasco, W.A. (1995) Design of a genetic immunotoxin to eliminate toxin immunogenicity. *Gene Therapy*. **2**: 116-123.

Chiorini, J.A., Kim, F., Yang, L. and Kotin, R.M. (1999) Cloning and characterization of adeno-associated virus type 5. *Journal of Virology*. **73**: 1309-1319.

Chu, C.J., Dijkstra, J., Lai, M.Z., Hong, K. and Szoka, F.C. (1990) Efficiency of cytoplasmic delivery by pH-sensitive liposomes to cells in culture. *Pharmaceutical Research*. **7**: 824-834.

Chung, L.A. and Thompson, T.E. (1996) Design of membrane-inserting peptides: Spectroscopic characterization with and without lipid bilayers. *Biochemistry*. **35**: 11343-11354.

Ciolina, C., Byk, G., Blanche, F., Thuillier, V., Scherman, D. and Wils, P. (1999) Coupling of nuclear localization signals to plasmid DNA and specific interaction of the conjugates with importin alpha. *Bioconjugate Chemistry*. **10**: 49-55.

Clarkson, M.J., Wells, J.R.E., Gibson, F., Saint, R. and Tremethick, D.J. (1999) Regions of variant histone His2AvD required for Drosophila development. *Nature*. **399**: 694-697.

Compton, S.H., Mecklenbeck, S., Mejia, J.E., Hart, S.L., Rice, M., Cervini, R., *et al* (2000) Stable integration of large (> 100 kb) PAC constructs in HaCaT keratinocytes using an integrin-targeting peptide delivery system. *Gene Therapy*. **7**: 1600-1605.

Conti, E., Uy, M., Leighton, L., Blobel, G. and Kuriyan, J. (1998) Crystallographic analysis of the recognition of a nuclear localization signal by the nuclear import factor karyopherin alpha. *Cell*. **94**: 193-204.

Cordes, V.C., Reidenbach, S. and Franke, W.W. (1995) High content of a nuclear pore complex protein in cytoplasmic annulate lamellae of Xenopus oocytes. *Eur J Cell Biol*. **68**: 240-255.

Costello, E., Munoz, M., Buetti, E., Meylan, P.R.A., Diggelmann, H. and Thali, M. (2000) Gene transfer into stimulated and unstimulated T lymphocytes by HIV-1-derived lentiviral vectors. *Gene Therapy*. **7**: 596-604.

Cullen, B.R. (1992) Mechanism of action of regulatory proteins encoded by complex retroviruses. *Microbiological Reviews*. **56**: 375-394.

Curiel, D.T. (1999) Strategies to adapt adenoviral vectors for targeted delivery. In *Anticancer Molecules: Structure, Function, and Design* New York: New York Academy of Sciences, pp. 158-171.

Curiel, D.T., Agarwal, S., Wagner, E. and Cotten, M. (1991) Adenovirus enhancement of transferrin polylysine-mediated gene delivery. *Proceedings of the National Academy of Sciences of the United States of America*. **88**: 8850-8854.

Dauty, E., Remy, J.S., Blessing, T. and Behr, J.P. (2001) Dimerizable cationic detergents with a low cmc condense plasmid DNA into nanometric particles and transfect cells in culture. *Journal of the American Chemical Society*. **123**: 9227-9234.

Dave, U.P., Jenkins, N.A. and Copeland, N.G. (2004) Gene therapy insertional mutagenesis insights. *Science*. **303**: 333.

Dean, D.A. (1997) Import of plasmid DNA into the nucleus is sequence specific. *Experimental Cell Research*. **230**: 293-302.

Dean, D.A., Dean, B.S., Muller, S. and Smith, L.C. (1999) Sequence requirements for plasmid nuclear import. *Experimental Cell Research*. **253**: 713-722.

Deas, O., Angevin, E., Cherbonnier, C., Senik, A., Charpentier, B., Levillain, J.P., *et al* (2002) In vivo-targeted gene delivery using antibody-based nonviral vector. *Human Gene Therapy*. **13**: 1101-1114.

Demirhan, I., Hasselmayer, O., Chandra, A., Ehemann, M. and Chandra, P. (1998) Histone-mediated transfer and expression of the HIV-1 tat gene in Jurkat cells. *Journal of Human Virology*. **1**: 430-440.

Dhillon, N. and Kamakaka, R.T. (2000) A histone variant, Htz1p, and a Sir1p-like protein, Esc2p, mediate silencing at HMR. *Molecular Cell*. **6**: 769-780.

Dilworth, S.M., Black, S.J. and Laskey, R.A. (1987) Two complexes that contain histones are required for nucleosome assembly in vitro: role of nucleoplasmin and N1 in Xenopus egg extracts. *Cell*. **51**: 1009-1018.

Ding, L., Lu, S. and Munshi, N.C. (1997) In vitro packaging of an infectious recombinant adeno-associated virus 2. *Gene Therapy*. **4**: 1167-1172.

Doenecke, D. and Tonjes, R. (1986) Differential distribution of lysine and arginine residues in the closely related histones H1 and H5. Analysis of a human H1 gene. *Journal of Molecular Biology*. **187**: 461-464.

Douglas, J.T., Rogers, B.E., Rosenfeld, M.E., Michael, S.I., Feng, M.Z. and Curiel, D.T. (1996) Targeted gene delivery by tropism-modified adenoviral vectors. *Nature Biotechnology*. **14**: 1574-1578.

Doukas, J., Hoganson, D.K., Ong, M., Ying, W.B., Lacey, D.L., Baird, A., *et al* (1999) Retargeted delivery of adenoviral vectors through fibroblast growth factor receptors involves unique cellular pathways. *FASEB Journal*. **13**: 1459-1466.

Dowty, M.E., Williams, P., Zhang, G., Hagstrom, J.E. and Wolff, J.A. (1995) Plasmid DNA entry into postmitotic nuclei of primary rat myotubes. *Proceedings of the National Academy of Sciences of the United States of America*. **92**: 4572-4576.

Dufresne, I., Desormeaux, A., Bestman-Smith, J., Gourde, P., Tremblay, M.J. and Bergeron, M.G. (1999) Targeting lymph nodes with liposomes bearing anti-HLA-DR Fab' fragments. *Biochimica et Biophysica Acta-Biomembranes*. **1421**: 284-294.

Dumas, T.D., McLaughlin, J.R., Ho, D.Y., Meier, T.J. and Sapolsky, R.M. (1999) Delivery of herpes simplex virus amplicon-based vectors to the dentate gyrus does not alter hippocampal synaptic transmission in vivo. *Gene Therapy*. **6**: 1679-1684.

Dworetzky, S.I. and Feldherr, C.M. (1988) Translocation of RNA-coated gold particles through the nuclear pores of oocytes. *Journal of Cell Biology*. **106**: 575-584.

Edwards, R.J., Carpenter, D.S. and Minchin, R.F. (1996) Uptake and intracellular trafficking of asialoglycoprotein-polylysine-DNA complexes in isolated rat hepatocytes. *Gene Therapy*. **3**: 937-940.

Efthymiadis, A., Briggs, L.J. and Jans, D.A. (1998) The HIV-1 Tat nuclear localization sequence confers novel nuclear import properties. *Journal of Biological Chemistry*. **273**: 1623-1628.

Efthymiadis, A., Shao, H.M., Hubner, S. and Jans, D.A. (1997) Kinetic characterization of the human retinoblastoma protein bipartite nuclear localization sequence (NLS) in vivo and in vitro - A comparison with the SV40 large T-antigen NLS. *Journal of Biological Chemistry*. **272**: 22134-22139.

Escriou, V., Carriere, M., Scherman, D. and Wils, P. (2003) NLS bioconjugates for targeting therapeutic genes to the nucleus. *Advanced Drug Delivery Reviews*. **55**: 295-306.

Escriou, V., Carriere, M., Bussone, F., Wils, P. and Scherman, D. (2001) Critical assessment of the nuclear import of plasmid during cationic lipid-mediated gene transfer. *Journal of Gene Medicine*. **3**: 179-187.

ESOGT (2003) French gene therapy group reports on the adverse event in a clinical trial of gene therapy for X-linked severe combined immune deficiency (X-SCID). Position statement from the European Society of Gene Therapy. *Journal of Gene Medicine*. **5**: 82-84.

Faast, R., Thonglairoam, V., Schulz, T.C., Beall, J., Wells, J.R., Taylor, H., *et al* (2001) Histone variant H2A.Z is required for early mammalian development. *Current Biology*. **11**: 1183-1187.

Fagotto, F., Gluck, U. and Gumbiner, B.M. (1998) Nuclear localization signal-independent and importin/karyopherin-independent nuclear import of beta-catenin. *Current Biology*. **8**: 181-190.

Fan, J.Y., Gordon, F., Luger, K., Hansen, J.C. and Tremethick, D.J. (2002) The essential histone variant H2A.Z regulates the equilibrium between different chromatin conformational states. *Nature Structural Biology*. **9**: 172-176.

Fasbender, A., Zabner, J., Chillon, M., Moninger, T.O., Puga, A.P., Davidson, B.L. and Welsh, M.J. (1997) Complexes of adenovirus with polycationic polymers and cationic lipids increase the efficiency of gene transfer in vitro and in vivo. *Journal of Biological Chemistry*. **272**: 6479-6489.

Federoff, H.J., Halterman, M.W. and Brooks, A.I. (1997) Use of the herpes amplicon system as a vehicle for somatic gene transfer. *Advanced Drug Delivery Reviews*. **27**: 29-39.

Felgner, P.L., Gadek, T.R., Holm, M., Roman, R., Chan, H.W., Wenz, M., *et al* (1987) Lipofection - a Highly Efficient, Lipid-Mediated DNA-Transfection Procedure. *Proceedings of the National Academy of Sciences of the United States of America*. **84**: 7413-7417.

Ferrari, F.K., Samulski, T., Shenk, T. and Samulski, R.J. (1996) Second-strand synthesis is a rate-limiting step for efficient transduction by recombinant adeno-associated virus vectors. *Journal of Virology*. **70**: 3227-3234.

Finlay, D.R., Newmeyer, D.D., Price, T.M. and Forbes, D.J. (1987) Inhibition of *in vitro* nuclear transport by a lectin that binds to nuclear pores. *Journal of Cell Biology*. **104**: 189-200.

Fisher, K.J. and Wilson, J.M. (1997) The transmembrane domain of diphtheria toxin improves molecular conjugate gene transfer. *Biochemical Journal*. **321**: 49-58.

Fisher, K.J., Choi, H., Burda, J., Chen, S.J. and Wilson, J.M. (1996) Recombinant adenovirus deleted of all viral genes for gene therapy of cystic fibrosis. *Virology*. **217**: 11-22.

Fisher, K.J., Jooss, K., Alston, J., Yang, Y.P., Haecker, S.E., High, K., *et al* (1997) Recombinant adeno-associated virus for muscle directed gene therapy. *Nature Medicine*. **3**: 306-312.

FisherAdams, G., Wong, K.K., Podsakoff, G., Forman, S.J. and Chatterjee, S. (1996) Integration of adeno-associated virus vectors in CD34(+) human hematopoietic progenitor cells after transduction. *Blood*. **88**: 492-504.

Fletcher, T.M. and Hansen, J.C. (1995) Core histone tail domains mediate oligonucleosome folding and nucleosomal DNA organization through distinct molecular mechanisms. *Journal of Biological Chemistry*. **270**: 25359-25362.

Flotte, T.R., Afione, S.A., Solow, R., Drumm, M.L., Markakis, D., Guggino, W.B., *et al* (1993) Expression of the cystic-Fibrosis transmembrane conductance regulator from a novel adeno-associated virus promoter. *Journal of Biological Chemistry*. **268**: 3781-3790.

Fominaya, J. and Wels, W. (1996) Target cell-specific DNA transfer mediated by a chimeric multidomain protein - Novel non-viral gene delivery system. *Journal of Biological Chemistry*. **271**: 10560-10568.

Forte, P., Leoni, L., Sampaolese, B. and Savino, M. (1989) Cooperativity in nucleosomes assembly on supercoiled pBR322 DNA. *Nucleic Acids Res*. **17**: 8683-8694.

Forwood, J.K. and Jans, D.A. (2002) Nuclear import pathway of the telomere elongation suppressor TRF1: inhibition by importin alpha. *Biochemistry*. **41**: 9333-9340.

Forwood, J.K., Lam, M.H.C. and Jans, D.A. (2001a) Nuclear import of CREB and AP-1 transcription factors requires importin-beta 1 and Ran but is independent of importin-alpha. *Biochemistry*. **40**: 5208-5217.

Forwood, J.K., Harley, V. and Jans, D.A. (2001b) The C-terminal nuclear localization signal of the sex-determining region Y (SRY) high mobility group domain mediates nuclear import through importin beta 1. *Journal of Biological Chemistry*. **276**: 46575-46582.

Foster, B.J. and Kern, J.A. (1997) HER2-targeted gene transfer. *Human Gene Therapy*. **8**: 719-727.

Fritz, J.D., Herweijer, H., Zhang, G.F. and Wolff, J.A. (1996) Gene transfer into mammalian cells using histone-condensed plasmid DNA. *Human Gene Therapy*. **7**: 1395-1404.

Fujiinakata, T., Ishimi, Y., Okuda, A. and Kikuchi, A. (1992) Functional-analysis of nucleosome assembly protein, Nap-1 - the negatively charged COOH-terminal region is not necessary for the intrinsic assembly activity. *Journal of Biological Chemistry*. **267**: 20980-20986.

Fyodorov, D.V. and Kadonaga, J.T. (2002) Dynamics of ATP-dependent chromatin assembly by ACF. *Nature*. **418**: 897-900.

Gao, L., Wagner, E., Cotten, M., Agarwal, S., Harris, C., Romer, M., *et al* (1993) Direct Invivo Gene-Transfer to Airway Epithelium Employing Adenovirus Polylysine DNA Complexes. *Human Gene Therapy*. **4**: 17-24.

Gao, X. and Huang, L. (1996) Potentiation of cationic liposome-mediated gene delivery by polycations. *Biochemistry*. **35**: 1027-1036.

Garner, J.A. (2003) Herpes simplex virion entry into and intracellular transport within mammalian cells. *Advanced Drug Delivery Reviews*. **55**: 1497-1513.

Garnett, M.C. (1999) Gene-delivery systems using cationic polymers. *Critical Reviews in Therapeutic Drug Carrier Systems*. **16**: 147-207.

Gershon, H., Ghirlando, R., Guttman, S.B. and Minsky, A. (1993) Mode of formation and structural features of DNA cationic liposome complexes used for transfection. *Biochemistry*. **32**: 7143-7151.

Gorlich, D., Henklein, P., Laskey, R.A. and Hartmann, E. (1996) A 41 amino acid motif in importin-alpha confers binding to importin-beta and hence transit into the nucleus. *EMBO Journal*. **15**: 1810-1817.

Gorlich, D., Vogel, F., Mills, A.D., Hartmann, E. and Laskey, R.A. (1995) Distinct Functions for the 2 Importin Subunits in Nuclear-Protein Import. *Nature*. **377**: 246-248.

Goto, T., Nishi, T., Tamura, T., Dev, S.B., Takeshima, H., Kochi, M., *et al* (2000) Highly efficient electro-gene therapy of solid tumor by using an expression plasmid for the herpes simplex virus thymidine kinase gene. *Proceedings of the National Academy of Sciences of the United States of America*. **97**: 354-359.

Gottschalk, S., Sparrow, J.T., Hauer, J., Mims, M.P., Leland, F.E., Woo, S.L. and Smith, L.C. (1996) A novel DNA-peptide complex for efficient gene transfer and expression in mammalian cells. *Gene Therapy*. **3**: 48-57.

Govind, S., Drier, E., Huang, L.H. and Steward, R. (1996) Regulated nuclear import of the Drosophila Rel protein Dorsal: Structure-function analysis. *Molecular and Cellular Biology*. **16**: 1103-1114.

Greco, A., Bausch, N., Coute, Y. and Diaz, J.J. (2000) Characterization by two-dimensional gel electrophoresis of host proteins whose synthesis is sustained or stimulated during the course of herpes simplex virus type 1 infection. *Electrophoresis*. **21**: 2522-2530.

Gruenheid, S., Gatzke, L., Meadows, H. and Tufaro, F. (1993) Herpes-simplex virus-infection and propagation in a mouse L-cell mutant lacking heparan-sulfate proteoglycans. *Journal of Virology*. **67**: 93-100.

Haberland, A., Dalluge, R., Zaitsev, S., Stahn, R. and Bottger, M. (1999) Ligand-histone H1 conjugates: increased solubility of DNA complexes, but no enhanced transfection activity. *Somatic Cell and Molecular Genetics*. **25**: 237-245.

Hacein-Bey-Abina, S., von Kalle, C., Schmidt, M., Le Deist, F., Wulffraat, N., McIntyre, E., *et al* (2003a) A serious adverse event after successful gene therapy for X-linked severe combined immunodeficiency. *New England Journal of Medicine*. **348**: 255-256.

Hacein-Bey-Abina, S., Le Deist, F., Carlier, F., Bouneaud, C., Hue, C., De Villartay, J.P., *et al* (2002) Sustained correction of X-linked severe combined immunodeficiency by ex vivo gene therapy. *N Engl J Med*. **346**: 1185-1193.

Hacein-Bey-Abina, S., Von Kalle, C., Schmidt, M., McCormack, M.P., Wulffraat, N., Leboulch, P., *et al* (2003b) LMO2-associated clonal T cell proliferation in two patients after gene therapy for SCID-X1. *Science*. **302**: 415-419.

Hagstrom, J.E., Sebestyen, M.G., Budker, V., Ludtke, J.J., Fritz, J.D. and Wolff, J.A. (1996) Complexes of non-cationic liposomes and histone H1 mediate efficient transfection of DNA without encapsulation. *Biochimica et Biophysica Acta*. **1284**: 47-55.

Hagstrom, J.E., Ludtke, J.J., Bassik, M.C., Sebestyen, M.G., Adam, S.A. and Wolff, J.A. (1997) Nuclear import of DNA in digitonin-permeabilized cells. *Journal of Cell Science*. **110**: 2323-2331.

Hall, M.N., Hereford, L. and Herskowitz, I. (1984) Targeting of Escherichia-Coli beta-galactosidase to the nucleus in yeast. *Cell*. **36**: 1057-1065.

Hall, M.N., Craik, C. and Hiraoka, Y. (1990) Homeodomain of yeast repressor alpha-2 contains a nuclear-localization signal. *Proceedings of the National Academy of Sciences of the United States of America*. **87**: 6954-6958.

Han, J. and Il Yeom, Y. (2000) Specific gene transfer mediated by galactosylated poly-L-lysine into hepatoma cells. *International Journal of Pharmaceutics*. **202**: 151-160.

Hansen, J.C. (2002) Conformational dynamics of the chromatin fiber in solution: determinants, mechanisms, and functions. *Annual Review of Biophysics and Biomolecular Structure*. **31**: 361-392.

Hansen, J.C. and Wolffe, A.P. (1992) Influence of chromatin folding on transcription initiation and elongation by RNA polymerase III. *Biochemistry*. **31**: 7977-7988.

Hansen, J.C., Lebowitz, J. and Demeler, B. (1994) Analytical ultracentrifugation of complex macromolecular systems. *Biochemistry*. **33**: 13155-13163.

Hansen, J.C., Ausio, J., Stanik, V.H. and van Holde, K.E. (1989) Homogeneous reconstituted oligonucleosomes, evidence for salt-dependent folding in the absence of histone H1. *Biochemistry*. **28**: 9129-9136.

Hansma, H.G., Golan, R., Hsieh, W., Lollo, C.P., Mullen-Ley, P. and Kwoh, D. (1998) DNA condensation for gene therapy as monitored by atomic force microscopy. *Nucleic Acids Res*. **26**: 2481-2487.

Hart, S.L., Arancibia-Carcamo, C.V., Wolfert, M.A., Mailhos, C., O'Reilly, N.J., Ali, R.R., *et al* (1998) Lipid-mediated enhancement of transfection by a nonviral integrin-targeting vector. *Human Gene Therapy*. **9**: 575-585.

Hasselmayer, O., Demirhan, I., Chandra, A., Bayer, M., Muller, R. and Chandra, P. (2001) Inhibition of histone-mediated gene transfer in eucaryotic cells by anti-histone IgG. *Anticancer Research*. **21**: 2377-2386.

Hayes, J.J. and Lee, K.M. (1997) *In vitro* reconstitution and analysis of mononucleosomes containing defined DNAs and proteins. *Methods-a Companion to Methods in Enzymology*. **12**: 2-9.

Hebbes, T.R., Clayton, A.L., Thorne, A.W. and Crane-Robinson, C. (1994) Core histone hyperacetylation co-maps with generalized DNase I sensitivity in the chicken beta-globin chromosomal domain. *EMBO Journal*. **13**: 1823-1830.

Heller, L., Jaroszeski, M.J., Coppola, D., Pottinger, C., Gilbert, R. and Heller, R. (2000) Electrically mediated plasmid DNA delivery to hepatocellular carcinomas *in vivo*. *Gene Therapy*. **7**: 826-829.

Henderson, B.R. and Percipalle, P. (1997) Interactions between HIV Rev and nuclear import and export factors: The Rev nuclear localisation signal mediates specific binding to human importin-beta. *Journal of Molecular Biology*. **274**: 693-707.

Herrlinger, U., Woiciechowski, C., Sena-Esteves, M., Aboody, K.S., Jacobs, A.H., Rainov, N.G., *et al* (2000) Neural precursor cells for delivery of replication-conditional HSV-1 vectors to intracerebral gliomas. *Molecular Therapy*. **1**: 347-357.

Himes, S.R. and Shannon, M.F. (2000) Assays for transcriptional activity based on the luciferase reporter gene. *Methods in Molecular Biology*. **130**: 165-174.

Himes, S.R., Coles, L.S., Katsikeros, R., Lang, R.K. and Shannon, M.F. (1993) HTLV-1 tax activation of the GM-CSF and G-CSF promoters requires the interaction of NF-kB with other transcription factor families. *Oncogene*. **8**: 3189-3197.

Hock, R., Scheer, U. and Bustin, M. (1998) Chromosomal proteins HMG-14 and HMG-17 are released from mitotic chromosomes and imported into the nucleus by active transport. *Journal of Cell Biology*. **143**: 1427-1436.

Horn, P.J. and Peterson, C.L. (2002) Molecular biology. Chromatin higher order folding-wrapping up transcription. *Science*. **297**: 1824-1827.

Hu, W. and Jans, D.A. (1999) Efficiency of importin alpha/beta-mediated nuclear localization sequence recognition and nuclear import - Differential role of NTF2. *Journal of Biological Chemistry*. **274**: 15820-15827.

Hu, Z.W. and Garen, A. (2000) Intratumoral injection of adenoviral vectors encoding tumor-targeted immunoconjugates for cancer immunotherapy. *Proceedings of the National Academy of Sciences of the United States of America*. **97**: 9221-9225.

Huard, J., Krisky, D., Oligino, T., Marconi, P., Day, C.S., Watkins, S.C. and Glorioso, J.C. (1997) Gene transfer to muscle using herpes simplex virus-based vectors. *Neuromuscular Disorders*. **7**: 299-313.

Hubner, S., Xiao, C.Y. and Jans, D.A. (1997) The protein kinase CK2 site (Ser(111/112)) enhances recognition of the Simian virus 40 large T-antigen nuclear localization sequence by importin. *Journal of Biological Chemistry*. **272**: 17191-17195.

Hubner, S., Smith, H.M.S., Hu, W., Chan, C.K., Rihs, H.P., Paschal, B.M., *et al* (1999) Plant importin alpha vinds nuclear localization sequences with high affinity and can mediate nuclear import independent of importin beta. *Journal of Biological Chemistry*. **274**: 22610-22617.

Im, D.S. and Muzyczka, N. (1989) Factors that bind to adeno-associated virus terminal repeats. *Journal of Virology*. **63**: 3095-3104.

Im, D.S. and Muzyczka, N. (1990) The Aav origin binding-protein Rep68 is an ATP-dependent site-specific endonuclease with DNA helicase activity. *Cell*. **61**: 447-457.

Im, D.S. and Muzyczka, N. (1992) Partial-purification of adenoassociated virus Rep78, Rep52, and Rep40 and their biochemical-characterization. *Journal of Virology*. **66**: 1119-1128.

Imamoto, N., Tachibana, T., Matsubae, M. and Yoneda, Y. (1995a) A karyophilic protein forms a stable complex with cytoplasmic components prior to nuclear pore binding. *Journal of Biological Chemistry*. **270**: 8559-8565.

Imamoto, N., Shimamoto, T., Takao, T., Tachibana, T., Kose, S., Matsubae, M., *et al* (1995b) *In-vivo* evidence for involvement of a 58 Kda component of nuclear pore-targeting complex in nuclear-protein import. *EMBO Journal*. **14**: 3617-3626.

Imazu, S., Nakagawa, S., Nakanishi, T., Mizuguchi, H., Uemura, H., Yamada, O. and Mayumi, T. (2000) A novel nonviral vector based on vesicular stomatitis virus. *Journal of Controlled Release*. **68**: 187-194.

Irvine, K.R., Rao, J.B., Rosenberg, S.A. and Restifo, N.P. (1996) Cytokine enhancement of DNA immunization leads to effective treatment of established pulmonary metastases. *Journal of Immunology*. **156**: 238-245.

Ito, T., Bulger, M., Kobayashi, R. and Kadonaga, J.T. (1996) Drosophila NAP-1 is a core histone chaperone that functions in ATP-facilitated assembly of regularly spaced nucleosomal arrays. *Molecular and Cellular Biology*. **16**: 3112-3124.

Izban, M.G. and Luse, D.S. (1992) Factor-stimulated RNA polymerase II transcribes at physiological elongation rates on naked DNA but very poorly on chromatin templates. *Journal of Biological Chemistry*. **267**: 13647-13655.

Jakel, S. and Gorlich, D. (1998) Importin beta, transportin, RanBP5 and RanBP7 mediate nuclear import of ribosomal proteins in mammalian cells. *EMBO Journal*. **17**: 4491-4502.

Jakel, S., Albig, W., Kutay, U., Bischoff, F.R., Schwamborn, K., Doenecke, D. and Gorlich, D. (1999) The importin beta/importin 7 heterodimer is a functional nuclear import receptor for histone H1. *EMBO Journal*. **18**: 2411-2423.

Jans, D.A. and Jans, P. (1994) Negative charge at the casein kinase-Ii site flanking the nuclear-localization signal of the Sv40 large T-antigen is mechanistically important for enhanced nuclear import. *Oncogene*. **9**: 2961-2968.

Jans, D.A., Xiao, C.Y. and Lam, M.H. (2000a) Nuclear targeting signal recognition: a key control point in nuclear transport? *Bioessays*. **22**: 532-544.

Jans, D.A., Moll, T., Nasmyth, K. and Jans, P. (1995) Cyclin-dependent kinase site-regulated signal-dependent nuclear-localization of the Swi5 yeast transcription factor in mammalian-cells. *Journal of Biological Chemistry*. **270**: 17064-17067.

Jans, D.A., Ackermann, M.J., Bischoff, J.R., Beach, D.H. and Peters, R. (1991) P34cdc2-mediated phosphorylation at T124 inhibits nuclear import of Sv40 T-antigen proteins. *Journal of Cell Biology*. **115**: 1203-1212.

Jans, D.A., Jans, P., Julich, T., Briggs, L.J., Xiao, C.Y. and Piller, S.C. (2000b) Intranuclear binding by the HIV-1 regulatory protein VPR is dependent on cytosolic factors. *Biochemical and Biophysical Research Communications*. **270**: 1055-1062.

Jenke, B.H., Fetzer, C.P., Stehle, I.M., Jonsson, F., Fackelmayer, F.O., Conradt, H., *et al* (2002) An episomally replicating vector binds to the nuclear matrix protein SAF-A in vivo. *EMBO Reports*. **3**: 349-354.

Johnson-Saliba, M. and Jans, D.A. (2001) Gene therapy: optimising DNA delivery to the nucleus. *Current Drug Targets*. **2**: 371-399.

Johnson-Saliba, M., Siddon, N.A., Clarkson, M.J., Tremethick, D.J. and Jans, D.A. (2000) Distinct importin recognition properties of histones and chromatin assembly factors. *FEBS Letters*. **467**: 169-174.

Jooss, K., Turka, L.A. and Wilson, J.M. (1998) Blunting of immune responses to adenoviral vectors in mouse liver and lung with CTLA4Ig. *Gene Therapy*. **5**: 309-319.

Kadonaga, J.T. (1998) Eukaryotic transcription: an interlaced network of transcription factors and chromatin-modifying machines. *Cell*. **92**: 307-313.

Kaffman, A., Rank, N.M. and O'Shea, E.K. (1998) Phosphorylation regulates association of the transcription factor Pho4 with its import receptor Psel/Kapl21. *Genes & Development*. **12**: 2673-2683.

Kalderon, D., Richardson, W.D., Markham, A.F. and Smith, A.E. (1984a) Sequence requirements for nuclear location of simian virus-40 large-T-antigen. *Nature*. **311**: 33-38.

Kalderon, D., Roberts, B.L., Richardson, W.D. and Smith, A.E. (1984b) A short amino-acid sequence able to specify nuclear location. *Cell*. **39**: 499-509.

Kamps, J., Koning, G.A., Velinova, M.J., Morselt, H.W.M., Wilkens, M., Gorter, A., *et al* (2000) Uptake of long-circulating immunoliposomes, directed against colon adenocarcinoma cells, by liver metastases of colon cancer. *Journal of Drug Targeting*. **8**: 235-245.

Kaneda, Y. (2000) Virosomes: evolution of the liposome as a targeted drug delivery system. *Advanced Drug Delivery Reviews*. **43**: 197-205.

Kaneda, Y., Iwai, K. and Uchida, T. (1989) Increased expression of DNA cointroduced with nuclear protein in adult rat liver. *Science*. **243**: 375-378.

Kaplitt, M.G., Leone, P., Samulski, R.J., Xiao, X., Pfaff, D.W., Omalley, K.L. and During, M.J. (1994) Long-term gene-expression and phenotypic correction using adenoassociated virus vectors in the mammalian brain. *Nature Genetics*. **8**: 148-154.

Katsel, P.L. and Greenstein, R.J. (2000) Eukaryotic gene transfer with liposomes: effect of differences in lipid structure. *Biotechnology Annual Review*. **5**: 197-220.

Kawakami, S., Wong, J., Sato, A., Hattori, Y., Yamashita, F. and Hashida, M. (2000) Biodistribution characteristics of mannosylated, fucosylated, and galactosylated liposomes in mice. *Biochimica et Biophysica Acta-General Subjects*. **1524**: 258-265.

Kearns, W.G., Afione, S.A., Fulmer, S.B., Pang, M.G., Erikson, D., Egan, M., *et al* (1996) Recombinant adeno-associated virus (AAV-CFTR) vectors do not integrate in a site-specific fashion in an immortalized epithelial cell line. *Gene Therapy*. **3**: 748-755.

Klebe, C., Prinz, H., Wittinghofer, A. and Goody, R.S. (1995) The kinetic mechanism of Ran - nucleotide exchange catalyzed by Rcc1. *Biochemistry*. **34**: 12543-12552.

Klein, T.M., Arentzen, R., Lewis, P.A. and Fitzpatrickmcelligott, S. (1992) Transformation of microbes, plants and animals by particle bombardment. *Bio-Technology*. **10**: 286-291.

Klibanov, A.L., Maruyama, K., Torchilin, V.P. and Huang, L. (1990) Amphipathic polyethyleneglycols effectively prolong the circulation time of liposomes. *FEBS Letters*. **268**: 235-237.

Kobe, B. (1999) Autoinhibition by an internal nuclear localization signal revealed by the crystal structure of mammalian importin alpha. *Nature Structural Biology*. **6**: 388-397.

Kochanek, S., Clemens, P.R., Mitani, K., Chen, H.H., Chan, S. and Caskey, C.T. (1996) A new adenoviral vector: Replacement of all viral coding sequences with 28 kb of DNA independently expressing both full-length dystrophin and beta-galactosidase. *Proceedings of the National Academy of Sciences of the United States of America*. **93**: 5731-5736.

Koeberl, D.D., Alexander, I.E., Halbert, C.L., Russell, D.W. and Miller, A.D. (1997) Persistent expression of human clotting factor IX from mouse liver after intravenous injection of adeno-associated virus vectors. *Proceedings of the National Academy of Sciences of the United States of America*. **94**: 1426-1431.

Kohler, M., Speck, C., Christiansen, M., Bischoff, F.R., Prehn, S., Haller, H., *et al* (1999) Evidence for distinct substrate specificities of importin alpha family members in nuclear protein import. *Molecular and Cellular Biology*. **19**: 7782-7791.

Kollen, W.J.W., Schembri, F.M., Gerwig, G.J., Vliegenthart, J.F.G., Glick, M.C. and Scanlin, T.F. (1999) Enhanced efficiency of lactosylated poly-L-lysine-mediated gene transfer into cystic fibrosis airway epithelial cells. *American Journal of Respiratory Cell and Molecular Biology*. **20**: 1081-1086.

Komeili, A. and O'Shea, E.K. (1999) Roles of phosphorylation sites in regulating activity of the transcription factor Pho4. *Science*. **284**: 977-980.

Kott, M., Haberland, A., Zaitsev, S., Buchberger, B., Morano, I. and Bottger, M. (1998) A new efficient method for transfection of neonatal cardiomyocytes using histone H1 in combination with DOSPER liposomal transfection reagent. *Somatic Cell and Molecular Genetics*. **24**: 257-261.

Krisky, D.M., Marconi, P.C., Oligino, T.J., Rouse, R.J.D., Fink, D.J., Cohen, J.B., *et al* (1998a) Development of herpes simplex virus replication-defective multigene vectors for combination gene therapy applications. *Gene Therapy*. **5**: 1517-1530.

Krisky, D.M., Wolfe, D., Goins, W.F., Marconi, P.C., Ramakrishnan, R., Mata, M., *et al* (1998b) Deletion of multiple immediate-early genes from herpes simplex virus reduces cytotoxicity and permits long-term gene expression in neurons. *Gene Therapy*. **5**: 1593-1603.

Kunze, K.K. and Netz, R.R. (2000) Salt-induced DNA-histone complexation. *Physical Review Letters*. **85**: 4389-4392.

Kuriyama, S., Mitoro, A., Tsujinoue, H., Nakatani, T., Yoshiji, H., Tsujimoto, T., *et al* (2000) Particle-mediated gene transfer into murine livers using a newly developed gene gun. *Gene Therapy*. **7**: 1132-1136.

Kurz, M., Doenecke, D. and Albig, W. (1997) Nuclear transport of H1 histones meets the criteria of a nuclear localization signal-mediated process. *Journal of Cellular Biochemistry*. **64**: 573-578.

Lachmann, R.H. and Efstathiou, S. (1999) Use of herpes simplex virus type I for transgene expression within the nervous system. *Clinical Science*. **96**: 533-541.

Lachmann, R.H., Sadarangani, M., Atkinson, H.R. and Efstathiou, S. (1999) An analysis of herpes simplex virus gene expression during latency establishment and reactivation. *Journal of General Virology*. **80**: 1271-1282.

Ladoux, B., Quivy, J.P., Doyle, P., du Roure, O., Almouzni, G. and Viovy, J.L. (2000) Fast kinetics of chromatin assembly revealed by single-molecule videomicroscopy and scanning force microscopy. *Proceedings of the National Academy of Sciences of the United States of America*. **97**: 14251-14256.

Lam, M.H.C., Briggs, L.J., Hu, W., Martin, T.J., Gillespie, M.T. and Jans, D.A. (1999) Importin beta recognizes parathyroid hormone-related protein with high affinity and mediates its nuclear import in the absence of importin alpha. *Journal of Biological Chemistry*. **274**: 7391-7398.

Lanford, R.E. and Butel, J.S. (1984) Construction and Characterization of an Sv40 Mutant Defective in Nuclear Transport of T-Antigen. *Cell*. **37**: 801-813.

Langer, T. (2000) Nuclear transport of histone 2b in mammalian cells is signal- and energy-dependent and different from the importin alpha/beta-mediated process. *Histochemistry and Cell Biology*. **113**: 455-465.

Larsen, C.E., Nir, S., Alford, D.R., Jennings, M., Lee, K.D. and Duzgunes, N. (1993) Human immunodeficiency virus type 1 (HIV-1) fusion with model membranes: kinetic analysis and the role of lipid composition, pH and divalent cations. *Biochimica et Biophysica Acta*. **1147**: 223-236.

Latchman, D.S. (2003) Herpes simplex virus vectors for Parkinson's disease. *International Reviews in Neurobiology*. **55**: 223-241.

Lechardeur, D., Sohn, K.J., Haardt, M., Joshi, P.B., Monck, M., Graham, R.W., *et al* (1999) Metabolic instability of plasmid DNA in the cytosol: a potential barrier to gene transfer. *Gene Therapy*. **6**: 482-497.

Lee, R.J. and Huang, L. (1996) Folate-targeted, anionic liposome-entrapped polylysine-condensed DNA for tumor cell-specific gene transfer. *Journal of Biological Chemistry*. **271**: 8481-8487.

Leuba, S.H., Bustamante, C., van Holde, K. and Zlatanova, J. (1998) Linker histone tails and N-tails of histone H3 are redundant: scanning force microscopy studies of reconstituted fibers. *Biophysical Journal*. **74**: 2830-2839.

Liang, W.W., Shi, X.L., Deshpande, D., Malanga, C.J. and Rojanasakul, Y. (1996) Oligonucleotide targeting to alveolar macrophages by mannose receptor-mediated endocytosis. *Biochimica et Biophysica Acta-Biomembranes*. **1279**: 227-234.

Lin, M.T.S., Pulkkinen, L., Uitto, J. and Yoon, K. (2000) The gene gun: current applications in cutaneous gene therapy. *International Journal of Dermatology*. **39**: 161-170.

Lin, P. and Clarke, H.J. (1996) Somatic histone H1 microinjected into fertilized mouse eggs is transported into the pronuclei but does not disrupt subsequent preimplantation development. *Molecular Reproduction and Development*. **44**: 185-192.

Lipps, H.J., Jenke, A.C., Nehlsen, K., Scinteie, M.F., Stehle, I.M. and Bode, J. (2003) Chromosome-based vectors for gene therapy. *Gene*. **304**: 23-33.

Liu, F., Qi, H., Huang, L. and Liu, D. (1997) Factors controlling the efficiency of cationic lipid-mediated transfection in vivo via intravenous administration. *Gene Therapy*. **4**: 517-523.

Logie, C. and Peterson, C.L. (1997) Catalytic activity of the yeast SWI/SNF complex on reconstituted nucleosome arrays. *EMBO Journal*. **16**: 6772-6782.

Lou, E. (2003) Oncolytic herpes viruses as a potential mechanism for cancer therapy. *Acta Oncologica*. **42**: 660-671.

Lucius, H., Haberland, A., Zaitsev, S., Dalluge, R., Schneider, M. and Bottger, M. (2001) Structure of transfection-active histone H1/DNA complexes. *Molecular Biology Reports*. **28**: 157-165.

Ludtke, J.J., Zhang, G., Sebestyen, M.G. and Wolff, J.A. (1999) A nuclear localization signal can enhance both the nuclear transport and expression of 1 kb DNA. *Journal of Cell Science*. **112**: 2033-2041.

Luger, K. (2003) Structure and dynamic behavior of nucleosomes. *Current Opinion in Genetics and Development*. **13**: 127-135.

Luger, K. and Richmond, T.J. (1998) The histone tails of the nucleosome. *Current Opinion in Genetics and Development*. **8**: 140-146.

Luger, K., Rechsteiner, T.J. and Richmond, T.J. (1999) Preparation of nucleosome core particle from recombinant histones. *Methods in Enzymology*. **304**: 3-19.

Luger, K., Mader, A.W., Richmond, R.K., Sargent, D.F. and Richmond, T.J. (1997) Crystal structure of the nucleosome core particle at 2.8 A resolution. *Nature*. **389**: 251-260.

Lukacs, G.L., Haggie, P., Seksek, O., Lechardeur, D., Freedman, N. and Verkman, A.S. (2000) Size-dependent DNA mobility in cytoplasm and nucleus. *Journal of Biological Chemistry*. **275**: 1625-1629.

Luo, D. and Saltzman, W.M. (2000) Synthetic DNA delivery systems. *Nature Biotechnology*. **18**: 33-37.

Mack, C.A., Song, W.R., Carpenter, H., Wickham, T.J., Kovesdi, I., Harvey, B.G., *et al* (1997) Circumvention of anti-adenovirus neutralizing immunity by administration of an adenoviral vector of an alternate serotype. *Human Gene Therapy*. **8**: 99-109.

Maeda, T., Kawasaki, K. and Ohnishi, S. (1981) Interaction of influenza-virus hemagglutinin with target membrane-lipids is a key step in virus-induced hemolysis and fusion at pH 5.2. *Proceedings of the National Academy of Sciences of the United States of America-Biological Sciences*. **78**: 4133-4137.

Mahvi, D.M., Burkholder, J.K., Turner, J., Culp, J., Malter, J.S., Sondel, P.M. and Yang, N.S. (1996) Particle-mediated gene transfer of granulocyte-macrophage colony-stimulating factor cDNA to tumor cells: Implications for a clinically relevant tumor vaccine. *Human Gene Therapy*. **7**: 1535-1543.

Marconi, P., Krisky, D., Oligino, T., Poliani, P.L., Ramakrishnan, R., Goins, W.F., *et al* (1996) Replication-defective herpes simplex virus vectors for gene transfer in vivo. *Proceedings of the National Academy of Sciences of the United States of America*. **93**: 11319-11320.

Martin, F.J. and Papahadjopoulos, D. (1982) Irreversible coupling of immunoglobulin fragments to preformed vesicles - an improved method for liposome targeting. *Journal of Biological Chemistry*. **257**: 286-288.

Maruyama, K. (2000) In vivo targeting by liposomes. *Biological & Pharmaceutical Bulletin*. **23**: 791-799.

Mathiesen, I. (1999) Electropermeabilization of skeletal muscle enhances gene transfer *in vivo*. *Gene Therapy*. **6**: 508-514.

Matsui, H., Johnson, L.G., Randell, S.H. and Boucher, R.C. (1997) Loss of binding and entry of liposome-DNA complexes decreases transfection efficiency in differentiated airway epithelial cells. *Journal of Biological Chemistry*. **272**: 1117-1126.

Michael, W.M., Eder, P.S. and Dreyfuss, G. (1997) The K nuclear shuttling domain: A novel signal for nuclear import and nuclear export in the hnRNP K protein. *EMBO Journal*. **16**: 3587-3598.

Miller, A.D., Miller, D.G., Garcia, J.V. and Lynch, C.M. (1993) Use of retroviral vectors for gene transfer and expression. *Methods in Enzymology*. **217**: 581-599.

Miller, D.G., Edwards, R.H. and Miller, A.D. (1994) Cloning of the cellular receptor for amphotropic murine retroviruses reveals homology to that for gibbon ape leukemia-virus. *Proceedings of the National Academy of Sciences of the United States of America*. **91**: 78-82.

Mir, L.M., Bureau, M.F., Gehl, J., Rangara, R., Rouy, D., Caillaud, J.M., *et al* (1999) High-efficiency gene transfer into skeletal muscle mediated by electric pulses. *Proceedings of the National Academy of Sciences of the United States of America*. **96**: 4262-4267.

Miyake, K., Suzuki, N., Matsuoka, H., Tohyama, T. and Shimada, T. (1998) Stable integration of human immunodeficiency virus-based retroviral vectors into the chromosomes of nondividing cells. *Human Gene Therapy*. **9**: 467-475.

Miyamoto, Y., Imamoto, N., Sekimoto, T., Tachibana, T., Seki, T., Tada, S., *et al* (1997) Differential modes of nuclear localization signal (NLS) recognition by three distinct classes of NLS receptors. *Journal of Biological Chemistry*. **272**: 26375-26381.

Miyatake, S.I., Tani, S., Feigenbaum, F., Sundaresan, P., Toda, H., Narumi, O., *et al* (1999) Hepatoma-specific antitumor activity of an albumin enhancer promoter regulated herpes simplex virus *in vivo*. *Gene Therapy*. **6**: 564-572.

Moll, T., Tebb, G., Surana, U., Robitsch, H. and Nasmyth, K. (1991) The role of phosphorylation and the Cdc28 protein-kinase in cell-cycle regulated nuclear import of the *Saccharomyces cerevisiae* transcription factor-Swi5. *Cell*. **66**: 743-758.

Moore, J.D., Yang, J., Truant, R. and Kornbluth, S. (1999) Nuclear import of Cdk/cyclin complexes: Identification of distinct mechanisms for import of Cdk2/cyclin E and Cdc2/cyclin B1. *Journal of Cell Biology*. **144**: 213-224.

Moreland, R.B., Langevin, G.L., Singer, R.H., Garcea, R.L. and Hereford, L.M. (1987) Amino acid sequences that determine the nuclear localization of yeast histone 2B. *Molecular and Cellular Biology*. **7**: 4048-4057.

Morishita, R., Gibbons, G.H., Kaneda, Y., Ogihara, T. and Dzau, V.J. (1994) Pharmacokinetics of antisense oligodeoxyribonucleotides (Cyclin-B-1 and Cdc-2 Kinase) in the vessel wall *in vivo* - enhanced therapeutic utility for restenosis by HVJ-liposome delivery. *Gene*. **149**: 13-19.

Moroianu, J., Blobel, G. and Radu, A. (1995a) Previously identified protein of uncertain function is karyopherin-alpha and together with karyopherin-beta docks import substrate at nuclear-pore complexes. *Proceedings of the National Academy of Sciences of the United States of America*. **92**: 2008-2011.

Moroianu, J., Hijikata, M., Blobel, G. and Radu, A. (1995b) Mammalian karyopherin alpha(1)beta and alpha(2)beta heterodimers - alpha(1) or alpha(2) subunit binds nuclear-localization signal and beta-subunit interacts with peptide repeat-containing nucleoporins. *Proceedings of the National Academy of Sciences of the United States of America*. **92**: 6532-6536.

Mosammaparast, N., Ewart, C.S. and Pemberton, L.F. (2002a) A role for nucleosome assembly protein 1 in the nuclear transport of histones H2A and H2B. *EMBO Journal*. **21**: 6527-6538.

Mosammaparast, N., Guo, Y., Shabanowitz, J., Hunt, D.F. and Pemberton, L.F. (2002b) Pathways mediating the nuclear import of histones H3 and H4 in yeast. *Journal of Biological Chemistry*. **277**: 862-868.

Mosammaparast, N., Jackson, K.R., Guo, Y., Brame, C.J., Shabanowitz, J., Hunt, D.F. and Pemberton, L.F. (2001) Nuclear import of histone H2A and H2B is mediated by a network of karyopherins. *Journal of Cell Biology*. **153**: 251-262.

Mosialos, G., Hamer, P., Capobianco, A.J., Laursen, R.A. and Gilmore, T.D. (1991) A protein kinase-a recognition sequence is structurally linked to transformation by P59v-Rel and cytoplasmic retention of P68c-Rel. *Molecular and Cellular Biology*. **11**: 5867-5877.

Moss, T., Cary, P.D., Abercrombie, B.D., Cranerobinson, C. and Bradbury, E.M. (1976) pH-dependent interaction between histones H2a and H2b involving secondary and tertiary folding. *European Journal of Biochemistry*. **71**: 337-350.

Muhlhausser, P., Muller, E.C., Otto, A. and Kutay, U. (2001) Multiple pathways contribute to nuclear import of core histones. *EMBO Reports*. **2**: 690-696.

Mui, B., Ahkong, Q.F., Chow, L. and Hope, M.J. (2000) Membrane perturbation and the mechanism of lipid-mediated transfer of DNA into cells. *Biochimica et Biophysica Acta-Biomembranes*. **1467**: 281-292.

Muramatsu, T., Nakamura, A. and Park, H.M. (1998) *In vivo* electroporation: A powerful and convenient means of nonviral gene transfer to tissues of living animals. *International Journal of Molecular Medicine*. **1**: 55-62.

Nadler, S.G., Tritschler, D., Haffar, O.K., Blake, J., Bruce, A.G. and Cleaveland, J.S. (1997) Differential expression and sequence-specific interaction of karyopherin alpha with nuclear localization sequences. *Journal of Biological Chemistry*. **272**: 4310-4315.

Nakagawa, T., Bulger, M., Muramatsu, M. and Ito, T. (2001) Multistep chromatin assembly on supercoiled plasmid DNA by nucleosome assembly protein-1 and ATP-utilizing chromatin assembly and remodeling factor. *Journal of Biological Chemistry*. **276**: 27384-27391.

Naldini, L., Blomer, U., Gage, F.H., Trono, D. and Verma, I.M. (1996a) Efficient transfer, integration, and sustained long-term expression of the transgene in adult rat brains injected with a lentiviral vector. *Proceedings of the National Academy of Sciences of the United States of America*. **93**: 11382-11388.

Naldini, L., Blomer, U., Gallay, P., Ory, D., Mulligan, R., Gage, F.H., *et al* (1996b) *In vivo* gene delivery and stable transduction of nondividing cells by a lentiviral vector. *Science*. **272**: 263-267.

Neumann, E. and Rosenheck, K (1972) Permeability Changes Induced by Electric Impulses in Vesicular Membranes. *Journal of Membrane Biology*. **10**: 279-290.

Neumann, E., Schaeferridder, M., Wang, Y. and Hofschneider, P.H. (1982) Gene-transfer into mouse lyoma cells by electroporation in high electric-fields. *EMBO Journal*. **1**: 841-845.

Neves, C., Byk, G., Scherman, D. and Wils, P. (1999a) Coupling of a targeting peptide to plasmid DNA by covalent triple helix formation. *FEBS Letters*. **453**: 41-45.

Neves, C., Escriou, V., Byk, G., Scherman, D. and Wils, P. (1999b) Intracellular fate and nuclear targeting of plasmid DNA. *Cell Biology and Toxicology*. **15**: 193-202.

Ng, K.W., Ridgway, P., Cohen, D.R. and Tremethick, D.J. (1997) The binding of a Fos/Jun heterodimer can completely disrupt the structure of a nucleosome. *EMBO Journal*. **16**: 2072-2085.

Nishi, T., Yoshizato, K., Yamashiro, S., Takeshima, H., Sato, K., Hamada, K., *et al* (1996) High-efficiency in vivo gene transfer using intraarterial plasmid DNA injection following in vivo electroporation. *Cancer Research*. **56**: 1050-1055.

Nishizaki, K., Mazda, O., Dohi, Y., Satoh, E., Kawata, T., Mizuguchi, K., *et al* (2000) *In vivo* gene transfer into rat hearts with Epstein-Barr virus-based episomal vectors using a gene gun. *Transplantation Proceedings*. **32**: 2413-2414.

Norris, J.L. and Manley, J.L. (1992) Selective nuclear transport of the Drosophila morphogen dorsal can be established by a signaling pathway involving the transmembrane protein Toll and protein kinase-A. *Genes & Development*. **6**: 1654-1667.

Ogier, G., Michal, Y., Thomas, V., Quash, G. and Rodwell, J.D. (1994) Inhibition of Type-5 adenovirus infectivity by periodate-oxidation. *Archives of Virology*. **135**: 43-60.

Oligino, T., Ghivizzani, S.C., Wolfe, D., Lechman, E.R., Krisky, D., Mi, Z., *et al* (1999) Intra-articular delivery of a herpes simplex virus IL-1Ra gene vector reduces inflammation in a rabbit model of arthritis. *Gene Therapy*. **6**: 1713-1720.

Orphanides, G. and Reinberg, D. (2000) RNA polymerase II elongation through chromatin. *Nature*. **407**: 471-475.

Parente, R.A., Nir, S. and Szoka, F.C. (1990) Mechanism of leakage of phospholipid vesicle contents induced by the peptide Gala. *Biochemistry*. **29**: 8720-8728.

Paul, R.W., Weisser, K.E., Loomis, A., Sloane, D.L., LaFoe, D., Atkinson, E.M. and Overell, R.W. (1997) Gene transfer using a novel fusion protein, GAL4/invasin. *Human Gene Therapy*. **8**: 1253-1262.

Pector, V., Backmann, J., Maes, D., Vandenbranden, M. and Ruysschaert, J.M. (2000) Biophysical and structural properties of DNA center dot diC(14)-amidine complexes - Influence of the DNA/lipid ratio. *Journal of Biological Chemistry*. **275**: 29533-29538.

Perales, J.C., Ferkol, T., Beegen, H., Ratnoff, O.D. and Hanson, R.W. (1994) Gene-transfer *in vivo* - sustained expression and regulation of genes introduced into the liver by receptor-targeted uptake. *Proceedings of the National Academy of Sciences of the United States of America*. **91**: 4086-4090.

Perales, J.C., Grossmann, G.A., Molas, M., Liu, G., Ferkol, T., Harpst, J., *et al* (1997) Biochemical and functional characterization of DNA complexes capable of targeting genes to hepatocytes via the asialoglycoprotein receptor. *Journal of Biological Chemistry*. **272**: 7398-7407.

Petersen, S.E. (1986) Accuracy and reliability of flow cytometric DNA analysis using a simple, one-step ethidium bromide staining protocol. *Cytometry*. **7**: 301-306.

Pieroni, L., Fipaldini, C., Monciotti, A., Cimini, D., Sgura, A., Fattori, E., *et al* (1998) Targeted integration of adeno-associated virus-derived plasmids in transfected human cells. *Virology*. **249**: 249-259.

Plank, C., Oberhauser, B., Mechtler, K., Koch, C. and Wagner, E. (1994) The influence of endosome-disruptive peptides on gene-transfer using synthetic virus-like gene-transfer systems. *Journal of Biological Chemistry*. **269**: 12918-12924.

Pollard, H., Toumaniantz, G., Amos, J.L., Avet-Loiseau, H., Guihard, G., Behr, J.P. and Escande, D. (2001) Ca^{2+}-sensitive cytosolic nucleases prevent efficient delivery to the nucleus of injected plasmids. *Journal of Gene Medicine*. **3**: 153-164.

Porter, C.D., Collins, M.K.L., Tailor, C.S., Parkar, M.H., Cosset, F.L., Weiss, R.A. and Takeuchi, Y. (1996) Comparison of efficiency of infection of human gene therapy target cells via four different retroviral receptors. *Human Gene Therapy*. **7**: 913-919.

Poste, G., Bucana, C., Raz, A., Bugelski, P., Kirsh, R. and Fidler, I.J. (1982) Analysis of the fate of systemically administered liposomes and implications for their use in drug delivery. *Cancer Research*. **42**: 1412-1422.

Pouton, C.W. and Seymour, L.W. (2001) Key issues in non-viral gene delivery. *Advanced Drug Delivery Reviews*. **46**: 187-203.

Prieve, M.G., Guttridge, K.L., Munguia, J. and Waterman, M.L. (1998) Differential importin-alpha recognition and nuclear transport by nuclear localization signals within the high-mobility-group DNA binding domains of lymphoid enhancer factor 1 and T-cell factor 1. *Molecular and Cellular Biology*. **18**: 4819-4832.

Radler, J.O., Koltover, I., Salditt, T. and Safinya, C.R. (1997) Structure of DNA-cationic liposome complexes: DNA intercalation in multilamellar membranes in distinct interhelical packing regimes. *Science*. **275**: 810-814.

Radu, A., Blobel, G. and Moore, M.S. (1995) Identification of a protein complex that is required for nuclear-protein import and mediates docking of import substrate to distinct nucleoporins. *Proceedings of the National Academy of Sciences of the United States of America*. **92**: 1769-1773.

Rakhmilevich, A.L., Janssen, K., Turner, J., Culp, J. and Yang, N.S. (1997) Cytokine gene therapy of cancer using gene gun technology: Superior antitumor activity of interleukin-12. *Human Gene Therapy*. **8**: 1303-1311.

Rakhmilevich, A.L., Timmins, J.G., Janssen, K., Pohlmann, E.L., Sheehy, M.J. and Yang, N.S. (1999) Gene gun-mediated IL-12 gene therapy induces antitumor effects in the absence of toxicity: A direct comparison with systemic IL-12 protein therapy. *Journal of Immunotherapy*. **22**: 135-144.

Ramani, K., Bora, R.S., Kumar, M., Tyagi, S.K. and Sarkar, D.P. (1997) Novel gene delivery to liver cells using engineered virosomes. *FEBS Letters*. **404**: 164-168.

Ramani, K., Hassan, Q., Venkaiah, B., Hasnain, S.E. and Sarkar, D.P. (1998) Site-specific gene delivery in vivo through engineered Sendai viral envelopes. *Proceedings of the National Academy of Sciences of the United States of America*. **95**: 11886-11890.

Rao, S., Procko, E. and Shannon, M.F. (2001) Chromatin remodeling, measured by a novel real-time polymerase chain reaction assay, across the proximal promoter region of the IL-2 gene. *J Immunol*. **167**: 4494-4503.

Reddy, J.A. and Low, P.S. (2000) Enhanced folate receptor mediated gene therapy using a novel pH-sensitive lipid formulation. *Journal of Controlled Release*. **64**: 27-37.

Reddy, J.A., Dean, D., Kennedy, M.D. and Low, P.S. (1999) Optimization of folate-conjugated liposomal vectors for folate receptor-mediated gene therapy. *Journal of Pharmaceutical Sciences*. **88**: 1112-1118.

Remy, J.S., Abdallah, B., Zanta, M.A., Boussif, O., Behr, J.P. and Demeneix, B. (1998) Gene transfer with lipospermines and polyethylenimines. *Advanced Drug Delivery Reviews*. **30**: 85-95.

Rexach, M. and Blobel, G. (1995) Protein Import into Nuclei - Association and Dissociation Reactions Involving Transport Substrate, Transport Factors, and Nucleoporins. *Cell*. **83**: 683-692.

Richmond, T.J., Searles, M.A. and Simpson, R.T. (1988) Crystals of a nucleosome core particle containing defined sequence DNA. *Journal of Molecular Biology*. **199**: 161-170.

Rihs, H.P., Jans, D.A., Fan, H. and Peters, R. (1991) The rate of nuclear cytoplasmic protein-transport Is determined by the casein kinase-Ii site flanking the nuclear-localization sequence of the Sv40 T-antigen. *EMBO Journal*. **10**: 633-639.

Rizzuto, G., Cappelletti, M., Maione, D., Savino, R., Lazzaro, D., Costa, P., *et al* (1999) Efficient and regulated erythropoietin production by naked DNA injection and muscle electroporation. *Proceedings of the National Academy of Sciences of the United States of America*. **96**: 6417-6422.

Robbins, J., Dilworth, S.M., Laskey, R.A. and Dingwall, C. (1991) 2 Interdependent basic domains in nucleoplasmin nuclear targeting sequence - identification of a class of bipartite nuclear targeting sequence. *Cell*. **64**: 615-623.

Robbins, P.D. and Ghivizzani, S.C. (1998) Viral vectors for gene therapy. *Pharmacology and Therapeutics*. **80**: 35-47.

Robello, M. and Gliozzi, A. (1989) Conductance transition induced by an electric-field in lipid bilayers. *Biochimica et Biophysica Acta*. **982**: 173-176.

Robinson, H.L. (1999) DNA vaccines: Basic mechanism and immune responses. *International Journal of Molecular Medicine*. **4**: 549-555.

Roe, T.Y., Reynolds, T.C., Yu, G. and Brown, P.O. (1993) Integration of murine leukemia-virus DNA depends on mitosis. *EMBO Journal*. **12**: 2099-2108.

Rolling, F. and Samulski, R.J. (1995) Aav as a viral vector for human gene therapy - generation of recombinant virus. *Molecular Biotechnology*. **3**: 9-15.

Rols, M.P. and Teissie, J. (1990) Electropermeabilization of mammalian cells - quantitative analysis of the phenomenon. *Biophysical Journal*. **58**: 1089-1098.

Rols, M.P., Coulet, D. and Teissie, J. (1992) Highly efficient transfection of mammalian cells by electric-field pulses - application to large volumes of cell-culture by using a flow system. *European Journal of Biochemistry*. **206**: 115-121.

Rosenberg, S.A., Aebersold, P., Cornetta, K., Kasid, A., Morgan, R.A., Moen, R., *et al* (1990) Gene-transfer into humans - immunotherapy of patients with advanced melanoma, using tumor-infiltrating lymphocytes modified by retroviral gene transduction. *New England Journal of Medicine*. **323**: 570-578.

Roth, J.A., Swisher, S.G., Merritt, J.A., Lawrence, D.D., Kemp, B.L., Carrasco, C.H., *et al* (1998) Gene therapy for non-small cell lung cancer: A preliminary report of a phase I trial of adenoviral p53 gene replacement. *Seminars in Oncology*. **25**: 33-37.

Roulon, T., Helene, C. and Escude, C. (2002) Coupling of a targeting peptide to plasmid DNA using a new type of padlock oligonucleotide. *Bioconjugate Chemistry*. **13**: 1134-1139.

Rouse, R.J.D., Seifried, W., Mistry, S.K., Goins, W.F. and Glorioso, J.C. (2000) Herpes simplex virus-enhanced cationic lipid/DNA-mediated transfection. *Biotechniques*. **29**: 810-814.

Rout, M.P. and Blobel, G. (1993) Isolation of the yeast nuclear pore complex. *Journal of Cell Biology*. **123**: 771-783.

Rout, M.P. and Aitchison, J.D. (2001) The nuclear pore complex as a transport machine. *Journal of Biological Chemistry*. **276**: 16593-16596.

Rout, M.P., Aitchison, J.D., Magnasco, M.O. and Chait, B.T. (2003) Virtual gating and nuclear transport: the hole picture. *Trends in Cell Biology*. **13**: 622-628.

Russell, D.W., Miller, A.D. and Alexander, I.E. (1994) Adenoassociated virus vectors preferentially transduce cells in S-phase. *Proceedings of the National Academy of Sciences of the United States of America*. **91**: 8915-8919.

Sakai, T., Hisaeda, H., Nakano, Y., Ishikawa, H., Maekawa, Y., Ishii, K., *et al* (2000) Gene gun-mediated delivery of an interleukin-12 expression plasmid protects against infections with the intracellular protozoan parasites Leishmania major and *Trypanosoma cruzi* in mice. *Immunology*. **99**: 615-624.

Salman, H., Zbaida, D., Rabin, Y., Chatenay, D. and Elbaum, M. (2001) Kinetics and mechanism of DNA uptake into the cell nucleus. *Proceedings of the National Academy of Sciences of the United States of America*. **98**: 7247-7252.

Samulski, R.J. (1993) Adeno-associated virus: integration at a specific chromosomal locus. *Current Opinion in Genetics and Development*. **3**: 74-80.

Sandaltzopoulos, R., Blank, T. and Becker, P.B. (1994) Transcriptional repression by nucleosomes but not H1 in reconstituted preblastoderm Drosophila chromatin. *EMBO Journal*. **13**: 373-379.

Saravolac, E.G., Ludkovski, O., Skirrow, R., Ossanlou, M., Zhang, Y.P., Giesbrecht, C., *et al* (2000) Encapsulation of plasmid DNA in stabilized plasmid-lipid particles composed of different cationic lipid concentration for optimal transfection activity. *Journal of Drug Targeting*. **7**: 423-437.

Schaeferridder, M., Wang, Y. and Hofschneider, P.H. (1982) Liposomes as Gene Carriers - Efficient Transformation of Mouse L-Cells by Thymidine Kinase Gene. *Science*. **215**: 166-168.

Schoen, P., Chonn, A., Cullis, P.R., Wilschut, J. and Scherrer, P. (1999) Gene transfer mediated by fusion protein hemagglutinin reconstituted in cationic lipid vesicles. *Gene Therapy*. **6**: 823-832.

Schwamborn, K., Albig, W. and Doenecke, D. (1998) The histone H1(0) contains multiple sequence elements for nuclear targeting. *Experimental Cell Research*. **244**: 206-217.

Schwarz, P.M. and Hansen, J.C. (1994) Formation and stability of higher order chromatin structures. Contributions of the histone octamer. *Journal of Biological Chemistry*. **269**: 16284-16289.

Sebestyen, M.G., Ludtke, J.J., Bassik, M.C., Zhang, G.F., Budker, V., Lukhtanov, E.A., *et al* (1998) DNA vector chemistry: The covalent attachment of signal peptides to plasmid DNA. *Nature Biotechnology*. **16**: 80-85.

Seglen, P.O. (1983) Inhibitors of lysosomal function. *Methods in Enzymology*. **96**: 737-764.

Seksek, O., Biwersi, J. and Verkman, A.S. (1997) Translational diffusion of macromolecule-sized solutes in cytoplasm and nucleus. *Journal of Cell Biology*. **138**: 131-142.

Seth, P., Fitzgerald, D.J., Willingham, M.C. and Pastan, I. (1984) Role of a low-pH environment in adenovirus enhancement of the toxicity of a Pseudomonas exotoxin-epidermal growth factor conjugate. *Journal of Virology*. **51**: 650-655.

Shirakawa, F. and Mizel, S.B. (1989) *In vitro* activation and nuclear translocation of NF-kappa-B catalyzed by cyclic AMP-dependent protein kinase and protein kinase C. *Molecular and Cellular Biology*. **9**: 2424-2430.

Siddon, N.A. and Tremethick, D.J. (1999) The role of histone acetylation in regulating gene expression. *Australian Biochemistry*. **30**: 5-7.

Simoes, S., Slepushkin, V., Gaspar, R., de Lima, M.C.P. and Duzgunes, N. (1998) Gene delivery by negatively charged ternary complexes of DNA, cationic liposomes and transferrin or fusigenic peptides. *Gene Therapy*. **5**: 955-964.

Simoes, S., Slepushkin, V., Pires, P., Gaspar, R., de Lima, M.C.P. and Duzgunes, N. (1999) Mechanisms of gene transfer mediated by lipoplexes associated with targeting ligands or pH-sensitive peptides. *Gene Therapy*. **6**: 1798-1807.

Simon, R.H. and Felsenfeld, G. (1979) New procedure for purifying histone pairs H2a + H2b and H-3 + H-4 from chromatin using hydroxylapatite. *Nucleic Acids Research*. **6**: 689-696.

Simpson, R.T., Thoma, F. and Brubaker, J.M. (1985) Chromatin reconstituted from tandemly repeated cloned DNA fragments and core histones: a model system for study of higher order structure. *Cell*. **42**: 799-808.

Singh, D. and Rigby, P.W. (1996) The use of histone as a facilitator to improve the efficiency of retroviral gene transfer. *Nucleic Acids Res*. **24**: 3113-3114.

Singh, M. (1999) Transferrin as a targeting ligand for liposomes and anticancer drugs. *Current Pharmaceutical Design*. **5**: 443-451.

Siomi, H., Shida, H., Maki, M. and Hatanaka, M. (1990) Effects of a highly basic region of human-immunodeficiency-virus Tat protein on nucleolar localization. *Journal of Virology*. **64**: 1803-1807.

Smith, H.M.S., Hicks, G.R. and Raikhel, N.V. (1997) Importin alpha from *Arabidopsis thaliana* is a nuclear import receptor that recognizes three classes of import signals. *Plant Physiology*. **114**: 411-417.

Smith, R.M. and Wu, G.Y. (1999) Hepatocyte-directed gene delivery by receptor-mediated endocytosis. *Seminars in Liver Disease*. **19**: 83-92.

Sonawane, N.D., Szoka, F.C., Jr. and Verkman, A.S. (2003) Chloride accumulation and swelling in endosomes enhances DNA transfer by polyamine-DNA polyplexes. *Journal of Biological Chemistry*. **278**: 44826-44831.

Sorgi, F.L., Bhattacharya, S. and Huang, L. (1997) Protamine sulfate enhances lipid-mediated gene transfer. *Gene Therapy*. **4**: 961-968.

Spiller, D.G., Giles, R.V., Grzybowski, J., Tidd, D.M. and Clark, R.E. (1998) Improving the intracellular delivery and molecular efficacy of antisense oligonucleotides in chronic myeloid leukemia cells: A comparison of streptolysin-O permeabilization, electroporation, and lipophilic conjugation. *Blood*. **91**: 4738-4746.

Srivastava, A., Lusby, E.W. and Berns, K.I. (1983) Nucleotide-sequence and organization of the adeno-associated virus-2 genome. *Journal of Virology*. **45**: 555-564.

Steward, R. (1989) Relocalization of the dorsal protein from the cytoplasm to the nucleus correlates with its function. *Cell*. **59**: 1179-1188.

Subbarao, N.K., Parente, R.A., Szoka, F.C., Jr., Nadasdi, L. and Pongracz, K. (1987) pH-dependent bilayer destabilization by an amphipathic peptide. *Biochemistry*. **26**: 2964-2972.

Subramanian, A., Ranganathan, P. and Diamond, S.L. (1999) Nuclear targeting peptide scaffolds for lipofection of nondividing mammalian cells. *Nature Biotechnology*. **17**: 873-877.

Summerford, C. and Samulski, R.J. (1998) Membrane-associated heparan sulfate proteoglycan is a receptor for adeno-associated virus type 2 virions. *Journal of Virology*. **72**: 1438-1445.

Summerford, C., Bartlett, J.S. and Samulski, R.J. (1999) alpha V beta 5 integrin: a co-receptor for adeno-associated virus type 2 infection. *Nature Medicine*. **5**: 78-82.

Surosky, R.T., Urabe, M., Godwin, S.G., McQuiston, S.A., Kurtzman, G.J., Ozawa, K. and Natsoulis, G. (1997) Adeno-associated virus Rep proteins target DNA sequences to a unique locus in the human genome. *Journal of Virology*. **71**: 7951-7959.

Suto, R.K., Clarkson, M.J., Tremethick, D.J. and Luger, K. (2000) Crystal structure of a nucleosome core particle containing the variant histone H2A.Z. *Nature Structural Biology*. **7**: 1121-1124.

Suzuki, S. and Shimada, T. (2000) A retroviral vector capable of targeted gene transfer into cells expressing HIV envelope glycoprotein. *Biochemical and Biophysical Research Communications*. **271**: 672-676.

Suzuki, T., Shin, B.C., Fujikura, K., Matsuzaki, T. and Takata, K. (1998) Direct gene transfer into rat liver cells by *in vivo* electroporation. *FEBS Letters*. **425**: 436-440.

Synnes, M., Prydz, K., Lovdal, T., Brech, A. and Berg, T. (1999) Fluid phase endocytosis and galactosyl receptor-mediated endocytosis employ different early endosomes. *Biochimica et Biophysica Acta-Biomembranes*. **1421**: 317-328.

Tanelian, D.L., Barry, M.A., Johnston, S.A., Le, T. and Smith, G. (1997) Controlled gene gun delivery and expression of DNA within the cornea. *Biotechniques*. **23**: 484-&.

Tanigawa, K., Yu, H., Sun, R., Nickoloff, B.J. and Chang, A.E. (2000) Gene gun application in the generation of effector T cells for adoptive immunotherapy. *Cancer Immunology Immunotherapy*. **48**: 635-643.

Thoma, F., Losa, R. and Koller, T. (1983) Involvement of the domains of histones H1 and H5 in the structural organization of soluble chromatin. *Journal of Molecular Biology*. **167**: 619-640.

Thomas, J.O. and Butler, P.J. (1977) Characterization of the octamer of histones free in solution. *Journal of Molecular Biology*. **116**: 769-781.

Toda, M., Rabkin, S.D., Kojima, H. and Martuza, R.L. (1999) Herpes simplex virus as an in situ cancer vaccine for the induction of specific anti-tumor immunity. *Human Gene Therapy*. **10**: 385-393.

Todryk, S., McLean, C., Ali, S., Entwistle, C., Boursnell, M., Rees, R. and Vile, R. (1999) Disabled infectious single-cycle herpes simplex virus as an oncolytic vector for immunotherapy of colorectal cancer. *Human Gene Therapy*. **10**: 2757-2768.

Tremethick, D.J. (1994) High-mobility group protein-14 and protein-17 can space nucleosomal particles deficient in histones H2a and H2b creating a template that is transcriptionally active. *Journal of Biological Chemistry*. **269**: 28436-28442.

Trotman, L.C., Mosberger, N., Fornerod, M., Stidwill, R.P. and Greber, U.F. (2001) Import of adenovirus DNA involves the nuclear pore complex receptor CAN/Nup214 and histone H1. *Nat Cell Biol*. **3**: 1092-1100.

Truant, R. and Cullen, B.R. (1999) The arginine-rich domains present in human immunodeficiency virus type 1 Tat and Rev function as direct importin beta-dependent nuclear localization signals. *Molecular and Cellular Biology*. **19**: 1210-1217.

Tse, C. and Hansen, J.C. (1997) Hybrid trypsinized nucleosomal arrays: identification of multiple functional roles of the H2A/H2B and H3/H4 N-termini in chromatin fiber compaction. *Biochemistry*. **36**: 11381-11388.

Turner, J.G., Tan, J., Crucian, B.E., Sullivan, D.M., Ballester, O.F., Dalton, W.S., *et al* (1998) Broadened clinical utility of gene gun-mediated, granulocyte-macrophage colony-stimulating factor cDNA-based tumor cell vaccines as demonstrated with a mouse myeloma model. *Human Gene Therapy*. **9**: 1121-1130.

Tuting, T., Gambotto, A., Baar, J., Davis, I.D., Storkus, W.J., Zavodny, P.J., *et al* (1997) Interferon-alpha gene therapy for cancer: retroviral transduction of fibroblasts and particle-mediated transfection of tumor cells are both effective strategies for gene delivery in murine tumor models. *Gene Therapy*. **4**: 1053-1060.

Uherek, C., Fominaya, J. and Wels, W. (1998) A modular DNA carrier protein based on the structure of diphtheria toxin mediates target cell-specific gene delivery. *Journal of Biological Chemistry*. **273**: 8835-8841.

Van Holde, K.E. and Weischet, W.O. (1978) Boundary analysis of sedimentaion velocity experients with monodisperse and paucidisperse solutes. *Biopolymers*. **17**: 1387-1403.

Van Holde, K.E., Allen, J.R., Tatchell, K., Weischet, W.O. and Lohr, D. (1980) DNA-histone interactions in nucleosomes. *Biophysical Journal*. **32**: 271-282.

Vancurova, I., Paine, T.M., Lou, W. and Paine, P.L. (1995) Nucleoplasmin associates with and is phosphorylated by casein kinase-Ii. *Journal of Cell Science*. **108**: 779-787.

Vanzeijl, M., Johann, S.V., Closs, E., Cunningham, J., Eddy, R., Shows, T.B. and Ohara, B. (1994) A human amphotropic retrovirus receptor is a 2nd member of the gibbon ape leukemia-virus receptor family. *Proceedings of the National Academy of Sciences of the United States of America*. **91**: 1168-1172.

Varga, C.M., Wickham, T.J. and Lauffenburger, D.A. (2000) Receptor-mediated targeting of gene delivery vectors: insights from molecular mechanisms for improved vehicle design. *Biotechnology and Bioengineering*. **70**: 593-605.

Vermaak, D., Ahmad, K. and Henikoff, S. (2003) Maintenance of chromatin states: an open-and-shut case. *Current Opinion in Cell Biology*. **15**: 266-274.

Vijayanathan, V., Thomas, T. and Thomas, T.J. (2002) DNA nanoparticles and development of DNA delivery vehicles for gene therapy. *Biochemistry*. **41**: 14085-14094.

Vitiello, L., Chonn, A., Wasserman, J.D., Duff, C. and Worton, R.G. (1996) Condensation of plasmid DNA with polylysine improves liposome-mediated gene transfer into established and primary muscle cells. *Gene Therapy*. **3**: 396-404.

Wade, P.A. and Wolffe, A.P. (1997) Histone acetyltransferases in control. *Current Biology*. 7: R82-84.

Wagner, E. (1998) Effects of membrane-active agents in gene delivery. *Journal of Controlled Release*. **53**: 155-158.

Wagner, E., Cotten, M., Foisner, R. and Birnstiel, M.L. (1991) Transferrin polycation DNA complexes - the effect of polycations on the structure of the complex and DNA delivery to cells. *Proceedings of the National Academy of Sciences of the United States of America*. **88**: 4255-4259.

Wagner, E., Zenke, M., Cotten, M., Beug, H. and Birnstiel, M.L. (1990) Transferrin-polycation conjugates as carriers for DNA uptake into cells. *Proceedings of the National Academy of Sciences of the United States of America*. **87**: 3410-3414.

Wagner, E.K. and Bloom, D.C. (1997) Experimental investigation of herpes simplex virus latency. *Clinical Microbiology Reviews*. **10**: 419-443.

Wang, C.Y. and Huang, L. (1984) Polyhistidine mediates an acid-dependent fusion of negatively charged liposomes. *Biochemistry*. **23**: 4409-4416.

Wang, Q., Guo, J. and Jia, W. (1997) Intracerebral recombinant HSV-1 vector does not reactivate latent HSV-1. *Gene Therapy*. **4**: 1300-1304.

Wang, X., Zhang, G.R., Yang, T., Zhang, W. and Geller, A.I. (2000) Fifty-one kilobase HSV-1 plasmid vector can be packaged using a helper virus-free system and supports expression in the rat brain. *Biotechniques*. **28**: 102-107.

Wangerek, L.A., Dahl, H.H.M., Senden, T.J., Carlin, J.B., Jans, D.A., Dunstan, D.E., *et al* (2001) Atomic force microscopy imaging of DNA - cationic liposome complexes optimised for gene transfection into neuronal cells. *Journal of Gene Medicine*. **3**: 72-81.

Ward, C.M. (2000) Folate-targeted non-viral DNA vectors for cancer gene therapy. *Current Opinion in Molecular Therapeutics*. **2**: 182-187.

Weger, S., Wistuba, A., Grimm, D. and Kleinschmidt, J.A. (1997) Control of adeno-associated virus type 2 cap gene expression: Relative influence of helper virus, terminal repeats, and rep proteins. *Journal of Virology*. **71**: 8437-8447.

Weiss, R.A. and Tailor, C.S. (1995) Retrovirus Receptors. *Cell*. **82**: 531-533.

Wells, D. and McBride, C. (1989) A comprehensive compilation and alignment of histones and histone genes. *Nucleic Acids Research*. **17**: 311-346.

Wells, J.M., Li, L.H., Sen, A., Jahreis, G.P. and Hui, S.W. (2000) Electroporation-enhanced gene delivery in mammary tumors. *Gene Therapy*. **7**: 541-547.

Whittaker, G.R., Kann, M. and Helenius, A. (2000) Viral entry into the nucleus. *Annual Review of Cell Developmental Biology*. **16**: 627-651.

Wickham, T.J., Mathias, P., Cheresh, D.A. and Nemerow, G.R. (1993) Integrin-alpha-V-beta-3 and integrin-alpha-V-beta-5 promote adenovirus internalization but not virus attachment. *Cell*. **73**: 309-319.

Wickham, T.J., Filardo, E.J., Cheresh, D.A. and Nemerow, G.R. (1994) Integrin alpha-V-beta-5 selectively promotes adenovirus-mediated cell-membrane permeabilization. *Journal of Cell Biology*. **127**: 257-264.

Wilke, M., Fortunati, E., van den Broek, M., Hoogeveen, A.T. and Scholte, B.J. (1996) Efficacy of a peptide-based gene delivery system depends on mitotic activity. *Gene Therapy*. **3**: 1133-1142.

Williams, R.S., Johnston, S.A., Riedy, M., Devit, M.J., McElligott, S.G. and Sanford, J.C. (1991) Introduction of foreign genes into tissues of living Mice by DNA-coated microprojectiles. *Proceedings of the National Academy of Sciences of the United States of America*. **88**: 2726-2730.

Wilson, G.L., Dean, B.S., Wang, G. and Dean, D.A. (1999) Nuclear import of plasmid DNA in digitonin-permeabilized cells requires both cytoplasmic factors and specific DNA sequences. *Journal of Biological Chemistry*. **274**: 22025-22032.

Wolf, H., Rols, M.P., Boldt, E., Neumann, E. and Teissie, J. (1994) Control by pulse parameters of electric field-mediated gene transfer in mammalian cells. *Biophysical Journal*. **66**: 524-531.

Wrobel, I. and Collins, D. (1995) Fusion of cationic liposomes with mammalian cells occurs after endocytosis. *Biochimica et Biophysica Acta*. **1235**: 296-304.

Wu, G.Y. and Wu, C.H. (1987) Receptor-mediated *in vitro* gene transformation by a soluble DNA carrier system. *Journal of Biological Chemistry*. **262**: 4429-4432.

Wu, G.Y. and Wu, C.H. (1988) Receptor-mediated gene delivery and expression *in vivo*. *Journal of Biological Chemistry*. **263**: 14621-14624.

Wyman, T.B., Nicol, F., Zelphati, O., Scaria, P.V., Plank, C. and Szoka, F.C. (1997) Design, synthesis, and characterization of a cationic peptide that binds to nucleic acids and permeabilizes bilayers. *Biochemistry*. **36**: 3008-3017.

Xiao, C.Y. and Jans, D.A. (1998) An engineered site for protein kinase C flanking the SV40 large T-antigen NLS confers phorbol ester-inducible nuclear import. *FEBS Letters*. **436**: 313-317.

Xiao, C.Y., Hubner, S. and Jans, D.A. (1997a) SV40 large tumor antigen nuclear import is regulated by the double-stranded DNA-dependent protein kinase site (serine 120) flanking the nuclear localization sequence. *Journal of Biological Chemistry*. **272**: 22191-22198.

Xiao, C.Y., Jans, P. and Jans, D.A. (1998) Negative charge at the protein kinase CK2 site enhances recognition of the SV40 large T-antigen NLS by importin: effect of conformation. *FEBS Letters*. **440**: 297-301.

Xiao, C.Y., Hubner, S., Elliott, R.M., Caon, A. and Jans, D.A. (1996a) A consensus cAMP-dependent protein kinase (PK-A) site in place of the CcN motif casein kinase II site of simian virus 40 large

T-antigen confers PK-A-mediated regulation of nuclear import. *Journal of Biological Chemistry*. **271**: 6451-6457.

Xiao, X., Xiao, W.D., Li, J. and Samulski, R.J. (1997b) A novel 165-base-pair terminal repeat sequence is the sole cis requirement for the adeno-associated virus life cycle. *Journal of Virology*. **71**: 941-948.

Xiao, X.A., Li, J.A. and Samulski, R.J. (1996b) Efficient long-term gene transfer into muscle tissue of immunocompetent mice by adeno-associated virus vector. *Journal of Virology*. **70**: 8098-8108.

Xu, Y. and Szoka, F.C., Jr. (1996) Mechanism of DNA release from cationic liposome/DNA complexes used in cell transfection. *Biochemistry*. **35**: 5616-5623.

Yanez, R.J. and Porter, A.C.G. (1999) Influence of DNA delivery method on gene targeting frequencies in human cells. *Somatic Cell and Molecular Genetics*. **25**: 27-31.

Yang, N.S. and Sun, W.H. (1995) Gene gun and other non-viral approaches for cancer gene therapy. *Nature Medicine*. **1**: 481-483.

Yang, Y.P. and Wilson, J.M. (1995) Clearance of adenovirus-infected hepatocytes by MHC class I-restricted CD4(+) CTLs *in vivo*. *Journal of Immunology*. **155**: 2564-2570.

Yano, L., Shimura, M., Taniguchi, M., Hayashi, Y., Suzuki, T., Hatake, K., *et al* (2000) Improved gene transfer to neuroblastoma cells by a monoclonal antibody targeting RET, a receptor tyrosine kinase. *Human Gene Therapy*. **11**: 995-1004.

Yao, J., Lowary, P.T. and Widom, J. (1991) Linker DNA bending induced by the core histones of chromatin. *Biochemistry*. **30**: 8408-8414.

Yeung, S.N., Bockhold, K. and Tufaro, F. (1999) Efficient infection of mature skeletal muscle with herpes simplex virus vectors by using dextran sulfate as a co-receptor. *Gene Therapy*. **6**: 1536-1544.

Yoshizato, K., Nishi, T., Goto, T., Dev, S.B., Takeshima, H., Kino, T., *et al* (2000) Gene delivery with optimized electroporation parameters shows potential for treatment of gliomas. *International Journal of Oncology*. **16**: 899-905.

Young, S.M., McCarty, D.M., Degtyareva, N. and Samulski, R.J. (2000) Roles of adeno-associated virus Rep protein and human chromosome 19 in site-specific recombination. *Journal of Virology*. **74**: 3953-3966.

Zabner, J., Fasbender, A.J., Moninger, T., Poellinger, K.A. and Welsh, M.J. (1995) Cellular and molecular barriers to gene-transfer by a cationic lipid. *Journal of Biological Chemistry*. **270**: 18997-19007.

Zaitsev, S.V., Haberland, A., Otto, A., Vorob'ev, V.I., Haller, H. and Bottger, M. (1997) H1 and HMG17 extracted from calf thymus nuclei are efficient DNA carriers in gene transfer. *Gene Therapy*. **4**: 586-592.

Zanta, M.A., Belguise-Valladier, P. and Behr, J.P. (1999) Gene delivery: A single nuclear localization signal peptide is sufficient to carry DNA to the cell nucleus. *Proceedings of the National Academy of Sciences of the United States of America*. **96**: 91-96.

Zasloff, M., Rosenberg, M. and Santos, T. (1982) Impaired nuclear transport of a human variant tRNAiMet. *Nature*. **300**: 81-84.

Zelenin, A.V., Kolesnikov, V.A., Tarasenko, O.A., Shafei, R.A., Zelenina, I.A., Mikhailov, V.V., *et al* (1997) Bacterial beta-galactosidase and human dystrophin genes are expressed in mouse skeletal muscle fibers after ballistic transfection. *FEBS Letters*. **414**: 319-322.

Zelphati, O. and Szoka, F.C., Jr. (1996) Mechanism of oligonucleotide release from cationic liposomes. *Proceedings of the National Academy of Sciences of the United States of America*. **93**: 11493-11498.

Zelphati, O., Liang, X., Hobart, P. and Felgner, P.L. (1999) Gene chemistry: functionally and conformationally intact fluorescent plasmid DNA. *Human Gene Therapy*. **10**: 15-24.

Zelphati, O., Liang, X., Nguyen, C., Barlow, S., Sheng, S., Shao, Z. and Felgner, P.L. (2000) PNA-dependent gene chemistry: stable coupling of peptides and oligonucleotides to plasmid DNA. *Biotechniques*. **28**: 304-310, 312-304, 316.

Zeng, M., Cerniglia, G.J., Eck, S.L. and Stevens, C.W. (1997) High-efficiency stable gene transfer of adenovirus into mammalian cells using ionizing radiation. *Human Gene Therapy*. **8**: 1025-1032.

Zhou, X. and Huang, L. (1994) DNA transfection mediated by cationic liposomes containing lipopolylysine: characterization and mechanism of action. *Biochimica et Biophysica Acta*. **1189**: 195-203.

Ziady, A.G., Ferkol, T., Dawson, D.V., Perlmutter, D.H. and Davis, P.B. (1999) Chain length of the polylysine in receptor-targeted gene transfer complexes affects duration of reporter gene expression both in vitro and in vivo. *Journal of Biological Chemistry*. **274**: 4908-4916.

Zlatanova, J.S., Srebreva, L.N., Banchev, T.B., Tasheva, B.T. and Tsanev, R.G. (1990) Cytoplasmic pool of histone H1 in mammalian cells. *Journal of Cell Science*. **96**: 461-468.

Zou, Y.Y., Zong, G., Ling, Y.H. and Perez-Soler, R. (2000) Development of cationic liposome formulations for intratracheal gene therapy of early lung cancer. *Cancer Gene Therapy*. **7**: 683-696.